A Study on Gain Scheduling of Auxiliary Noise for Online Secondary and Feedback Path Modeling in Active Noise Control Systems

by

Shakeel Ahmed

A thesis submitted in partial fulfilment
of the requirments for the degree of
Doctor of Engineering

Department of Communication Engineering and Informatics
Graduate School of Informatics and Engineering
The University of Electro-Communications
1-5-1 Chofugaoka, Chofu, 182-8585, Tokyo, Japan

March, 2015

DEDICATION

To my beloved parents, father *Muhammad Javed*; mother *Sabia Beigum*, and proficient teachers for their invaluable support, and for guiding me to where I am today

GLOSSARY

ADC	Analog to digital converter.
ANC	Active noise control.
ANP	Auxiliary-noise-power.
CEMFxLMS	Computationally efficient modified filtered-x-least-mean-square.
DAC	Digital to analog converter.
DSP	Digital signal processing.
EMFN	Even mirror Fourier non-linear.
FBPM	Feedback path modeling.
FBPN	Feedback path neutralization.
FBPMN	Feedback path modeling and neutralization.
FDAF	Frequency domain adaptive filter.
FFT	Fast Fourier transform.
FIR	Finite impulse response.
FN	Fourier non-linear.
FsLMS	Filtered-s-least-mean-square.
FxLMS	Filtered-x-least-mean-square.

IIR	Infinite impulse response.
LMS	Least-mean-square.
MFxLMS	Modified filtered-x-least-mean-square.
MFxNLMS	Modified filtered-x-normalized-least-mean-square.
MNR	Mean-noise-reduction.
MSE	Mean-square-error.
NLMS	Normalized-least-mean-square.
NRP	Noise-reduction-performance.
OSPM	Online secondary path modeling.
PPSEQ	Perfect-periodic-sequences.
SNR	Signal to noise ratio.
SPM	Secondary path modeling.
VFxLMS	Volterra filtered-x-least-mean-square.
VSS	Variable step-size.
WGN	White Gaussian noise.

SYMBOLS

$d(n)$	Desired response/ Unwanted noise at the summing junction.
$E[\cdot]$	Mathematical expectation operator.
E_q	Energy of signal $q(n)$.
$e(n)$	Residual error signal.
$e_q(n)$	Error signal of any adaptive filter $Q(z)$.
f	Signal frequency.
$F(z)$	Feedback path transfer function with impulse response $f(n)$.
$\hat{F}(z)$	Estimate of $F(z)$ with impulse response $\hat{f}(n)$.
$G(n)$	Time-varying gain.
$\boldsymbol{G}(n)$	Diagonal gain matrix.
$\boldsymbol{G}^{-1}(n)$	Inverse of diagonal gain matrix.
k	Frequency index.
L_q	Length of any filter $Q(z)$ and its estimate $\hat{Q}(z)$.
n	Time index.
$P(z)$	Primary path transfer function with impulse response $p(n)$.
P_q	Power of signal $q(n)$.

$Q(z)$	Filter transfer function with impulse response $q(n)$.
$Q^{-1}(z)$	Inverse filter of $Q(z)$ with impulse response $q^{-1}(n)$.
$\hat{Q}(z)$	Estimate of filter $Q(z)$ with impulse response $\hat{q}(n)$.
$\hat{Q}_o(z)$	Optimal value of the estimate $\hat{Q}(z)$.
$\hat{Q}^{-1}(z)$	Inverse filter of $\hat{Q}(z)$ with impulse response $\hat{q}^{-1}(n)$.
$\boldsymbol{q}(n)$	Vector of length L_q containing tap-weights of filter $Q(z)$
$\overline{Q}(k)$	Complex conjugate of $Q(k)$.
$r(n)$	Noise from a noise source at reference microphone.
$R_{qq}(n)$	Autocorrelation function of a signal $q(n)$
$R_{pq}(n)$	Cross-correlation function of signal $p(n)$ with $q(n)$.
$S(z)$	Secondary path transfer function with impulse response $s(n)$.
$\hat{S}(z)$	Estimate of $S(z)$ with impulse response $\hat{s}(n)$.
$v(n)$	Auxiliary WGN used for system identification.
$v_d(n)$	Measurement noise.
$v_g(n)$	Output of White noise generator.
$v_f(n)$	Output of $F(z)$ corresponding to input $v(n)$.
$v_{\hat{f}}(n)$	Output of $\hat{F}(z)$ corresponding to input $v(n)$.
$v_s(n)$	Output of $S(z)$ corresponding to input $v(n)$.
$v_{\hat{s}}(n)$	Output of $\hat{S}(z)$ corresponding to input $v(n)$.
$x(n)$	Input excitation signal/ Noise signal from a noise source.
$\boldsymbol{x}_{q(n),x(n)}(n)$	Input signal vector of filter $Q(z)$ with input $x(n)$ at iteration n
$y_q(n)$	Output signal of any adaptive filter $Q(z)$.
$y_{pq}(n)$	Output of series combination of filters $P(z)$ and $Q(z)$ with input signal filtered first through $P(z)$ and then through $Q(z)$.
$*$	Convolution operator.

Δ	Delay.
$\Delta D_q(n)$	Relative modeling error of filter $Q(z)$.
$\delta(n)$	Unit sample function.
ΔX	Mean-square-error in the signal $r(n)$.
$\|\| \cdot \|\|^2$	Square of the Euclidean norm.
λ	Forgetting factor.
μ	Fixed step-size parameter for an adaptive filter.
$\mu_q(n)$	Time-varying step-size parameter for adaptive filter $Q(z)$.
$\boldsymbol{\mu}_q(n)$	Diagonal matrix of time-varying step-size parameters for adaptive filter $Q(z)$.

概　　要

アンチノイズ信号を生成して音響ノイズをキャンセルする非常に興味深い手法は，1936 年に P. Lueg によって提案された．フィードフォワード型アクティブノイズコントロール (ANC) システムでは，アンチノイズ信号は，基準マイクとエラーマイク，ANC フィルタに基づく適応 FxLMS (Filtered-x-Least-Mean-Square) アルゴリズム及び電気音響二次経路により生成される．ANC システムが安定に動作するには，FxLMS アルゴリズムが二次経路の推定が必要である．スピーカーで生成されたアンチノイズ信号が基準マイク信号と干渉を引き起こす．この干渉はスピーカーと基準マイクの間にフィードバック経路と呼ばれる電気音響経路が存在することに起因する．よって，このフィードバック経路の影響を中和する必要があり，フィードバック経路の推定が必要である．

二次経路とフィードバック経路のオンラインモデリングのために，付加的な補助ノイズが注入される．この補助ノイズは，残留誤差を招き，ANC システムのノイズ低減性能 (NRP) を劣化させる．NRP を改善するために，ゲインスケジューリング手法が使われ，注入された補助ノイズの電力を変化させる．ゲインスケジューリングの目的は，二次経路とフィードバック経路のモデル推定値が実際の未知経路とかけ離れているとき，大きい補助ノイズを注入して高速に収束させることである．推定値が実際の未知経路に近いときは，補助ノイズを小さい値に低減させる．したがって，ゲインスケジューリングは，二次経路とフィードバック経路のモデル推定に役に立つと同時に，定常状態では NRP を改善できる．本論文では，二つの重要な問題：オンライン二次経路モデリング (OSPM) と、オンラインフィードバック経路モデリングとニュートラリゼション (FBPMN) について，ゲインスケジューリングの幾つか異なる方法を提案する．

第 1 章では，まず ANC システムの基礎となる物理的原理と構成について概説する．異なるシステム同定において，ANC システム，すなわち，適応フィルタの基本構成ブロックの適用について議論し，ANC システムの中で最もよく使われている適応アルゴリズム，すなわち，FxLMS アルゴリズムを一般的な二次経路のために導出する．また，ANC システムにおける二つの基本的な問題：OSPM とオンライン FBPMN について説明し，システム同定のための最適な励起信号，すなわち，完全スイープ信号の使用についても述べる．

第 2 章では，分散値を固定した補助ノイズを使用した条件でゲインスケジューリングなしの OSPM について，既存の手法を解説し，修正された FxLMS (MFxLMS) と OSPM のための簡単な構造を持つ適応アルゴリズムを提案する．提案した簡単な構造の利点は，ANC システムの性能を維持しなが

ら，MFxLMS アルゴリズムに基づく OSPM の計算量を低減できることである．また，シミュレーションを行い，その結果を用いて既存の方法と性能を比較する．

第 3 章では，まず，ゲインスケジューリングを用いた OSPM について，既存の手法を解説する．既存のゲインスケジューリング手法の利点と欠点を分析し，新しいゲインスケジューリング手法を提案し，SPM フィルタのモデリング精度および ANC システムの NRP を改善する．既存の方法では，ANC システムの収束状態の情報のみを持つ残差信号の電力に基づいてゲインを変動させる．一方，提案法では，SPM フィルタのエラー信号の電力に基づいてゲインを変動させている．SPM フィルタのエラー信号の電力は ANC システムと SPM フィルタの両方の収束状態に関する情報を持つため，ゲインを制御するより望ましい手法である．また，シミュレーションを行い，その結果を用いて既存の方法と性能を比較する．

第 4 章では，ANC システムのフィードフォワード構成に関連するオンライン FBPMN の問題について議論する．はじめに，ゲインスケジューリングを使用しないオンライン FBPMN について，既存の方法とそれらの問題点を説明する．つぎに，ゲインスケジューリングを使用しないオンライン FBPMN のための新しい構造を提案し，シミュレーションを行い，既存の方法と性能を比較する．新しい構造では，既存構造の特長が組み合わせられ，予測器を使って適応 FBPMN フィルタのエラー信号から予測可能な干渉項を除去する．加えて，FBPM フィルタと FBPN フィルタが単一の FBPMN フィルタとして結合される．既存構造に比較して，新しい構造の利点は，ANC フィルタの入力信号にフィードバックカップリングする作用をより良く中和でき，ANC システムの収束性を改善することができる．後半では，ANC システムの NRP を改善するために，ゲインスケジューリング手法を提案する．また，FBPMN フィルタのステップサイズが一致する自己同調 ANP スケジューリング手法も提案する．この自己同調 ANP スケジューリング手法では，チューニングパラメータを必要とせず，ANC システムの NRP をさらに改善できる．

第 5 章では，本論文の結論と今後の研究課題等について述べる．

ABSTRACT

The idea of cancelling the acoustic noise by generating an anti-noise signal is very fascinating, and was first proposed by P. Lueg in 1936. In feedforward active noise control (ANC) systems, the anti-noise signal is generated with the help of reference and error microphones, an adaptive filtered-x-LMS (FxLMS) algorithm based ANC filter, and an electro-acoustic path named as the secondary path. For stable operation of ANC systems, the FxLMS algorithm needs an estimate of the secondary path. The anti-noise signal generated by the loudspeaker (part of secondary path) causes interference with the reference microphone signal. This interference is due to the presence of electro-acoustic path, named as feedback path, between the loudspeaker and the reference microphone. It is required to neutralize the effect of this feedback path, and hence an estimate of the feedback path is required.

For online modeling of the secondary and feedback paths, an additional auxiliary noise is injected. This auxiliary noise contributes to the residual error, and thus degrades the noise-reduction-performance (NRP) of ANC system. In order to improve the NRP, a gain scheduling strategy is used to vary the variance of the injected auxiliary noise. The purpose of the gain scheduling is that when the model estimates of the secondary and the feedback paths are far from the actual unknown paths, auxiliary noise with large variance is injected. Once the model estimates are closer to the actual unknown paths, the variance of auxiliary noise is reduced to a small value. In this way, on one hand the gain scheduling can help us to achieve the required model estimates of secondary and feedback paths, and on the other hand to improve the NRP at the steady-state. In this thesis, we discuss the two most important issues, i.e., 1) online secondary path modeling (OSPM), and 2) online feedback path modeling and neutralization (FBPMN) with gain scheduling.

In **chapter 1**, the basic underlying physical principle and configurations of active noise control (ANC) systems are explained. The application of the basic building block of an ANC system i.e. *An adaptive filter*, in different system identification scenarios is discussed. The most popular adaptive algorithm for ANC system, i.e., *FxLMS algorithm* is derived for the general secondary path. A brief overview is given for the two fundamental issues in ANC systems, i.e., 1) OSPM

and 2) online FBPMN. The use of optimal excitation signal, i.e., *Perfect sweep signals* for system identification is described.

In **chapter 2**, the existing methods for OSPM without gain scheduling, where the auxiliary noise with fixed variance is used in all operating conditions, are discussed. In this chapter a simplified structure for OSPM with the modified FxLMS (MFxLMS) adaptive algorithm is proposed. The advantage of the simplified structure is that it reduces the computational complexity of the MFxLMS algorithm based OSPM without having any compromise on the performance of ANC system.

In **chapter 3**, the existing methods for OSPM with gain scheduling are discussed. The drawbacks with the existing gain scheduling strategies are highlighted, and some new gain scheduling strategies are proposed to improve the modeling accuracy of SPM filter and the NRP of an ANC system. In existing methods, the gain is varied based on the power of residual error signal which carries information only about the convergence status of ANC system. In the Proposed methods the gain is varied based on the power of error signal of SPM filter. This is more desirable way of controlling the gain because the power of error signal of SPM filter carries information about the convergence status of both the ANC system and the SPM filter. The performance comparison is carried out through the simulation results.

In **chapter 4**, the second most important issue associated with the feedforward configuration of ANC system, i.e., the issue of online FBPMN is deal with. In the first part, the existing methods for online FBPMN without gain scheduling are discussed. A new structure is proposed for online FBPMN without gain scheduling. The performance of the existing methods is compare with the proposed method through the simulation results. In the new structure the good features from the existing structures are combined together. The predictor is used in the new structure to remove the predictable interference term from the error signal of adaptive FBPMN filter. In addition to this, the action of FBPM filter and the FBPN filter is combined into a single FBPMN filter. The advantage of the new structure over the existing structures is that it can better neutralize the effect of feedback coupling on the input signal of ANC filter, thus improves the convergence of ANC system. In the second part, a gain scheduling strategy is proposed to improve the NRP of ANC system. In addition to this, a self-tuned ANP scheduling strategy with matching step-size for FBPMN filter is also proposed that requires no tuning parameters and further improves the NRP of ANC systems.

In **chapter 5**, the concluding remarks and some future research directions are given.

Contents

Chapter 1

Introduction

1.1 Active Noise Control (ANC)

Noise is an unwanted or an undesired signal. The unintended and undesired sound in the acoustic domain is called acoustic noise. The major sources of the acoustic noise include industries, and transportation. Broadly speaking the acoustic noise can be classified into two major types; 1) Narrow band noise, having energy concentrated at specific frequencies, e.g., noise from rotating machines and engines etc., and 2) Broad-band noise, having energy distribution over a broad range of audible frequencies, e.g., pink noise, white noise etc [1]-[5].

The traditional approach for acoustic noise cancellation is to use the passive techniques. These techniques include the use of sound absorbing materials, si-

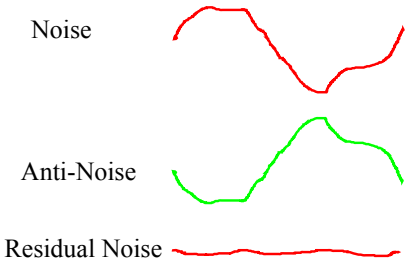

Figure 1.1: Physical concept of active noise cancellation.

lencers, enclosures, barriers, and mufflers [1, 2] for noise attenuation. These passive techniques are effective at high frequencies, and become ineffective, large in size, and costly at low frequencies (for $f < 500Hz$). The alternate solution at low frequency is to use active techniques for noise cancellation [3]- [5].

Physical concept of ANC: The basic building block of an ANC system is an adaptive filter [6]-[8], and the underlying physical concept is the principle of superposition. In feedforward configuration of ANC systems, using the reference microphone signal, the electrical adaptive controller followed by the secondary path will generate an anti-noise signal. The anti-noise signal will interfere destructively with the unwanted noise signal at the summing junction, and will cancel the original noise. The better cancellation will be achieved if the magnitude of the anti-noise is same and phase is exactly opposite to that of original unwanted noise. The idea of noise cancellation with an anti-noise signal is shown in Fig. 1.1. It is difficult to achieve the desired performance with analog circuits, hence it is required for the controller of ANC system to be digital [4].

The idea of using the microphones and the secondary source (loudspeaker) to generate the anti-noise signal was first proposed by P. Lueg in 1936 [9]. Since the characteristics of the unwanted noise, and the acoustic paths are time-varying, therefore the idea presented in [9] did not have the practical applications until the

development of adaptive signal processing algorithm and DSP hardware. The idea became practically realizable with the development of adaptive signal processing algorithm and DSP hardware in 1980. The application of adaptive signal processing to cancel the noise in a duct was proposed in [10]-[12], where the adaptive filters adjust its coefficients to minimize some cost functions.

Basic configurations of ANC systems: Based on the structure, the ANC systems can be classified into following two types: 1) Feedforward Single/Multi channel ANC system, and 2) Feedback Single/Multi channel ANC system. The feedforward ANC system can be used to cancel both the narrow-band (predictable) as well as the broad-band (unpredictable) noise signals, whereas the feedback ANC system is used to cancel only the narrow-band signal. The feedback ANC system can not be employed for the cancellation of broad-band noise signal due to inherent delay associated with the feedback configuration. The details for the feedforward and feedback ANC system can be found in [3]- [5].

ANC applications: When the unwanted noise to be canceled is at high frequency, the need of high sampling rate will limit the use of active techniques, so passive techniques are the best choice. However on the other hand, when the unwanted noise is at low frequency, active techniques are the obvious choice due to size and cost constraints. ANC has found many applications such as in cars, locomotives, air-planes, particularly hi-tech propeller driven air crafts, helicopters, ships, and boats to cancel the unwanted noise coming from an engine. ANC can be employed in smart-phones, earphones, and blue-tooth head sets to cancel the background noise and allow the user to hear a clean audio of a song, or news etc. The most popular applications of ANC systems are in ventilations, air conditioning ducts used in seminar rooms, hospitals, concert halls and meeting rooms [4].

In this thesis, our focus will be on the application of ANC in acoustic duct.

1.2 Adaptive Filtering in ANC

The adaptive filter is one of the basic building block of an adaptive ANC system. An adaptive filter can be realized using FIR or IIR structure. In this thesis, the FIR structure will be used for the implementation of an adaptive filter. In an adaptive filter, the coefficients are adjusted automatically such that a certain cost function is minimized. The adaptive filtering finds many applications in area of an unknown system identification [7], prediction [13], and inverse filtering.

System identification: The block diagram for an unknown system identification using an adaptive filter is shown in Fig. 1.2, where $W(z)$ is the transfer function of an unknown system, $\hat{W}(z)$ is an adaptive filter and represents an estimate of $W(z)$, $y_w(n)$ and $y_{\hat{w}}(n)$ are the outputs of $W(z)$ and $\hat{W}(z)$, respectively, corresponding to input excitation signal $x(n)$, $v_d(n)$ is a measurement noise and usually modeled as additive white Gaussian noise (WGN), $d(n)$ is the desired response of adaptive filter, and $e_{\hat{w}}(n)$ is the error signal of adaptive filter $\hat{W}(z)$. The adaptive filter updates its coefficient at each iteration such that the certain cost function is minimized. Acoustic echo cancellation [14] is one of the practical application where system identification is required.

Prediction: The general block diagram of an adaptive linear predictor is shown in Fig. 1.3. It is called predictor because the current value of the input $x(n)$ is predicted from the past sample values of $x(n)$. If it is assumed that the adaptive filter has length L_w, then the output $y_{\hat{w}}(n)$ can be written as the linear

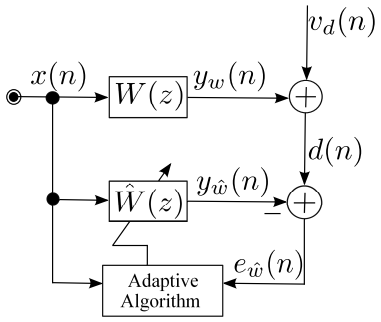

Figure 1.2: Adaptive system identification.

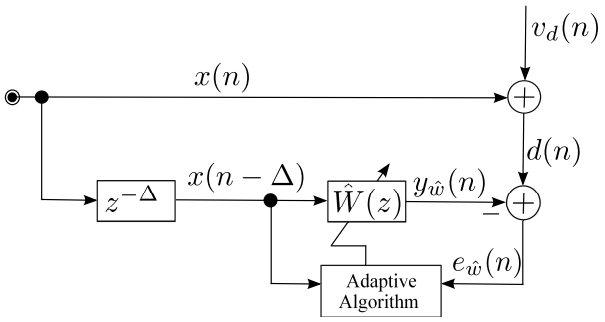

Figure 1.3: Adaptive linear prediction.

combination of the past sample values of $x(n)$, and is computed as

$$y_{\hat{w}}(n) = \hat{w}(n) * x(n-\Delta) = \hat{\boldsymbol{w}}^T(n)\boldsymbol{x}_{\hat{w}(n),x(n-\Delta)}(n), \tag{1.1}$$

where $\hat{w}(n)$ is the impulse response of $\hat{W}(z)$, $x(n-\Delta)$ is the delayed version of $x(n)$, $\hat{\boldsymbol{w}}(n) = [\hat{w}_0(n), \hat{w}_1(n), \cdots, \hat{w}_{L_w-1}(n)]^T$ is the impulse response coefficient vector of adaptive filter $\hat{W}(z)$ at time n, $\boldsymbol{x}_{\hat{w}(n),x(n-\Delta)}(n) = [x(n-\Delta), x(n-\Delta-1), \cdots, x(n-\Delta-L_w+1)]^T$ is the input signal vector of $\hat{W}(z)$ with input $x(n-\Delta)$ at time n, and Δ represents the delay. This technique is useful in some applications where it is required to separate the predictable signal from the unwanted random background noise.

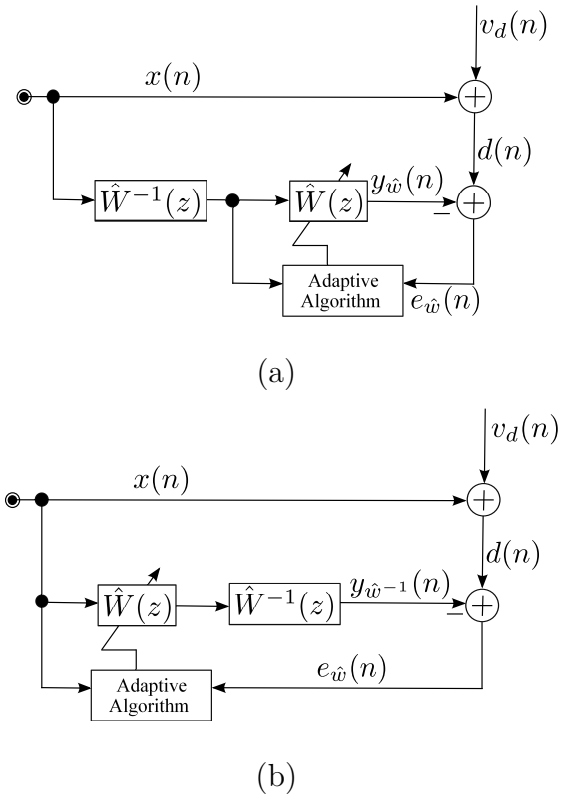

Figure 1.4: Adaptive inverse filtering: (a) Unknown system followed by an adaptive filter, (b) Adaptive filter followed by an unknown system.

Inverse filtering: The general block diagram for inverse filtering in two scenarios is shown in Fig. 1.4. In inverse filtering, the coefficients of the adaptive filter $\hat{W}(z)$ are updated in such a way that the overall impulse response is the unit sample function, i.e, $\hat{w}(n) * \hat{w}^{-1}(n) = \delta(n)$, where $\hat{w}(n)$ is the impulse response of $\hat{W}(z)$, $\hat{w}^{-1}(n)$ is the impulse response of $\hat{W}^{-1}(z)$, and $\delta(n)$ is the unit sample function. The block diagram in Fig. 1.4(a) is used in communication systems, where it is required to equalize the effect of the channel on the transmitted signal. The block diagram in Fig. 1.4(b) has found application in ANC, where the controller is required to equalize the effect of the secondary path [4].

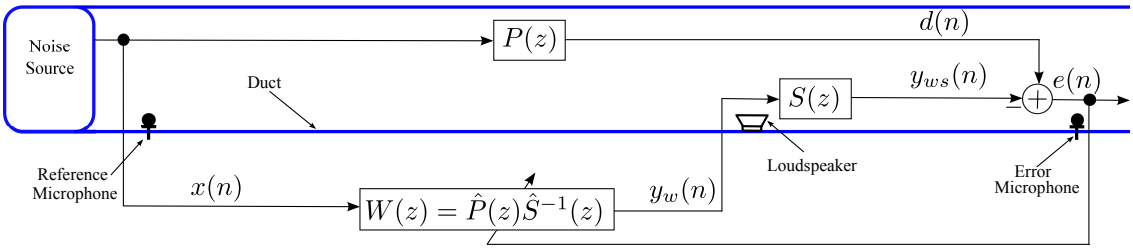

Figure 1.5: LMS adaptive algorithm based ANC for acoustic duct: An example of indirect system identification.

Direct VS Indirect system identification: In direct system identification the output of an adaptive filter is subtracted from the desired response $d(n)$, as shown in Fig. 1.2 $\sim$ Fig. 1.4(a), whereas in indirect system identification, the output of an adaptive filter has to pass through some filters before being subtracted from the desired response, as shown in Fig. 1.4(b). The practical example of an indirect system identification is an ANC system, where the electrical adaptive controller is followed by an electro-acoustic secondary path.

ANC for acoustic duct (an example of indirect system identification): The block diagram of a single channel feedforward LMS adaptive algorithm based ANC system for acoustic duct is shown in Fig. 1.5. Here $x(n)$ is the unwanted noise to be canceled. This unwanted noise travels through an electro-acoustic path $P(z)$. The transfer function $P(z)$ represents the combination of the transfer functions $P'(z)$ and $R(z)$, i. e., $P(z) = P'(z)R(z)$. The transfer function $P'(z)$ includes the transfer function of the acoustic path from the reference microphone to the summing junction, and $R(z)$ is the residual transfer function from the summing junction to the residual error signal $e(n)$. The transfer function $R(z)$ includes not only the transfer function of the acoustic path from the summing junction to the error microphone, but also the transfer functions of error microphone, pre-

amplifier, anti-aliasing filter, and analog to digital converter (ADC). The signal $x(n)$ is also picked-up by the reference microphone and is given to the controller $W(z)$. The output $y_w(n)$ of $W(z)$ is applied to secondary path transfer function $S(z)$ to generate $y_{ws}(n)$ (estimate of $d(n)$). Similar to $P(z)$, the secondary path transfer function $S(z)$ also represents the combination of the transfer functions $S'(z)$ and $R(z)$. The transfer function $S'(z)$ includes the transfer function from the controller output $y_w(n)$ to the summing junction [4]. The transfer functions $P(z)$ and $W(z)S(z)$ will transform the signal $x(n)$ to $d(n)$ and $y_{ws}(n)$, respectively. The signal $d(n)$ and its estimate $y_{ws}(n)$ will interfere with each other destructively (note the negative sign at the error microphone in Fig. 1.5 to reduce the noise at the summing junction.

In Fig. 1.5, the controller $W(z)$ will simultaneously identify $P(z)$ (indirect system identification) and equalize $S(z)$, i.e., $W(z) = \hat{P}(z)\hat{S}^{-1}(z)$, where $\hat{P}(z)$ and $\hat{S}^{-1}(z)$ are the estimate of $P(z)$, and inverse transfer function of $S(z)$. If it is assumed that the secondary path is linear, then the filters $W(z)$, and $S(z)$ can commute. With this commutation the problem of indirect system identification is now transformed to direct system identification and is shown in Fig. 1.6. It is clear from Fig. 1.6 that the input signal $x(n)$ is filtered through the secondary path before being applied to the adaptive algorithm of $W(z)$. Therefore, the assumption of the linearity of the secondary path led to the foundation of the most popular filtered-x-LMS (FxLMS) algorithm [15]. The FxLMS algorithm was also derived independently by Burgess and Widrow in [10], and [16], respectively. The equivalent block diagram of FxLMS algorithm based single channel feedforward ANC system for duct is shown in Fig. 1.7, where $\hat{S}(z)$ represents the estimate of $S(z)$.

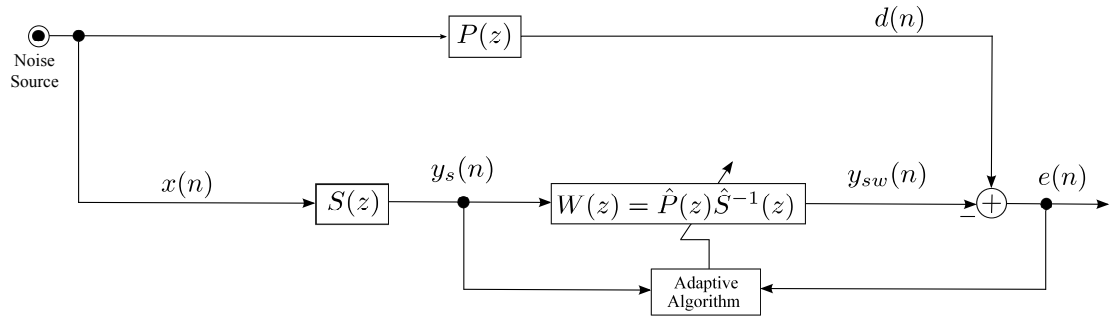

Figure 1.6: Block diagram of ANC system with secondary path followed by controller.

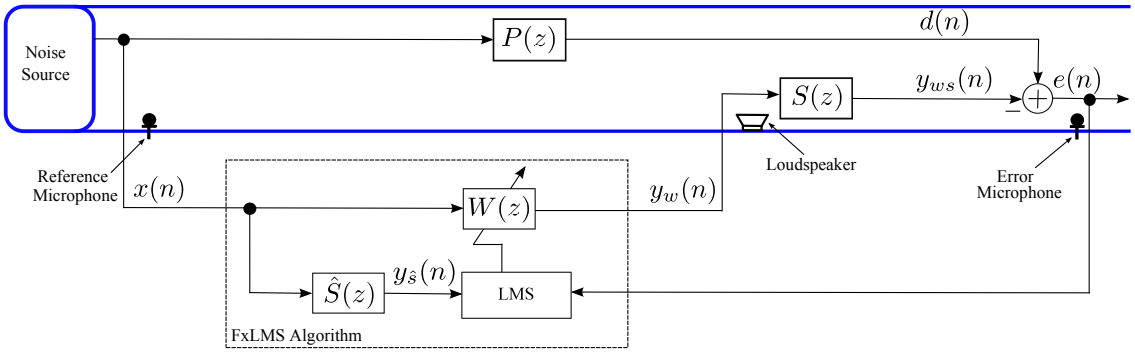

Figure 1.7: FxLMS algorithm based single channel feedforward ANC system for duct.

1.2.1 FxLMS Algorithm for General Secondary Path

In the case of ANC systems the secondary path can be linear or nonlinear. In this section, at first the expression of FxLMS algorithm is derived for general secondary path. After that, the assumption of the linearity of the secondary path is incorporated into the general expression to have an expression for the FxLMS with linear secondary path. From Fig. 1.7, the residual error signal $e(n)$ is given by

$$e(n) = d(n) - y_{ws}(n), \tag{1.2}$$

where

$$d(n) = p(n) * x(n) = \boldsymbol{p}^T(n)\boldsymbol{x}_{p(n),x(n)}(n), \tag{1.3}$$

and

$$y_{ws}(n) = s(n) * y_w(n) = \boldsymbol{s}^T(n)\boldsymbol{x}_{s(n),y_w(n)}(n), \tag{1.4}$$

where $d(n)$ is the unwanted noise at the summing junction, $p(n)$ is the impulse response of the primary path, $\boldsymbol{p}(n) = [p_0(n), p_1(n), \cdots, p_{L_p-1}(n)]^T$ is the impulse response coefficient vector of primary path at time n, $\boldsymbol{x}_{p(n),x(n)}(n) = [x(n), x(n-1), \cdots, x(n-L_p+1)]^T$ is the input signal vector of filter $P(z)$ with input $x(n)$ at time n, L_p is the tap-weight length of the primary path, $y_{ws}(n)$ is the estimate of $d(n)$ at the summing junction, $\boldsymbol{s}(n) = [s_0(n), s_1(n), \cdots, s_{L_s-1}(n)]^T$ is the impulse response coefficient vector of secondary path at time n, $\boldsymbol{x}_{s(n),y_w(n)}(n) = [y_w(n), y_w(n-1), \cdots, y_w(n-L_s+1)]^T$ is the input signal vector of filter $S(z)$ with input $y_w(n)$ at time n, L_s is the tap-weight length of the secondary path, and $y_w(n)$ is controller output being computed as

$$y_w(n) = w(n) * x(n) = \boldsymbol{w}^T(n)\boldsymbol{x}_{w(n),x(n)}(n), \tag{1.5}$$

where $w(n)$ is the impulse response of $W(z)$, $\boldsymbol{w}(n) = [w_0(n), w_1(n), \cdots, w_{L_w-1}(n)]^T$ is the impulse response coefficient vector of $W(z)$ at time n, $\boldsymbol{x}_{w(n),x(n)}(n) = [x(n), x(n-1), \cdots, x(n-L_w+1)]^T$ is the input signal vector of filter $W(z)$ with input $x(n)$ at time n, and L_w is the tap-weight length of $W(z)$. At each iteration the weight of controller are adjusted in such away as to minimize the cost function given by

$$J(\boldsymbol{w}(n))(n) = E\{e^2(n)\} = E\{(d(n) - y_{ws}(n))^2\}, \tag{1.6}$$

where the cost function $J(\boldsymbol{w}(n))(n)$ is a quadratic w.r.t the filter coefficients. Using the steepest descent method, the weight update equation for the controller $W(z)$

can be written as

$$\begin{aligned} \boldsymbol{w}(n+1) &= \boldsymbol{w}(n) - \frac{1}{2}\mu E\left\{\frac{\partial J(\boldsymbol{w}(n))(n)}{\partial \boldsymbol{w}(n)}\right\} \\ &= \boldsymbol{w}(n) + \mu E\left\{e(n)\frac{\partial y_{ws}(n)}{\partial \boldsymbol{w}(n)}\right\}, \end{aligned} \tag{1.7}$$

where μ is the step-size parameter, and it control the convergence and stability of the adaptive algorithm, and

$$\frac{\partial y_{ws}(n)}{\partial \boldsymbol{w}(n)} = \sum_{m=0}^{L_s-1} \frac{\partial y_{ws}(n)}{\partial y_w(n-m)} \frac{\partial y_w(n-m)}{\partial \boldsymbol{w}(n)}, \tag{1.8}$$

where $\frac{\partial y_{ws}(n)}{\partial y_w(n-m)}$ is the I/O gradient of the secondary path. Using (1.5), $y_w(n-m)$ can be written as

$$y_w(n-m) = \boldsymbol{w}^T(n-m)\boldsymbol{x}_{w(n-m),x(n-m)}(n-m). \tag{1.9}$$

Assuming that $\boldsymbol{w}(n)$ is slowly varying, the term $\frac{\partial y_w(n-m)}{\partial \boldsymbol{w}(n)}$ in (1.8) can be written as

$$\frac{\partial y_w(n-m)}{\partial \boldsymbol{w}(n)} \approx \boldsymbol{x}_{w(n),x(n-m)}(n-m). \tag{1.10}$$

Define the signal

$$g(n,m) = \frac{\partial y_{ws}(n)}{\partial y_w(n-m)}. \tag{1.11}$$

Using (1.8), (1.10), and (1.11), and approximating the expectation with the instantaneous values, the weight update equation in (1.7) can be written as

$$\boldsymbol{w}(n+1) \approx \boldsymbol{w}(n) + \mu e(n) \sum_{m=0}^{L_s-1} g(n,m)\boldsymbol{x}_{w(n),x(n-m)}(n-m)). \tag{1.12}$$

This update equation was derived in [17]. In [18] the concept of virtual secondary path, $\tilde{\boldsymbol{s}}(n)$, is introduced and is given by

$$\begin{aligned} \tilde{\boldsymbol{s}}(n) &= [g(n,0), g(n,1), \cdots, g(n,L_s-1)]^T \\ &= \left[\frac{\partial y_{ws}(n)}{\partial y_w(n)}, \frac{\partial y_{ws}(n)}{\partial y_w(n-1)}, \cdots, \frac{\partial y_{ws}(n)}{\partial y_w(n-L_s+1)}\right]^T. \end{aligned} \tag{1.13}$$

Now if it is assumed that the secondary path $S(z)$ is known exactly, i.e., $\hat{S}(z) = S(z)$ and is linear then from (1.4) and (1.13) it can be concluded that

$$\tilde{\boldsymbol{s}}(n) = \hat{\boldsymbol{s}}(n) = \boldsymbol{s}(n) = [\hat{s}_0(n), \hat{s}_1(n), \cdots, \hat{s}_{L_s-1}(n)]^T = [s_0(n), s_1(n), \cdots, s_{L_s-1}(n)]^T. \tag{1.14}$$

Using (1.13) and (1.14) in (1.12), the FxLMS algorithm weight update equation for linear secondary path is given by

$$\boldsymbol{w}(n+1) \approx \boldsymbol{w}(n) + \mu e(n)[\boldsymbol{X}_{w(n),x(n)}(n)\hat{\boldsymbol{s}}(n)] = \boldsymbol{w}(n) + \mu e(n)\boldsymbol{x}_{\text{LMS},y_{\hat{s}}(n)}(n), \tag{1.15}$$

where $\boldsymbol{X}_{w(n),x(n)}(n) = \sum_{m=0}^{L_s-1} \hat{s}_m(n)\boldsymbol{x}_{w(n),x(n-m)}(n-m)$ is a matrix of dimension $L_w \times L_s$ with m^{th} column represented by $\boldsymbol{x}_{w(n),x(n-m)}(n-m) = [x(n-m), x(n-m-1), \cdots, x(n-m-L_w+1)]^T$ for $m = 0, 1, \cdots, L_s-1$, $\hat{\boldsymbol{s}}(n)$ is the impulse response coefficient vector of secondary path $\hat{S}(z)$ having coefficients $\hat{s}_m(n)$, and $\boldsymbol{x}_{\text{LMS},y_{\hat{s}}(n)}(n) = \boldsymbol{X}_{w(n),x(n)}(n)\hat{\boldsymbol{s}}(n) = [y_{\hat{s}}(n), y_{\hat{s}}(n-1), \cdots, y_{\hat{s}}(n-L_w+1)]^T$ is the input signal vector of adaptive LMS algorithm of $W(z)$ at time n and is referred as the filtered reference signal vector.

The FxLMS algorithm is the most popular adaptive algorithm for ANC system due to its simplicity of implementation and robustness. It is found in [15] that the ANC system will remain stable as long as the phase error between $S(z)$ and its estimate $\hat{S}(z)$ is within $\pm 90°$. The effect of the error, between $S(z)$ and its estimate $\hat{S}(z)$, on the stability of the FxLMS algorithm implemented in the time domain was also studied by Snyder and Hansen in [19]. They found that the phase error effect is not symmetric about the $0°$ phase error point and may cause the stability of the algorithm to increase for some values of error. They concluded that while a maximum phase error of $\pm 90°$ is a bound for stability, there is no simple relationship between error and stability within this region.

1.2.2 Modified FxLMS Algorithm

In the case of FxLMS algorithm the maximum value of the step-size μ for which the algorithm in (1.15) will be stable is given by [20]

$$\mu = \frac{2}{(L_w + \Delta)P_{y_{\hat{s}}}(n)}, \tag{1.16}$$

where L_w is the tap-weight length of controller $W(z)$, $P_{y_{\hat{s}}}(n) \approx E\{y^2_{\hat{s}}(n)\}$ is the power or mean-square value of the signal $y_{\hat{s}}(n)$, and Δ is the delay due to the presence of the secondary path. The value of delay Δ is equal to the tap-weight length of $S(z)$. Therefore the long filter length of $S(z)$ will result in a large value of Δ. From (1.16), it is clear that the large value of Δ will reduce the maximum allowable value of the step-size for which the algorithm will be stable, and hence will result in slow convergence of the adaptive filter $W(z)$. The solution to the problem is to use modified FxLMS (MFxLMS) algorithm [5]. The block diagram of MFxLMS algorithm for single channel feedforward ANC system is shown in Fig. 1.8. In the case of MFxLMS algorithm, two extra filters $W(z)$ and $\hat{S}(z)$ are used to generate the estimate $y_{\hat{s}w}(n)$ of the desired response $\hat{d}(n)$ for $W(z)$, and thus transforming the problem of indirect system identification to the problem of direct system identification. For MFxLMS algorithm, the allowable maximum value of the step-size is given by

$$\mu = \frac{2}{L_w P_{y_{\hat{s}}}(n)}. \tag{1.17}$$

From the comparison of (1.16) and (1.17), it is clear that the maximum allowable value of step-size for stable operation of ANC system is higher for MFxLMS algorithm compared to FxLMS algorithm, and thus can result in fast convergence of controller $W(z)$. The disadvantage of the MFxLMS algorithm is that the computational complexity is higher than the FxLMS algorithm. This is due to the use

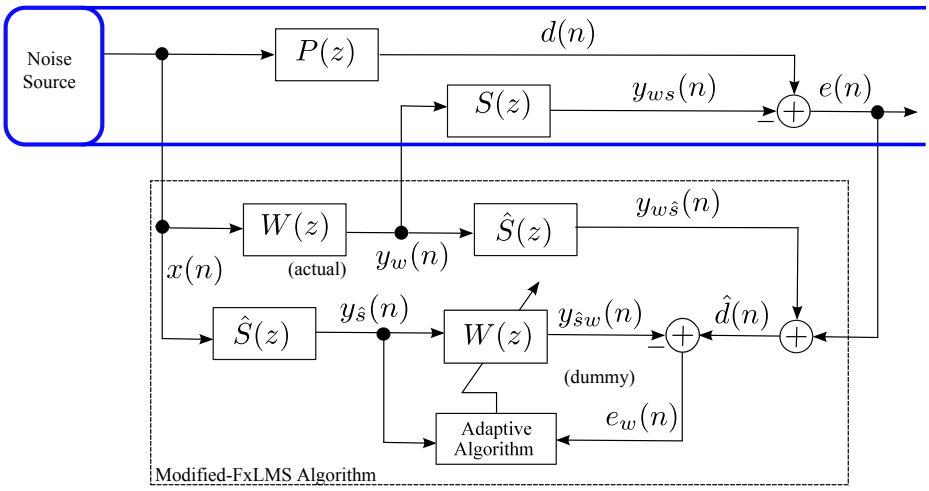

Figure 1.8: MFxLMS algorithm based single channel feedforward ANC system for duct.

of two extra filters in MFxLMS algorithm.

1.3 Secondary Path Modeling

For stable operation of FxLMS and MFxLMS adaptive algorithms, the estimate of the secondary path is required to filter the reference signal. If the secondary path $S(z)$ is assumed to be time-invariant, then the estimate can be obtained, prior to the operation of ANC system, using the offline modeling techniques. The detail of offline modeling techniques can be found in [4]. In actual practice, the secondary path is time-varying as it includes the acoustic path transfer function and the transfer functions of many electronic components whose characteristics may change with temperature, ageing etc. Therefore, in order to keep the phase error between $S(z)$ and $\hat{S}(z)$ to within $\pm 90^\circ$ bound, online modeling of $S(z)$ is required.

Direct secondary path modeling: The block diagram for direct online secondary path modeling (OSPM) [6] is shown in Fig. 1.9. The LMS algorithm based adaptive filter $\hat{S}(z)$ is connected in parallel with $S(z)$. The output of controller $W(z)$ is used as an excitation signal for the adaptive filter $\hat{S}(z)$. Based on the input excitation signal $y_w(n)$, and the error signal $e_{\hat{s}}(n)$, the coefficients of $\hat{S}(z)$ are updated in order to minimize the mean-square vale of the error signal $e_{\hat{s}}(n)$. The error signal $e_{\hat{s}}(n)$ can be written in the z domain as

$$E_{\hat{s}}(z) = -E(z) - \hat{S}(z)Y_w(z) = -[P(z)X(z) - S(z)Y_w(z)] - \hat{S}(z)Y_w(z). \quad (1.18)$$

Assuming that $\hat{S}(z)$ is of sufficient order, and $x(n)$ is a persistent excitation signal, the error signal $e_{\hat{s}}(n)$ will converge to zero. Therefore from (1.18) the steady-state solution $\hat{S}_o(z)$ is given by

$$\hat{S}_o(z) = S(z) - \frac{P(z)X(z)}{Y_w(z)} = S(z) - \frac{P(z)}{W(z)}. \quad (1.19)$$

It is clear from (1.19) that $\hat{S}_o(z) = S(z)$ only if $P(z) = 0$ (i.e. $d(n) = 0$), otherwise this technique will result in a biased solution. From Fig. 1.9 the optimal value of controller is $W_o(z) = P(z)S^{-1}(z)$, and hence from (1.19) it is clear that this optimal value of controller will result in the vale of $\hat{S}_o(z) = 0$ (undesirable solution). This shows that the estimation of $S(z)$ is affected by the adaptation of $W(z)$, which is undesirable.

Online secondary path modeling with additive white noise: The block diagram of Eriksson's method [21] for OSPM is shown in Fig. 1.10. Here an additional auxiliary noise $v(n)$ being modeled as white noise is injected for OSPM. The signal $v(n)$ is uncorrelated with the original unwanted noise $x(n)$. The use of white noise as an excitation signal for system identification is well known due to having flat power spectrum over entire frequency range. In Fig. 1.10, the

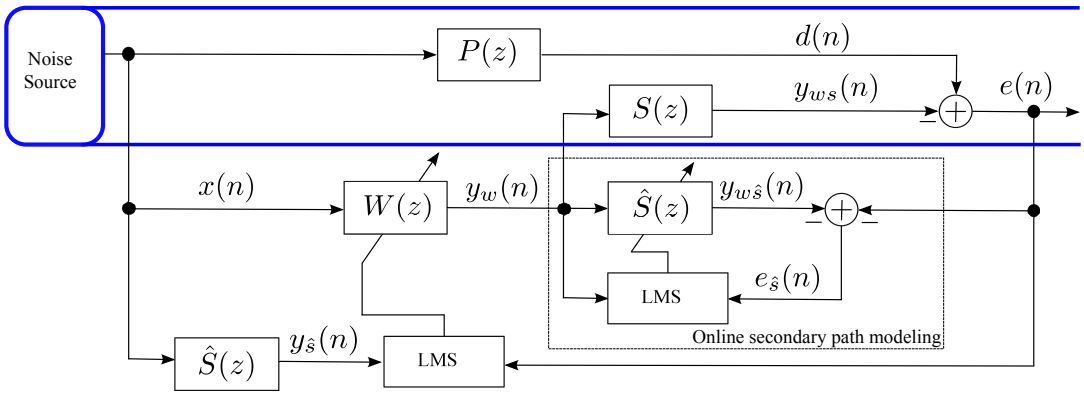

Figure 1.9: Online secondary path modeling [6].

signal $v(n)$ together with controller output $y_w(n)$ will derive the loudspeaker. The output of the loudspeaker will interfere destructively with the original noise at the summing junction. The remaining residual error picked-up by the error microphone is given by

$$e(n) = [d(n) - y_{ws}(n)] + v_s(n), \tag{1.20}$$

where $v_s(n) = s(n) * v(n)$ is the response of $S(z)$ corresponding to the auxiliary noise $v(n)$. In $e(n)$, the first term $[d(n) - y_{ws}(n)]$ is the desired error signal for adaptation of $W(z)$, and acts as an interference for adaptation of SPM filter $\hat{S}(z)$. The output of the SPM filter $v_{\hat{s}}(n)$ is computed as

$$v_{\hat{s}}(n) = \hat{s}(n) * v(n) = \hat{\boldsymbol{s}}^T(n)\boldsymbol{x}_{\hat{s}(n),v(n)}(n), \tag{1.21}$$

where $\hat{\boldsymbol{s}}(n) = [\hat{s}_0(n), \hat{s}_1(n), \cdots, \hat{s}_{L_s-1}(n)]^T$ is the impulse response coefficient vector of $\hat{S}(z)$ at time n, $\boldsymbol{x}_{\hat{s}(n),v(n)}(n) = [v(n), v(n-1), \cdots, v(n-L_s+1)]^T$ is the input signal vector of filter $\hat{S}(z)$ with input $v(n)$ at time n, $\hat{s}(n)$ is the impulse response of SPM filter $\hat{S}(z)$, and L_s is the tap-weight length of $\hat{S}(z)$. The output of $\hat{S}(z)$ is subtracted from $e(n)$ to compute $e_{\hat{s}}(n)$ as

$$e_{\hat{s}}(n) = e(n) - v_{\hat{s}}(n) = [d(n) - y_{ws}(n)] + [v_s(n) - v_{\hat{s}}(n)]. \tag{1.22}$$

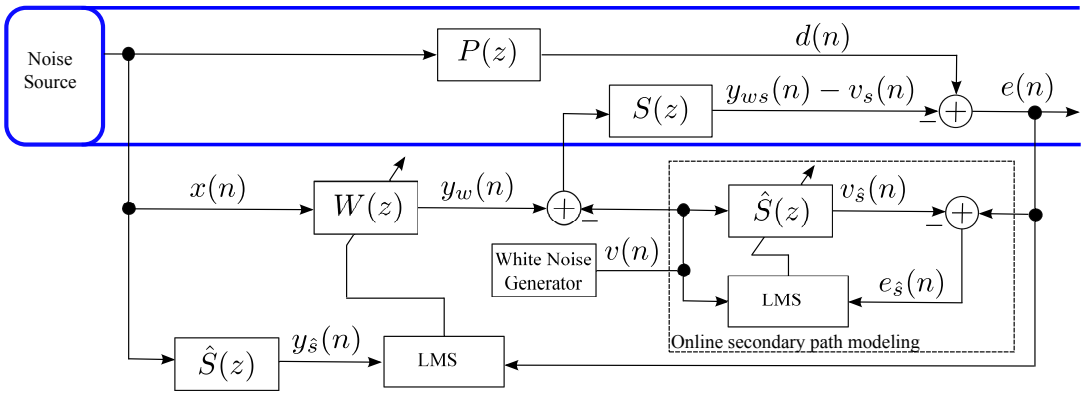

Figure 1.10: Block diagram of Eriksson's method for online secondary path modeling [21].

Using LMS algorithm, the SPM filter will update its weights based on the the error signal $e_{\hat{s}}(n)$ and input signal vector $\boldsymbol{x}_{\hat{s}(n),v(n)}(n)$ as

$$\hat{\boldsymbol{s}}(n+1) = \hat{\boldsymbol{s}}(n)+\mu[v_s(n)-v_{\hat{s}}(n)]\boldsymbol{x}_{\hat{s}(n),v(n)}(n)+\mu[d(n)-y_{ws}(n)]\boldsymbol{x}_{\hat{s}(n),v(n)}(n), \quad (1.23)$$

where μ is the step-size parameter. The last term $\mu[d(n) - y_{ws}(n)]\boldsymbol{x}_{\hat{s}(n),v(n)}(n)$ in the weight update equation of $\hat{S}(z)$ acts as an interference and thus will degrade the convergence of $\hat{S}(z)$.

1.4 Feedback Path Modeling and Neutralization

In ANC systems, the anti-noise signal generated by the loudspeaker will not only propagate downstream to cancel the original noise at the summing junction but also radiate upstream and corrupt the reference signal. This is the well known feedback effect in ANC system. For stable operation of ANC system it is required to neutralize this feedback effect using the feedback path neutralization (FBPN) filter.

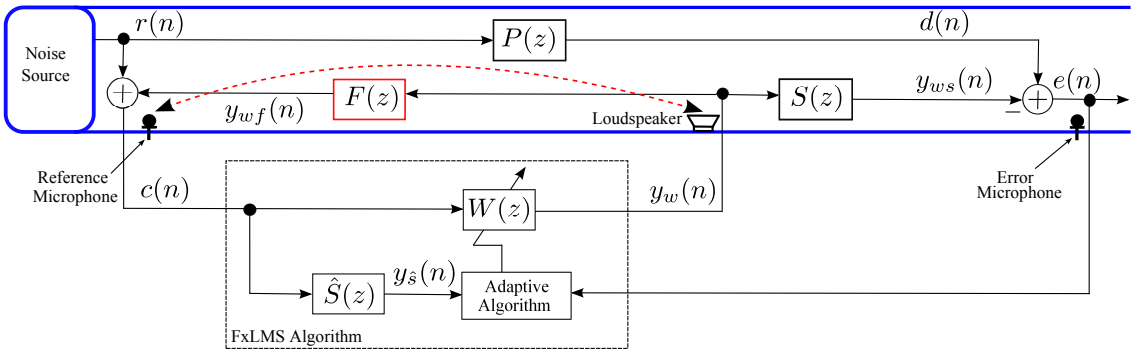

Figure 1.11: Block diagram of single channel feedforward ANC system with feedback coupling.

Need for feedback path neutralization: A block diagram of single channel feedforward ANC system with feedback coupling is shown in Fig. 1.11. Here $F(z)$ is the feedback path transfer function from the output of $W(z)$ to the reference microphone. It includes the transfer functions of digital to analog converter (DAC), smoothing filter, power amplifier, loudspeaker, acoustic path from the loudspeaker to the reference microphone, pre-amplifier, anti-aliasing filter, and ADC [4]. From Fig. 1.11, the reference signal (corrupted) $c(n)$ picked-up by the reference microphone is given by

$$c(n) = r(n) + y_{wf}(n) = r(n) + (f(n) * y_w(n)), \tag{1.24}$$

where $r(n)$ is the original noise at the reference microphone, $y_{wf}(n)$ is the feedback coupling signal and represents the response of the filter $F(z)$ corresponding to input $y_w(n)$. The objective of ANC system is to cancel the unwanted noise at the summing junction, i.e., to reduce the mean-square value of the error signal $e(n)$. In order to see the effect of feedback coupling on the error signal $e(n)$, consider the z-transform of the error signal which is given by the expression

$$E(z) = P(z)R(z) - S(z)\frac{W(z)R(z)}{1 - W(z)F(z)}. \tag{1.25}$$

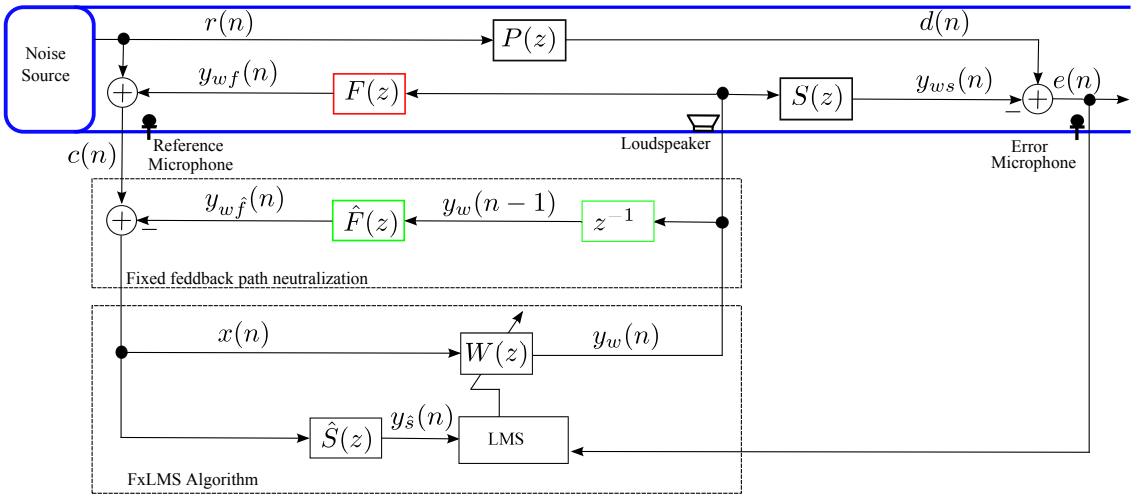

Figure 1.12: Block diagram of single channel feedforward ANC system with fixed feedback path neutralization.

It is clear from (1.25) that ANC system may become unstable if at some frequency $W(z)F(z) = 1$. It is therefore necessary to neutralize the effect of this feedback. This neutralization can be done either by using the offline modeling or online modeling of $F(z)$. The block diagram of single channel feedforward ANC system with fixed FBPN is shown in Fig. 1.12. The fixed FBPN filter $\hat{F}(z)$ can be obtained offline, i.e., prior to operation of ANC system. Here z^{-1} is the inherent delay associated with the feedback path $F(z)$. In order to neutralize the effect of $F(z)$ it is required that $\hat{F}(z)z^{-1} = F(z)$. The output $y_{w\hat{f}}$ of $\hat{F}(z)$ is subtracted from the reference microphone signal, $c(n)$, in order to generate the desired reference signal for $W(z)$ as

$$x(n) = c(n) - y_{w\hat{f}} = x(n) - (\hat{f}(n) * y_w(n-1)) = x(n) - (\hat{\boldsymbol{f}}^T(n))\boldsymbol{x}_{\hat{f}(n),y_w(n-1)}(n-1)), \tag{1.26}$$

where $\hat{f}(n)$ is the impulse response of $\hat{F}(z)$, $\hat{\boldsymbol{f}}(n) = [\hat{f}_0(n), \hat{f}_1(n), \cdots, \hat{f}_{L_f-1}(n)]^T$ is the impulse response coefficient vector of $\hat{F}(z)$ at time n, $\boldsymbol{x}_{\hat{f}(n),y_w(n-1)}(n-1) =$

$[y_w(n-1), y_w(n-2), \cdots, y_w(n-L_f)]^T$ is the input signal vector of filter $\hat{F}(z)$ with input $y_w(n-1)$ at time n, and L_f is the tap-weight length of $\hat{F}(z)$. The detail for the offline modeling of $F(z)$ can be found in [4]. The procedure of offline modeling works well if the acoustic paths are time invariant, however in actual practice, the acoustic paths are time-varying, and hence online modeling is needed to track variations in feedback path. In this thesis, our focus will be the online feedback path modeling and neutralization (FBPMN). One of the basic online methods, proposed by Warnaka [12], is shown in Fig. 1.13. The purpose of adaptive FBPMN filter $\hat{F}(z)$ is to cancel only the feedback part of the reference microphone signal $c(n)$ using $y_w(n)$ as the input excitation signal. However, as the signal $y_w(n)$ is highly correlated with the original unwanted noise $r(n)$, therefore the filter $\hat{F}(z)$ will adapt in such away as to incorrectly cancel the original primary noise as well along with the feedback signal. Thus this structure will not allow filter $W(z)$ to receive the signal $r(n)$ at its input. This is the major problem with this structure and hence more sophisticated techniques, in which an additional auxiliary noise being modeled as white noise is injected for system identification of unknown feedback path [4, 5], are used for online FBPMN.

1.5 NLMS Adaptive Algorithm and Optimal Excitation Signal

NLMS adaptive algorithm: It is shown in [22] that for LMS adaptive algorithm in Fig. 1.2, the convergence of the mean-square-error (MSE) is guaranteed if the step-size is selected within the bounds given by

$$0 < \mu < \frac{2}{3L_w P_x(n)} \tag{1.27}$$

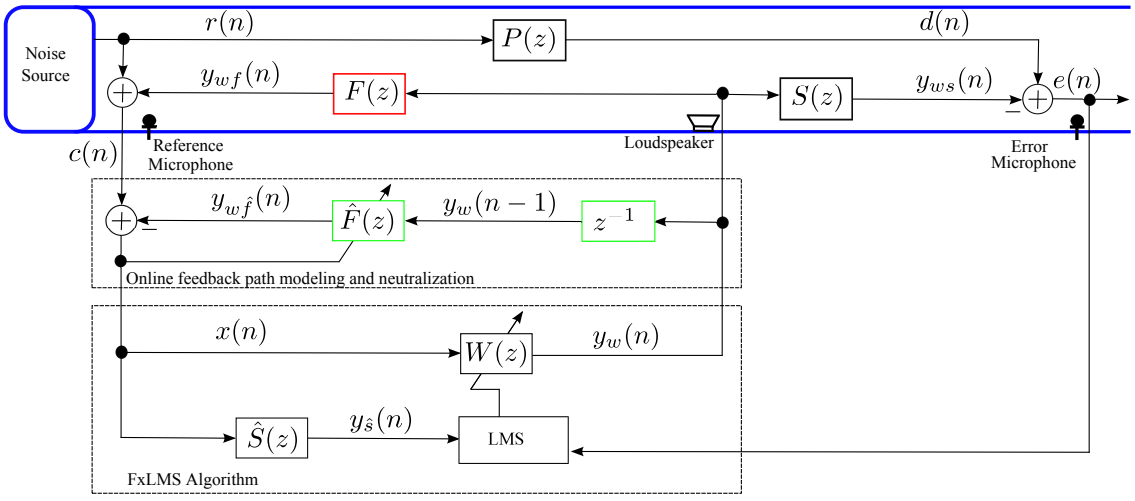

Figure 1.13: Block diagram of single channel feedforward ANC system with online feedback path modeling and neutralization.

where $P_x(n)$ is the power of input excitation signal of an adaptive algorithm. It is clear from (1.27) that in the case of LMS adaptive algorithm, the prior knowledge of the input signal power is required for the selection of step-size within the stability bounds. If the power of the input signal is time-varying, then the selection of a constant (fixed) step-size may drive the algorithm unstable. The solution to the problem is to use normalized LMS (NLMS) algorithm [6]. The popularity of NLMS algorithm is due to its simplicity and automatic adjustment of initially selected step-size corresponding to varying input signal power. Considering Fig. 1.2 the weight update equation for NLMS algorithm is given by

$$\hat{\boldsymbol{w}}(n+1) = \hat{\boldsymbol{w}}(n) + \mu \frac{e(n)\boldsymbol{x}_{\hat{w}(n),x(n)}(n)}{\boldsymbol{x}^T_{\hat{w}(n),x(n)}(n)\boldsymbol{x}_{\hat{w}(n),x(n)}(n)}, \tag{1.28}$$

where $\hat{\boldsymbol{w}}(n) = [\hat{w}_0(n), \hat{w}_1(n), \cdots, \hat{w}_{L_w-1}(n)]^T$ is the impulse response coefficient vector of $\hat{W}(z)$ at time n, and $\boldsymbol{x}_{\hat{w}(n),x(n)}(n) = [x(n), x(n-1), \cdots, x(n-L_w+1)]^T$ is the input signal vector of filter $\hat{W}(z)$ with input $x(n)$ at time n. If the weight error vector is defined as $\boldsymbol{e}_w(n) = \boldsymbol{w} - \hat{\boldsymbol{w}}(n)$, where $\boldsymbol{w} = [w_0, w_1, \cdots, w_{L_w-1}]^T$ is

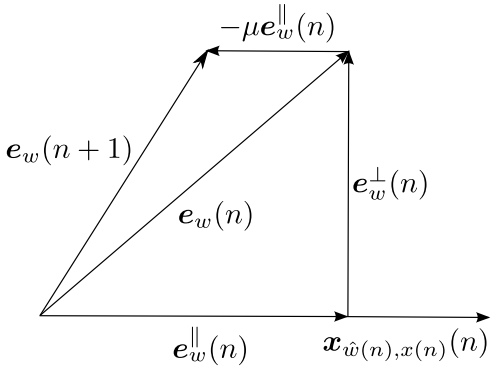

Figure 1.14: Geometrical interpretation of (1.30).

the impulse response coefficient vector of unknown system $W(z)$, then using (1.28), $\boldsymbol{e}_w(n+1)$ can be written as

$$\boldsymbol{e}_w(n+1) = \boldsymbol{e}_w(n) - \mu \frac{e(n)\boldsymbol{x}_{\hat{w}(n),x(n)}(n)}{\boldsymbol{x}^T_{\hat{w}(n),x(n)}(n)\boldsymbol{x}_{\hat{w}(n),x(n)}(n)} = \boldsymbol{e}_w(n) - \mu \frac{e(n)\boldsymbol{x}_{\hat{w}(n),x(n)}(n)}{||\boldsymbol{x}_{\hat{w}(n),x(n)}(n)||^2}. \tag{1.29}$$

From Fig. 1.2, with $v(n) = 0$, the update equation for $\boldsymbol{e}_w(n)$ can be written as

$$\boldsymbol{e}_w(n+1) = \boldsymbol{e}_w(n) - \mu \frac{(\boldsymbol{w} - \hat{\boldsymbol{w}}(n))^T \boldsymbol{x}_{\hat{w}(n),x(n)}(n)}{||\boldsymbol{x}_{\hat{w}(n),x(n)}(n)||} \frac{\boldsymbol{x}_{\hat{w}(n),x(n)}(n)}{||\boldsymbol{x}_{\hat{w}(n),x(n)}(n)||} = \boldsymbol{e}_w(n) - \mu \boldsymbol{e}_w^{\parallel}(n), \tag{1.30}$$

where $\frac{\boldsymbol{x}_{\hat{w}(n),x(n)}(n)}{||\boldsymbol{x}_{\hat{w}(n),x(n)}(n)||}$ is a unit vector, and $\boldsymbol{e}_w^{\parallel}(n)$ is the component of vector $\boldsymbol{e}_w(n)$ parallel to input vector $\boldsymbol{x}_{\hat{w}(n),x(n)}(n)$. The geometrical interpretation of (1.30) is shown in Fig. 1.14. It is clear from Fig. 1.14 that the $\boldsymbol{e}_w^{\parallel}(n)$ component of $\boldsymbol{e}_w(n)$ can contribute to its desirable reduction for

$$0 < \mu < 2, \tag{1.31}$$

where the range of step-size μ in (1.31) is the stability criterion for NLMS algorithm. The convergence of NLMS algorithm degrades for correlated input signal having large eigenvalue ratio [8]. Therefore, for better convergence of NLMS algorithm the selection of the optimal input excitation signal is very important.

Optimal excitation signal: From the theory of signal processing, it is known that the cross-correlation $R_{xy}(n)$ between input $x(n)$ and output $y(n)$ of a linear filter is equal to the convolution of the autocorrelation of input $R_{xx}(n)$ with system impulse response $w(n)$, and is computed as

$$R_{xy}(n) = R_{xx}(n) * w(n). \tag{1.32}$$

For input excitation signal with impulse like autocorrelation function, i.e., $R_{xx}(n) = \delta(n)$, the cross-correlation is the measure of the impulse response of system. Therefore it is required that the input excitation signal must have the ideal impulse like autocorrelation function. The selection of the excitation signal for adaptive filter depends upon specific applications. When the designer is provided with a choice for the selection of input excitation signal, one choice could be the random white noise due to having wide range of frequency components and flat power spectrum over the entire frequency range. However, it is shown in [23]-[29] that the optimal excitation signal that shows high energy efficiency and improves the convergence of NLMS algorithm is a deterministic *Perfect-Periodic-Sequences* (PPSEQ) having period equal to the tap-weight length of adaptive filter and shows desired autocorrelation properties given by

$$R_{xx}(i) = \sum_{n=0}^{L_w-1} x(n)x(n+i) = \begin{cases} E_x & (\text{if} \quad i = 0 \pmod{L_w}) \\ 0 & (\text{Otherwise}) \end{cases}, \tag{1.33}$$

where E_x is the energy of one period of the signal. Furthermore, in [30] it is shown that in the practical set-ups, due to the presence of nonlinearities, the property of high energy efficiency associated with PPSEQ can not be achieved. Therefore a new class of excitation signals referred as *perfect-sweeps* are introduced in [31]. The perfect-sweep signal is a time-stretched pulse [32] having the desired properties of

PPSEQ along with high immunity against distortions. For perfect-sweep signal, the general construction formula is given

$$P(k) = \begin{cases} \exp\left(\frac{-j4m\pi k^2}{L_w^2}\right) & (0 \leq k \leq \frac{L_w}{2}) \\ \overline{P}(L_w - k) & (\frac{L_w}{2} < k < L_w) \end{cases}, \tag{1.34}$$

where k is the frequency index, L_w is the length of one period of signal, m determines the stretch of the time-stretched pulse, and $\overline{P}(k)$ represents the complex conjugate of $P(k)$. The signal in the time domain is obtained by taking the inverse transform of $P(k)$.

The geometric interpretation of NLMS algorithm in Fig. 1.14 shows that for $\mu = 1$ the parallel component $\boldsymbol{e}_w^{\parallel}(n)$ can be completely eliminated. Similarly all the L_w components of $\boldsymbol{e}_w(n)$ can be compensated if the L_w consecutive input vectors to an adaptive filter $\hat{W}(z)$ are orthogonal. In the case of random white noise input excitation signal $x(n)$, the L_w consecutive input vectors of infinite length, denoted by $\boldsymbol{x}'_{\hat{w}(n),x(n)}(n), \boldsymbol{x}'_{\hat{w}(n),x(n-1)}(n-1), \cdots, \boldsymbol{x}'_{\hat{w}(n),x(n-L_w+1)}(n-L_w+1)$, are orthogonal in the infinite vector space. The vectors of length L_w, denoted by $\boldsymbol{x}_{\hat{w}(n),x(n)}(n), \boldsymbol{x}_{\hat{w}(n),x(n-1)}(n-1), \cdots, \boldsymbol{x}_{\hat{w}(n),x(n-L_w+1)}(n-L_w+1)$, represents, respectively, the projection of vectors denoted by $\boldsymbol{x}'_{\hat{w}(n),x(n)}(n), \boldsymbol{x}'_{\hat{w}(n),x(n-1)}(n-1), \cdots, \boldsymbol{x}'_{\hat{w}(n),x(n-L_w+1)}(n-L_w+1)$ onto the L_w dimensional vector space. For the projected vectors in the L_w dimensional space the orthogonality is not guaranteed, therefore it can be concluded that the random white noise is not an optimal excitation signal [26]. For the PPSEQ, it is clear from the autocorrelation property given in (1.33) that the L_w consecutive vectors are orthogonal and thus represents the optimal excitation signal. As stated earlier, in practical set-ups the presence of nonlinear distortion can limit the performance of PPSEQ. Therefore, in this case the perfect-sweep excitation signal, having all the desired properties of PPSEQ

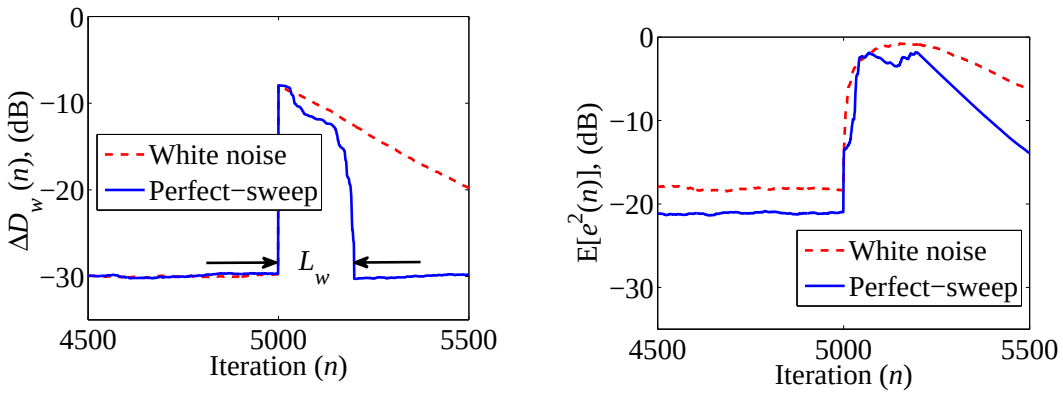

Figure 1.15: Simulation results for Case 1 (SNR=30 dB): (a) Relative modeling error, $\Delta D_w(n)$(dB), (b) Mean-square-error, MSE (dB).

and shows improved performance with nonlinear distortion, can be the best choice for system identification [33]. The simulation results of NLMS algorithm based system identification for Case 1: with SNR=∞ dB, i.e., $v(n) = 0$, and Case 2: with SNR=30 dB, are shown, respectively, in Fig. 1.15 and Fig. 1.16. The performance comparison is carried out on the basis of following performance measures.

- Relative modeling error $\Delta D_w(n)$ in dB, being defined as

$$\Delta D_w(n) = 10\log_{10}\frac{||\boldsymbol{w}(n) - \hat{\boldsymbol{w}}(n)||^2}{||\boldsymbol{w}(n)||^2} \quad \text{dB}. \tag{1.35}$$

- MSE $E[e^2(n)]$ in dB.

For the simulation results, the data for the unknown system is selected from [4], the length of unknown system and adaptive filters is selected as $L_w = 200$. The acoustic paths are perturbed in the middle of simulation, and all the results are averaged over 10 independent realizations. The rest of the simulation parameters are the

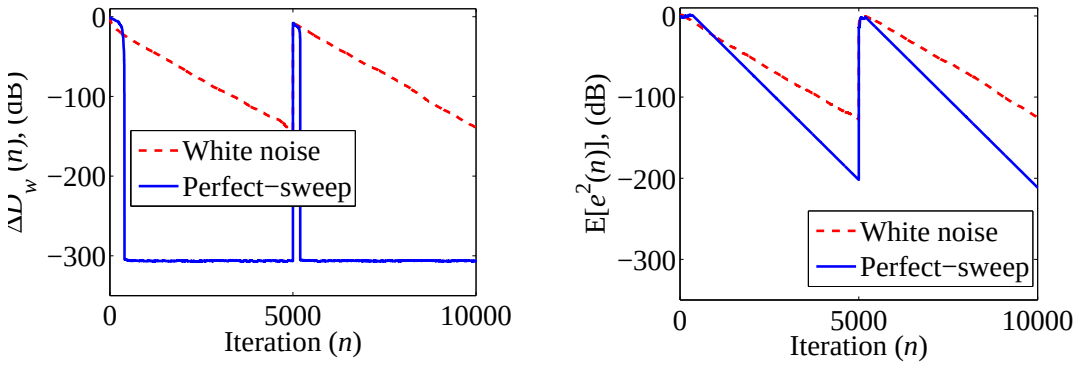

Figure 1.16: Simulation results for Case 2 (SNR=∞ dB i.e $v(n) = 0$): (a) Relative modeling error, $\Delta D_w(n)$(dB), (b) Mean-square-error, MSE (dB).

same as in [33]. It is clear from Fig.1.15(a) and Fig. 1.16(a) that with perfect-sweep input excitation signal the system can be identified in L_w iterations, while the convergence of the system with white noise input is slow and requires more than L_w iterations. The curves for the MSE in Case 1 and Case 2, respectively, are shown in Fig.1.15(b) and Fig. 1.16(b). From these curves it is clear that identification with perfect-sweep excitation signal results in lower steady-state MSE.

1.6 Need of Gain Scheduling of Auxiliary Noise

For stable operation of ANC systems, the estimates (identification) of the unknown secondary path and the feedback path are required [4]. In order to obtain these estimates, an additional auxiliary noise is required to be injected into the ANC system [21]. On one hand, the injection of auxiliary noise into the ANC system is useful to get the required estimates of secondary and feedback path, but on the other hand, the injection of auxiliary noise contributes to the residual error (which

we want to minimize) and will degrade the noise-reduction-performance (NRP) of ANC system. The solution, for improving the NRP, is to use gain scheduling strategy to vary the variance of auxiliary noise. At the start (when ANC system is far from steady-state), it is required that the gain scheduling strategy must allow the auxiliary noise to have large variance to obtain the better estimates of the unknown secondary and feedback paths. At the steady-state, it is required that the gain scheduling strategy must reduce the variance of auxiliary noise to a small value to improve the NRP of ANC system.

From [33], it can be concluded that the perfect sweep signal can be the optimal auxiliary input excitation signal for system identification purpose. However, in ANC literature [4, 5] the most common choice of auxiliary input excitation signal for system identification is the WGN. In this thesis the WGN will be used as an auxiliary noise signal for OSPM and online FBPMN.

1.7 Summary

In this introductory chapter, the underlying physical principle used for acoustic noise cancellation is explained. In order to show the importance of this idea, some practical examples where this idea can be employed are given, and the brief overview of the most popular application of ANC system for acoustic duct is provided.

The idea of direct and indirect system identification is discussed, and the derivation of the most popular adaptive FxLMS algorithm for ANC systems is described. The idea of MFxLMS algorithm to convert the problem of indirect system identification in ANC system to a problem of direct system identification is explained.

The two fundamental issues in ANC systems, i.e., OSPM and online FBPMN

are discussed. A brief overview of some basic techniques used for OSPM and online FBPMN is given, while the detail will be given in the coming chapters.

The role of the input excitation signal for NLMS algorithm based identification of an unknown system is explained, and it is found that perfect-sweep excitation signal is the optimal choice. Finally the need of gain scheduling of auxiliary noise has been discussed.

In the following chapter 2 and chapter 3 the focus is on OSPM. In chapter 2, the existing methods for OSPM without gain scheduling (auxiliary noise with fixed variance is used in all operating conditions) will be discussed. In chapter 3, the existing methods of OSPM using gain scheduling of auxiliary noise are explained. In addition to this, new strategies for gain scheduling of auxiliary noise are proposed. In existing methods, the gain is varied based on the power of residual error signal which carries information only about the convergence status of ANC system. In the proposed methods the gain is varied based on the power of error signal of SPM filter. This is more desirable way of controlling the gain because the power of error signal of SPM filter carries information about the convergence status of both the ANC system and SPM filter. The simulations are carried out to show that the proposed gain scheduling strategies improve both the modeling accuracy of SPM filter and the NRP of overall ANC systems.

In chapter 4, the issue of online FBPMN with and without gain scheduling of auxiliary noise is explained. In the first part of this chapter, the existing methods for online FBPMN without gain scheduling are discussed. A new structure is proposed that combines the good features of the existing structures to better neutralize the effect of the feedback coupling and to improve the convergence of ANC system. In the second part of this chapter, a gain scheduling strategy is

proposed, for online FBPMN, to improve the NRP of ANC system. In addition to this, a self-tuned ANP scheduling strategy with matching step-size for FBPMN filter is also proposed that requires no tuning parameters and further improves the NRP of ANC systems.

In chapter 5, the concluding remarks and the future research directions are given.

Chapter 2

Online Secondary Path Modeling Without Gain Scheduling

With the invention of high speed digital hardware and the development of adaptive signal processing algorithms, the field of active noise control (ANC) has found a great attention of the researchers since the last three decades. The basic crux of ANC system is the principle of superposition in which the acoustic waves of the original unwanted noise interfere destructively with the acoustic waves generated by the combination of ANC filter followed by the secondary path. In order for the ANC systems to converge properly, it is necessary to compensate for the effects of the secondary path. For some applications the secondary path can be estimated offline, i.e., prior to the operation of an ANC system. However, for most of the practical applications the secondary path is time-varying and therefore on-

line secondary path modeling (OSPM) is required, i.e., when ANC system is in operation.

OSPM with higher modeling accuracy and faster convergence is desirable in ANC systems to ensure large stability margins. There are two different approaches for OSPM in ANC systems. The first approach models the secondary path using the output of ANC filter $W(z)$ as an input excitation signal of secondary path modeling (SPM) filter. The second approach involves injection of additional random noise into the output of $W(z)$, and utilizes a system identification method to model the secondary path. The additional noise injected is uncorrelated with the original unwanted noise. The comparison of the two approaches for OSPM can be found in [34], where it is concluded that the second approach is superior to the first one when compared in terms of convergence rate, and speed of response to changes in original unwanted noise. In this chapter, the use of second approach is considered for OSPM, however additional noise with fixed variance is injected, i.e., no gain scheduling is used.

In the first part of this chapter, various existing methods using filtered-x-LMS (FxLMS) adaptive algorithm for ANC filter $W(z)$, are briefly explained for OSPM.

In the second part of this chapter, a method using modified-filtered-x-LMS (MFxLMS) adaptive algorithm [5] for ANC filter $W(z)$, is explained for OSPM. In this second part, a new computationally efficient MFxLMS (CEMFxLMS) algorithm is proposed. The proposed structure is simple than the original structure using MFxLMS algorithm for OSPM. The performance of the MFxLMS algorithm based ANC system with OSPM is compared with the proposed CEMFxLMS algorithm through computer simulations. We will see that the performance of the proposed CEMFxLMS algorithm is same as obtained with the original MFxLMS al-

gorithm. However, CEMFxLMS algorithm has lower computational requirements compared to MFxLMS algorithm.

2.1 FxLMS Algorithm Based ANC Systems

For OSPM without gain scheduling an additional white Gaussian noise (WGN), here after called as auxiliary noise, with fixed variance is injected in all operating conditions. In this section a brief overview of Eriksson's method [21], Kuo's method [35], Bao's method [36], Zhang's method [37], and Akhtar's method [38] is given. This section also describes a variable step-size (VSS) method [39] for OSPM without gain scheduling. In all these methods FxLMS algorithm is used for ANC filter $W(z)$, and auxiliary noise with fixed variance is injected for SPM filter. The performance of all previously mentioned methods are compared through the simulation results, and it is found that the VSS approach in [39] outperforms in terms of improving the modeling accuracy of SPM filter compared to other existing methods.

2.1.1 Eriksson's Method

The block diagram of Eriksson's structure [21] for OSPM is shown in Fig. 2.1. Here $G(n) = 1$ shows that no gain scheduling is used, and auxiliary noise with fixed variance is injected in all operating conditions. From Fig. 2.1, the error signal is given by

$$e(n) = [d(n) - y_{ws}(n)] + v_s(n). \tag{2.1}$$

In Eriksson's method, the signal $e(n)$ acts both as an error signal for $W(z)$ and as a desired response of SPM filter. The following are the problems associated with the Eriksson's structure.

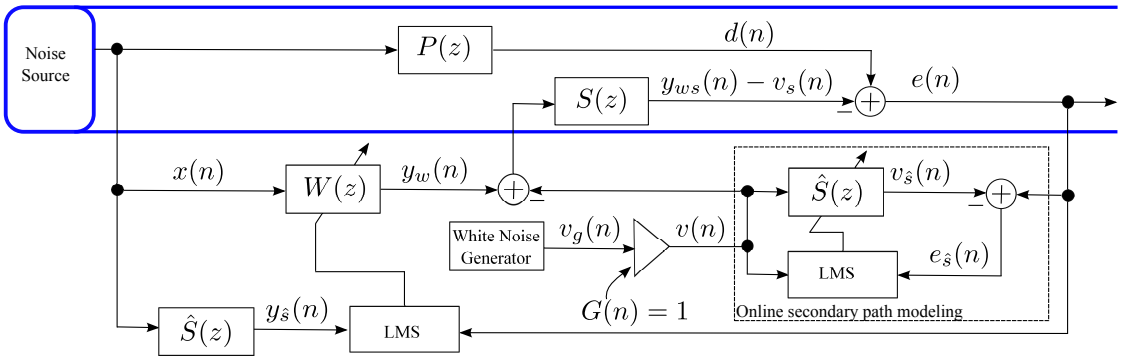

Figure 2.1: Block diagram of Eriksson's method for ANC systems with online secondary path modeling [21].

- In $e(n)$, the first term in square brackets acts as an interference for SPM filter, and thus may affect the convergence of SPM filter.
- The last term $v_s(n)$ in $e(n)$ acts as an interference for ANC filter $W(z)$, thus affects its convergence.

2.1.2 Kuo's Method

The block diagram of Kuo's structure [35] for OSPM is shown in Fig. 2.2. In addition to ANC filter $W(z)$ and SPM filter $\hat{S}(z)$, a third adaptive filter $K(z)$ (termed as the prediction error filter) is used to remove the interference from the desired response of the $\hat{S}(z)$. Here, the error signal $e_k(n)$ of adaptive filter $K(z)$ acts as a desired response of SPM filter and is computed as

$$e_k(n) = e(n) - y_k(n), \tag{2.2}$$

where $y_k(n)$ is the output of prediction error filter $K(z)$, and is computed as

$$y_k(n) = k(n) * e(n - \Delta) = \boldsymbol{k}^T(n)\boldsymbol{x}_{k(n),e(n-\Delta)}(n - \Delta), \tag{2.3}$$

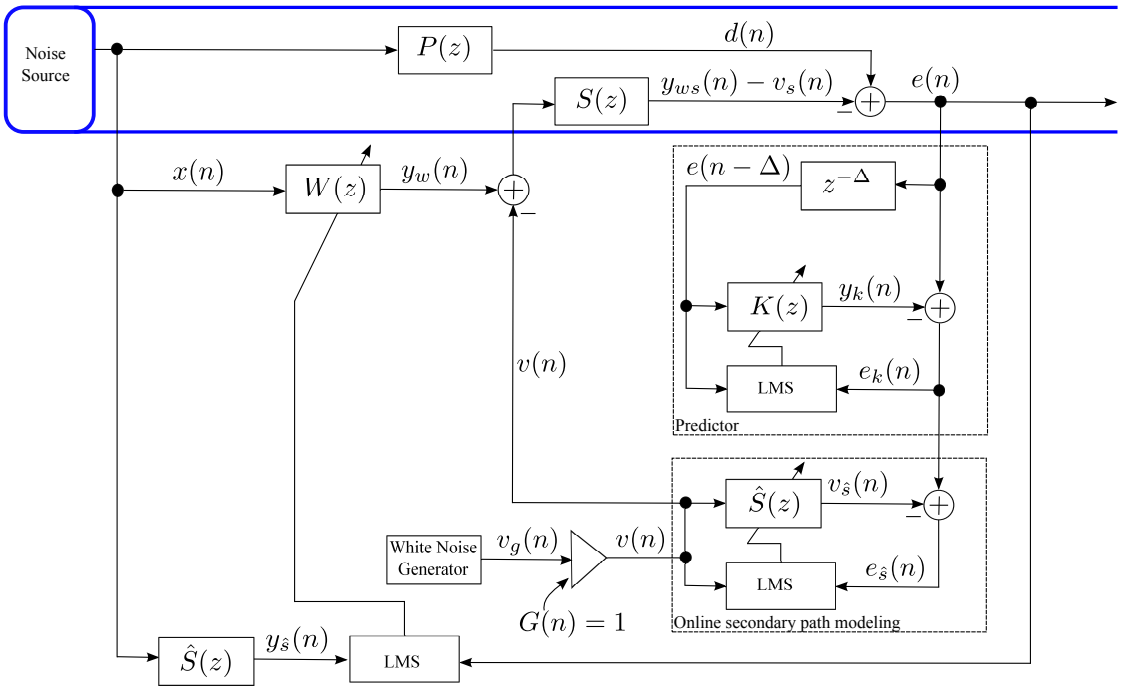

Figure 2.2: Block diagram of Kuo's method for ANC systems with online secondary path modeling [35].

where $k(n)$ is the impulse response of $K(z)$, Δ is the delay, $e(n-\Delta)$ is the delayed version of $e(n)$, $\boldsymbol{k}(n) = [k_0(n), k_1(n), \cdots, k_{L_k-1}(n)]^T$ is the impulse response coefficient vector of $K(z)$ at time n, and $\boldsymbol{x}_{k(n),e(n-\Delta)}(n-\Delta) = [e(n-\Delta), e(n-\Delta-1), \cdots, e(n-\Delta-L_k+1)]^T$ is the input signal vector of filter $K(z)$ with input $e(n-\Delta)$ at time n.

From the theory of adaptive filtering, it is known that the adaptive filter output converges to that part of its desired response which is correlated with the input excitation signal. It is shown in [35], for $\Delta \geq L_s$ the term $v_s(n-\Delta)$ in $e(n-\Delta)$ becomes uncorrelated with the term $v_s(n)$ in $e(n)$. As a result, at the steady-state, $y_k(n) \rightarrow [d(n) - y_{ws(n)}]$, and $e_k(n) \rightarrow v_s(n)$. Thus the Kuo's structure is capable of removing the interference term $[d(n) - y_{ws(n)}]$ from the desired response, $e_k(n)$,

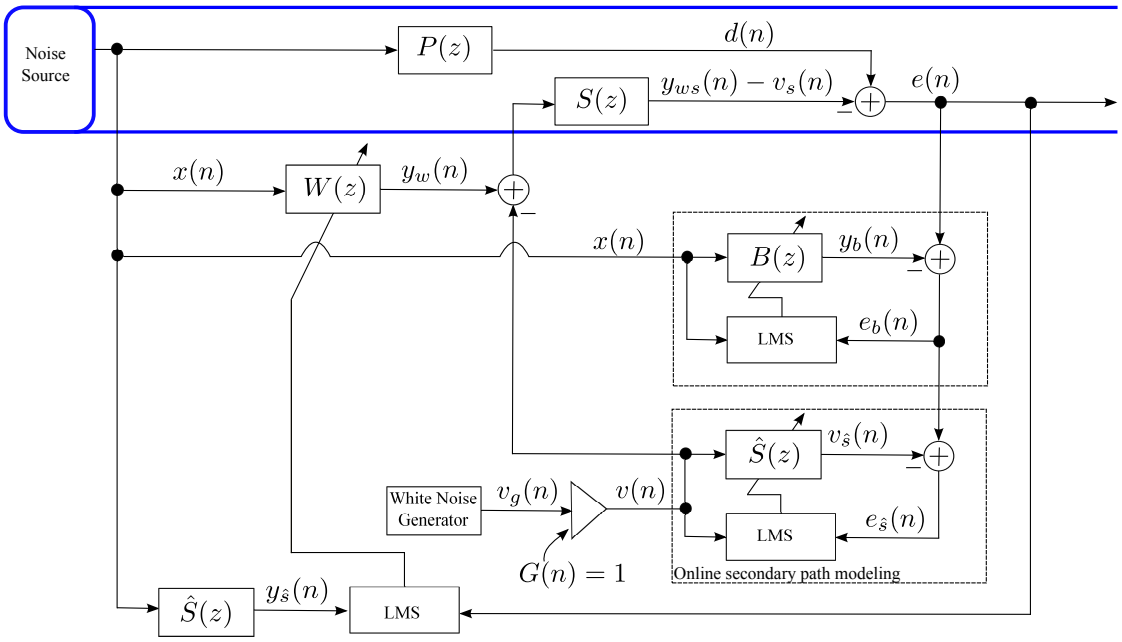

Figure 2.3: Block diagram of Bao's method for ANC systems with online secondary path modeling [36].

of SPM filter. The problem with Kuo's structure are as follows

- We need to know the length of the secondary path, L_s, in order to select the proper value of the decorrelation delay Δ.
- The prediction error filter will work properly only if the original unwanted noise is predictable such as narrow-band noise.
- The term $v_s(n)$ in $e(n)$ (see (2.1)) acts as an interference for ANC filter $W(z)$, and for prediction error filter $K(z)$, thus affects the convergence of overall ANC system.

2.1.3 Bao's Method

The block diagram of Bao's structure [36] for OSPM is shown in Fig. 2.3. An additional adaptive filter, represented by $B(z)$, is used to remove the interference term $[d(n)-y_{ws(n)}]$ from the desired response, $e_b(n)$, of SPM filter, where the signal $e_b(n)$ is computed as

$$e_b(n) = e(n) - y_b(n), \tag{2.4}$$

where $y_b(n)$ is the output of adaptive filter $B(z)$ corresponding to input $x(n)$, and is computed as

$$y_b(n) = b(n) * x(n) = \boldsymbol{b}^T(n)\boldsymbol{x}_{b(n),x(n)}(n), \tag{2.5}$$

where $b(n)$ is the impulse response of $B(z)$, $x(n)$ is the original unwanted noise picked-up by the reference microphone, $\boldsymbol{b}(n) = [b_0(n), b_1(n), \cdots, b_{L_b-1}(n)]^T$ is the impulse response coefficient vector of $B(z)$ at time n, and $\boldsymbol{x}_{b(n),x(n)}(n) = [x(n), x(n-1), \cdots, x(n-L_b+1)]^T$ is the input signal vector of filter $B(z)$ with input $x(n)$ at time n. When ANC system converges, $y_b(n) \to [d(n) - y_{ws(n)}]$, and hence the desired response of SPM filter $e_b(n) \to v_s(n)$. Thus the filter $B(z)$ is capable of removing the interference $[d(n) - y_{ws(n)}]$ from the desired response of SPM filter. Unlike Kuo's method, the Bao's method works well both for narrow-band and broad-band original unwanted noise. The problem with Bao's method are as follows

- The term $v_s(n)$ in $e(n)$ (see (2.1)) acts as an interference for ANC filter $W(z)$, and for filter $B(z)$, thus affects the convergence of overall ANC system.

2.1.4 Zhang's Method

The block diagram of Zhang's structure [37] for OSPM is shown in Fig. 2.4. In this method, three cross updated adaptive filters are used to reduce the perturbation effect of the original unwanted noise on SPM filter. The method not only removes the interference $[d(n) - y_{ws(n)}]$ from the desired response, $d_{\hat{s}}(n)$, of SPM filter but also reduces the perturbation effect of injected random noise $v_s(n)$ on convergence of adaptive filters $H(z)$, and $W(z)$. The signal $d_h(n)$ acts both as a desired response of $H(z)$ and as an error signal of ANC filter $W(z)$, and the interference term $v_s(n)$ is removed from the signal $d_h(n)$ by subtracting the output of SPM filter from $e(n)$, i.e., $d_h(n) = e(n) - v_{\hat{s}}(n)$. In this method, as the ANC system converges all the error signals of adaptive filters will converge towards zero. This is because as ANC system converges $[d(n) - y_{ws(n)}] \rightarrow 0$, $y_h(n) \rightarrow [d(n) - y_{ws(n)}]$, $d_h(n) \rightarrow [d(n) - y_{ws(n)}]$, $e_h(n) \rightarrow 0$, $d_{\hat{s}}(n) \rightarrow v_s(n)$, and $e_{\hat{s}}(n) \rightarrow 0$. This shows that in Zhang's method a perturbation free error signals for all the three adaptive filters are obtained.

In Kuo's, Bao's and Zhang's structures, three adaptive filters are used for OSPM. In [38], and [40, 41] a two adaptive filter based structure (almost similar to Eriksson's structure) is proposed by Akhtar. In [40, 41] adaptive filtering with averaging based FxLMS algorithm is used for $W(z)$, and improved performance, in terms of modeling accuracy of SPM filter and the noise-reduction-performance (NRP) of ANC system, is realized compared to previous methods. However, the improved performance is attained with higher computational complexity compared to previous methods. In [38] a new VSS adaptive algorithm is proposed by Akhtar for SPM filter. The brief detail of the method in [38] is given below.

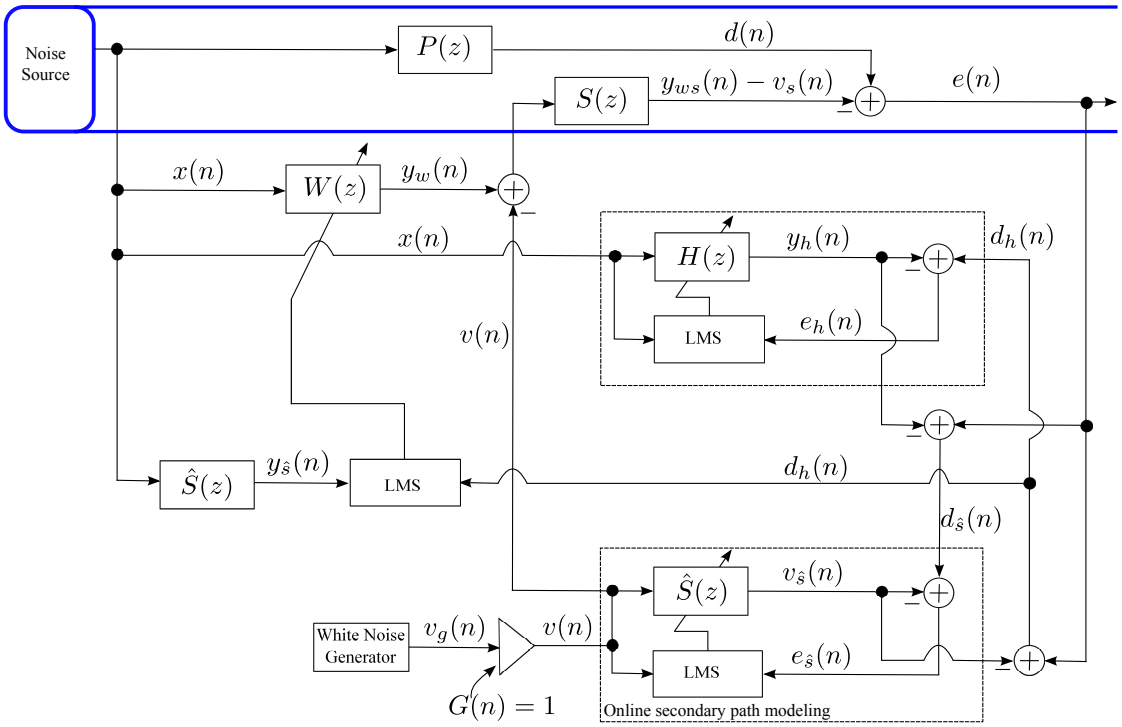

Figure 2.4: Block diagram of Zhang's method for ANC systems with online secondary path modeling [37].

2.1.5 Akhtar's Method

The block diagram of Akhtar's structure [38] for OSPM is shown in Fig. 2.5. The main features of Akhtar's method are: 1) Similar to Eriksson structure, only two adaptive filters are used to remove the effects of interference terms on the convergence performance of adaptive filters in ANC systems, however, as opposed to Eriksson's structure same error signal, $e_{\hat{s}}(n)$, is used to update the coefficients of both the SPM filter and the ANC filter, and 2) a VSS is used for SPM filter. In Akhtar's method the variable step-size for SPM filter, $\mu_s(n)$, is computed as

$$\mu_s(n) = \rho(n)\mu_{\min} + (1 - \rho(n))\mu_{\max}, \tag{2.6}$$

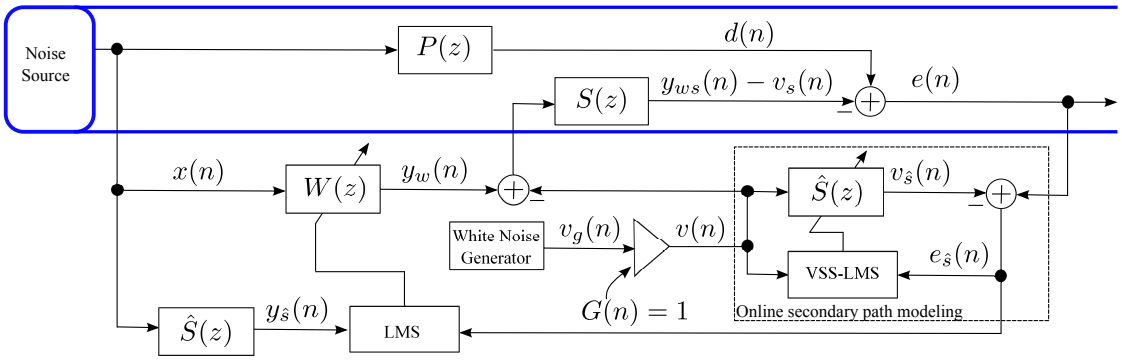

Figure 2.5: Block diagram of Akhtar's method for ANC systems with online secondary path modeling [38].

where the tuning parameters $\mu_{\min}$ and $\mu_{\max}$ are, respectively, the minimum and the maximum values of $\mu_s(n)$, and $\rho(n)$ is a parameter being computed as

$$\rho(n) = \frac{P_{e_{\hat{s}}}(n)}{P_e(n)} = \frac{P_{[d(n)-y_{ws}(n)]} + P_{[v_s(n)-v_{\hat{s}}(n)]}}{P_{[d(n)-y_{ws}(n)]} + P_{v_s(n)}}, \tag{2.7}$$

where $P_{e_{\hat{s}}}(n)$ and $P_e(n)$ are estimates of power of error signals $e_{\hat{s}}(n)$ and $e(n)$, respectively and are given by

$$P_{e_{\hat{s}}}(n) = \lambda P_{e_{\hat{s}}}(n-1) + (1-\lambda)e^2_{\hat{s}}(n)), \tag{2.8}$$

$$P_e(n) = \lambda P_e(n-1) + (1-\lambda)e^2(n)), \tag{2.9}$$

where λ is a forgetting factor $(0.9 < \lambda < 1)$. It is clear from (2.7) that $\rho(0) \approx 1$ and as $n \to \infty$, $P_{[d(n)-y_{ws}(n)]} \to 0$, $P_{[v_s(n)-v_{\hat{s}}(n)]} \to 0$, $P_{v_s(n)} >> P_{[d(n)-y_{ws}(n)]}$ and $\rho(n) \to 0$. The basic idea of the Akhtar's VSS algorithm stems from the fact that the disturbance signal in the desired response of the modeling filter is decreasing in nature (ideally converging to zero). Hence, initially when the power of the disturbance signal is large a small step-size is used for SPM filter, and later at the

steady-state when the power of the disturbance signal is reduced to a small value, large value of step-size is selected for SPM filter.

The problem with Akhtar's method is that the step-size variation of SPM filter is such that it is minimum at the start-up of ANC system and increases to a maximum value as the ANC system converges. For LMS-based adaptive SPM filter with input $v(n)$, the excess mean-square-error (MSE) is given by [4]

$$\xi_{\text{excess}} \approx 0.5\mu_s L_s P_v \xi_{\min}, \tag{2.10}$$

where μ_s is the fixed step-size parameter, P_v is the power of input signal of $\hat{S}(z)$, and $\xi_{\min}$ is the minimum MSE corresponding to Weiner solution. It is very easy to conclude from (2.10) that in Akhtar's method the large value of step-size in the steady-state will result in large excess MSE, and thus affects the convergence of SPM filter. In order to over come this difficulty a new VSS adaptive algorithm is given for SPM filter in [39], the detail of which is given below

2.1.6 Variable Step-size Method

The structure of the VSS method [39] is exactly the same as that of Akhtar's method shown in Fig. 2.5. Assuming that $W(z)$ is an FIR filter, the output $y_w(n)$ is given as

$$y_w(n) = w(n) * x(n) = \boldsymbol{w}^T(n)\boldsymbol{x}_{w(n),x(n)}(n), \tag{2.11}$$

where $w(n)$ is the impulse response of $W(z)$, $\boldsymbol{w}(n) = [w_0(n), w_1(n), \cdots, w_{L_w-1}(n)]^T$ is the impulse response coefficient vector of $W(z)$ at time n, and $\boldsymbol{x}_{w(n),x(n)}(n) = [x(n), x(n-1), \cdots, x(n-L_w+1)]^T$ is the input signal vector of filter $W(z)$ with input $x(n)$ at time n. The weight update equation for ANC filter $W(z)$ is given as

$$\boldsymbol{w}(n+1) = \boldsymbol{w}(n) + \mu_w e_{\hat{s}}(n)\boldsymbol{x}_{\text{LMS},y_{\hat{s}}(n)}(n), \tag{2.12}$$

where μ_w is the step-size parameter, $e_{\hat{s}}(n)$ is the error signal of both the SPM filter and ANC filter, and $\boldsymbol{x}_{\text{LMS},y_{\hat{s}}(n)}(n) = [y_{\hat{s}}(n), y_{\hat{s}}(n-1), \cdots, y_{\hat{s}}(n-L_w+1)]^T$ is the input signal vector of adaptive LMS algorithm of $W(z)$ at time n and is referred as the filtered reference signal vector. The reference signal $x(n)$ filtered through $\hat{S}(z)$ is computed as

$$y_{\hat{s}}(n) = \hat{s}(n) * x(n) = \hat{\boldsymbol{s}}^T(n)\boldsymbol{x}_{\hat{s}(n),x(n)}(n), \tag{2.13}$$

where $\hat{s}(n)$ is the impulse response of $\hat{S}(z)$, $\hat{\boldsymbol{s}}(n) = [\hat{s}_0(n), \hat{s}_1(n), \cdots, \hat{s}_{L_s-1}(n)]^T$ is the impulse response coefficient vector of $\hat{S}(z)$ at time n, and $\boldsymbol{x}_{\hat{s}(n),x(n)}(n) = [x(n), x(n-1), \cdots, x(n-L_s+1)]^T$ is the input signal vector of filter $\hat{S}(z)$ with input $x(n)$ at time n. The residual error signal $e(n)$ picked-up by the error microphone is given by (2.1). The output of SPM filter is subtracted from $e(n)$ to compute $e_{\hat{s}}(n)$ as

$$e_{\hat{s}}(n) = e(n) - v_{\hat{s}}(n), \tag{2.14}$$

where the signal $v_{\hat{s}}(n)$ is computed as

$$v_{\hat{s}}(n) = \hat{s}(n) * v(n) = \hat{\boldsymbol{s}}^T(n)\boldsymbol{x}_{\hat{s}(n),v(n)}(n), \tag{2.15}$$

where $\hat{s}(n)$ is the impulse response of $\hat{S}(z)$, $\hat{\boldsymbol{s}}(n) = [\hat{s}_0(n), \hat{s}_1(n), \cdots, \hat{s}_{L_s-1}(n)]^T$ is the impulse response coefficient vector of $\hat{S}(z)$ at time n, and $\boldsymbol{x}_{\hat{s}(n),v(n)}(n) = [v(n), v(n-1), \cdots, v(n-L_s+1)]^T$ is the input signal vector of filter $\hat{S}(z)$ with input $v(n)$ at time n. Using $e_{\hat{s}}(n)$, the SPM filter $\hat{S}(z)$ is adapted as

$$\hat{\boldsymbol{s}}(n+1) = \hat{\boldsymbol{s}}(n) + \mu_s(n)e_{\hat{s}}(n)\boldsymbol{x}_{\hat{s}(n),v(n)}(n), \tag{2.16}$$

where $\mu_s(n)$ is the VSS step-size parameter, and is computed as

$$\mu_s(n) = (1 - \rho(n))\mu(n), \tag{2.17}$$

where $\rho(n)$ is given by (2.7) for Akhtar's method, and $\mu(n)$ is another variable step-size [42] being computed as

$$\mu(n) = \begin{cases} \mu_{\min} & (\beta(n) < \mu_{\min}) \\ \beta(n) & (\mu_{\min} \leq \beta(n) \leq \mu_{\max}) \\ \mu_{\max} & (\beta(n) > \mu_{\max}) \end{cases}, \tag{2.18}$$

where $\mu_{\min}$ and $\mu_{\max}$ are, respectively, the minimum and the maximum values of $\mu(n)$, chosen to guarantee tracking capability and stability, and $\beta(n)$ is recursively computed as

$$\beta(n) = \alpha\beta(n-1) + (1-\alpha)e_{\hat{s}}^2(n), \tag{2.19}$$

where α is a control parameter. The step-size $\mu(n)$ in (2.17) is bounded by $\mu_{\min}$ and $\mu_{\max}$, and in between this limit the step-size $\mu(n)$ is proportional to $e_{\hat{s}}^2(n)$ (see (2.18) and 2.19). It is shown in [42], when adaptive filter $\hat{S}(z)$ is far from $S(z)$, the large value of $e_{\hat{s}}(n)$ will cause the step-size $\mu(n)$ to increase to provide faster convergence while a small value of $e_{\hat{s}}(n)$, when adaptive filter $\hat{S}(z)$ is close to $S(z)$, will result in a decrease in the step-size $\mu(n)$ to yield small excess MSE.

- **purpose of factor $(1-\rho(n))$ in (2.17)**

Using (2.1) and (2.15), the instantaneous value of the error signal $e_{\hat{s}}(n)$ of SPM filter can be written as

$$e_{\hat{s}}(n) = (d(n) - y_{ws}(n)) - v_{\hat{s}}(n). \tag{2.20}$$

In VSS method [39], if $\mu_s(n) = \mu(n)$, then at the start when ANC system is far from steady state, the large value of the disturbance term $(d(n) - y_{ws}(n))$ in $e_{\hat{s}}(n)$ causes the value of step-size $\mu_s(n)$ to be large, and thus may cause the ANC system to become unstable. In order to avoid this the factor $(1-\rho(n))$ (which is close to

zero when ANC system is far from steady state) is multiplied with $\mu(n)$ to keep the overall step-size $\mu_s(n)$ small. This will result in small value of step-size $\mu_s(n)$ at the start as in Akhtar's method. However, in Akhtar's method large value of the step-size, $\mu_s(n)$, at the steady state will not allow the weights of the modeling filter to converge to their optimum value (see (2.10)). In order to avoid this problem, it is required that the step-size should be small in the steady state. In VSS method [39], at steady-state, the factor $(1-\rho(n)) \rightarrow 1$ and $\mu_s(n) \approx \mu(n)$. It is clear from (2.18) that $\mu(n)$ has a decreasing trend and hence the overall step-size $\mu_s(n)$ will also have a decreasing trend and will settle down to a small value at the steady-state. Therefore, in VSS method [39] (see (2.17)) the step-size variation is such that $\mu_s(n)$ has small value both at the start as in Akhtar's method and at the steady state as in [42]. The algorithm for the VSS method [39] is shown in Table. 2.1.

2.1.7 Simulation Results

In this subsection, simulation results are presented, for FxLMS algorithm based ANC systems with OSPM, to compare the performance of the VSS method [39] with Eriksson's method [21], Kuo's method [35], Bao's method [36], Zhang's method [37], and Akhtar's method [38]. The performance comparison is carried out on the basis of following performance measures.

- Relative modeling error of the secondary path $S(z)$ being defined as

$$\Delta D_s(n) = 10\log_{10}\frac{||\boldsymbol{s}-\hat{\boldsymbol{s}}(n)||^2}{||\boldsymbol{s}||^2} \quad \text{dB}. \tag{2.21}$$

- Mean-noise-reduction (MNR) at the error microphone being defined as

$$\text{MNR}(n) = 10\log_{10}\frac{E[e^2(n)]}{E[d^2(n)]} \quad \text{dB}. \tag{2.22}$$

Table 2.1: Algorithm for the VSS method [39].

$d(n) = \boldsymbol{p}^T(n)\boldsymbol{x}_{p(n),x(n)}(n);\ y_w(n) = \boldsymbol{w}^T(n)\boldsymbol{x}_{w(n),x(n)}(n)$
$v(n) = G(n)v_g(n)$
$y_{ws}(n) - v_s(n) = \boldsymbol{s}^T(n)\boldsymbol{x}_{s(n),(y_w(n)-v(n))}(n)$
$e(n) = d(n) - y_{ws}(n) + v_s(n)$
$v_{\hat{s}}(n) = \hat{\boldsymbol{s}}^T(n)\boldsymbol{x}_{\hat{s}(n),v(n)}(n);\ e_{\hat{s}}(n) = e(n) - v_{\hat{s}}(n)$
$y_{\hat{s}}(n) = \hat{\boldsymbol{s}}^T(n)\boldsymbol{x}_{\hat{s}(n),x(n)}(n)$
$P_{e_{\hat{s}}}(n) = \lambda P_{e_{\hat{s}}}(n-1) + (1-\lambda)e^2_{\hat{s}}(n))$
$P_e(n) = \lambda P_e(n-1) + (1-\lambda)e^2(n))$
$\rho(n) = \frac{P_{e_{\hat{s}}}(n)}{P_e(n)}$
$\beta(n) = \alpha\beta(n-1) + (1-\alpha)e^2_{\hat{s}}(n)$
$\mu(n)$ is computed using (2.18)
$\mu_s(n) = (1-\rho(n))\mu(n)$
$\hat{\boldsymbol{s}}(n+1) = \hat{\boldsymbol{s}}(n) + \mu_s(n)e_{\hat{s}}(n)\boldsymbol{x}_{\hat{s}(n),v(n)}(n)$
$\boldsymbol{w}(n+1) = \boldsymbol{w}(n) + \mu_w e_{\hat{s}}(n)\boldsymbol{x}_{\mathrm{LMS},y_{\hat{s}}(n)}(n)$

Using data from [4], the acoustic paths $P(z)$, and $S(z)$ are modeled as FIR filters of tap-weight lengths 48, 16, respectively. The adaptive filters $W(z)$, $\hat{S}(z)$, $K(z)$, $B(z)$ and $Z(z)$ are selected as FIR filters of tap-weight length 32, 16, 16, 16, and 16, respectively. The ANC filter $W(z)$, the filter $K(z)$, the filter $B(z)$ and the filter $H(z)$ are initialized by null vectors. In all methods, -5dB offline modeling is used for $\hat{S}(z)$. The original unwanted noise signal $x(n)$, at the reference microphone, is a multi-tonal input with frequencies 100, 200, 300, and 400 Hz, and

Table 2.2: Simulation parameters for filtered-x-LMS algorithm based active noise control systems: Online secondary path modeling without gain scheduling.

	Parameters
Eriksson's method [21]	$\mu_w = 5 \times 10^{-4}$, $\mu_s(n) = \mu_s = 1 \times 10^{-2}$.
Kuo's method [35]	$\mu_w = 5 \times 10^{-4}$, $\mu_s(n) = \mu_s = 1 \times 10^{-2}$, $\mu_k = 1 \times 10^{-2}$, $\Delta = 16$.
Bao's method [36]	$\mu_w = 5 \times 10^{-4}$, $\mu_s(n) = \mu_s = 1 \times 10^{-2}$, $\mu_b = 1 \times 10^{-2}$.
Zhang's method [37]	$\mu_w = 5 \times 10^{-4}$, $\mu_s(n) = \mu_s = 1 \times 10^{-2}$, $\mu_h = 1 \times 10^{-2}$.
Akhtar's method [38]	$\mu_w = 5 \times 10^{-4}$, $\mu_{s_{\min}} = 7.5 \times 10^{-3}$, $\mu_{s_{\max}} = 2.5 \times 10^{-2}$, $P_e(0) = P_{e_{\hat{s}}}(0) = 1$.
VSS method [39]	$\mu_w = 5 \times 10^{-4}$, $\mu_{s_{\min}} = 7.5 \times 10^{-3}$, $\mu_{s_{\max}} = 5 \times 10^{-2}$, $P_e(0) = P_{e_{\hat{s}}}(0) = \beta(0) = 1$, $\alpha = 0.999$.

its variance is adjusted to 1. A zero-mean WGN with variance 0.001 is added with $x(n)$ to account for any measurement noise. The modeling excitation signal $v_g(n)$ is a zero-mean WGN with variance 0.05. As no gain scheduling is used, therefore in all the methods $G(n) = 1$ and $v_g(n) = v(n)$. The sampling frequency is 2kHz, and the forgetting factor is selected as 0.99. The step-size parameters are experimentally adjusted for fast and stable convergence for various methods. The step-sizes and other simulation parameters for various methods are given in Table. 2.2. The jumps in the middle of all the simulation results is due to the perturbation in the impulse responses of the acoustic paths $P(z)$ and $S(z)$. The impulse responses of $P(z)$ and $S(z)$ are perturbed from their nominal values by

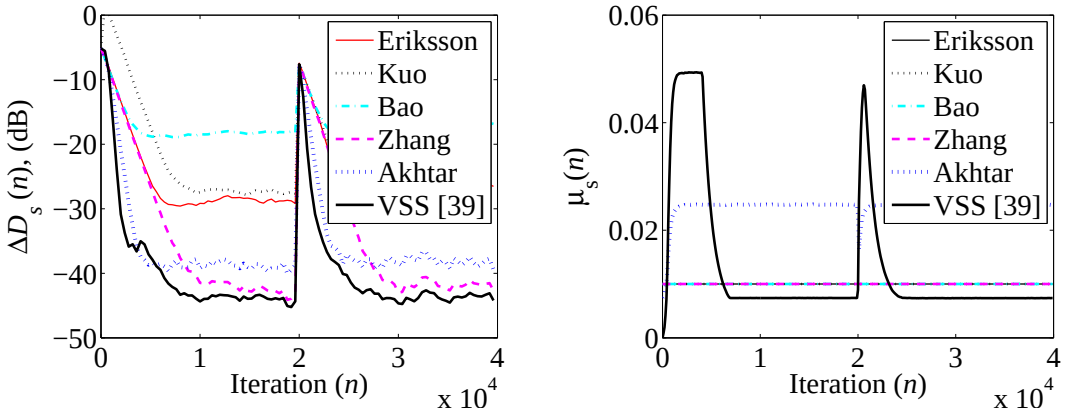

(a) (b)

Figure 2.6: (a) Relative modeling error, $\Delta D_s(n)$(dB), (b) Step-size variation for secondary path modeling filter, $\mu_s(n)$.

adding random WGN. All the simulation results are averaged over 10 independent realizations.

In Fig. 2.6(a) the curves for relative modeling error, as defined in (2.21), are plotted in dB for different methods. It is clear from Fig. 2.6(a) that the VSS method not only gives fast initial convergence as in Akhtar's method but it also gives much lower steady state value of $\Delta D_s(n)$ in comparison with other existing methods. As mentioned before, the reason of getting the improved modeling accuracy of SPM filter is due to different step-size variation for $\hat{S}(z)$ as plotted in Fig. 2.6(b). In the VSS method a smaller step-size is used at the start because of larger disturbance and then step-size is increased accordingly to allow fast convergence of SPM filter. Finally, at the steady-state, the step-size in the VSS method is brought back to minimum value to allow the excess MSE to a small value. This will lead to faster convergence at the start as in Akhtar's method and also provides better performance in steady state. The step-size for modeling filter in case of Akhtar's

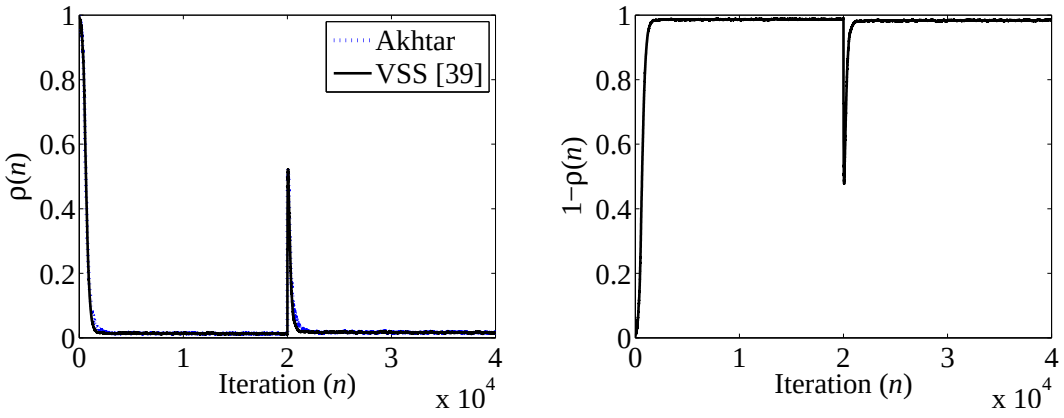

Figure 2.7: (a) Variation of $\rho(n) = P_{e_{\hat{s}}}/P_e(n)$, (b) Variation of $(1 - \rho(n))$ in VSS method (see (2.17)).

method is small at the start but it remains high in the steady state as shown in Fig. 2.6(b). The variation of $\rho(n)$ in Akhtar and VSS methods are plotted in Fig. 2.7(a). It is clear from Fig. 2.7(a), that $\rho(n)$ is close to one when ANC system is far from steady-state and $\rho(n) \to 0$ as ANC system converges. The two factors, $(1 - \rho(n))$ and $\mu(n)$, of $\mu_s(n)$ in VSS method [39] are plotted in Fig. 2.7(b) and Fig. 2.8(a), respectively. It is clear from Fig. 2.8(a) that the value of $\mu(n)$ is large when ANC system is far from steady-state and decreases towards $\mu_{\min}$ as ANC system converges. The overall step-size of SPM filter, $\mu_s(n)$, is the product of factor $(1 - \rho(n))$ and $\mu(n)$. In Fig. 2.8(b) the curves for MNR, as defined in (2.22), are plotted in dB for different methods. It is clear from Fig. 2.8(b) that the performance of all the methods is almost the same in terms of MNR value. From this we can conclude that when the estimation of the secondary-path reaches to certain level of accuracy (-15dB in this case), further improvement of modeling accuracy does not necessarily contribute to the further reduction of MNR value in

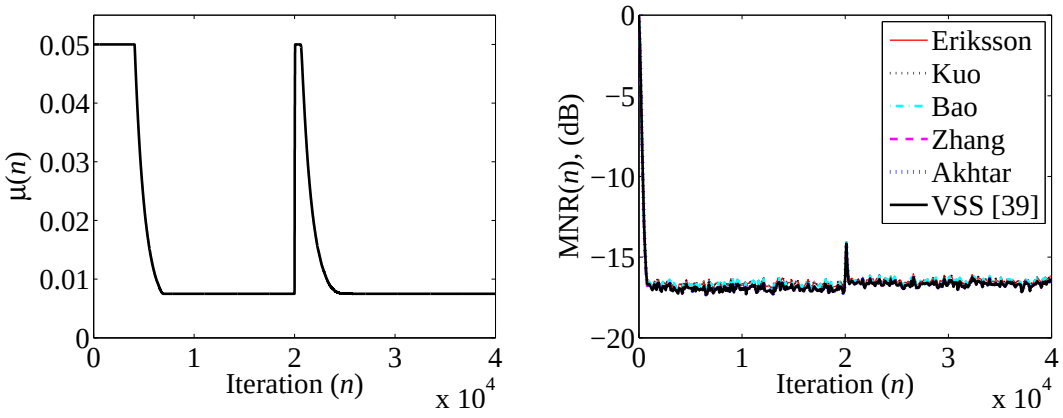

(a) (b)

Figure 2.8: (a) Variation of $\mu(n)$ in VSS method (see (2.17)), (b) Mean-noise-reduction, MNR(n) (dB).

a significant way. All the methods discussed in this paper can achieve the desired modeling accuracy of -15 dB, so the performance of all the methods in terms of MNR value is almost same. However, the advantage of having the improved modeling accuracy of SPM filter is that this will increase the stability margins of ANC systems.

2.2 MFxLMS Algorithm Based ANC Systems

2.2.1 MFxLMS Algorithm

The block diagram of MFxLMS algorithm based single channel feedforward ANC system is shown in Fig. 2.9. In case of MFxLMS algorithm two extra filters $W(z)$ and $\hat{S}(z)$ are used to generate the estimate $y_{\hat{s}w}(n)$ of the estimated desired response $\hat{d}(n)$ (estimate of $d(n)$) of $W(z)$, and thus transforming the problem of indirect system identification in ANC system to the problem of direct system

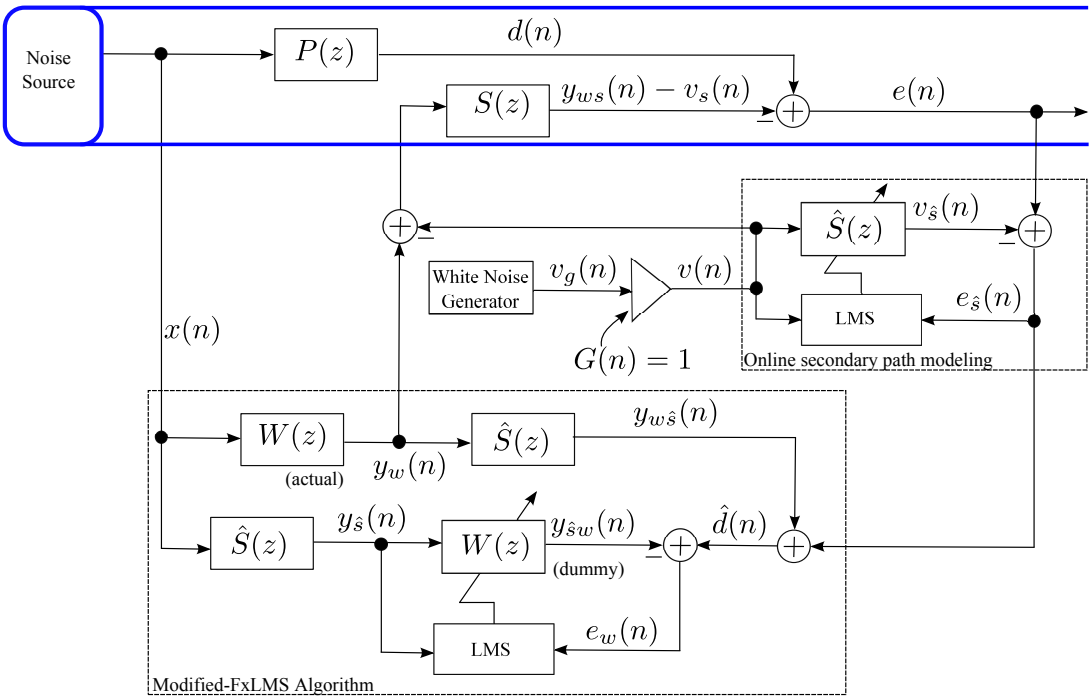

Figure 2.9: Modified-filtered-x-LMS algorithm based ANC system with online secondary path modeling.

identification. For MFxLMS algorithm the allowable maximum value of step-size, for stable operation of ANC system, is higher than FxLMS algorithm [5], and thus can results in fast convergence of ANC filter $W(z)$. The disadvantage of the MFxLMS algorithm is that the computational complexity is higher than the FxLMS algorithm. This is due to the use of two extra filters in MFxLMS algorithm.

In [43], a simplified structure for MFxLMS algorithm based ANC systems is proposed, hereafter referred as CEMFxLMS algorithm. In [43] the variance of auxiliary noise is also made variable. However, in this chapter since we are dealing with OSPM without gain scheduling. Therefore, in this chapter, we will assume $G(n) = 1$ for CEMFxLMS algorithm.

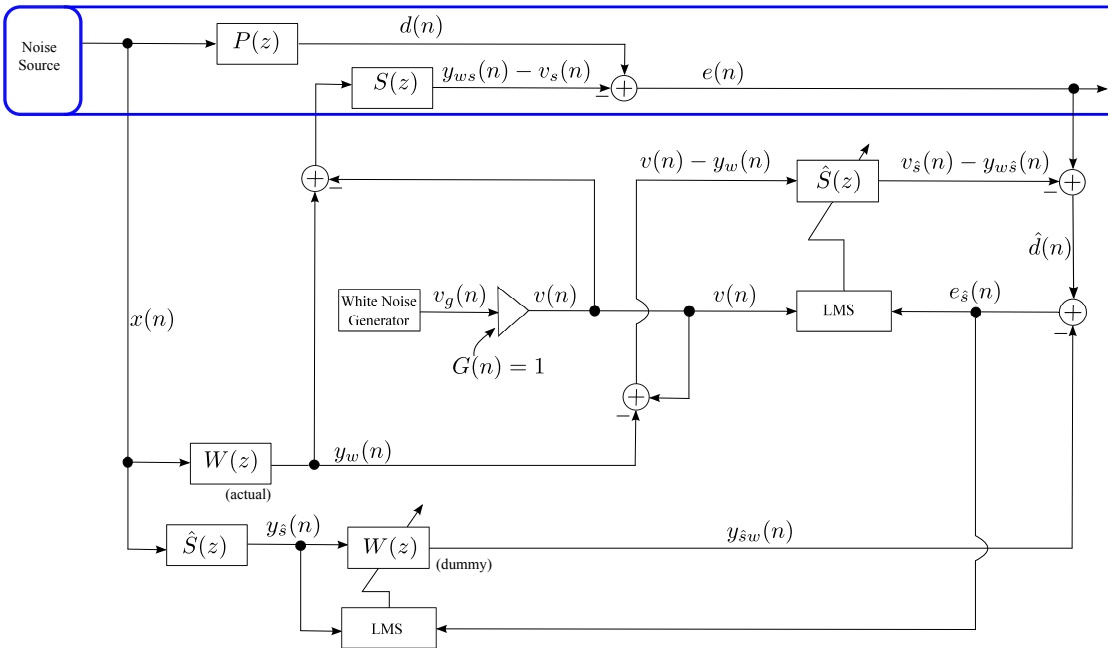

Figure 2.10: Proposed structure: Computationally efficient modified-filtered-x-LMS algorithm based ANC system with online secondary path modeling.

2.2.2 CEMFxLMS Algorithm

The block diagram of CEMFxLMS algorithm based ANC system with OSPM is shown in Fig. 2.10. From comparison of Fig. 2.7, and Fig. 2.8, it is clear that the CEMFxLMS algorithm based ANC system is structurally simpler than the MFxLMS algorithm based ANC system. This is because the action of filter $\hat{S}(z)$ with input $y_w(n)$ (see Fig. 2.7) and filter $\hat{S}(z)$ with input $v(n)$ (see Fig. 2.7) is combined into one filter $\hat{S}(z)$ with input $(v(n) - y_w(n))$ (see Fig. 2.8). This will results in a computational saving of L_s multiplications and $(L_s - 1)$ additions per iteration. In Fig. 2.8, the same error signal $e_{\hat{s}}(n)$ is used to update both the coefficients of $\hat{S}(z)$ and $W(z)$. The signal $e_{\hat{s}}(n)$ is computed as

$$e_{\hat{s}}(n) = \hat{d}(n) - y_{\hat{s}w}(n), \tag{2.23}$$

where $y_{\hat{s}w}(n)$ is computed as

$$y_{\hat{s}w}(n) = w(n) * y_{\hat{s}}(n) = \boldsymbol{w}^T(n)\boldsymbol{x}_{w(n),y_{\hat{s}}(n)}(n), \tag{2.24}$$

where $w(n)$ is the impulse response of $W(z)$, $\boldsymbol{w}(n) = [w_0(n), w_1(n), \cdots, w_{L_w-1}(n)]^T$ is the impulse response coefficient vector of $W(z)$ at time n, and $\boldsymbol{x}_{w(n),y_{\hat{s}}(n)}(n) = [y_{\hat{s}}(n), y_{\hat{s}}(n-1), \cdots, y_{\hat{s}}(n-L_w+1)]^T$ is the input signal vector of filter $W(z)$ with input $y_{\hat{s}}(n)$ at time n. The signal $\hat{d}(n)$ (estimate of $d(n)$) in (2.23) is computed as

$$\hat{d}(n) = e(n) - v_{\hat{s}}(n) + y_{w\hat{s}(n)} = d(n) - (y_{ws}(n) - y_{w\hat{s}}(n)) + (v_s(n) - v_{\hat{s}}(n)), \tag{2.25}$$

where $y_{w\hat{s}}(n)$ is the output of $\hat{S}(z)$ corresponding to input $y_w(n)$. As the ANC system converges, the terms $(y_{ws}(n) - y_{w\hat{s}}(n)) \to 0$ and $(v_s(n) - v_{\hat{s}}(n)) \to 0$, $\hat{d}(n) \to d(n)$, $y_{\hat{s}w}(n) \to \hat{d}(n) \to d(n)$, and $e_{\hat{s}}(n) \to 0$. For CEMFxLMS algorithm based ANC system, the weight update equation for ANC filter $W(z)$ is given as

$$\boldsymbol{w}(n+1) = \boldsymbol{w}(n) + \mu_w e_{\hat{s}}(n)\boldsymbol{x}_{w(n),y_{\hat{s}}(n)}(n), \tag{2.26}$$

where μ_w is the step-size parameter, $e_{\hat{s}}(n)$ is the error signal of both the SPM filter and ANC filter, and $\boldsymbol{x}_{w(n),y_{\hat{s}}(n)}(n) = [y_{\hat{s}}(n), y_{\hat{s}}(n-1), \cdots, y_{\hat{s}}(n-L_w+1)]^T$ is the input signal vector of filter $W(z)$ with input $y_{\hat{s}}(n)$ at time n. In the proposed method, the weight update equation for SPM filter $\hat{S}(z)$ is given as

$$\hat{\boldsymbol{s}}(n+1) = \hat{\boldsymbol{s}}(n) + \mu_s e_{\hat{s}}(n)\boldsymbol{x}_{\mathrm{LMS},v(n)}(n), \tag{2.27}$$

where μ_s is the fixed step-size parameter, and $\boldsymbol{x}_{\mathrm{LMS},v(n)}(n) = [v(n), v(n-1), \cdots, v(n-L_s+1)]^T$ is the input signal vector of adaptive LMS algorithm of $\hat{S}(z)$ at time n. The CEMFxLMS algorithm [43] for $G(n) = 1$ is shown in Table. 2.3.

2.2.3 Simulation Results

In this subsection simulation results are presented to compare the performance of ANC system using CEMFxLMS algorithm [43] and original MFxLMS algorithm.

Table 2.3: CEMFxLMS algorithm with $G(n) = 1 \; \forall \; n$ [43].

$$d(n) = \boldsymbol{p}^T(n)\boldsymbol{x}_{p(n),x(n)}(n)$$

$$y_w(n) = \boldsymbol{w}^T(n)\boldsymbol{x}_{w(n),x(n)}(n)$$

$$v(n) = G(n)v_g(n)$$

$$y_{ws}(n) - v_s(n) = \boldsymbol{s}^T(n)\boldsymbol{x}_{s(n),(y_w(n)-v(n))}(n)$$

$$e(n) = d(n) - y_{ws}(n) + v_s(n)$$

$$v_{\hat{s}}(n) - y_{w\hat{s}}(n) = \hat{\boldsymbol{s}}^T(n)\boldsymbol{x}_{\hat{s}(n),(v(n)-y_w(n))}(n)$$

$$\hat{d}(n) = e(n) - v_{\hat{s}}(n) + y_{w\hat{s}}(n)$$

$$y_{\hat{s}}(n) = \hat{\boldsymbol{s}}^T(n)\boldsymbol{x}_{\hat{s}(n),x(n)}(n)$$

$$y_{\hat{s}w}(n) = \boldsymbol{w}^T(n)\boldsymbol{x}_{w(n),y_{\hat{s}}(n)}(n)$$

$$e_{\hat{s}}(n) = \hat{d}(n) - y_{\hat{s}w}(n)$$

$$\hat{\boldsymbol{s}}(n+1) = \hat{\boldsymbol{s}}(n) + \mu_s e_{\hat{s}}(n)\boldsymbol{x}_{\text{LMS},v(n)}(n)$$

$$\boldsymbol{w}(n+1) = \boldsymbol{w}(n) + \mu_w e_{\hat{s}}(n)\boldsymbol{x}_{w(n),y_{\hat{s}}(n)}(n)$$

The performance comparison is carried out on the basis of 1) Relative modeling error, $\Delta D_s(n)$, of the secondary path $S(z)$ as defined in (2.21), and 2) Mean-noise-reduction (MNR) at the error microphone as defined in (2.22).

Using data from [4], the acoustic paths $P(z)$, and $S(z)$ are modeled as FIR filters of tap-weight lengths 48, 16, respectively. The adaptive filters $W(z)$, and $\hat{S}(z)$ are selected as FIR filters of tap-weight length 32, and 16, respectively. The ANC filter, $W(z)$, is initialized with null vectors, and -5dB offline modeling is used for $\hat{S}(z)$. The original unwanted noise signal $x(n)$, at the reference microphone, is a multi-tonal input with frequencies 100, 200, 300, and 400 Hz, and its variance is adjusted to 1. A zero-mean WGN with variance 0.001 is added with $x(n)$ to

account for any measurement noise. The modeling excitation signal $v_g(n)$ is a zero-mean WGN with variance 0.05. As no gain scheduling is used, therefore $G(n) = 1$ and $v_g(n) = v(n)$. The step-size parameters are experimentally adjusted for fast and stable convergence and are given as: $\mu_w = 5 \times 10^{-4}$; $\mu_s = 1 \times 10^{-2}$. The jumps in the middle of the simulation results is due to the perturbation in the impulse responses of the acoustic paths $P(z)$ and $S(z)$. The impulse responses of $P(z)$ and $S(z)$ are perturbed from their nominal values by adding random WGN. The sampling frequency is 2kHz. All the simulation results are averaged over 10 independent realizations.

In Fig. 2.11(a), the curves for relative modeling error, as defined in (2.21), are plotted in dB for original MFxLMS algorithm based ANC system and for CEMFxLMS algorithm based ANC system. Similarly in Fig. 2.11(b) the curves for MNR, as defined in (2.22), are plotted in dB. It is clear from Fig. 2.11(a) and Fig. 2.11(b) that the performance of CEMFxLMS algorithm is almost same as that of original MFxLMS algorithm. However, the advantage of the CEMFxLMS algorithm is that the same performance is achieved with less computational complexity. As mentioned earlier that the CEMFxLMS algorithm reduces L_s multiplications and $(L_s - 1)$ additions per iteration.

2.3 Computational Complexity Comparison

The computational complexity requirements of all the methods discussed in this chapter are given in Table. 2.4. In case of FxLMS algorithm based ANC systems, Eriksson's method has the lowest computational complexity. In case of MFxLMS algorithm based ANC systems, the CEMFxLMS has the lower computational complexity.

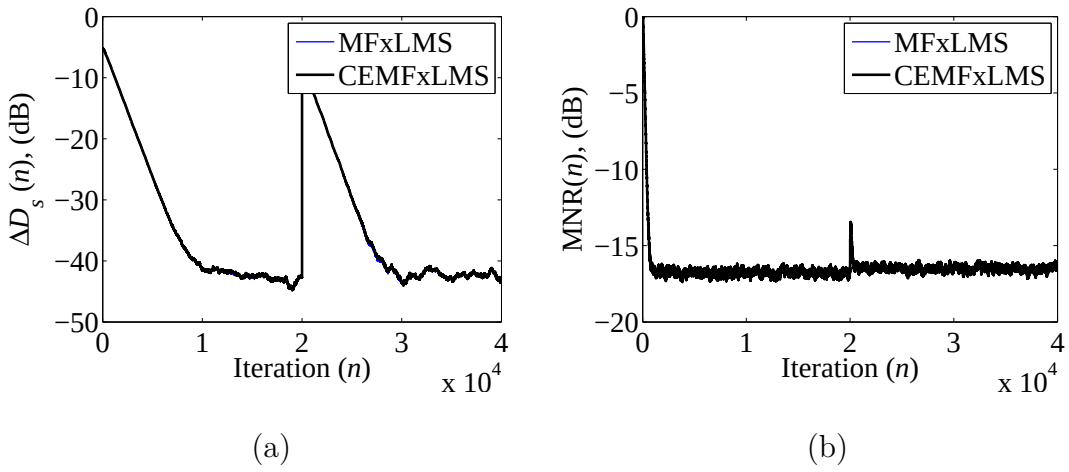

(a) (b)

Figure 2.11: (a) Relative modeling error, $\Delta D_s(n)$(dB), (b) Mean-noise-reduction, MNR(n) (dB).

2.4 Summary

In this chapter, some methods using auxiliary WGN as an excitation signal for OSPM are discussed. In all the methods auxiliary noise with fixed variance is injected, i.e., $G(n) = 1$, and $v_g(n) = v(n)$.

In the first part of this chapter, FxLMS algorithm based methods for OSPM without gain scheduling are discussed. It is found through the simulation results that the VSS method [39] performs better compared to other existing methods in terms of improving the modeling accuracy of SPM filter. It is also concluded from the simulation results that higher modeling accuracy of SPM filter does not mean less MNR value. The modeling accuracy up to certain extent is required to keep the ANC system stable. Any further improvement in the modeling accuracy can only improve the stability margins and may not affect (improve) the MNR value of ANC systems.

In the second part of this chapter, a computationally efficient structure is pro-

Table 2.4: Computational complexity comparison (Number of computations per iteration)

Name	$\times$	$+$	$\div$
FxLMS algorithm based ANC systems			
Eriksson [21]	$2L_w + 3L_s + 2$	$2L_w + 3L_s - 1$	–
Kuo [35]	$2L_w + 2L_k + 3L_s + 3$	$2L_w + 2L_k + 3L_s - 1$	–
Bao [36]	$2L_w + 2L_b + 3L_s + 3$	$2L_w + 2L_b + 3L_s - 1$	–
Zhang [37]	$2L_w + 2L_h + 3L_s + 3$	$2L_w + 2L_h + 3L_s + 1$	–
Akhtar [38]	$2L_w + 3L_s + 10$	$2L_w + 3L_s + 4$	1
Proposed [39]	$2L_w + 3L_s + 12$	$2L_w + 3L_s + 5$	1
MFxLMS algorithm based ANC systems			
MFxLMS	$3L_w + 4L_s + 2$	$3L_w + 4L_s - 1$	–
CEMFxLMS [43]	$3L_w + 3L_s + 2$	$3L_w + 3L_s$	–

posed for ANC system using MFxLMS adaptive algorithm. It is found through the simulation results that the CEMFxLMS algorithm achieves almost the same performance as that of original MFxLMS algorithm. However the computational complexity of the CEMFxLMS algorithm is lower than that of the original MFxLMS algorithm.

The goal of an ANC system is to reduce the unwanted noise at the summing junction. In order to compensate for the secondary path effects and to keep the ANC system stable, an additional auxiliary noise injected into the ANC system. This auxiliary noise contributes to the residual error at the summing junction. This

contribution of auxiliary noise will degrades the NRP of ANC system especially at steady-state when the original unwanted noise is reduced to a small value due to the convergence of an ANC system. In all the methods, discussed in this chapter, auxiliary noise with fixed variance is injected. In the next chapter the methods for OSPM with gain scheduling are discussed. In these methods, instead of injecting the auxiliary noise with fixed variance, the time-varying gain $G(n)$ is used to change (decrease) the variance of auxiliary noise with the convergence status of ANC system. This gain scheduling will reduce the contribution of auxiliary noise to the residual error and thus improves the NRP of ANC systems.

Chapter 3

Online Secondary Path Modeling With Gain Scheduling

In the last chapter the methods, for on-line secondary path modeling (OSPM), in which an additional auxiliary noise with fixed variance is injected in all operating conditions were discussed. The objective of active noise control (ANC) system is to reduce the residual noise at the summing junction. The auxiliary noise injected for OSPM contributes to the residual error, and hence degrades the noise-reduction-performance (NRP) of ANC system. In this chapter, instead of injecting auxiliary noise with fixed variance, a gain scheduling scheme is used to vary the power of auxiliary noise. The auxiliary noise power is varied in accordance with the convergence status of ANC system. When ANC system is far from steady-state, the gain scheduling strategy is such that to allow injection of

auxiliary noise with large variance. This will result in fast convergence of SPM filter. At early stages of adaptation of ANC system, the large variance of auxiliary noise is masked by the large variance of the residual unwanted noise, and hence the contribution corresponding to auxiliary noise remains unnoticeable by the subject (observer). However, with the convergence of ANC system the original unwanted noise is reduced due to cancellation by the anti-noise, and is not able to mask the large value of auxiliary noise. Therefore, it is desirable that as the ANC system converges the gain scheduling strategy will allow the power of auxiliary noise to decrease. This will reduce the contribution of auxiliary noise to the residual error, and thus improves the NRP fo ANC system.

In this chapter we will discuss the existing methods for OSPM with gain scheduling. It includes Akhtar's method [44] and the best know Carini's method [45, 46]. In addition to these existing methods our proposed strategies [43], [47]-[49] for gain scheduling were discussed and compared with the existing methods through the simulation results.

3.1 Existing Methods

3.1.1 Akhtar's Method

The block diagram of Akhtar's method [44] for OSPM with gain scheduling is shown in Fig. 3.1. Here the signal $v_d(n)$ is used to model the background noise, and is assumed to be equal to zero unless otherwise stated. In order to compensates for the secondary path effects, a modified filtered-x-LMS (MFxLMS) adaptive algorithm is used for ANC filter $W(z)$. A variable step-size (VSS) LMS adaptive algorithm is used for SPM filter $\hat{S}(z)$. The weight update equation for ANC filter

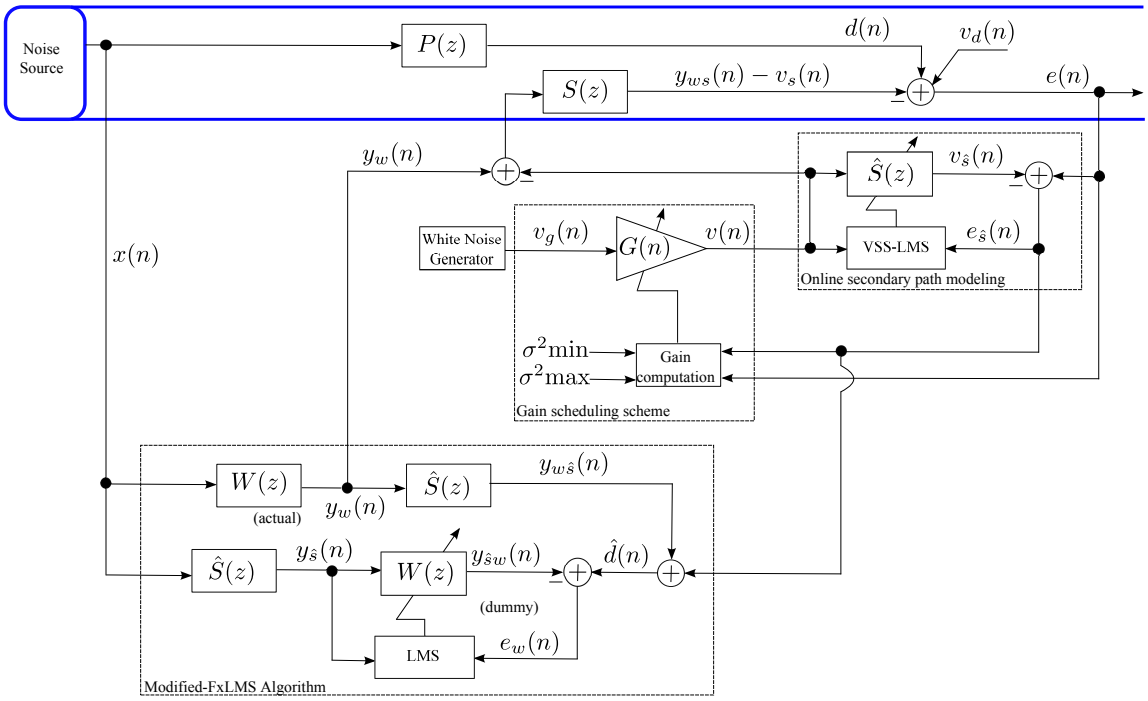

Figure 3.1: Block diagram of Akhtar's method for Online secondary path modeling with gain scheduling [44].

$W(z)$ is given as

$$\boldsymbol{w}(n+1) = \boldsymbol{w}(n) + \mu_w e_w(n) \boldsymbol{x}_{\text{LMS},y_{\hat{s}}(n)}(n), \tag{3.1}$$

where μ_w is the fixed step-size parameter, $e_w(n)$ is the error signal of ANC filter $W(z)$, and $\boldsymbol{x}_{\text{LMS},y_{\hat{s}}(n)}(n) = [y_{\hat{s}}(n), y_{\hat{s}}(n-1), \cdots, y_{\hat{s}}(n-L_w+1)]^T$ is the input signal vector of adaptive LMS algorithm of $W(z)$ at time n and is referred as the filtered reference signal vector. The reference signal $x(n)$ filtered through $\hat{S}(z)$ is computed as

$$y_{\hat{s}}(n) = \hat{s}(n) * x(n) = \hat{\boldsymbol{s}}^T(n) \boldsymbol{x}_{\hat{s}(n),x(n)}(n), \tag{3.2}$$

where $\hat{s}(n)$ is the impulse response of $\hat{S}(z)$, $\hat{\boldsymbol{s}}(n) = [\hat{s}_0(n), \hat{s}_1(n), \cdots, \hat{s}_{L_s-1}(n)]^T$ is the impulse response coefficient vector of $\hat{S}(z)$ at time n, and $\boldsymbol{x}_{\hat{s}(n),x(n)}(n) =$

$[x(n), x(n-1), \cdots, x(n-L_s+1)]^T$ is the input signal vector of filter $\hat{S}(z)$ with input $x(n)$ at time n. The weight update equation for SPM filter is given by

$$\hat{\boldsymbol{s}}(n+1) = \hat{\boldsymbol{s}}(n) + \mu_s(n) e_{\hat{s}}(n) \boldsymbol{x}_{\hat{s}(n),v(n)}(n), \tag{3.3}$$

where $\mu_s(n)$ is the VSS, $e_{\hat{s}}(n)$ is the error signal of SPM filter, and $\boldsymbol{x}_{\hat{s}(n),v(n)}(n) = [v(n), v(n-1), \cdots, v(n-L_s+1)]$ is the input signal vector of filter $\hat{S}(z)$ with input $v(n)$ at time n.

VSS for SPM Filter in Akhtar's Method [44]: In Akhtar's method, the VSS, $\mu_s(n)$, in the weight update equation of SPM filter (see (3.3)) is computed as

$$\mu_s(n) = \rho(n)\mu_{s_{\min}} + (1-\rho(n))\mu_{s_{\max}}, \tag{3.4}$$

where $\mu_{s_{\min}}$ and $\mu_{s_{\max}}$ are minimum and maximum values of $\mu_s(n)$, respectively, selected for fast and stable convergence of ANC system. At the start, when ANC system is far from steady-state, the term $\rho(n) \approx 1$ and hence $\mu_s(n) = \mu_{s_{\min}}$. As the SPM filter and ANC system converges $\rho(n) \to 0$ and $\mu_s(n) = \mu_{s_{\max}}$. The variation of $\rho(n)$ in Akhtar's method is explained below

Variation of $\rho(n)$ in Akhtar's Method [44]: From Fig. 3.1, the term $\rho(n)$ is defined as

$$\rho(n) = \frac{P_{e_{\hat{s}}}(n)}{P_e(n)} = \frac{E[(d(n) - y_{ws}(n))^2] + E[(v_s(n) - v_{\hat{s}}(n))^2]}{E[(d(n) - y_{ws}(n))^2] + E[(v_s(n))^2]}, \tag{3.5}$$

where $E[\cdot]$ is the expectation operator and

$$P_q(n) = \lambda P_q(n-1) + (1-\lambda) q^2(n), \tag{3.6}$$

where $q(n)$ is the signal of interest, and $0.9 < \lambda < 1$ is a forgetting factor. At the start-up of ANC system, $P_{e_{\hat{s}}}(0) \approx P_e(0)$, $\rho(0) = P_{e_{\hat{s}}}(0)/P_e(0) = 1$, and as the SPM

filter converges $\hat{\boldsymbol{s}}(n) \rightarrow \boldsymbol{s}(n) \Rightarrow v_{\hat{s}}(n) \rightarrow v_s(n)$. In Akhtar's method [44], at steady-state $E[(v_s(n))^2] > E[(d(n) - y_{ws}(n))^2]$ and $E[(v_s(n))^2] >> E[(v_s(n) - v_{\hat{s}}(n))^2]$, and hence from (3.5) $\rho(n) \rightarrow 0$.

Gain Scheduling in Akhtar's Method [44]: The input signal vector $\boldsymbol{x}_{\hat{s}(n),v(n)}(n)$ in the weight update equation of SPM filter (see (3.3)) can be written as

$$\begin{aligned}
\boldsymbol{x}_{\hat{s}(n),v(n)}(n) &= [v(n), v(n-1), \cdots, v(n-L_s+1)]^T \\
&= [G(n)v_g(n), G(n-1)v_g(n-1), \cdots, G(n-L_s+1)v_g(n-L_s+1)]^T \\
&= \boldsymbol{G}(n)\boldsymbol{x}_{\hat{s}(n),v_g(n)}(n), \qquad (3.7)
\end{aligned}$$

where $\boldsymbol{G}(n) = \text{diag}[G(n), G(n-1), \cdots, G(n-L_s+1)]$ is a diagonal matrix of dimensions $L_s \times L_s$, $\boldsymbol{x}_{\hat{s}(n),v_g(n)}(n) = [v_g(n), v_g(n-1), \cdots, v_g(n-L_s+1)]^T$ is a vector of length L_s, $v_g(n)$ is a random WGN signal, $v(n) = G(n)v_g(n)$ is the input excitation signal of SPM filter, and $G(n)$ is the time-varying gain. In Akhtar's method [44], the gain $G(n)$ is computed as

$$G(n) = \sqrt{\rho(n)\sigma^2_{\max} + (1-\rho(n))\sigma^2_{\min}}, \qquad (3.8)$$

where $\sigma^2_{\min}$ and $\sigma^2_{\max}$ are experimentally determined parameters. In Akhtar's method, the value of the parameter $\rho(n)$ is never zero in steady-state and $\sigma^2_{\max}$ in (3.8) contributes to the steady-state value of auxiliary-noise-power (ANP) and hence degrades the NRP of ANC system.

3.1.2 Carini's Method

The block diagram of Carini's method for OSPM with gain scheduling [45] and with optimal normalized LMS (NLMS) adaptive algorithms for ANC and SPM filters [46] is shown in Fig. 3.2. A delay coefficient technique [50] is used to compute the optimal normalized step-size parameter, $\mu_s(n)$, for SPM filter. For this purpose an

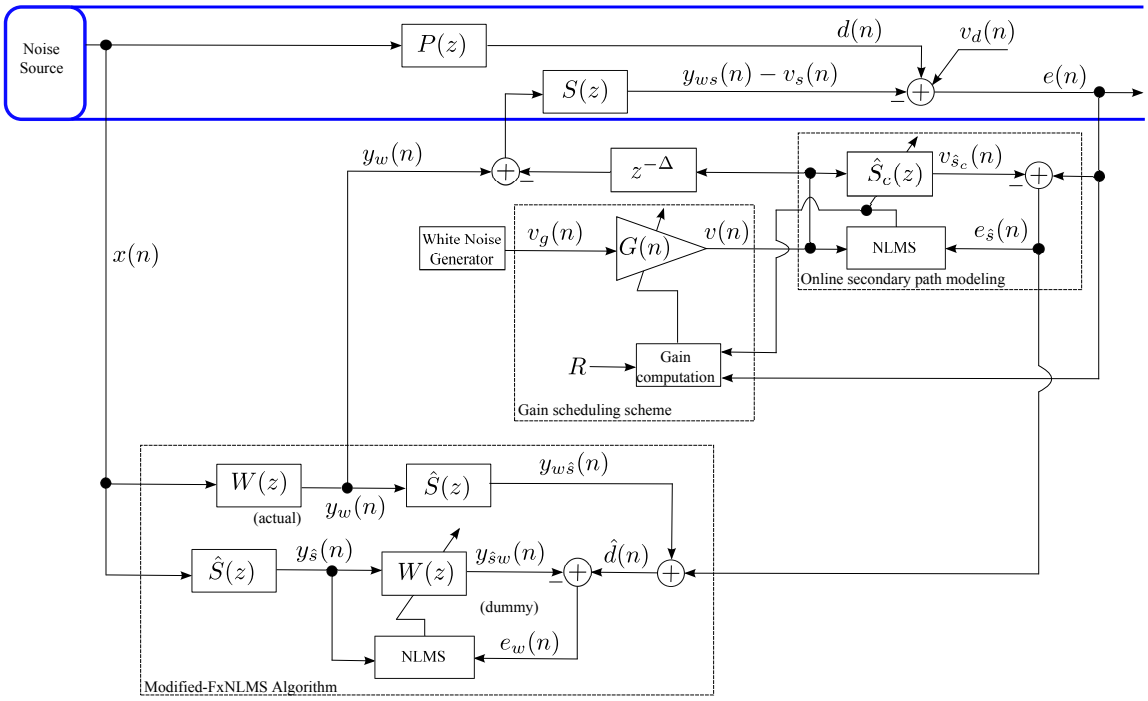

Figure 3.2: Block diagram of Carini's method for Online secondary path modeling with gain scheduling [46].

artificial delay $z^{-\Delta}$ is used as shown in Fig. 3.2. The SPM filter $\hat{S}_c(z)$ of length $(\Delta + L_s)$ has to model the series combination of $z^{-\Delta}$ followed by $S(z)$, where Δ is the length of delay. The impulse response coefficient vector of $\hat{S}_c(z)$ is given by

$$\hat{\boldsymbol{s}}_c(n) = [\hat{\boldsymbol{s}}_0^T(n) \qquad \hat{\boldsymbol{s}}^T(n)]^T, \tag{3.9}$$

where $\hat{\boldsymbol{s}}_0(n) = [\hat{s}_0(n), \hat{s}_1(n), \cdots, \hat{s}_{\Delta-1}(n),]^T$ is a vector of the first Δ samples of $\hat{\boldsymbol{s}}_c(n)$, and $\hat{\boldsymbol{s}}(n) = [\hat{s}_\Delta(n), \hat{s}_{\Delta+1}(n), \cdots, \hat{s}_{\Delta+L_s-1}(n),]^T$ is a vector of the last L_s samples of $\hat{\boldsymbol{s}}_c(n)$.

Gain Scheduling in Carini's Method [45]: In [45], a self-tuned gain scheduling (to vary ANP) strategy is proposed by Carini and Malatini. The gain

scheduling strategy is such that the ratio $R(n)$ given by

$$R(n) = \frac{E\left[(d(n) - y_{ws}(n))^2\right]}{E\left[(v_s(n))^2\right]} = \text{constant}\,\forall\, n, \tag{3.10}$$

is kept constant in every operating conditions, where $E[\cdot]$ is the expectation operator. From Fig. 3.2, the power of residual error signal, $E[e^2(n)]$, can be written as

$$\begin{aligned} E[e^2(n)] &= E[(d(n) - y_{ws}(n))^2] + E[(v_s(n))^2] \\ &= E[(d(n) - y_{ws}(n))^2] + G^2(n)||\boldsymbol{s}(n)||^2 E[(v_g(n))^2], \end{aligned} \tag{3.11}$$

Where $E[(v_g(n))^2] = 1$, as $v_g(n)$ is a zero mean, unit variance random WGN, and $||\boldsymbol{s}(n)||^2$ is the square of the Euclidean norm of impulse response of unknown secondary path. Using $E[(v_g(n))^2] = 1$ in (3.11) we get

$$E[e^2(n)] = E[(d(n) - y_{ws}(n))^2] + E[(v_s(n))^2] = E[(d(n) - y_{ws}(n))^2] + G^2(n)||\boldsymbol{s}(n)||^2. \tag{3.12}$$

Dividing both sides of (3.12) with $E[(v_s(n))^2]$ and using $R(n)$ from (3.10) we get

$$\frac{E[e^2(n)]}{E[(v_s(n))^2]} = R(n) + 1 = \frac{E[e^2(n)]}{G^2(n)||\boldsymbol{s}(n)||^2} \approx \frac{P_e(n)}{G^2(n)P_s(n)}, \tag{3.13}$$

where $P_e(n)$ is the power estimate of the error signal $e(n)$ being computed using (3.6). Since the secondary path is unknown, therefore the term $P_s(n)$ can not be computed exactly. However, its estimate can be computed using the coefficients of SPM filter as

$$P_{\hat{s}}(n) = \lambda P_{\hat{s}}(n-1) + (1-\lambda)\hat{\boldsymbol{s}}^T(n)\hat{\boldsymbol{s}}(n), \tag{3.14}$$

where $P_{\hat{s}}(n)$ is the estimate of $P_s(n)$, $\hat{\boldsymbol{s}}(n)$ is the same as defined in (3.9), and $0.9 < \lambda < 1$ is a forgetting factor. Using (3.14) in (3.13) and rearranging the equation the time-varying gain $G(n)$ in Carini's method is computed as

$$G(n) = \sqrt{\frac{P_e(n)}{(R(n)+1)P_{\hat{s}}(n)}}. \tag{3.15}$$

Optimal Normalized Step-size Computation for $W(z)$ and $\hat{S}(z)$ in Carini's Method [46]: A heuristic approach is used to estimate the optimal normalized step-size parameter, $\mu_w(n)$, for $W(z)$ and is given by

$$\mu_w(n) = \frac{\hat{N}_w(n)}{P_{e_w}(n)\left(\boldsymbol{x}^T_{\text{NLMS},y_{\hat{s}}(n)}(n)\boldsymbol{x}_{\text{NLMS},y_{\hat{s}}(n)}(n)\right)}, \tag{3.16}$$

where $P_{e_w}(n)$ is the power estimate of the error signal $e_w(n)$ being computed using (3.6), $\boldsymbol{x}_{\text{NLMS},y_{\hat{s}}(n)}(n) = [y_{\hat{s}}(n), y_{\hat{s}}(n-1), \cdots, y_{\hat{s}}(n-L_w+1)]^T$ is the input signal vector of adaptive NLMS algorithm of $W(z)$ with input $y_{\hat{s}}(n)$ at time n, and $\hat{N}_w(n)$ is computed as

$$\hat{N}_w(n) = \lambda\hat{N}_w(n-1) + (1-\lambda)e_w(n)\hat{\boldsymbol{m}}^T(n)\boldsymbol{x}_{\text{NLMS},y_{\hat{s}}(n)}(n), \tag{3.17}$$

where $\hat{\boldsymbol{m}}(n)$ is computed as

$$\hat{\boldsymbol{m}}(n) = \hat{\lambda}\hat{\boldsymbol{m}}(n-1) + \frac{(1-\hat{\lambda})e_w(n)\boldsymbol{x}_{\text{NLMS},y_{\hat{s}}(n)}(n)}{\boldsymbol{x}^T_{\text{NLMS},y_{\hat{s}}(n)}(n)\boldsymbol{x}_{\text{NLMS},y_{\hat{s}}(n)}(n)}, \tag{3.18}$$

and $\hat{\lambda}$ is selected in the range [0.6, 0.9].

Finally, the optimal normalized step-size parameter $\mu_s(n)$ for SPM filter $\hat{S}_c(z)$ is computed as

$$\mu_s(n) = \begin{cases} \frac{\hat{N}_s(n)}{P_{e_{\hat{s}}}(n)\left(\boldsymbol{x}^T_{\hat{s}_c(n),v(n)}(n)\boldsymbol{x}_{\hat{s}_c(n),v(n)}(n)\right)} & \left(\frac{\hat{N}_s(n)}{P_{e_{\hat{s}}}(n)} > \mu_{s_{\min}}\right) \\ \frac{\mu_{s_{\min}}}{\boldsymbol{x}^T_{\hat{s}_c(n),v(n)}(n)\boldsymbol{x}_{\hat{s}_c(n),v(n)}(n)} & (\text{Otherwise}) \end{cases}, \tag{3.19}$$

where $\boldsymbol{x}_{\hat{s}_c(n),v(n)}(n) = [v(n), v(n-1), \cdots, v(n-L_s-\Delta+1)]^T$ is the input signal vector of adaptive NLMS algorithm of $\hat{S}_c(z)$ with input $v(n)$ at time n, and $\hat{N}_s(n)$ is computed as

$$\hat{N}_s(n) = \lambda\hat{N}_s(n-1) + \frac{1-\lambda}{\Delta}\left(\hat{\boldsymbol{s}}_0^T(n)\hat{\boldsymbol{s}}_0(n)\boldsymbol{x}^T_{\hat{s}_c(n),v(n)}(n)\boldsymbol{x}_{\hat{s}_c(n),v(n)}(n)\right), \tag{3.20}$$

where $\hat{\boldsymbol{s}}_0(n) = [\hat{s}_0(n), \hat{s}_1(n), \cdots, \hat{s}_{\Delta-1}(n),]^T$ represents the first Δ coefficients of $\hat{\boldsymbol{s}}_c(n)$ (see (3.9)).

In Carini's method [46], the weight update equation for $W(z)$ is almost same as used in Akhtar's method [44] (see (3.1)). In Carini's method, instead of μ_w, an optimal normalized step-size, $\mu_w(n)$, given by (3.16), is used for the weight updation of $W(z)$. In Carini's method, the SPM filter is represented by $\hat{S}_c(z)$, and has the weight update equation given by

$$\hat{\boldsymbol{s}}_c(n+1) = \hat{\boldsymbol{s}}_c(n) + \mu_s(n) e_{\hat{s}}(n) \boldsymbol{x}_{\hat{s}_c(n),v(n)}(n), \tag{3.21}$$

where $\mu_s(n)$ (see (3.19)) is the optimal step-size parameter for $\hat{S}_c(z)$ computed using the delay coefficient technique [50], and $\boldsymbol{x}_{\hat{s}_c(n),v(n)}(n)$ is the input signal vector of $\hat{S}_c(z)$ with input $v(n)$ at time n.

Few Remarks Regarding Carini's method:

1. The first part of $\hat{\boldsymbol{s}}_c(n)$, i.e., $\hat{\boldsymbol{s}}_0(n)$, is to model the artificially introduced delay $z^{-\Delta}$, so after the convergence of ANC system, the term $\left(\hat{\boldsymbol{s}}_0^T(n)\hat{\boldsymbol{s}}_0(n)\right)$ in (3.20) is very small (ideally zero) $\Rightarrow \hat{N}_s(n) \approx 0$. The perturbation in acoustic paths would cause an increase in the power of $e_{\hat{s}}(n)$, so the term $P_{e_{\hat{s}}}(n)$ in the denominator of (3.19) will drive the condition $\hat{N}_s(n)/P_{e_{\hat{s}}}(n) > \mu_{s_{\min}}$ to be false, and hence the step-size for $\hat{\boldsymbol{s}}_c(n)$ will be determined by $\mu_{s_{\min}} / \left(\boldsymbol{x}^T_{\hat{s}_c(n),v(n)}(n)\boldsymbol{x}_{\hat{s}_c(n),v(n)}(n)\right)$. This means that in Carini's method once the ANC system converges, the step-size for SPM filter will stay at small value even if there is a perturbation in the acoustic paths. The small value of step-size, even when the acoustic paths are perturbed, is undesirable and thus resulting in a poor tracking performance. Here $\mu_{s_{\min}}$ is used to avoid freezing completely the adaptation in these conditions.

2. The overall computational complexity of Carini's method is very high. The high computational cost is mainly due to the online estimation of optimal normalized step-size parameters for ANC filter and SPM filter.

3. The ratio $R(n)$ in (3.10) is constant in all operating conditions (The value of the constant is selected as 1 for Carini's method). This means, that $E[(v_s(n))^2] = G^2(n)||\boldsymbol{s}(n)||^2 E[v_g^2(n)] = E[(d(n) - y_{ws}(n))^2]$ is always satisfied. As $E[v_g^2(n)] = 1$, and at steady-state the term $||\boldsymbol{s}(n)||^2$ is almost constant, therefore gain $G(n)$ at steady-state is proportional to $\sqrt{E[(d(n) - y_{ws}(n))^2]}$. After the convergence of ANC system: 1) the step-size for $\hat{\boldsymbol{s}}_c(n)$ is determined by second part of (3.19) (step-size stays small), and 2) the input signal power for $\hat{\boldsymbol{s}}_c(n)$ is determined by the $E[(d(n) - y_{ws}(n))^2]$. These two conditions results in slow convergence of SPM filter, when there is a perturbation in the acoustic paths.

4. The presence of uncorrelated disturbance $v_d(n)$ (used to model the background noise) at the error microphone contributes to the power of residual error signal, $P_e(n)$. The signal $v_d(n)$ with large variance results in large value of the gain $G(n)$ (see (3.15)), thus degrades the NRP of ANC system.

3.2 Proposed Methods

3.2.1 Proposed Method-1

. The block diagram of proposed method-1 [47] is shown in Fig. 3.3. Here fixed step-size LMS adaptive algorithm is used for both the SPM filter and ANC filter. The use of fixed step-size LMS adaptive algorithms, instead of optimal NLMS adaptive algorithms, reduces the computational complexity of the proposed method-1 compared to Carini's method. In order to solve the first of the above mentioned problems with Carini's method [46], i.e., to efficiently track the time-varying secondary path even after the convergence of ANC system, a new gain scheduling

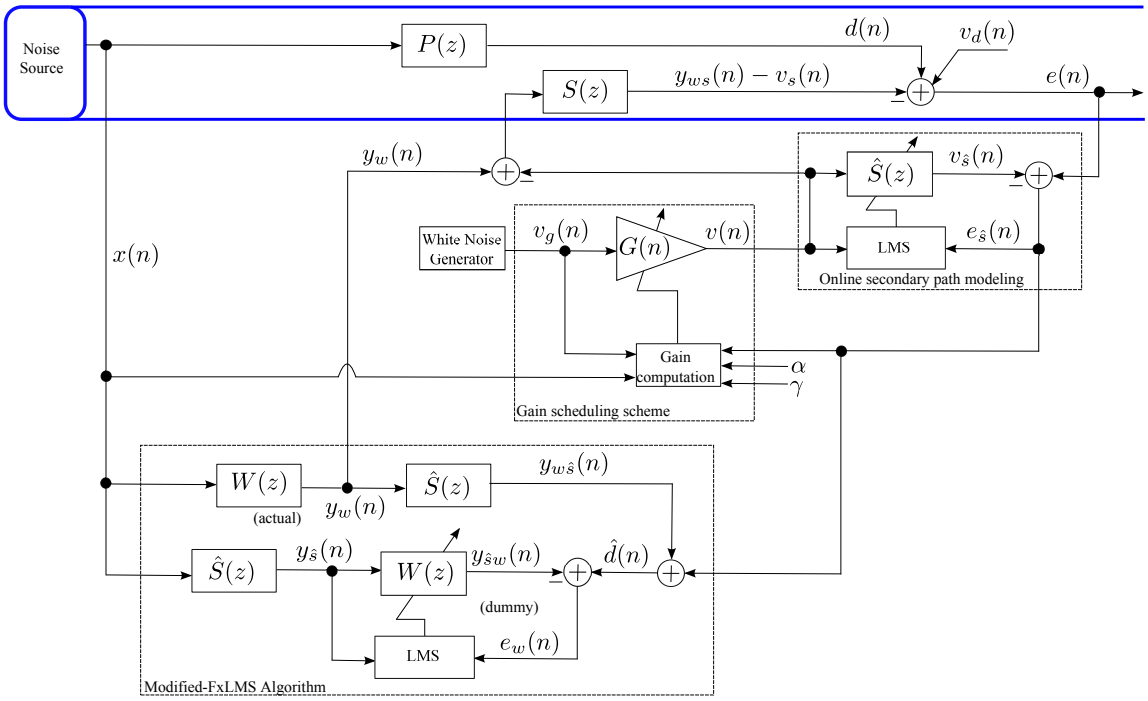

Figure 3.3: Block diagram of proposed method-1 for Online secondary path modeling with gain scheduling [47].

strategy based on the error signal, $e_{\hat{s}}(n)$, of the $\hat{S}(z)$ is proposed. The time-varying gain $G(n)$ in proposed method-1 [47] is computed as

$$G(n) = \begin{cases} P_x/P_{v_g} & (\beta(n) > P_x) \\ \beta(n)/P_{v_g} & (\text{Otherwise}) \end{cases}, \tag{3.22}$$

where P_x and P_{v_g}, respectively, are the powers of the reference signal, $x(n)$, and auxiliary noise $v_g(n)$ which can be estimated using (3.6), and the time-varying term $\beta(n)$ can be computed as

$$\beta(n) = \alpha\beta(n-1) + \gamma e_{\hat{s}}^2(n), \tag{3.23}$$

where $0 < \alpha < 1$ and $\gamma > 0$ are controlling parameters, and $e_{\hat{s}}(n)$ is the error signal of SPM filter.

At the start-up, when ANC system is far from steady-state, the error signal $e_{\hat{s}}(n)$ is large, therefore setting the gain $G(n)$ to a higher value, upper bounded by the P_x/P_{v_g}. This will increase the convergence speed of $\hat{S}(z)$. The error signal $e_{\hat{s}}(n)$ is decreasing in nature. As the ANC system converges the signal $e_{\hat{s}}(n)$ and hence the gain $G(n)$ decreases, thereby reducing the contribution of the auxiliary noise in residual error signal $e(n)$. In the case of perturbation in acoustic paths the error signal $e_{\hat{s}}(n)$ will increase, setting the gain, $G(n)$, again to a larger value, allowing the SPM filter to converge quickly, and hence can efficiently track the perturbation in the acoustic paths.

In proposed method-1, the weight update equations for ANC filter and SPM filter are the same as used for Akhtar's method [44] (see (3.1) and (3.3)) with two exceptions. First fixed step-size μ_s, instead of VSS $\mu_s(n)$, is used in the weight update equation of SPM filter, and second, instead of using (3.8), the gain in proposed method-1 is computed using (3.22) and (3.23). The algorithm for the proposed method-1 is given in Table. 3.1

3.2.2 Proposed Method-2

In proposed method-1, MFxLMS adaptive LMS algorithm is used for ANC filter. In chapter 2 (see Fig. 2.10) a computationally efficient structure is proposed for MFxLMS algorithm based ANC system. In proposed method-2 the structure of Fig. 2.10 is used in combination with the time-varying gain computed using (3.22) and (3.23). The proposed method-2 is computationally efficient than proposed method-1 and can save $(2L_s - 1)$ computations per iteration. It will be shown in the simulation results that the performance of proposed method-2 is almost same as that of proposed method-1.

Table 3.1: Algorithm for the proposed method-1 [47].

$d(n) = \boldsymbol{p}^T(n)\boldsymbol{x}_{p(n),x(n)}(n)$; $y_w(n) = \boldsymbol{w}^T(n)\boldsymbol{x}_{w(n),x(n)}(n)$
$v(n) = G(n)v_g(n)$ ($G(n) = 1$ for first iteration)
$y_{ws}(n) - v_s(n) = \boldsymbol{s}^T(n)\boldsymbol{x}_{s(n),(y_w(n)-v(n))}(n)$
$e(n) = d(n) - y_{ws}(n) + v_s(n)$
$v_{\hat{s}}(n) = \hat{\boldsymbol{s}}^T(n)\boldsymbol{x}_{\hat{s}(n),v(n)}(n)$; $e_{\hat{s}}(n) = e(n) - v_{\hat{s}}(n)$
$y_{w\hat{s}}(n) = \hat{\boldsymbol{s}}^T(n)\boldsymbol{x}_{\hat{s}(n),y_w(n)}$; $\hat{d}(n) = e_{\hat{s}}(n) + y_{w\hat{s}}(n)$
$y_{\hat{s}}(n) = \hat{\boldsymbol{s}}^T(n)\boldsymbol{x}_{\hat{s}(n),x(n)}(n)$; $y_{\hat{s}w}(n) = \boldsymbol{w}^T(n)\boldsymbol{x}_{w(n),y_{\hat{s}}(n)}(n)$
$e_w(n) = \hat{d}(n) - y_{\hat{s}w}(n)$
$\hat{\boldsymbol{s}}(n+1) = \hat{\boldsymbol{s}}(n) + \mu_s e_{\hat{s}}(n)\boldsymbol{x}_{\hat{s}(n),v(n)}(n)$
$\boldsymbol{w}(n+1) = \boldsymbol{w}(n) + \mu_w e_w(n)\boldsymbol{x}_{\mathrm{LMS},y_{\hat{s}}(n)}(n)$
Using (3.6) compute P_x, and P_{v_g}
$\beta(n) = \alpha\beta(n-1) + \gamma e_{\hat{s}}^2(n)$
Compute $G(n)$ using (3.22)

The weight update equations of $W(z)$ and $\hat{S}(z)$ are same as in proposed method-1 with two exception. The vector $\boldsymbol{x}_{\mathrm{LMS},v(n)}(n) = [v(n), v(n-1), \cdots, v(n-L_s+1)]^T$ is used in the update equation of SPM filter, and instead of using $e_w(n)$, in proposed method-2 the signal $e_{\hat{s}}(n)$ is used in the weight update equation of $W(z)$. The algorithm for the proposed method-2 is given in Table. 3.2

Table 3.2: Algorithm for the proposed method-2.

$d(n) = \boldsymbol{p}^T(n)\boldsymbol{x}_{p(n),x(n)}(n)$; $y_w(n) = \boldsymbol{w}^T(n)\boldsymbol{x}_{w(n),x(n)}(n)$
$v(n) = G(n)v_g(n)$ ($G(n) = 1$ for first iteration)
$y_{ws}(n) - v_s(n) = \boldsymbol{s}^T(n)\boldsymbol{x}_{s(n),(y_w(n)-v(n))}(n)$
$e(n) = d(n) - y_{ws}(n) + v_s(n)$
$v_{\hat{s}}(n) - y_{w\hat{s}}(n) = \hat{\boldsymbol{s}}^T(n)\boldsymbol{x}_{\hat{s}(n),(v(n)-y_w(n))}(n)$
$\hat{d}(n) = e(n) - v_{\hat{s}}(n) + y_{w\hat{s}}(n)$
$y_{\hat{s}}(n) = \hat{\boldsymbol{s}}^T(n)\boldsymbol{x}_{\hat{s}(n),x(n)}(n)$; $y_{\hat{s}w}(n) = \boldsymbol{w}^T(n)\boldsymbol{x}_{w(n),y_{\hat{s}}(n)}(n)$
$e_{\hat{s}}(n) = \hat{d}(n) - y_{\hat{s}w}(n)$
$\hat{\boldsymbol{s}}(n+1) = \hat{\boldsymbol{s}}(n) + \mu_s e_{\hat{s}}(n)\boldsymbol{x}_{\text{LMS},v(n)}(n)$
$\boldsymbol{w}(n+1) = \boldsymbol{w}(n) + \mu_w e_{\hat{s}}(n)\boldsymbol{x}_{\text{LMS},y_{\hat{s}}(n)}(n)$
Using (3.6) compute P_x, and P_{v_g}
$\beta(n) = \alpha\beta(n-1) + \gamma e_{\hat{s}}^2(n)$
Compute $G(n)$ using (3.22)

3.2.3 Simulation Results

In this section, simulation results are presented, to compare the the performance of MFxLMS based ANC system without gain scheduling, Akhtar's method [44], Carini's method [46], proposed method-1 [47], and proposed method-2. The performance comparison is carried out on the basis of following performance measures.

- Relative modeling error of the secondary path $S(z)$ being defined as

$$\Delta D_s(n) = 10\log_{10}\frac{||\boldsymbol{s} - \hat{\boldsymbol{s}}(n)||^2}{||\boldsymbol{s}||^2} \quad \text{dB}. \tag{3.24}$$

- Mean-noise-reduction (MNR) at the error microphone being defined as

$$\text{MNR}(n) = 10\log_{10}\frac{E[e^2(n)]}{E[d^2(n)]} \quad \text{dB}. \tag{3.25}$$

Using data from [4], the acoustic paths $P(z)$, and $S(z)$ are modeled as FIR filters of tap-weight lengths 48, 16, respectively. The adaptive filters $W(z)$, $\hat{S}(z)$ and $\hat{S}_c(z)$ (in Carini's method) are selected as FIR filters of tap-weight length 32, 16 and $16+\Delta$ respectively. The value of Δ and other simulation parameters are given in Table 3.3. The step-size parameters are experimentally adjusted for fast and stable convergence of ANC system. In all methods, the adaptive filter weights are initialized by null vectors. In Carini's method the coefficients of the first part of $\hat{\boldsymbol{s}}_c(n)$, i.e., $\hat{\boldsymbol{s}}_0(n)$ are initialized by all ones. The original unwanted noise signal $x(n)$, at the reference microphone, is a multi-tonal input with frequencies 100, 200, 300, and 400 Hz, and its variance is adjusted to 2. A zero-mean WGN with variance 0.002 is added with $x(n)$ to account for any measurement noise. The modeling excitation signal $v_g(n)$ is a zero-mean WGN with variance 1 for all methods.

For stable operation of MFxLMS/MFxNLMS algorithm based ANC system the phase error between $\boldsymbol{s}(n)$ and SPM filter must be within the bound of $\pm 90^0$ [15], [19]. Since the secondary path $\boldsymbol{s}(n)$ is unknown, therefore one option could be the offline modeling ($d(n) = 0$) of the secondary path to satisfy the $\pm 90^0$ bound at the start-up of ANC system. The other option (with $d(n)$ present) is to keep ANC filter in sleep state for a while and only the SPM is adapted. In this chapter, the second option is used and ANC filter is in sleep state from $n = 0$ to $n = 5000$ as did by Carini and Malatini in [45, 46]. In all the simulation results the background noise, $v_d(n)$, is assumed to be zero. The sampling frequency is 2kHz, and the forgetting factor is selected as 0.99. The jumps in the middle of all the simulation results is due to the perturbation in the impulse responses of the acoustic paths

Table 3.3: Simulation parameters for online secondary path modeling 1) without gain scheduling (modified filtered-x-LMS algorithm) and 2) with gain scheduling (All other methods).

	Parameters
MFxLMS	$\mu_w = 5 \times 10^{-5}$, $\mu_s(n) = \mu_s = 1 \times 10^{-2}$.
Akhtar's method [44]	$\mu_w = 5 \times 10^{-5}$, $\mu_{s_{\min}} = 1 \times 10^{-3}$, $\mu_{s_{\max}} = 1 \times 10^{-2}$, $\sigma_{\min} = 0.001$, $\sigma_{\text{miax}} = 1$.
Carini's method [46]	$\mu_{s_{\min}} = 4 \times 10^{-3}$, $\Delta = 8$, $\hat{\lambda} = 0.6$, $R(n) = 1$
Proposed method-1 [47]	$\mu_w = 5 \times 10^{-5}$, $\mu_s(n) = \mu_s = 7 \times 10^{-3}$, $\alpha = 0.9985$, $\gamma = 0.004$.
Proposed method-2	$\mu_w = 5 \times 10^{-5}$, $\mu_s(n) = \mu_s = 7 \times 10^{-3}$, $\alpha = 0.9985$, $\gamma = 0.004$.

$P(z)$ and $S(z)$. The data for the perturbed acoustic paths is also taken from [4]. All the simulation results are averaged over 10 independent realizations.

In Fig. 3.4(a) the curves for relative modeling error, as defined in (3.24), are plotted in dB for different methods. It is clear from Fig. 3.4(a) that Carini's method results in poor modeling accuracy of SPM filter. Since in Carini's method, after the convergence of ANC system, the step-size for SPM filter freezes to a small value, therefore slower convergence of SPM filter is observed in Carini's method after acoustic path perturbation. All other methods including the proposed method-1 and proposed method-2 performs almost similarly, and results in improved modeling accuracy of SPM filter compared to Carini's method.

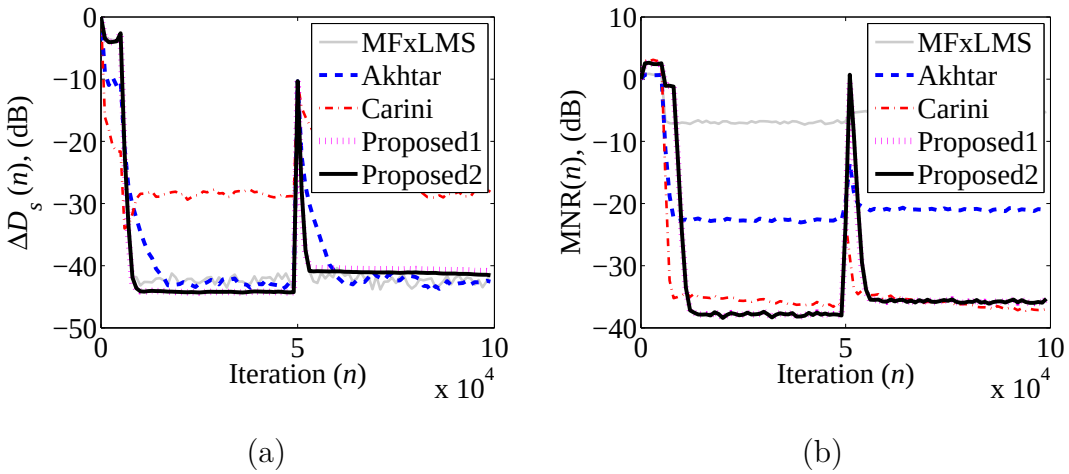

(a) (b)

Figure 3.4: (a) Relative modeling error, $\Delta D_s(n)$(dB), (b) Mean-noise-reduction, MNR(n) (dB).

As stated earlier, higher modeling accuracy does not mean less residual error. However, improved modeling accuracy is desirable to have large stability margins. In Fig. 3.4(b) the curves for MNR, as defined in (3.25), are plotted in dB for different methods. It is clear from Fig. 3.4(b), that MFxLMS algorithm without gain scheduling degrades the NRP of ANC system. Akhtar's method gives improved NRP compared to MFxLMS algorithm without gain scheduling. This improved NRP performance of Akhtar's method is due to gain scheduling strategy given in (3.8). However, for Akhtar's method the value of $\rho(n)$ is never zero in steady-state, and $\sigma^2_{\max}$ will affect the NRP of ANC system. Although Carini method has poor modeling accuracy, but the gain scheduling strategy of Carini's method is efficient than Akhtar's method, and hence results in improved NRP of ANC system. The performance of proposed method-1 and proposed method-2 is almost similar. Both the proposed method-1 and proposed method-2 gives modeling accuracy almost equal to the one achieved by Akhtar's method, and NRP as achieved by Carini's method.

3.2.4 Effect of γ on $\Delta D_s(n)$ and MNR(n)

From (3.22) and (3.23) it is clear, that the large value of γ will result in large value of $\beta(n)$. The gain at steady-state is determined by $\beta(n)/P_{v_g}(n)$ (see (3.23)). The large value of $\beta(n)$ at steady-state will result in large gain and thus degrades the NRP of ANC system. However, if we select a small value of γ, then it means that we are giving less weightage to the error signal $e_{\hat{s}}(n)$ (see 3.23). The small value of γ thus results in poor modeling accuracy of SPM filter. In order to meet the conflicting requirements of having good tracking capability of SPM filter and improved NRP, it is desirable that the parameter γ is made time-varying. When SPM filter is far from steady-state, the large value of γ is required to give more weightage to the error signal $e_{\hat{s}}(n)$ and thus allow the SPM filter to converge properly. The small value of γ is required at steady-state to reduce the gain to a lower steady-state value, and hence to improve the NRP of ANC system. In order to show the effect of using different values of γ on $\Delta D_s(n)$ and MNR(n), a simulation experiment is performed for proposed method-1 with same simulation parameters as in Table. 3.3 and with values of $\gamma_{\max} = 0.01$ and $\gamma_{\min} = 0.001$. The simulation results are shown in Fig. 3.5. It is clear from Fig. 3.5(b) that with $\gamma = \gamma_{\min}$ improved NRP is achieved. This is because, with small value of γ the gain drops quickly and settles to a lower steady-state value. This quick drop of the gain $G(n)$ will reduce the variance of input excitation signal of SPM filter, and thus freezing the adaptation of SPM filter. In this case the SPM filter may not converge to the optimal value. On the other hand, the large value of $\gamma = \gamma_{\max}$ will not allow the gain to drop very quickly, thus avoids freezing of the adaptation process of SPM filter. It is clear form Fig. 3.5(b) that for $\gamma = \gamma_{\max}$ the SPM filter continues adaptation and settles to a lower steady state value. However, it is clear

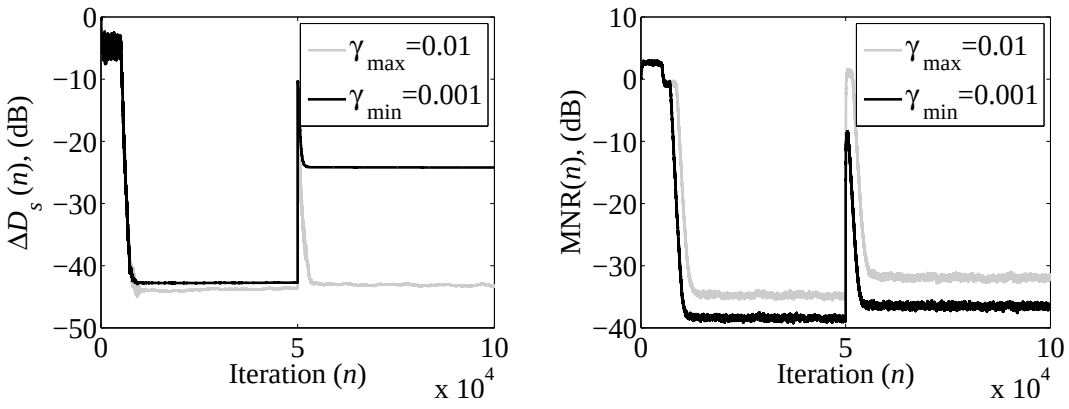

(a) (b)

Figure 3.5: In proposed method-1, the effect of γ on (a) Relative modeling error, $\Delta D_s(n)$(dB), (b) Mean-noise-reduction, MNR(n) (dB).

from Fig. 3.5(b) that $\gamma = \gamma_{\max}$ degrades the MNR(n) value.

The above discussion of the effect of using different values of γ on $\Delta D_s(n)$ and MNR(n) in proposed method-1 is equally applicable to proposed method-2 as well.

3.2.5 Remarks Regarding Proposed Method-1 and Method-2

1. In proposed method-1 and proposed method-2, LMS adaptive algorithm is used for ANC filter and SPM filter. For LMS adaptive algorithm the allowable range of step-size parameter, μ, for which the algorithm remains stable is given by [4]

$$0 < \mu < \frac{2}{3LP_x}, \tag{3.26}$$

where L is the length of adaptive filter, P_x is the power of the input excitation signal of adaptive filter. It is clear from (3.26), that the LMS adaptive

algorithm is not suitable for non-stationary input excitation signal. This is because the time-varying variance of the input excitation signal may drive the initially selected stable step-size parameter μ out of the allowable stable range of operation. For non-stationary input signal it is desirable that the step-size parameter μ should adjust its value to stay with in the allowable range. The solution to the problem is to use normalized LMS (NLMS) algorithm [51]-[54].

2. In proposed method-1 and proposed method-2 fixed value of γ is used for gain scheduling. As discussed previously, in order to meet the conflicting requirements of good modeling accuracy of SPM filter and improved NRP of ANC system, the value of γ should be time-varying.

3. At steady-state, The NRP of proposed method-1 and proposed method-2 is inferior to that of Carini's method. This is clear from Fig. 3.4(b), that the MNR(n) curves of proposed methods have already converged to steady-state value, while that of Carini's method has a decreasing trend and can settle to lower steady state value if the time duration of simulation is increased.

In order to address the above mentioned problems, a new gain scheduling strategy with time-varying parameter γ is proposed. In addition to this, NLMS adaptive algorithm is used for both the ANC filter and the SPM filter to deal with non-stationary input excitation signals.

3.2.6 Proposed Method-3

The structure of the proposed method-3 [48] is almost the same as given in Fig. 3.3, with two exceptions: 1) NLMS adaptive algorithm is used for ANC filter and SPM

filter to deal with non-stationary input excitations signals, and 2) For time-varying γ, two parameters $\gamma_{\min}$ and $\gamma_{\max}$ are given as an input to the gain computation block in Fig. 3.3.

The normalized step-size for ANC filter is computed as $\mu_w(n)$

$$\mu_w(n) = \frac{\mu_w}{\boldsymbol{x}^T_{\text{NLMS},y_{\hat{s}}(n)}(n)\boldsymbol{x}_{\text{NLMS},y_{\hat{s}}(n)}(n) + \delta}, \tag{3.27}$$

where μ_w is the fixed step-size parameter, δ is a small positive number to avoid division by zero, and $\boldsymbol{x}_{\text{NLMS},y_{\hat{s}}(n)}(n)$ is the input signal vector of NLMS adaptive algorithm for $W(z)$ as defined in (3.16). Similarly the normalized step-size for SPM filter is computed as $\mu_s(n)$

$$\mu_s(n) = \min\left(\frac{\mu_s}{\boldsymbol{x}^T_{\hat{s}(n),v(n)}(n)\boldsymbol{x}_{\hat{s}(n),v(n)}(n)}, \mu_s\right), \tag{3.28}$$

where μ_s is the fixed step-size parameter, and $\boldsymbol{x}_{\hat{s}(n),v(n)}(n) = [G(n)v_g(n), G(n-1)v_g(n-1), \cdots, G(n-L_s+1)v_g(n-L_s+1)]^T$ is the input signal vector of SPM filter. The gain $G(n)$ in proposed method-3 is computed as

$$G(n) = \begin{cases} P_x(n)/P_{v_g} & (\beta(n) \geq P_x(n)/P_{v_g}) \\ \beta(n) & \text{(Otherwise)} \end{cases}, \tag{3.29}$$

where $P_x(n)$ (the index n is used to emphasize that now the power of input excitation signal is time-varying) and P_{v_g}, respectively, are the powers of the reference signal $x(n)$ and auxiliary noise $v_g(n)$ both of which can be estimated using (3.6), and the time-varying term $\beta(n)$ can be computed as

$$\beta(n) = \alpha\beta(n-1) + \gamma(n)\frac{P_{e_{\hat{s}}}(n)}{P_x(n) + P_{v_g}}, \tag{3.30}$$

where $0 < \alpha < 1$ and $\gamma(n) > 0$ are controlling parameters, and $e_{\hat{s}}(n)$ is the error signal of SPM filter. The value of the time-varying parameter $\gamma(n)$ can be computed as

$$\gamma(n) = \rho(n)\gamma_{\min} + ((1-\rho(n))\gamma_{\max}), \tag{3.31}$$

where $\gamma_{\min}$ and $\gamma_{\max}$ are minimum and maximum values of $\gamma(n)$, respectively, that are selected by trial and error method. It is important to note that the variation of $\rho(n)$ in proposed method is different from that of Akhtar's method. This is because of using different gain scheduling strategies in these methods. In proposed method, when SPM filter is far from steady-state $\rho(n) \approx 0 \Rightarrow \gamma(n) = \gamma_{\max}$, and after the convergence of SPM filter and ANC system $\rho(n) \rightarrow 1 \Rightarrow \gamma(n) = \gamma_{\min}$. The variation of $\rho(n)$ in proposed method-3 is explained in the next section.

The weight update equations for ANC filter and SPM filter are same as for proposed method-1 with following exceptions: 1) Instead of μ_w, $\mu_w(n)$ (see (3.27)) is used for ANC filter, 2) Instead of μ_s, $\mu_s(n)$ (see (3.28)) is used for SPM filter, and 3) The gain is computed using (3.29)-(3.31). Also it is important to note that the step-size $\mu_s(n)$ for the SPM filter is upper bounded by μ_s (see (3.28)) to avoid very large value of step-size. The reason behind the large value of step-size is the small value of the denominator term $(\boldsymbol{x}^T_{\hat{s}(n),v(n)}(n)\boldsymbol{x}_{\hat{s}(n),v(n)}(n))$ in (3.28) due to proposed gain scheduling. The algorithm for the proposed method-3 is given in Table. 3.4

Variation of $\rho(n)$ in proposed Method-3 [48]: For convenience, the equation for $\rho(n)$ as defined in (3.5) is repeated here, and is given by

$$\rho(n) = \frac{P_{e_{\hat{s}}}(n)}{P_e(n)} = \frac{E[(d(n) - y_{ws}(n))^2] + E[(v_s(n) - v_{\hat{s}}(n))^2]}{E[(d(n) - y_{ws}(n))^2] + E[(v_s(n))^2]}, \tag{3.32}$$

It is important to note that the same equation is used to compute the parameter $\rho(n)$ in Akhtar's method and proposed method-3. However, the variation of the parameter $\rho(n)$ is different for Akhtar's and proposed method-3. This is due to different gain scheduling strategies of Akhtar's and proposed method-3. The variation of $\rho(n)$ for Akhtar's method is already explained, and it is clear form that explanation that when ANC system is far from steady-state $\rho(n) \approx 1$, and

Table 3.4: Algorithm for the proposed method-3 [48].

$d(n) = \boldsymbol{p}^T(n)\boldsymbol{x}_{p(n),x(n)}(n)$; $y_w(n) = \boldsymbol{w}^T(n)\boldsymbol{x}_{w(n),x(n)}(n)$
$v(n) = G(n)v_g(n)$ ($G(n) = 1$ for first iteration)
$y_{ws}(n) - v_s(n) = \boldsymbol{s}^T(n)\boldsymbol{x}_{s(n),(y_w(n)-v(n))}(n)$
$e(n) = d(n) - y_{ws}(n) + v_s(n)$
$v_{\hat{s}}(n) = \hat{\boldsymbol{s}}^T(n)\boldsymbol{x}_{\hat{s}(n),v(n)}(n)$; $e_{\hat{s}}(n) = e(n) - v_{\hat{s}}(n)$
$y_{w\hat{s}}(n) = \hat{\boldsymbol{s}}^T(n)\boldsymbol{x}_{\hat{s}(n),y_w(n)}$; $\hat{d}(n) = e_{\hat{s}}(n) + y_{w\hat{s}}(n)$
$y_{\hat{s}}(n) = \hat{\boldsymbol{s}}^T(n)\boldsymbol{x}_{\hat{s}(n),x(n)}(n)$; $y_{\hat{s}w}(n) = \boldsymbol{w}^T(n)\boldsymbol{x}_{w(n),y_{\hat{s}}(n)}(n)$
$e_w(n) = \hat{d}(n) - y_{\hat{s}w}(n)$
$\mu_w(n)$ and $\mu_s(n)$ are computed, respectively, using (3.27), (3.28)
$\hat{\boldsymbol{s}}(n+1) = \hat{\boldsymbol{s}}(n) + \mu_s(n)e_{\hat{s}}(n)\boldsymbol{x}_{\hat{s}(n),v(n)}(n)$
$\boldsymbol{w}(n+1) = \boldsymbol{w}(n) + \mu_w(n)e_w(n)\boldsymbol{x}_{\text{LMS},y_{\hat{s}}(n)}(n)$
Using (3.6) compute $P_x(n)$, $P_{e_{\hat{s}}}(n)$, $P_e(n)$, and P_{v_g}
Compute $\rho(n)$, $\gamma(n)$, and $\beta(n)$, respectively, using (3.5), (3.31), and (3.30).
Compute $G(n)$ using (3.29)

$\rho(n) \to 0$ as SPM filter and ANC system converges.

The variation of $\rho(n)$ in proposed method-3 is almost apposite to that of Akhtar's method. In proposed method-3 when SPM filter is far from steady-state $\rho(n) \approx 0$ and $\rho(n) \to 1$ as SPM filter and ANC system converges. When SPM filter is far from steady state, the gain scheduling of the proposed method-3 is such that it results in $E[(v_s(n))^2] >> E[(d(n)-y_{ws}(n))^2]$ and $\rho(n) \approx 0$. After SPM filter and ANC system converges, the gain scheduling strategy of proposed method-3 reduces the gain $G(n)$ to very small value ensuring $E[(d(n) - y_{ws}(n))^2] >> E[(v_s(n))^2]$,

and hence $\rho(n) \rightarrow 1$.

3.2.7 Simulation Results

In this section simulation results are presented to compare the performance of the proposed method-3, with Akhtar's [44] and Carini's method [46]. The original unwanted noise signal $x(n)$ is assumed to be non-stationary. The signal $x(n)$ is a multi-tonal input with frequencies 100, 200, 300, and 400 Hz, and initially its variance is adjusted to 2. The variance of the signal $x(n)$ is changed to 6, 5, and 1, respectively, at $n = 20000$, $n = 50000$, and $n = 70000$. A zero-mean WGN with variance 0.002 is added with $x(n)$ to account for any measurement noise. The simulation parameters for the proposed method-3 are given by: $\mu_w = 5 \times 10^{-1}$, $\mu_s = 7 \times 10^{-3}$, $\alpha = 0.995$, $\gamma_{\min} = 0.02$, and $\gamma_{\max} = 0.1$. The rest of the simulation parameters are the same as used for the simulation results of Fig. 3.4. The jumps in the middle of all the simulation results is due to: 1) acoustic paths perturbation, and 2) change in the variance of $x(n)$ from 6 to 5. All the simulation results are averaged over 10 independent realizations.

In Fig. 3.6(a), the curves for relative modeling error, as defined in (3.24) are plotted in dB for different methods. It is clear from Fig. 3.6(a) that the performance of proposed method-3 is almost same as that of Crini's method. As stated earlier that higher modeling accuracy does not mean less MNR value. The objective of ANC system is to reduce the noise at the summing junction. It is clear from Fig.3.6(b) that the proposed method-3 outperforms than Akhtar's and Carini's method in terms of improving the MNR value at the steady-state.

Fig. 3.7(a) shows the variation of parameter $\rho(n)$ in Akhtar's and proposed method-3. Due to different gain scheduling strategies of Akhtar's and proposed

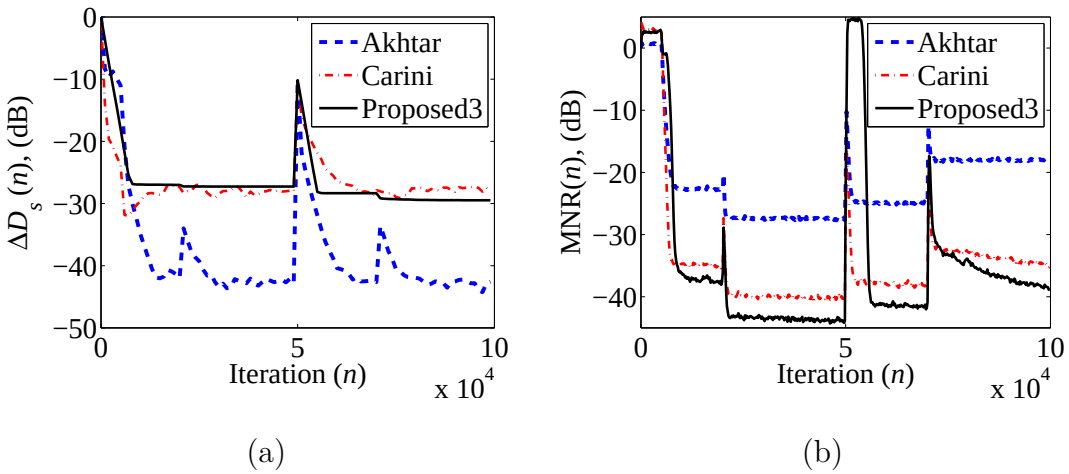

Figure 3.6: (a) Relative modeling error, $\Delta D_s(n)$(dB), (b) Mean-noise-reduction, MNR(n) (dB).

method-3, the variation of $\rho(n)$ is different. In Akhtar's method, when ANC system is far from steady-state $\rho(n) \approx 1$, and $\rho(n) \to 0$ as the SPM filter and ANC system converges. In proposed method-3, the variation of $\rho(n)$ is such that it is close to zero when SPM filter is far from steady-state and $\rho(n) \to 1$ as SPM filter and ANC system converges.

Fig. 3.7(b) shows the variation of parameter $\gamma(n)$ in proposed method-3 as defined in (3.21). When ANC system is far from staedy-state $\rho(n) \approx 0 \Rightarrow \gamma(n) = \gamma_{\max}$. As the ANC system converges $\rho(n) \to 1 \Rightarrow \gamma(n) \to \gamma_{\min}$.

Fig. 3.8(a) and 3.8(b), respectively shows the plot of normalized step-size $\mu_s(n)$ and $\mu_w(n)$. As stated earlier, instead of offline modeling of SPM filter, the ANC filter is in sleep state from $n = 0$ to $n = 5000$ and only the SPM filter is allowed to update its coefficients. Therefore the step-size parameter $\mu_w(n)$ is not allowed to update during this period, and this can be observed form Fig. 3.8(b) where $\mu_w(n)$ is not defined for $n = 0$ to $n = 5000$

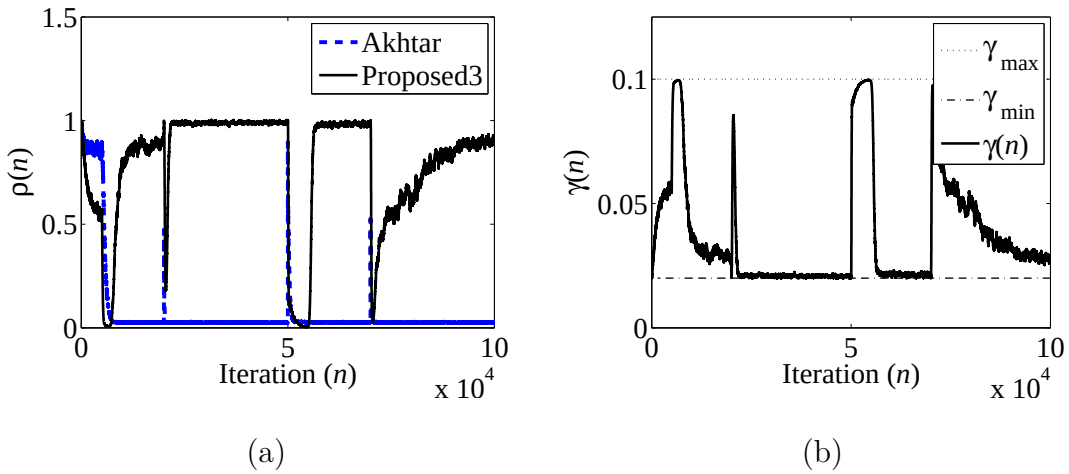

Figure 3.7: (a) Variation of parameter $\rho(n)$ as defined in (3.5), (b) Variation of parameter $\gamma(n)$ as defined in (3.31).

3.2.8 Remarks Regarding Proposed Method-3

1. In proposed method-3, NLMS adaptive algorithms are used for adaptive filters, so it can work fine with non-stationary input excitation signals.

2. The gain scheduling strategy of proposed method-3 is such that it improves the MNR(n) value of ANC system at steady-state, however the modeling accuracy of SPM filter is degraded compared to proposed method-1 and proposed method-2. It is desirable to have both the good modeling accuracy to increase the stability margins, and lower MNR(n) value at steady-state.

3. The gain in proposed method-1, proposed method-2, and proposed method-3 is upper bounded by the power ratio ($P_x(n)/P_{v_g}$) (see (3.22), and (3.29)), where $P_x(n)$ and P_{v_g}, respectively, are the powers of original unwanted noise signal $x(n)$ sensed by the reference microphone, and auxiliary random WGN signal. The term ($d(n)-y_{ws}(n)$) in the error signal $e(n)$ acts as an interference

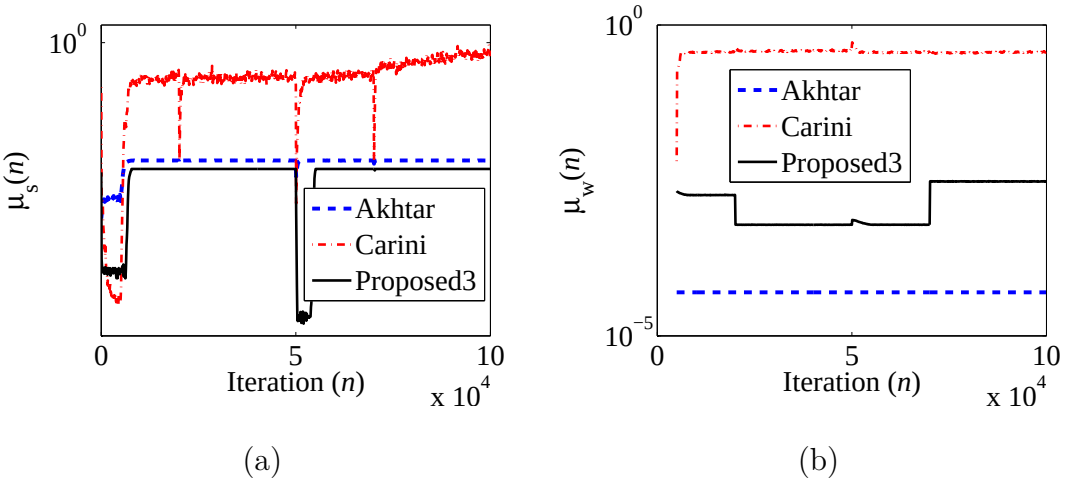

Figure 3.8: (a) Time-varying step-size parameter $\mu_s(n)$ as defined in (3.28), (b) Time-varying step-size parameter $\mu_w(n)$ as defined in (3.27).

for SPM filter, while the term $v_s(n)$ (function of $G(n)$, see (3.12)) in $e(n)$ is the desired signal for SPM filter. In case of strong perturbation in acoustic paths, the interference term of SPM filter $(d(n) - y_{ws}(n))$ may be very large. Under this scenario, if the gain is upper bounded by the ratio $(P_x(n)/P_{v_g})$, than it may result in a very low SNR, $(v_s(n)/(d(n) - y_{ws}(n)))$, value for SPM filter, and ANC system may become unstable. The simulation results with strong perturbation in acoustic paths are shown in Fig. 3.9. All the simulation conditions are the same as used for Fig. 3.6 except that instead of mild perturbation in acoustic paths, a strong perturbation is introduced in the middle of simulation. The strong perturbation is simulated by giving 2 samples right circular shift to the impulse response of original acoustic paths. It is clear from Fig. 3.9, that the proposed method-3 is unstable after the acoustic paths perturbation in the middle of simulation.

4. The gain $G(n)$ in all the existing methods and in the proposed methods

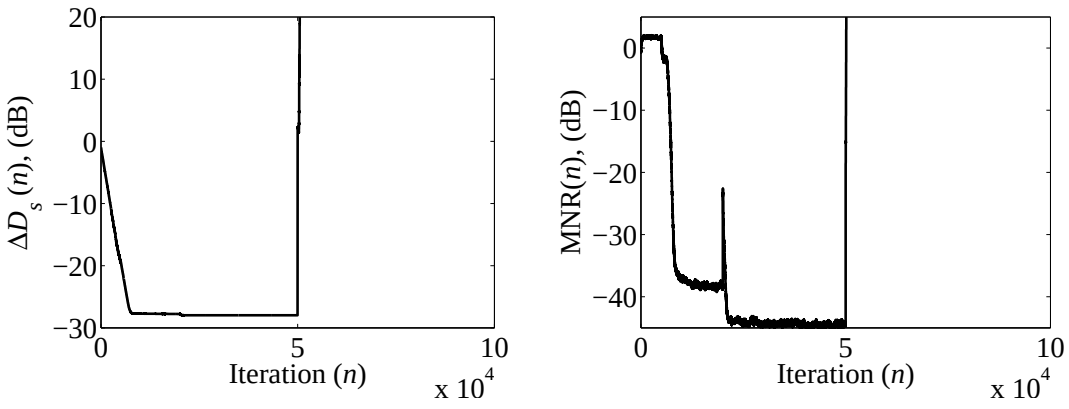

(a) (b)

Figure 3.9: Proposed method-3 with strong perturbation in acoustic paths: (a) Relative modeling error, $\Delta D_s(n)$(dB), (b) Mean-noise-reduction, MNR(n) (dB).

depends either on the signal $e(n)$ or on the signal $e_{\hat{s}}(n)$. The uncorrelated WGN disturbance $v_d(n)$ (to model the background noise) at the error microphone (see Fig. 3.3) directly contributes to both $e(n)$ and $e_{\hat{s}}(n)$. This means that the large value of $v_d(n)$ results in large value of gain $G(n)$. At the steady-state, the large value of $G(n)$ degrades the NRP of ANC system which is undesirable.

In order to solve the above mentioned problems a new gain scheduling strategy is proposed in [49].

3.2.9 Proposed Method-4

The block diagram of the proposed method-4 [49] is shown in Fig. 3.10. Here a new gain scheduling strategy is proposed which

- improves the convergence speed of SPM filter,
- improves the NRP of ANC system at steady-state,

- improves the performance of ANC system in the presence of uncorrelated WGN at error sensor,
- makes the ANC system more robust, so that it should remain stable even for very strong perturbations in acoustic paths, and
- reduces the computational cost of the algorithm compared to Carini's method.

Assuming $v_d(n) = 0$ in Fig. 3.10, it is evident from (3.11) that the time-varying gain $G(n)$ can be employed to control the contribution of $E[(v_s(n))^2]$ to $E[e^2(n)]$. In the proposed approach the gain $G(n)$ is computed such that the ratio $R(n)$ (defined in (3.10)) is time-varying. As long as $\hat{\boldsymbol{s}}(n)$ is away from $\boldsymbol{s}(n)$, the ratio $R(n)$ is lower than 0 dB, i.e., $E[(v_s(n))^2] > E[(d(n)-yws(n))^2]$, guaranteeing fast convergence of SPM filter. The fast convergence of SPM filter is desirable, because accurate model of $\boldsymbol{s}(n)$ is needed for modified filtered-x normalized least-mean-square (MFxNLMS) algorithm-based adaptation of ANC filter. After convergence of the SPM filter, $R(n)$ becomes greater than 0 dB ensuring that $E[(v_s(n))^2] < E[(d(n) - y_{ws}(n))^2]$, which in turn improves the NRP.

Gain Scheduling Strategy of the proposed Method-4: In proposed method-4 [49], a new two-stage gain scheduling strategy is proposed to compute the time-varying gain, $G(n)$. The two stages are described as

Stage 1: When the ANC system is very far from steady-state i.e, when $P_{e_{\hat{s}}}(n) > P_x(n)$. This situation can occur

- at the start-up of ANC system, and
- when there is a strong perturbation in the acoustic paths.

Stage 2: When the ANC system is close to steady-state i.e, when $P_{e_{\hat{s}}}(n) \leq P_x(n)$.

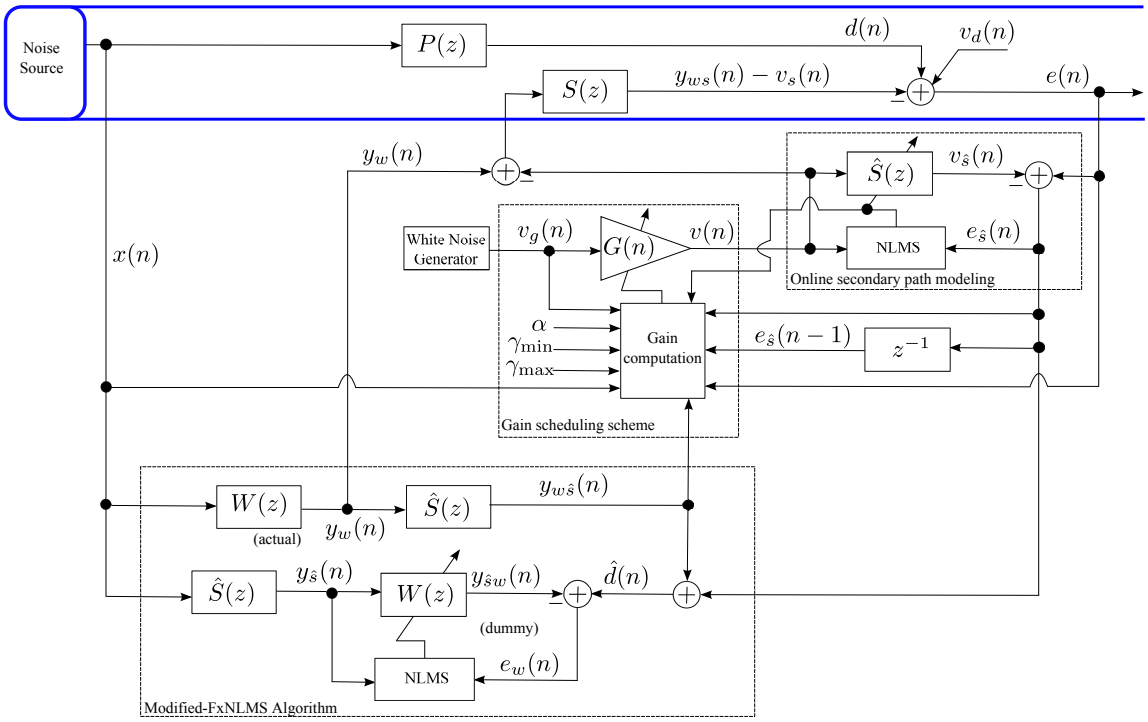

Figure 3.10: Online secondary path modeling with gain scheduling, proposed method-4 [49].

The subsequent discussion will explain the computation of $G(n)$ for each of these stages one by one.

Stage 1: $P_{e_{\hat{s}}}(n > P_x(n)$, When the ANC System is Very Far From Steady-State. From Fig. 3.10 the error signal, $e_{\hat{s}}(n)$ can be computed as

$$e_{\hat{s}}(n) = [d(n) - y_{ws}(n)] + [v_s(n) - v_{\hat{s}}(n)], \tag{3.33}$$

where the first part $(d(n) - y_{ws}(n))$ carries information about the convergence of the ANC filter $\boldsymbol{w}(n)$, and acts as an interference to the adaptation of the SPM filter. The second part $(v_s(n) - v_{\hat{s}}(n))$ plays exactly the reverse role, i.e., carries information about the convergence of $\hat{\boldsymbol{s}}(n)$ and acts as an interference for $\boldsymbol{w}(n)$.

The power of the error signal of $\hat{\boldsymbol{s}}(n)$, can be written as:

$$P_{e_{\hat{s}}}(n) = P_{d-y_{ws}}(n) + P_{v_s-v_{\hat{s}}}(n), \tag{3.34}$$

where $P_{d-y_{ws}}(n)$ denotes the estimate of the power of interference term $(d(n) - y_{ws}(n))$ in the error signal of $\hat{\boldsymbol{s}}(n)$, and $P_{v_s-v_{\hat{s}}}(n)$ denotes the estimate of the power of the desired term $(v_s(n) - v_{\hat{s}}(n))$ in the error signal of $\hat{\boldsymbol{s}}(n)$. At this stage, the interference term $(d(n) - y_{ws}(n))$ for $\hat{\boldsymbol{s}}(n)$ is strong, therefore the gain $G(n)$ is varied in accordance with 1) the convergence status of $\boldsymbol{w}(n)$ (power of interference term $P_{d-y_{ws}}(n)$), 2) the convergence status of $\hat{\boldsymbol{s}}(n)$. At this stage the gain $G(n)$ is computed by making the power $P_{v_s}(n)$ to be equal to the power $P_{e_{\hat{s}}}(n-1)$. In the case of ANC systems, the signal $v_s(n)$ is not accessible, therefore the following condition

$$P_{v_{\hat{s}}}(n) = P_{e_{\hat{s}}}(n-1), \tag{3.35}$$

is forced to be satisfied, where $P_{e_{\hat{s}}}(n-1))$ is estimated online using (3.6), and $P_{v_{\hat{s}}}(n)$ can be expressed as

$$P_{v_{\hat{s}}}(n) \approx G^2(n)||\hat{\boldsymbol{s}}(n)||^2 E[v_g^2(n)] = G^2(n)||\hat{\boldsymbol{s}}(n)||^2, \tag{3.36}$$

where $E[v_g^2(n)] = 1$. Equating the right hand sides of (3.35) and (3.36), and solving for $G(n)$, we get

$$G(n) = \sqrt{\frac{P_{e_{\hat{s}}}(n-1)}{||\hat{\boldsymbol{s}}(n)||^2}} = \sqrt{\frac{P_{d-y_{ws}}(n-1) + P_{v_s-v_{\hat{s}}}(n-1)}{||\hat{\boldsymbol{s}}(n)||^2}}. \tag{3.37}$$

As long as $\hat{\boldsymbol{s}}(n)$ is away from $\boldsymbol{s}(n)$, the gain $G(n)$ will keep on increasing due to the presence of the term $P_{v_s-v_{\hat{s}}}(n-1)$ in $P_{e_{\hat{s}}}(n-1)$. This will ensure fast convergence of $\hat{\boldsymbol{s}}(n)$ and result in the ratio $R(n) < 0$ dB. When $\hat{\boldsymbol{s}}(n) \to \boldsymbol{s}(n)$, $v_{\hat{s}}(n) \to v_s(n)$, and $e_{\hat{s}}(n) \to (d(n) - y_{ws}(n))$, the positive feedback scenario for the gain $G(n)$ will automatically breakup and the ratio $R(n) \to 0$ dB.

Stage 2: $P_{e_{\hat{s}}}(n) \leq P_x(n)$, When the ANC System is Close to Steady-State. If only (3.37) is used for computing gain, $G(n)$, then the maximum performance we can achieve in steady-state can result in $R(n) = 0$ dB. However, to have improved NRP at steady-state, it is desirable to have $R(n) > 0$ dB. When the condition $P_{e_{\hat{s}}}(n) \leq P_x(n)$ is satisfied, the ANC system is close to steady-state, and in this case the gain $G(n)$ is computed as

$$G(n) = \begin{cases} \sqrt{\frac{P_x(n)}{P_{v_g}}} & (\beta(n) > \frac{P_x(n)}{P_{v_g}}) \\ \beta(n) & (\text{Otherwise}) \end{cases}, \tag{3.38}$$

where $P_x(n)$ and P_{v_g}, respectively, are the powers of the reference signal, $x(n)$, and auxiliary noise $v_g(n)$ which can be estimated using (3.6), and the time-varying term $\beta(n)$ can be computed as

$$\beta(n) = \alpha\beta(n-1) + \gamma(n)\left(\frac{P_{e_{\hat{s}}d}(n)}{P_{v_g}}\right)^2, \tag{3.39}$$

where $0 < \alpha < 1$ and $\gamma(n) > 0$ (will be explained later in this section) are controlling parameters, and $P_{e_{\hat{s}}d}(n)$ is computed as

$$E[e_{\hat{s}}(n)e_{\hat{s}}(n-1)] \approx P_{e_{\hat{s}}d}(n) = \lambda P_{e_{\hat{s}}d}(n-1) + (1-\lambda)e_{\hat{s}}(n)e_{\hat{s}}(n-1), \tag{3.40}$$

where $E[e_{\hat{s}}(n)e_{\hat{s}}(n-1)]$ is the autocorrelation between $e_{\hat{s}}(n)$ and $e_{\hat{s}}(n-1)$. When switching occurs from first stage of gain scheduling to second stage, the condition $(\beta(n) > (P_x(n)/P_{v_g}))$ may be true. In such a situation, if we make $G(n) = \beta(n)$ then a large value of $\beta(n)$ will result in large value of $G(n)$, thus resulting in a large value of the interference term $(v_s(n) - v_{\hat{s}}(n))$ in the error signal of $\boldsymbol{w}(n)$. This may result in the divergence of $\boldsymbol{w}(n)$, and hence the whole ANC system may become unstable. In order to avoid such a situation the value of the $G(n)$ is upper bounded by $(\sqrt{\frac{P_x(n)}{P_{v_g}}})$ (see 3.38), until the condition $(\beta(n) > (P_x(n)/P_{v_g}))$ is false; otherwise the gain will follow the variation of $\beta(n)$.

In the presence of an uncorrelated disturbance $v_d(n)$ at the error microphone $E[e_{\hat{s}}(n)e_{\hat{s}}(n-1)]$ can be expressed as

$$\begin{aligned} E[e_{\hat{s}}(n)e_{\hat{s}}(n-1)] &= E[(d(n)-y_{ws}(n))(d(n-1)-y_{ws}(n-1))]+ \\ & E[(v_s(n)-v_{\hat{s}}(n))(v_s(n-1)-v_{\hat{s}}(n-1)]+ \\ & E[v_d(n)v_d(n-1)]. \end{aligned} \tag{3.41}$$

where $E[v_d(n)v_d(n-1)]=0$ as $v_d(n)$ is assumed as uncorrelated zero mean WGN. Thus the correlation $E[e_{\hat{s}}(n)e_{\hat{s}}(n-1)] \approx P_{e_{\hat{s}}d}(n)$ is independent of the uncorrelated disturbance signal $v_d(n)$. In (3.41) a delay of at least L_s (length of secondary path) samples is needed for correlation term corresponding to $v(n)$ (second term on R.H.S of (3.41)) to vanish [35]. It is worth mentioning that, in the presence of an uncorrelated disturbance $v_d(n)$, the gain $G(n)$ computed using instantaneous energy of the signal $e_{\hat{s}}(n)$ has large steady-state value [55]. Therefore, in proposed method-4, employing $P_{e_{\hat{s}}d}(n)$ in computing $\beta(n)$ and hence the gain $G(n)$ results in small steady-state gain even in the presence of $v_d(n)$ at the error microphone.

For a typical simulation the effect of $\gamma(n)$ on the relative modeling error $\Delta D_s(n)$ and ANP, $E[(v_s(n))^2]$, is studied in Fig. 3.11. If there is a perturbation in the acoustic paths, large value of $\gamma(n)$ is desirable to have good modeling accuracy. However a large value of $\gamma(n)$ at steady-state would result in a large value for $E[(v_s(n))^2]$, and thus degrades the NRP (see (3.11)). On the other hand, a small value of $\gamma(n)$ reduces the contribution of $E[(v_s(n))^2]$, but the performance is not good in terms of $\Delta S(n)$. In order to meet the conflicting requirements of a small steady-state value for $E[(v_s(n))^2]$, and a good modeling accuracy, the value of $\gamma(n)$ in (3.39) is made adaptive and is computed as

$$\gamma(n) = \rho(n)\gamma_{\min} + (1-\rho(n))\gamma_{\max}, \tag{3.42}$$

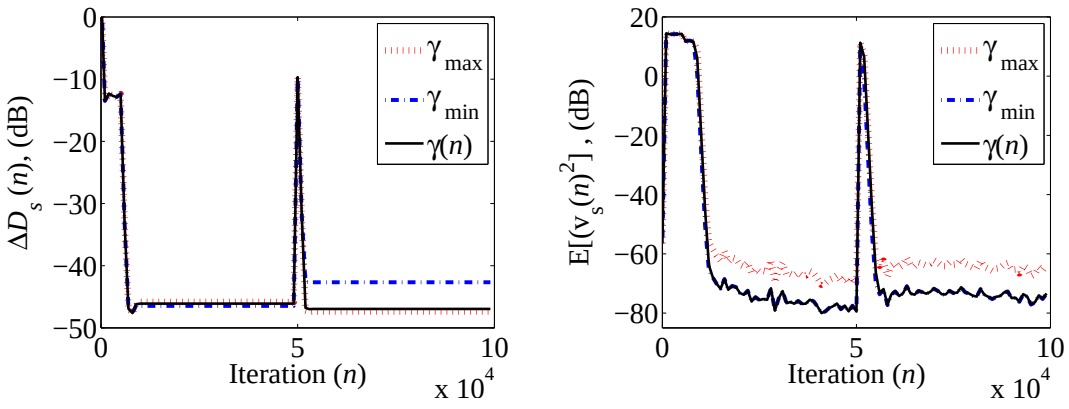

(a) (b)

Figure 3.11: Proposed method-4: Effect of different values of γ on (a) Relative modeling error, $\Delta D_s(n)$(dB), (b) Auxiliary-noise-power, ANP (dB): $\gamma_{\max} = 0.9$, $\gamma_{\min} = 0.3$, and $\gamma(n)$ as defined (3.41).

where $\rho(n) = P_{e_{\hat{s}}}(n)/P_e(n)$ (see (3.32)), and is varying between 0 and 1. The variation of $\rho(n)$ in proposed method-4 is same as explained in proposed method-3. When SPM filter is far from steady-state $\rho(n) \approx 0 \Rightarrow \gamma(n) = \gamma_{\max}$. After the convergence of SPM filter and ANC system $\rho(n) \to 1 \Rightarrow \gamma(n) = \gamma_{\min}$.

Step-Size Variation: In contrast to Carini's method, in the proposed method-4 normalized step-sizes (instead of optimal normalized step-sizes) are employed for $\boldsymbol{w}(n)$ and $\hat{\boldsymbol{s}}(n)$. This reduces the computations required to estimate the optimal step-size parameters. In proposed method-4, the normalized step-size parameter, $\mu_w(n)$, for ANC filter is computed as

$$\mu_w(n) = \frac{\mu_w}{\boldsymbol{x}^T_{\text{NLMS},y_{\hat{s}}(n)}(n)\boldsymbol{x}_{\text{NLMS},y_{\hat{s}}(n)}(n) + P_{e_w}(n)}, \tag{3.43}$$

where μ_w is the fixed step-size parameter, $\boldsymbol{x}_{\text{NLMS},y_{\hat{s}}(n)}(n)$ is the input signal vector of adaptive NLMS algorithm of $W(z)$ at time n as defined in (3.16), and $P_{e_w}(n)$ is the power of error signal of ANC filter (can be estimated using (3.6)). It is shown

Table 3.5: Algorithm for the proposed method-4 [49].

$d(n) = \boldsymbol{p}^T(n)\boldsymbol{x}_{p(n),x(n)}(n)$; $y_w(n) = \boldsymbol{w}^T(n)\boldsymbol{x}_{w(n),x(n)}(n)$
$v(n) = G(n)v_g(n)$ ($G(n) = 1$ for first iteration)
$y_{ws}(n) - v_s(n) = \boldsymbol{s}^T(n)\boldsymbol{x}_{s(n),(y_w(n)-v(n))}(n)$; $e(n) = d(n) - y_{ws}(n) + v_s(n)$
$v_{\hat{s}}(n) = \hat{\boldsymbol{s}}^T(n)\boldsymbol{x}_{\hat{s}(n),v(n)}(n)$; $e_{\hat{s}}(n) = e(n) - v_{\hat{s}}(n)$
$y_{w\hat{s}}(n) = \hat{\boldsymbol{s}}^T(n)\boldsymbol{x}_{\hat{s}(n),y_w(n)}$; $\hat{d}(n) = e_{\hat{s}}(n) + y_{w\hat{s}}(n)$
$y_{\hat{s}}(n) = \hat{\boldsymbol{s}}^T(n)\boldsymbol{x}_{\hat{s}(n),x(n)}(n)$; $y_{\hat{s}w}(n) = \boldsymbol{w}^T(n)\boldsymbol{x}_{w(n),y_{\hat{s}}(n)}(n)$; $e_w(n) = \hat{d}(n) - y_{\hat{s}w}(n)$
$\mu_w(n)$ and $\mu_s(n)$ are computed, respectively, using (3.43), (3.44)
$\hat{\boldsymbol{s}}(n+1) = \hat{\boldsymbol{s}}(n) + \mu_s(n)e_{\hat{s}}(n)\boldsymbol{x}_{\hat{s}(n),v(n)}(n)$
$\boldsymbol{w}(n+1) = \boldsymbol{w}(n) + \mu_w(n)e_w(n)\boldsymbol{x}_{\text{LMS},y_{\hat{s}}(n)}(n)$; Using (3.40) compute $P_{e_{\hat{s}}d}(n)$
Using (3.6) compute $P_x(n)$,$P_{e_{\hat{s}}}(n)$, $P_{e_{\hat{s}}}(n-1)$, $P_e(n)$, and P_{v_g}
Compute $\rho(n)$, $\gamma(n)$, and $\beta(n)$, respectively, using (3.5), (3.42), and (3.39)
if $\left(P_{e_{\hat{s}}(n)} > P_x(n)\right)$ $G(n) = \sqrt{\frac{P_{e_{\hat{s}}}(n-1)}{\|\hat{\boldsymbol{s}}(n)\|^2}}$ else compute $G(n)$ using (3.38)

in [56] that the term $P_{e_w}(n)$ in (3.43) plays a very important role. In the case of perturbation terms, $v_d(n)$ and $(v_s(n) - v_{\hat{s}}(n))$, in the error signal, $e_w(n)$, of ANC filter, the step-size decreases to a small value thus preventing ANC system from divergence. The normalized step-size parameter for $\hat{\boldsymbol{s}}(n)$, $\mu_s(n)$, is computed as

$$\mu_s(n) = \frac{\mu_s}{\boldsymbol{x}^T_{\hat{s}(n),v(n)}(n)\boldsymbol{x}_{\hat{s}(n),v(n)}(n) + P_{y_{w\hat{s}}}(n)}, \tag{3.44}$$

where μ_s is another fixed step-size parameter, and $\boldsymbol{x}_{\hat{s}(n),v(n)}(n)$ is the input signal vector of SPM filter as defined in (3.28). The term $P_{y_{w\hat{s}}}(n)$ (estimated using estimator like (3.6)) is employed to have some upper bound on $\mu_s(n)$. This upper bound in (3.44) is needed to avoid the possibility of very large step-size value, when

Table 3.6: Simulation parameters for online secondary path modeling with gain scheduling.

	Parameters
Akhtar's method [44]	$\mu_w = 5 \times 10^{-4}$, $\mu_{s_{\min}} = 1 \times 10^{-3}$, $\mu_{s_{\max}} = 1 \times 10^{-2}$, $\sigma_{\min} = 0.001$, $\sigma_{\max} = 0.1$.
Carini's method [46]	$\mu_{s_{\min}} = 4 \times 10^{-3}$, $\Delta = 8$, $\hat{\lambda} = 0.6$, $R(n) = 1$
Proposed method-4 [49]	$\mu_w = 3 \times 10^{-1}$, $\mu_s = 8 \times 10^{-2}$, $\alpha = 0.997$, $\gamma_{\min} = 0.3$, $\gamma_{\max} = 0.9$.

the term $(\boldsymbol{x}^T_{\hat{s}(n),v(n)}(n)\boldsymbol{x}_{\hat{s}(n),v(n)}(n))$ becomes very small in steady-state due to the proposed gain scheduling.

In proposed method-4, the weight update equations for ANC filter and SPM filter are the same as used for Akhtar's method [44] (see (3.1) and (3.3)) with following exceptions. First normalized step-sizes $\mu_w(n)$ (see (3.43)) and $\mu_s(n)$ (see (3.44)), respectively, are used for ANC filter and SPM filter, and second the gain $G(n)$ in proposed method-4 is computed using (3.38) -(3.40) and (3.42). The algorithm for the proposed method-4 is given in Table. 3.5.

3.2.10 Simulation Results

In this section, extensive simulation results for four different cases are presented to compare the performance of the proposed method-4 with Akhtar's [44], and Carini's method [46]. The performance comparison is carried out on the basis of following performance measures.

- Relative modeling error of secondary path, $\Delta D_s(n)$, as defined in (3.24)
- Mean-squared error (MSE) at the error microphone, $E[e^2(n)]$.
- Steady-state value of the time-varying gain, $G(n)$.

For all the four cases, the simulation parameters used are shown in Table. 3.6. The selection of step-size parameter for adaptive filter depends upon the adaptation method, power of input signal of adaptive filter (except for NLMS algorithm), and the power of interference term in the error signal of the adaptive filter. The adaptation strategies for ANC filter and SPM filter in Akhtar's, Carini's, and the proposed method-4 are different. In addition to this, a different gain scheduling strategy results in different power of input signal for $\hat{\boldsymbol{s}}(n)$, and different power of the interference term in the error signal $e_w(n)$ of ANC filter, therefore, the step-size parameters are tuned for each method to achieve the fast and stable convergence of the adaptive filters. In all methods, the adaptive filter weights are initialized by null vectors (in the proposed method-4 $\hat{\boldsymbol{s}}(n)$, and in Carini's method $\hat{\boldsymbol{s}}_0(n)$ are initialized by all ones). All other simulation parameters are same as used for the simulation results of Fig. 3.4.

For stable operation of MFxNLMS algorithm based ANC system the phase error between $\boldsymbol{s}(n)$ and $\hat{\boldsymbol{s}}(n)$ must be within the bound of $\pm 90^0$ [15], [19], [57]-[59]. Since the secondary path $\boldsymbol{s}(n)$ is unknown, therefore offline modeling ($d(n) = 0$) of the secondary path can be used to satisfy the $\pm 90^0$ bound at the start-up of ANC system. The other option (with $d(n)$ present) is to keep ANC filter in sleep state for a while and only the modeling filter $\hat{\boldsymbol{s}}(n)$ is adapted. As stated earlier, in this chapter, the second option is used in which ANC filter is in sleep state from $n = 0$ to $n = 5000$ as done in [45], and [46]. In all plots for simulation results, the vertical line at $n = 5000$ marks the end of this phase.

Case 1: Multi-Tonal Input With Time-Varying Power: In this case, the reference signal, $x(n)$, is a multi-tonal input with frequencies 100, 200, 300, and 400 Hz. Initially variance of $x(n)$ is selected as 2, and then changed to 6, and 1 at time $n = 25000$, and $n = 75000$, respectively. A WGN with zero-mean and variance 0.002 is added to $x(n)$ to account for any measurement noise. The simulation results for Case 1 are presented in Fig. 3.12, Fig. 3.13 and Fig. 3.14.

- Fig. 3.12(a) shows the plots for $P_{e_{\hat{s}}}(n)/P_x(n)$, $P_x(n)/P_{v_g}$, and $\beta(n)$. These time-varying quantities are involved in the selection of (3.37) or (3.38) for gain $G(n)$ computation. The horizontal line (dashed-dotted) with amplitude 1 is plotted as a reference line to show that as long as $P_{e_{\hat{s}}}(n) > P_x(n) \Rightarrow \frac{P_{e_{\hat{s}}}(n)}{P_x(n)} > 1$, (3.37) is used for computing $G(n)$. It is found from Fig. 3.12(a) that from $n = 0$ to $n = 5247$ the ratio $P_{e_{\hat{s}}}(n)/P_x(n) > 1$, therefore (3.37) is used for $G(n)$. After $n = 5247$ the condition $P_{e_{\hat{s}}}(n)/P_x(n) > 1$ is false and the $G(n)$ is computed using (3.38). It is clear from Fig. 3.12(a) that at the start of second stage ($P_{e_{\hat{s}}}(n)/P_x(n) \leq 1$) of gain scheduling strategy the value of $\beta(n)$ is greater than $P_x(n)/P_{v_g}$ and the gain is determined by the input reference signal power, otherwise the gain follows the variation of $\beta(n)$. After convergence of the ANC system the change in the variance of the input reference signal, $x(n)$, changes the error signal $e_{\hat{s}}(n)$, therefore causing a change in $P_{e_{\hat{s}}d}(n)$ and $\beta(n)$.

- The plot for the time-varying gain $G(n)$ is shown in Fig. 3.12(b). In Akhtar's method the value of $\rho(n)$ is never zero, and hence $G(n)$ is higher in steady-state. In Carini's method the gain is determined by $E[(d(n) - y_{ws}(n))^2]$ in all operating conditions, while in the proposed method the gain, at steady-state, is varied on the basis of the correlation estimate of the two adjacent

values of the error signal $e_{\hat{s}}(n)$ of SPM filter. This results in a much smaller steady-state value of $G(n)$ as compared to that of Carini's method. After convergence of ANC system the change in the variance of the input reference signal $x(n)$ changes the signal $e_{\hat{s}}(n)$, therefore causing a change in $G(n)$.

- As $E[(v_s(n))^2] = G^2(n)||\boldsymbol{s}(n)||^2$, so a small value of the gain $G(n)$ results in a small ANP at the error microphone. The curves for the mean-square value of the auxiliary noise at the error microphone are shown in Fig. 3.12(c). The change in the variance of $x(n)$ changes $P_{e_{\hat{s}}}(n)$. The change in $P_{e_{\hat{s}}}(n)$ causes a change in $G(n)$ and therefore changes $E[(v_s(n))^2]$.

- Fig. 3.13(a) shows the plot of relative modeling error $\Delta D_s(n)$, as defined in (3.24). To explain the fast convergence of the SPM filter in the proposed method consider $n \geq 5247$ where the gain $G(n)$ is computed using (3.38). As stated earlier, as long as in the second stage of gain scheduling the value of $\beta(n) > P_x(n)/P_{v_g}$ the gain is determined by the input reference signal power and is higher than Akhtar's and Carni's methods (see Fig. 3.12(b)). This large value of the gain $G(n)$ results in a large power of input signal, $E[(v(n))^2]$, for $\hat{\boldsymbol{s}}(n)$ and hence a large value for $E[e^2(n)]$. This results in the fast convergence of the SPM filter $\hat{\boldsymbol{s}}(n)$. It is shown in [60] that after the convergence of ANC system the norms of the adaptive filters $\hat{\boldsymbol{s}}(n)$ and $\boldsymbol{w}(n)$ should remain insensitive to changes in input reference signal power. In Fig. 3.13(a), we observe that there is no change in $\Delta D_s(n)$ in the proposed method even when the variance of the input reference signal $x(n)$ changes. This is in accordance with the theory mentioned in [60].

- In Fig. 3.13(b) MSE curves are plotted for various methods. For changes

in the input reference signal variance at time $n = 25000$ and $n = 75000$, the value of $E[e^2(n)]$ in the proposed method is almost same as in Carini's methods. When ANC system is in early stages of adaptation or when the acoustic paths are perturbed, in both these situation fast convergence of $\hat{\boldsymbol{s}}(n)$ is desirable. The proposed gain scheduling scheme is such that as far as $\hat{\boldsymbol{s}}(n)$ is away from $\boldsymbol{s}(n)$ the ratio $R(n) < 0$ dB, $E[(v_s(n))^2] > E[(d(n) - y_{ws}(n))^2]$ and hence resulting in large $E[e^2(n)]$ in early stages of adaptation, and in situations when acoustic paths are perturbed. We observe that the proposed method improves steady-state noise-reduction performance as compared to the existing methods. The reason for an improved noise-reduction performance is the proposed strategy for gain scheduling which results in a small contribution of $E[(v_s(n))^2]$ in $E[e^2(n)]$ at steady-state.

- The variation of $R(n)$ in the Carini's and the proposed methods is shown in Fig. 3.13(c). It is clear that ratio $R(n) = \text{constant} \,\forall\, n$ in Carini's method, where as $R(n)$ is allowed to vary in the proposed method. As long as $\hat{\boldsymbol{s}}(n)$ is away from $\boldsymbol{s}(n)$, $R(n) < 0$ dB, and $R(n) > 0$ dB as $\hat{\boldsymbol{s}}(n)$ converges to $\boldsymbol{s}(n)$. After ANC system converges, the change in the variance of input reference signal results in an increase in the gain $G(n)$. The increase in $G(n)$ causes the value of $E[(v_s(n))^2]$ to increase and therefore the value of $R(n)$ decreases.

- The time-varying step-size for SPM filter, $\mu_s(n)$, in Akhtar's, Carini's and the proposed methods is plotted in Fig. 3.14(a). In Akhtar's method, the step-size $\mu_s(n)$ is set to a minimum value at the start-up and later increased to a maximum value. In Carini's method the variation of step-size $\mu_s(n)$ depends upon the distance of $\hat{\boldsymbol{s}}_0(n)$ from $[0, 0, ...0]^T$, and the step-size $\mu_s(n)$ increases because of decrease of term $\boldsymbol{x}^T_{\hat{s}_c(n),v(n)}(n)\boldsymbol{x}_{\hat{s}_c(n),v(n)}(n)$ in the denominator of

(3.19). In proposed method-4, normalized step-size, as defined in (3.44), is used for SPM filter. It is clear from Fig. 3.14(a) that as the ANC system converges the step-size for SPM filter increase. This is because of the decrease in the denominator term ($\boldsymbol{x}^T_{\hat{s}(n),v(n)}(n)\boldsymbol{x}_{\hat{s}(n),v(n)}(n)$) due to gain scheduling.

- The time-varying step-size for ANC filter, $\mu_w(n)$, is plotted in Fig. 3.14(b). As the normalization factor is involved in computing $\mu_w(n)$, therefore the large input signal power results in small step-size and vice versa.

- Fig. 3.14(c) shows the variation of $\rho(n)$ in Akhtar's and the proposed methods. In Akhtar's method the value of $\rho(n)$ decrease from one to zero, where as in the proposed method the value of $\rho(n)$ is almost one in steady-state.

Case 2: Multi-Tonal Input and Strong Acoustic Path Perturbation:

The existing methods work fine for slight variations in the acoustic paths. In actual practice significant changes in the acoustic paths may be encountered due to the movement of the error microphone or the loudspeaker. In this case study a strong perturbation in the acoustic paths is simulated by giving two sample right circular shift to the truncated impulse responses of $\boldsymbol{p}(n)$ and $\boldsymbol{s}(n)$ [49]. The simulation results for this case study are presented in Fig. 3.15 Fig. 3.16, and Fig. 3.17, where jumps at $n = 5 \times 10^4$ indicate a perturbation in the acoustic paths.

- From Fig. 3.15(a), it is clear that just before the acoustic paths perturbation the gain in the proposed method is following the variations of $\beta(n)$, and is computed using (3.38). The perturbation in acoustic paths results in $P_{e_{\hat{s}}}(n) > P_x(n)$ and the gain is computed using (3.37) until the condition $P_{e_{\hat{s}}}(n) > P_x(n)$ is false.

- The variation of the gain $G(n)$ is shown in Fig. 3.15(b). In Akhtar's method,

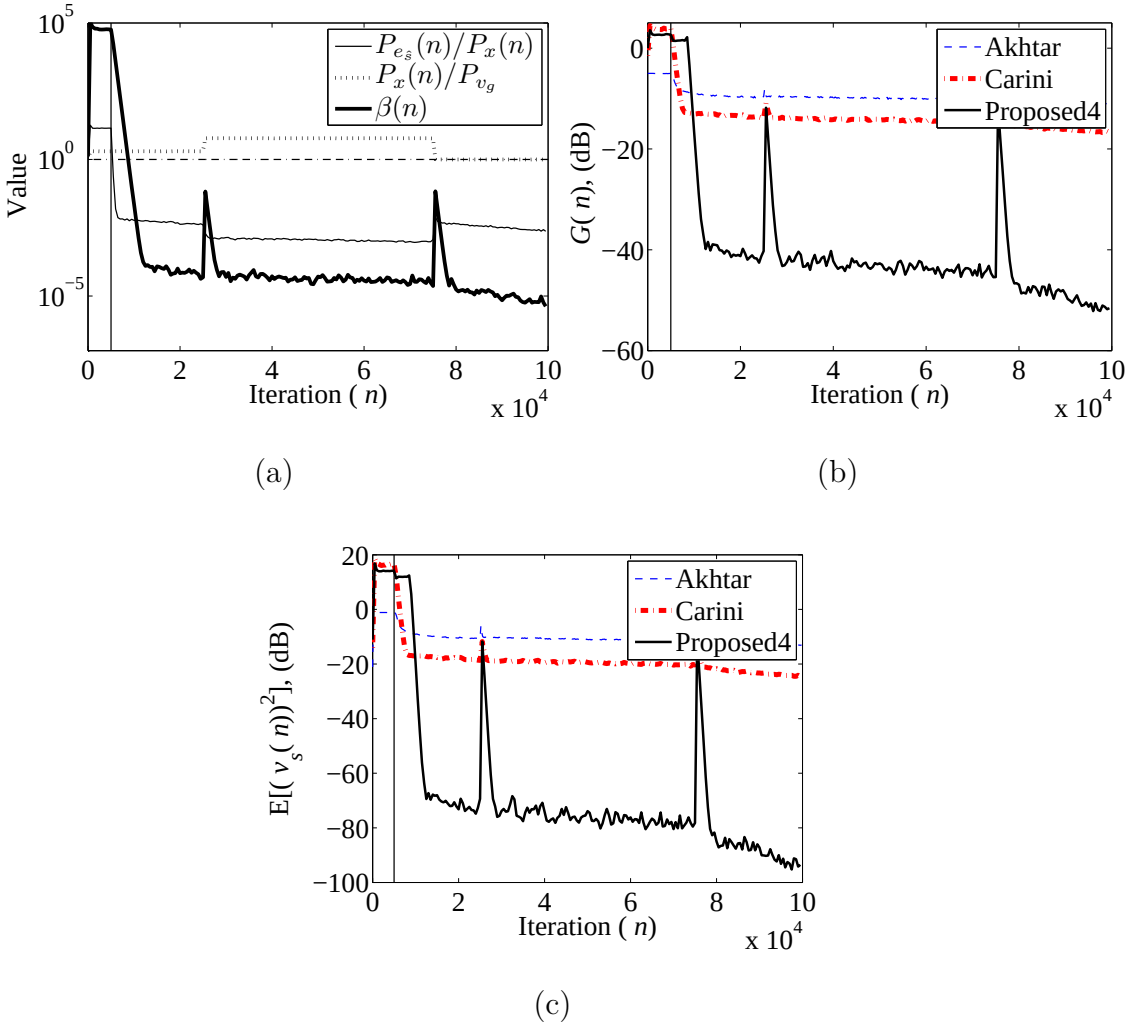

Figure 3.12: Simulation results in Case 1: (a) Variation of $P_{e_{\hat{s}}}(n)/P_x(n)$, $P_x(n)/P_{v_g}$, and $\beta(n)$ in the proposed method-4, (b) The time-varying gain $G(n)$(dB), (c) Mean-squared auxiliary noise, $E[(v_s(n))^2]$(dB).

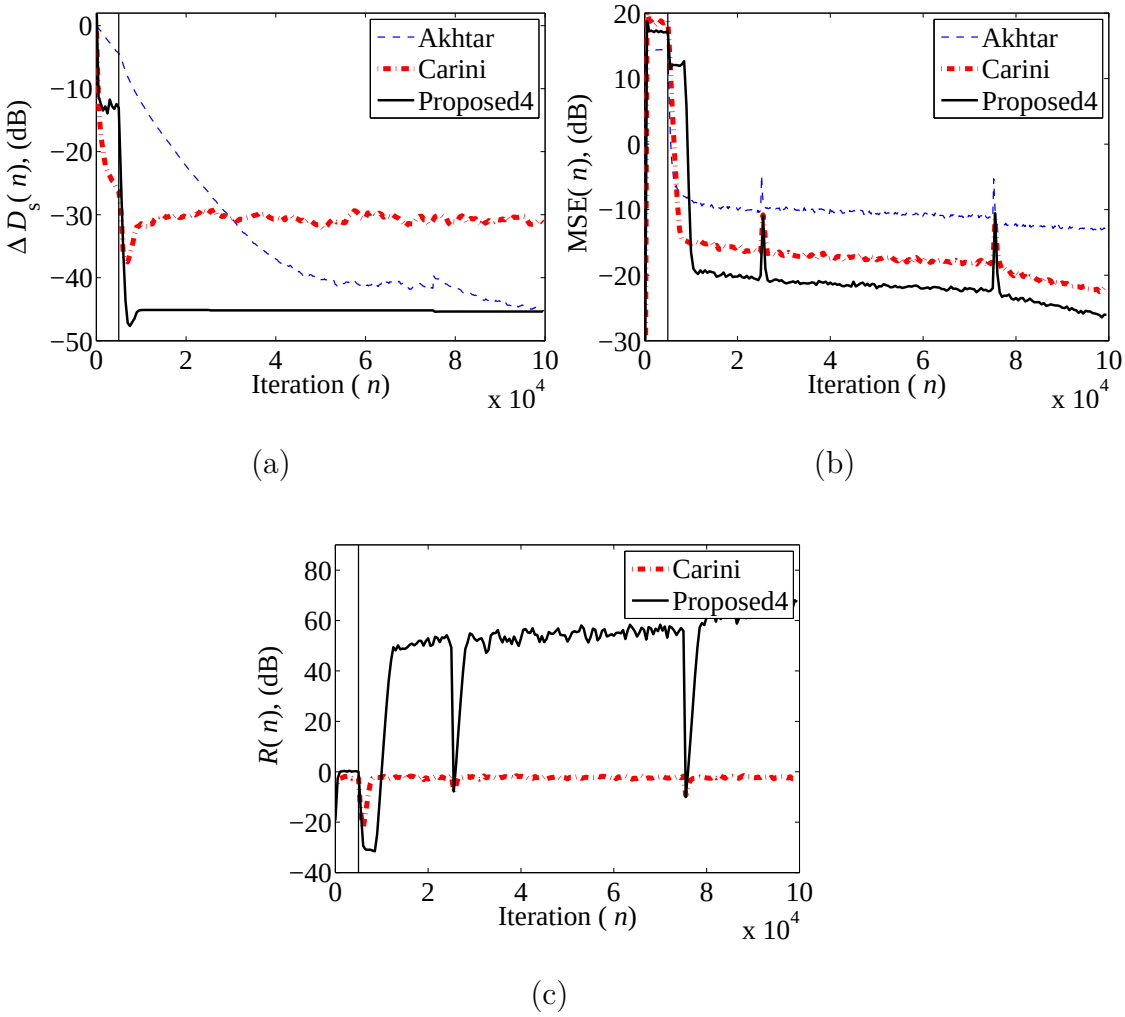

Figure 3.13: Simulation results in Case 1: (a) Relative modeling error, $\Delta D_s(n)$(dB), (b) Mean-square-error, MSE (dB), (c) The ratio $R(n)$(dB).

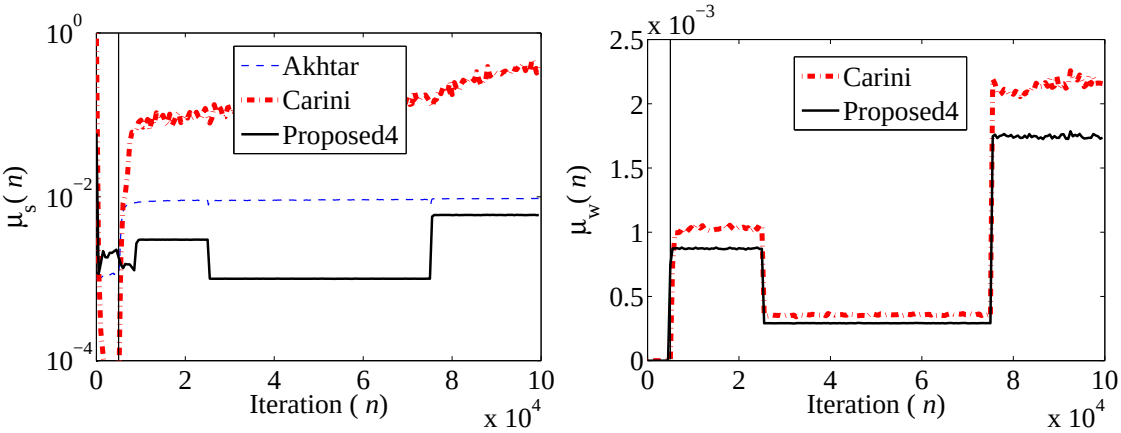

(a) (b)

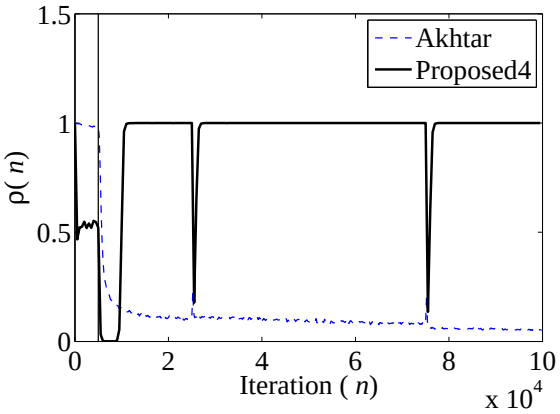

(c)

Figure 3.14: Simulation results in Case 1: (a) The time-varying step-size parameter $\mu_s(n)$, (b) The time-varying step-size parameters $\mu_w(n)$, (c) The variation of the parameter $\rho(n)$ as defined in (3.32).

the gain $G(n)$ is not able to increase in accordance with the power of the interference term $E[(d(n) - y_{ws}(n))^2]$, so the strong perturbation results in a large interference $(d(n) - y_{ws}(n))$ in the error signal $e_{\hat{s}}(n)$ of SPM filter, resulting in the divergence of SPM and hence the overall ANC system. In Carini's method, the step-size $\mu_w(n)$ jumps to higher value after perturbation (see Fig. 3.17(b)). The large value of the step-size in the presence of a strong perturbation term $(v_s(n) - v_{\hat{s}}(n))$ results in the divergence of ANC filter, thus resulting in very large value of $E[(d(n) - y_{ws}(n))^2]$. To keep the ratio $R(n) = 0$ dB, the gain $G(n)$ also increases to a very large value. Only the proposed method is convergent and gain $G(n)$ reduces to a small value even after the perturbation in the acoustic paths.

- Fig. 3.15(c) shows the plot of $E[(v_s(n))^2]$. As expected, a large value of $G(n)$ results in a large value of $E[(v_s(n))^2]$ and vice versa.

- Fig. 3.16(a) show the curves for $\Delta D_s(n)$. In the proposed method a fast convergence of the SPM filter is obtained before and after the acoustic path perturbation. The reason for the fast convergence is the same as explained in Case 1. The fast convergence of SPM filter quickly neutralizes the effect of the perturbation term $(v_s(n) - v_{\hat{s}}(n))$ from the error signal $k(n)$ of ANC filter $\boldsymbol{w}(n)$, and thus the ANC system remains stable even for a strong perturbation in the acoustic paths. The behavior of $\Delta D_s(n)$ for Carini's method is quite interesting. The ANC filter is diverged, but the modeling filter still manages to converge. The reason is quite simple, a large value of $E[(d(n) - y_{ws}(n))^2]$ results in a large $E[(v_s(n))^2]$ to keep the ratio $R(n)$ constant, thus resulting in a very small step-size (see Fig. 3.17(a) for variation in $\mu_s(n)$). A very small value of the step-size allows SPM filter to converge even for a very

strong perturbation term $(d(n) - y_{ws}(n))$ in the error signal $e_{\hat{s}}(n)$ of SPM filter.

Case 3: Multi-Tonal Input and the Uncorrelated WGN at Error Sensor: In this case study a zero-mean WGN $v_d(n)$ with variance 0.05; uncorrelated with the reference and auxiliary noise; is assumed to be present at the error microphone. The noise at the error microphone contributes to the residual error signal $e(n)$, thus the gain in Carini's method (see (3.15)) will be higher as compared with the gain for $v_d(n) = 0$. This large value of the gain $G(n)$ results in $E[(v_s(n))^2] > E[(d(n) - y_{ws}(n))^2]]$, thus making $R(n) < 0$ dB $\forall\, n$. In the proposed method the gain $G(n)$ in steady-state depends upon $\beta(n)$, however $\beta(n)$ itself depends upon the estimate of autocorrelation of $e_{\hat{s}}(n)$ and $e_{\hat{s}}(n-1)$, therefore the gain $G(n)$ is independent of error sensor noise $v_d(n)$ (see (3.41)).

The simulation results for Case 3 are shown in Fig. 3.18, Fig. 3.19, and Fig. 3.20, where we observe that the performance of the proposed method is better than the existing methods in terms of modeling accuracy of the SPM filter, the power of the residual error signal at the error microphone, and steady-state value of the time-varying gain $G(n)$.

Case 4: Broad-Band Input: The practical example of the broad-band feed-forward ANC system is the control of acoustic noise in long, narrow ducts, such as exhaust pipes and ventilation systems [4]. The objective of this case study is to compare the performance of the proposed algorithm for broad-band input reference signal $x(n)$. The broad-band input signal $x(n)$ is generated by filtering a WGN signal with variance 2 through a bandpass FIR filter of order 128 with a passband of [100 500] Hz. An uncorrelated WGN with zero-mean and variance 0.002 is added with $x(n)$ to account for the measurement noise. The simulation

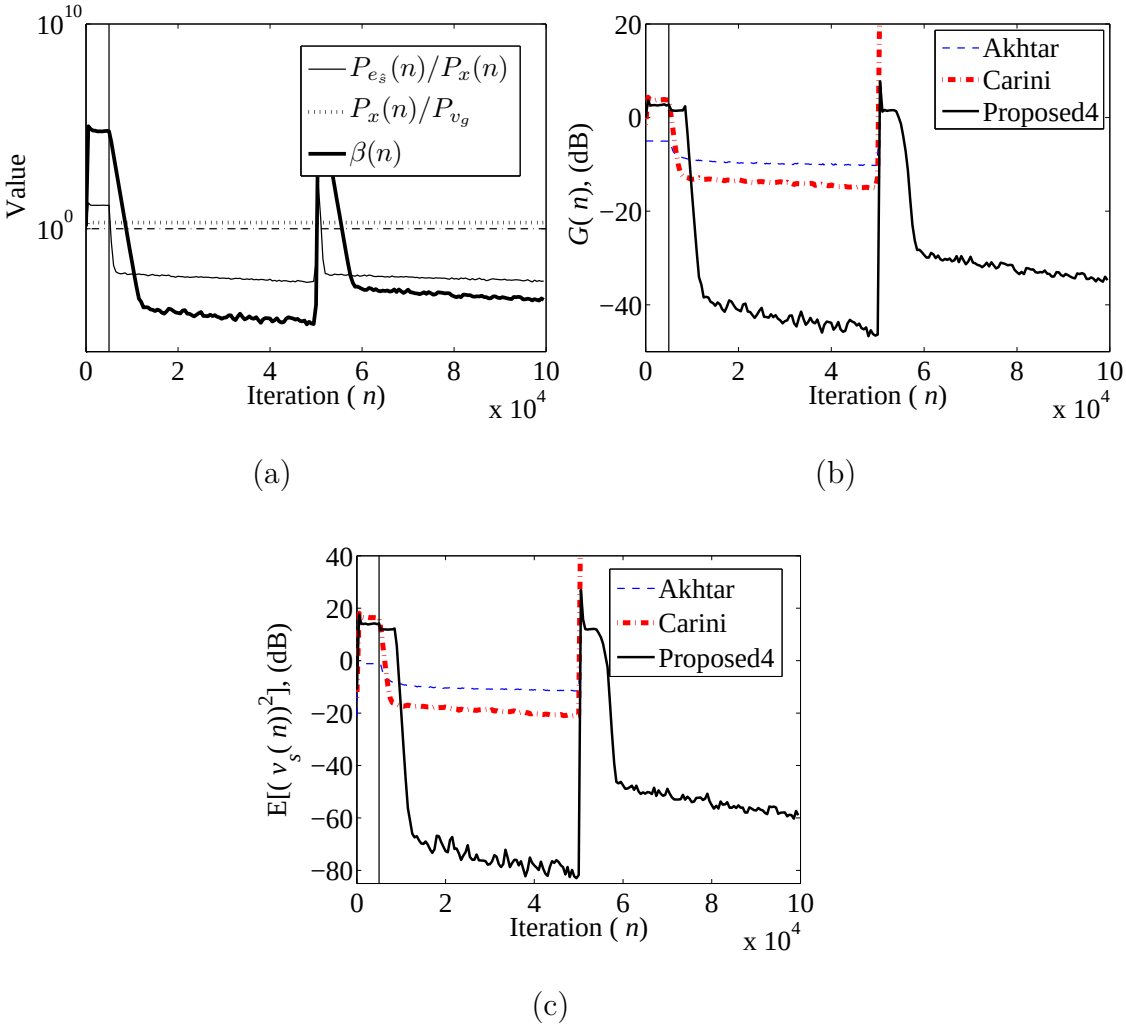

Figure 3.15: Simulation results in Case 2: (a) Variation of $P_{e_{\hat{s}}}(n)/P_x(n)$, $P_x(n)/P_{v_g}$, and $\beta(n)$ in the proposed method-4, (b) The time-varying gain $G(n)$(dB), (c) Mean-squared auxiliary noise, $E[(v_s(n))^2]$(dB).

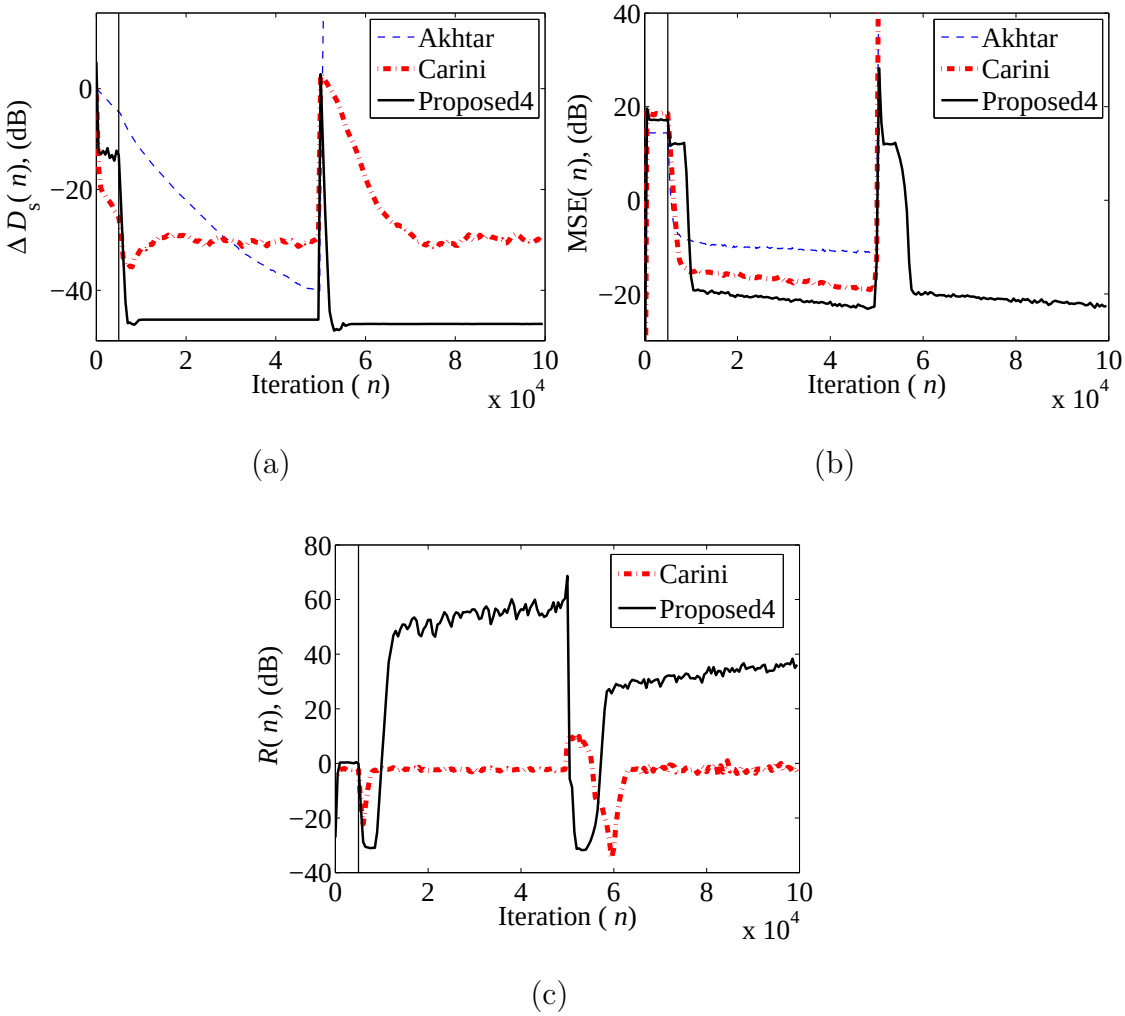

Figure 3.16: Simulation results in Case 2: (a) Relative modeling error, $\Delta D_s(n)$(dB), (b) Mean-square-error, MSE (dB), (c) The ratio $R(n)$(dB).

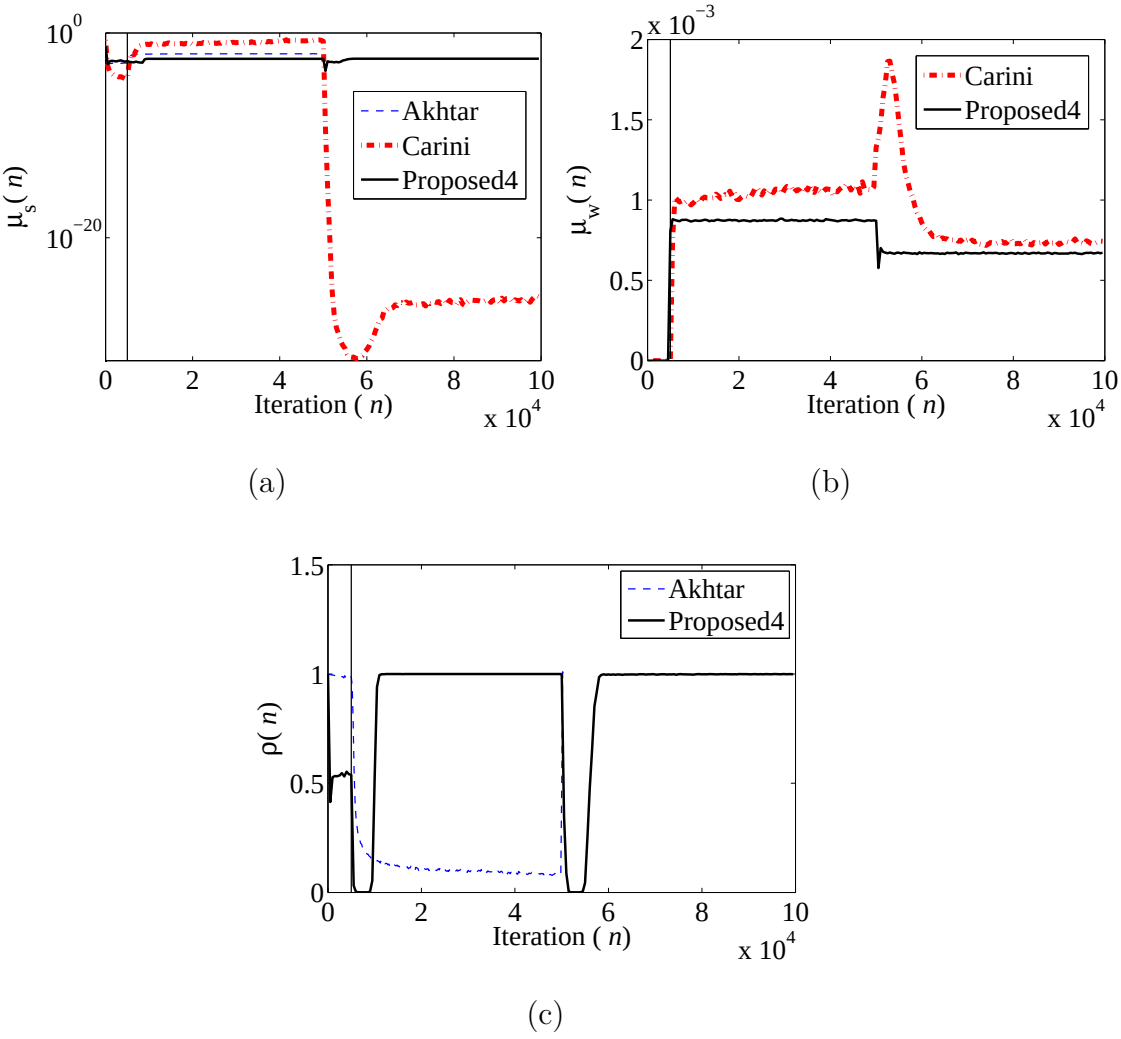

Figure 3.17: Simulation results in Case 2: (a) The time-varying step-size parameter $\mu_s(n)$, (b) The time-varying step-size parameters $\mu_w(n)$, (c) The variation of the parameter $\rho(n)$ as defined in (3.32).

Table 3.7: Computational complexity comparison (Number of computations per iteration)

Name	$\times$	$+$	$\div$	$\sqrt{}$
MFxLMS	$3L_w + 4L_s + 2$	$3L_w + 4L_s - 1$	–	–
Akhtar [44]	$3L_w + 4L_s + 13$	$3L_w + 4L_s + 4$	1	1
Carini [46]	$7L_w + 6L_s + 4\Delta + 19$	$6L_w + 6L_s + 4\Delta - 1$	6	1
Proposed-1 [47]	$3L_w + 4L_s + 11$	$3L_w + 4L_s + 3$	2	–
Proposed-2	$3L_w + 3L_s + 11$	$3L_w + 3L_s + 4$	2	–
Proposed-3 [48]	$4L_w + 5L_s + 18$	$4L_w + 5L_s + 6$	5	–
Proposed-4 [49]	$4L_w + 6L_s + 29$	$4L_w + 6L_s + 7$	5	1

results for Case 4 are shown in Fig. 3.21, Fig. 3.22, and Fig. 3.23. As in previous cases, the proposed method performs better than the existing methods.

3.3 Computational Complexity Comparison

The computational complexity requirements of all the methods discussed in this chapter are given in Table. 3.7. The computational complexity of Carini's method [46] is higher than all the other methods. This is because of computation of optimal normalized step-sizes for ANC filter and SPM filter in Carini's method. The proposed method-2 uses the proposed simplified structure of MFxLMS algorithm (see Fig. 2.10), and has the lowest computational complexity than all the other methods using ANP scheduling.

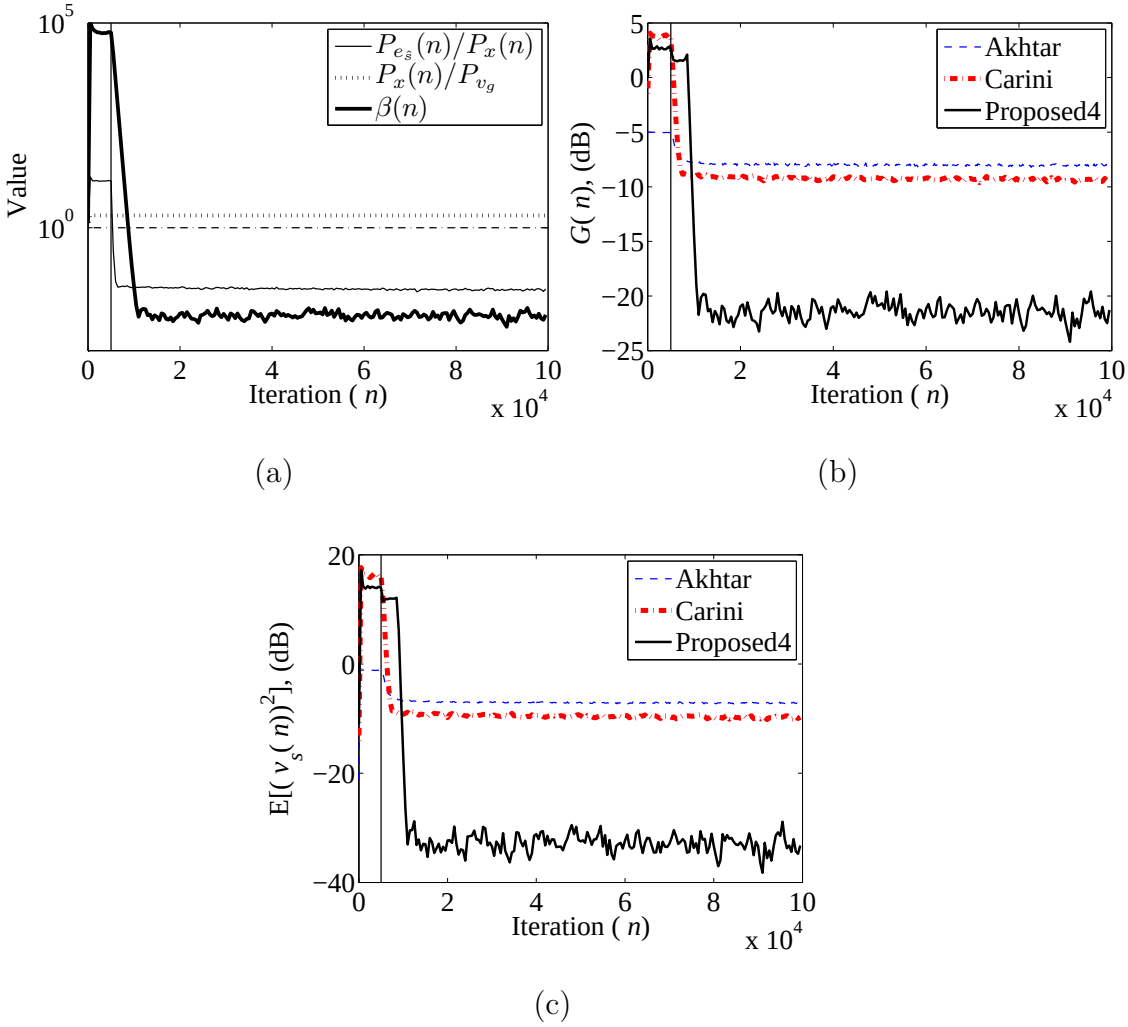

Figure 3.18: Simulation results in Case 3: (a) Variation of $P_{e_{\hat{s}}}(n)/P_x(n)$, $P_x(n)/P_{v_g}$, and $\beta(n)$ in the proposed method-4, (b) The time-varying gain $G(n)$(dB), (c) Mean-squared auxiliary noise, $E[(v_s(n))^2]$(dB).

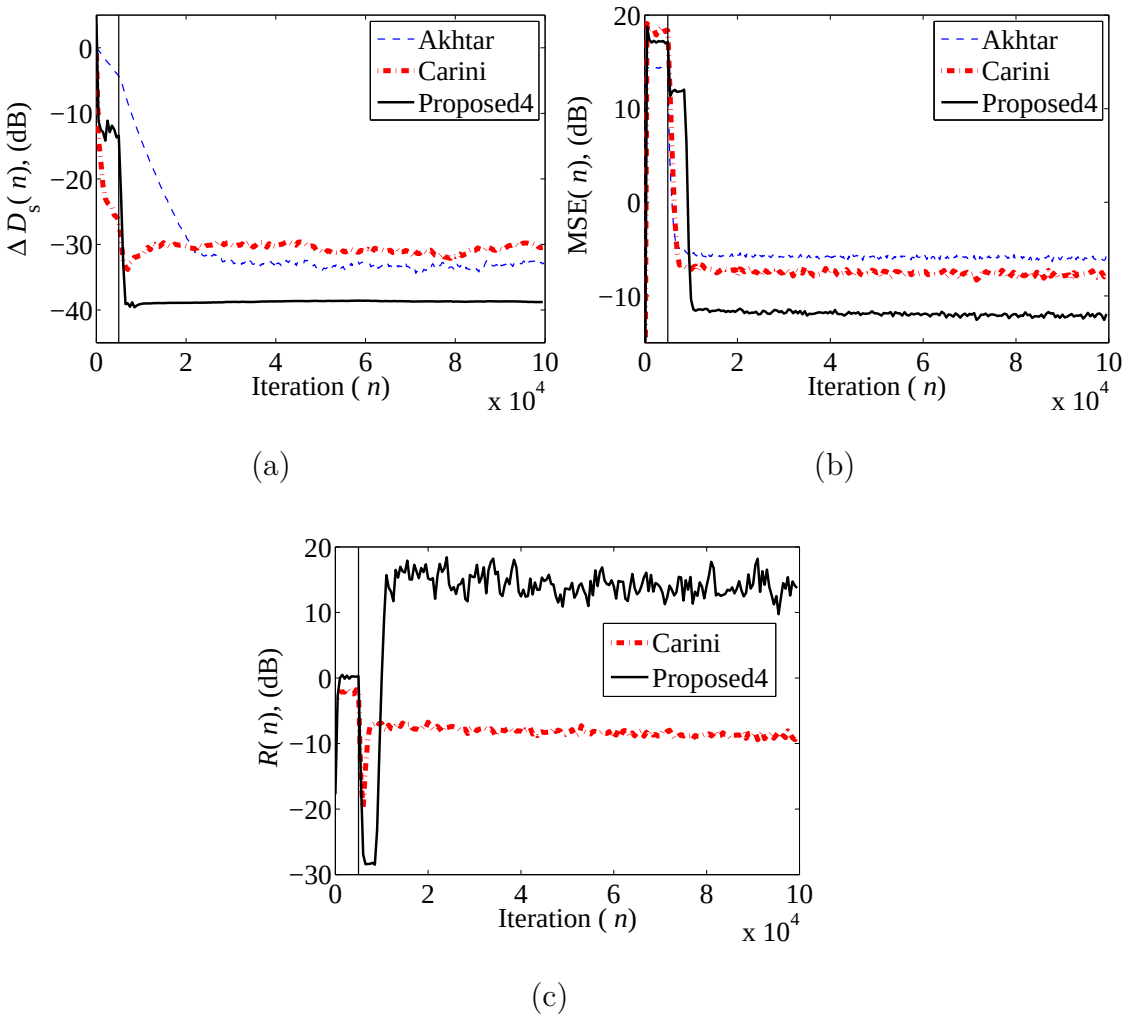

Figure 3.19: Simulation results in Case 3: (a) Relative modeling error, $\Delta D_s(n)$(dB), (b) Mean-square-error, MSE (dB), (c) The ratio $R(n)$(dB).

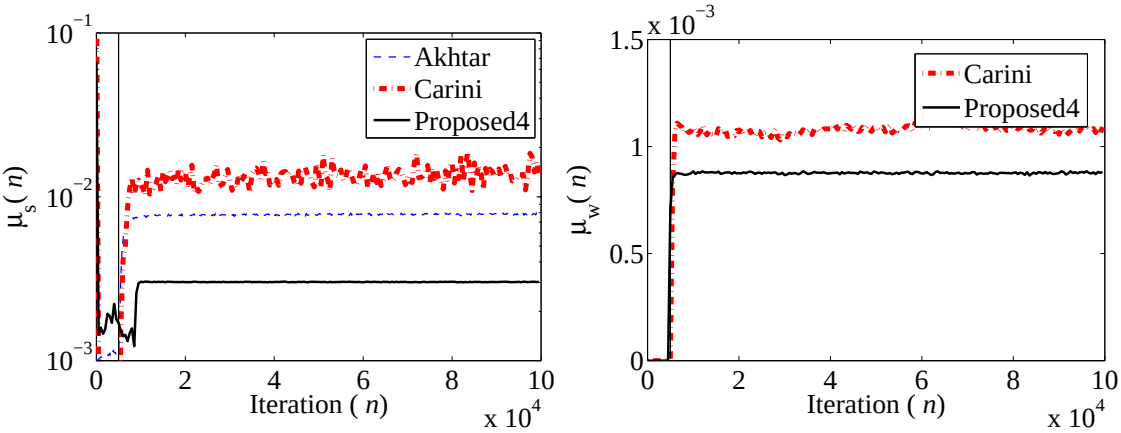

(a)

(b)

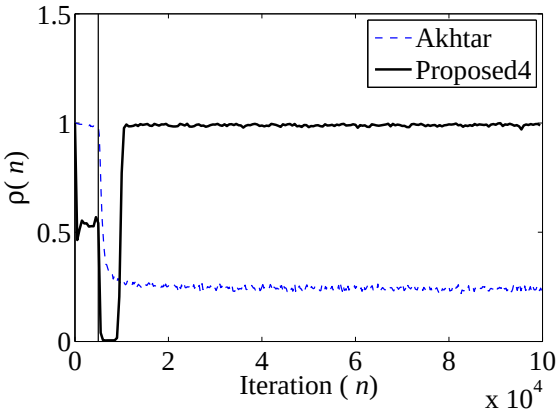

(c)

Figure 3.20: Simulation results in Case 3: (a) The time-varying step-size parameter $\mu_s(n)$, (b) The time-varying step-size parameters $\mu_w(n)$, (c) The variation of the parameter $\rho(n)$ as defined in (3.32).

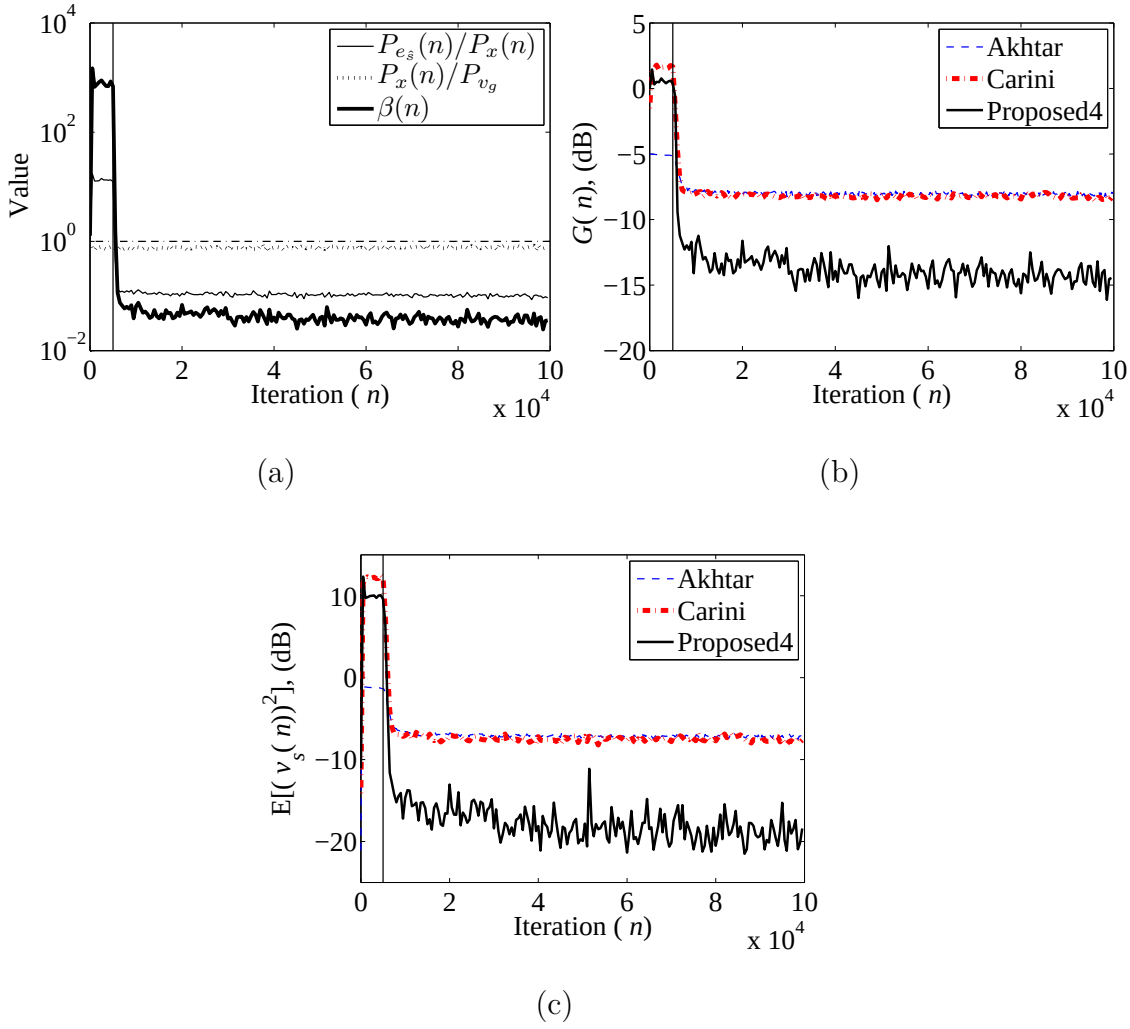

Figure 3.21: Simulation results in Case 4: (a) Variation of $P_{e_{\hat{s}}}(n)/P_x(n)$, $P_x(n)/P_{v_g}$, and $\beta(n)$ in the proposed method-4, (b) The time-varying gain $G(n)$(dB), (c) Mean-squared auxiliary noise, $E[(v_s(n))^2]$(dB).

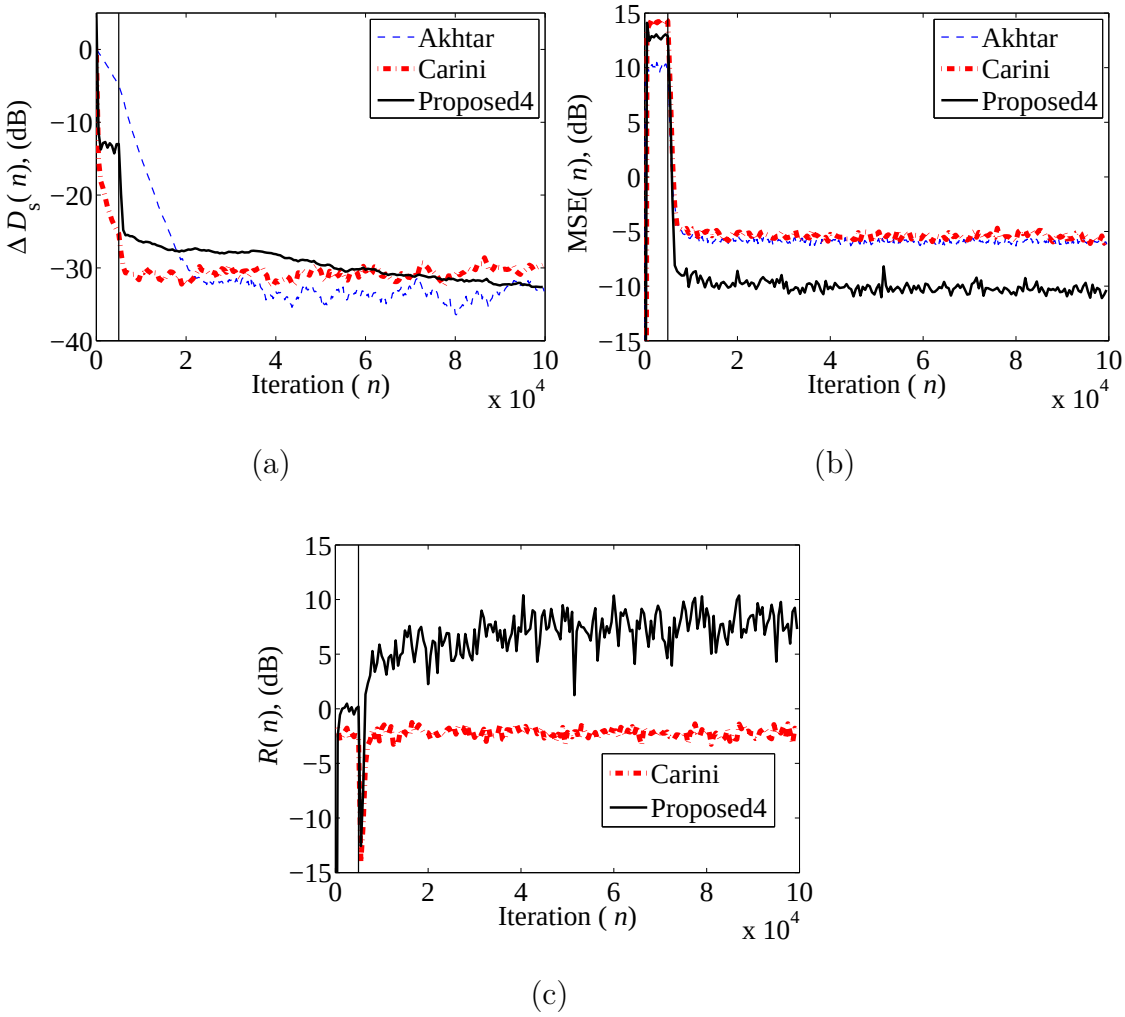

Figure 3.22: Simulation results in Case 4: (a) Relative modeling error, $\Delta D_s(n)$(dB), (b) Mean-square-error, MSE (dB), (c) The ratio $R(n)$(dB).

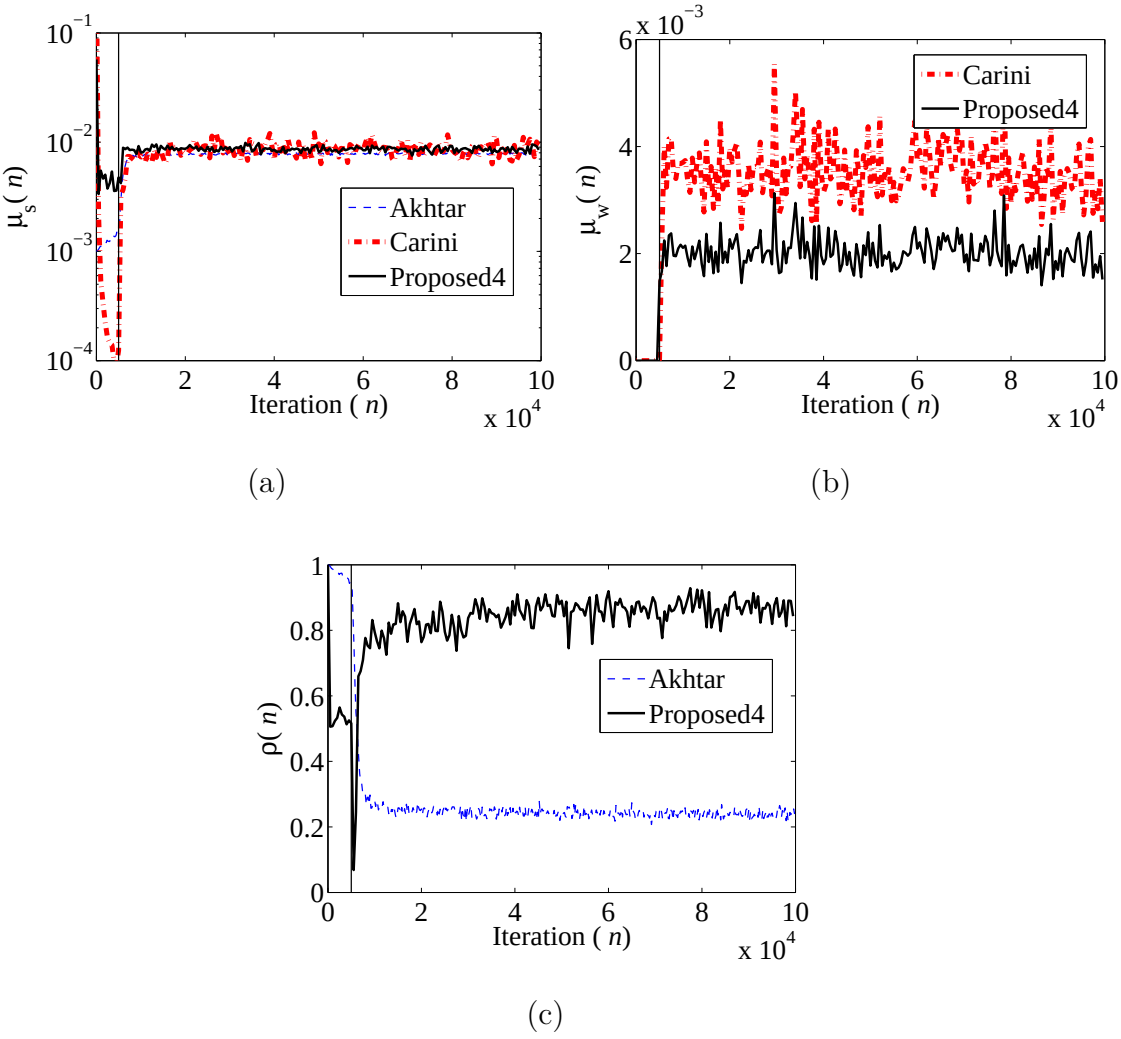

Figure 3.23: Simulation results in Case 4: (a) The time-varying step-size parameter $\mu_s(n)$, (b) The time-varying step-size parameters $\mu_w(n)$, (c) The variation of the parameter $\rho(n)$ as defined in (3.32).

3.4 Summary

The goal of an ANC system is to reduce the unwanted noise at the summing junction. For online SPM, an additional auxiliary noise is injected. This auxiliary noise contributes to the residual error, and thus degrades the NRP of ANC system.

In this chapter, various existing gain scheduling strategies were discussed. The drawbacks with the existing gain scheduling strategies were highlighted, and various new gain scheduling strategies were proposed. The proposed schemes were compared with the existing methods through the simulation results, and it is found that the proposed method-4 is better than the existing methods in terms of improving the modeling accuracy of SPM filter and in improving the NRP of ANC system

Chapter 4

Online Feedback Path Modeling and Neutralization With Gain Scheduling

The two important issues in feedforward configuration of active noise control (ANC) systems are: 1) online secondary path modeling (OSPM), 2) online feedback path modeling and neutralization (FBPMN). The details about OSPM with and without gain scheduling are discussed in the previous chapters. In this chapter the second important issue of feedforward ANC system, i.e., online FBPMN will be discussed.

The objective of an ANC system is to reduce the unwanted noise at the summing junction. The original unwanted noise at the summing junction is reduced by generating an anti-noise signal through the cancelling loudspeaker. In feedforward

ANC systems, the anti-noise signal generated by the loudspeaker will not only travel down stream to reduce the original unwanted noise, but will also propagates upstream through electro-acoustic feedback path and will corrupt the signal sensed by the reference microphone (see Fig. 1.11). The electro-acoustic feedback path, hereafter referred as feedback path for simplicity, includes the transfer functions of digital to analog converter (DAC), smoothing filter, power amplifier, loudspeaker, acoustic path from the loudspeaker to the reference microphone, pre-amplifier, anti-aliasing filter, and analog to digital converter (ADC) [4]. In the presence of feedback path, the reference signal picked-up by the reference microphone, hereafter referred as the corrupted reference signal, has two parts: 1) corresponding to original unwanted noise, 2) corresponding to anti-noise (due to the presence of feedback path). The presence of the feedback path may cause the ANC system to become unstable (see (1.25)). It is, therefore necessary to neutralize the effect of the feedback path.

There are various types of strategies that have been reported in the literature to solve the problem of the feedback path in the ANC systems. These include 1) directional (array of) microphones and speakers [61, 62], 2) non-acoustic sensors such as tachometer to acquire the reference signal [63, 64], 3) adaptive feedback ANC employing only the error microphone [65, 66], 4) adaptive IIR filter based feedback path compensation [67, 68], 5) fixed feedback path neutralization (FBPN) filter (obtained through offline modeling) [4], [12], and 6) adaptive FBPN using an FIR filter [69]-[75]. The structure-based approaches mentioned in (1)-(3) are either expensive or have limited applicabilities. Among the signal processing based approaches (4)-(6), the IIR filter based methods have an inherent problem of stability. Moreover, the IIR filter may converge to a local minimum. The FBPN based

on fixed filter offers a simplest solution (see Fig. 1.12). However in actual practice the feedback path may be time-varying, and hence online modeling is required to track variation in the feedback path. In online modleing techniques, the FBPMN filter is made adaptive. The coefficients of the FBPMN filter are adjusted according to some criterion (depending upon the adaptive algorithm), using, generally, random WGN (auxiliary noise) as an input excitation signal of adaptive filter. As discussed in previous chapters, the auxiliary noise injected for online FBPMN will contribute to the residual error and thus degrades the noise-reduction-performance (NRP) of ANC system. The solution to this problem is to use gain scheduling to reduce the contribution of auxiliary noise to the residual error at steady-state.

In the first part of this chapter existing methods [70], and [75] for online FBPMN without gain scheduling are discussed. In [76] a new structure is proposed, hereafter referred as proposed method-1, for online FBPMN. The performance of the proposed method-1 is compared with the existing methods through the simulation results.

In the second part of this chapter online FBPMN with gain scheduling are discussed. A new gain scheduling strategy is proposed for online FBPMN. The gain scheduling strategy when combined with Akhtar's structure [75] will result in method referred as proposed method-2 [77]. The same gain scheduling strategy when combined with the structure of proposed method-1 will result in a method referred as proposed method-3 [76]. In addition to this, in the second part of this chapter, a self tuned gain scheduling strategy with matching step-size is introduced and combined with the structure of proposed method-1. This will lead to a method referred as proposed method-4 [78]. The performance of the proposed strategies

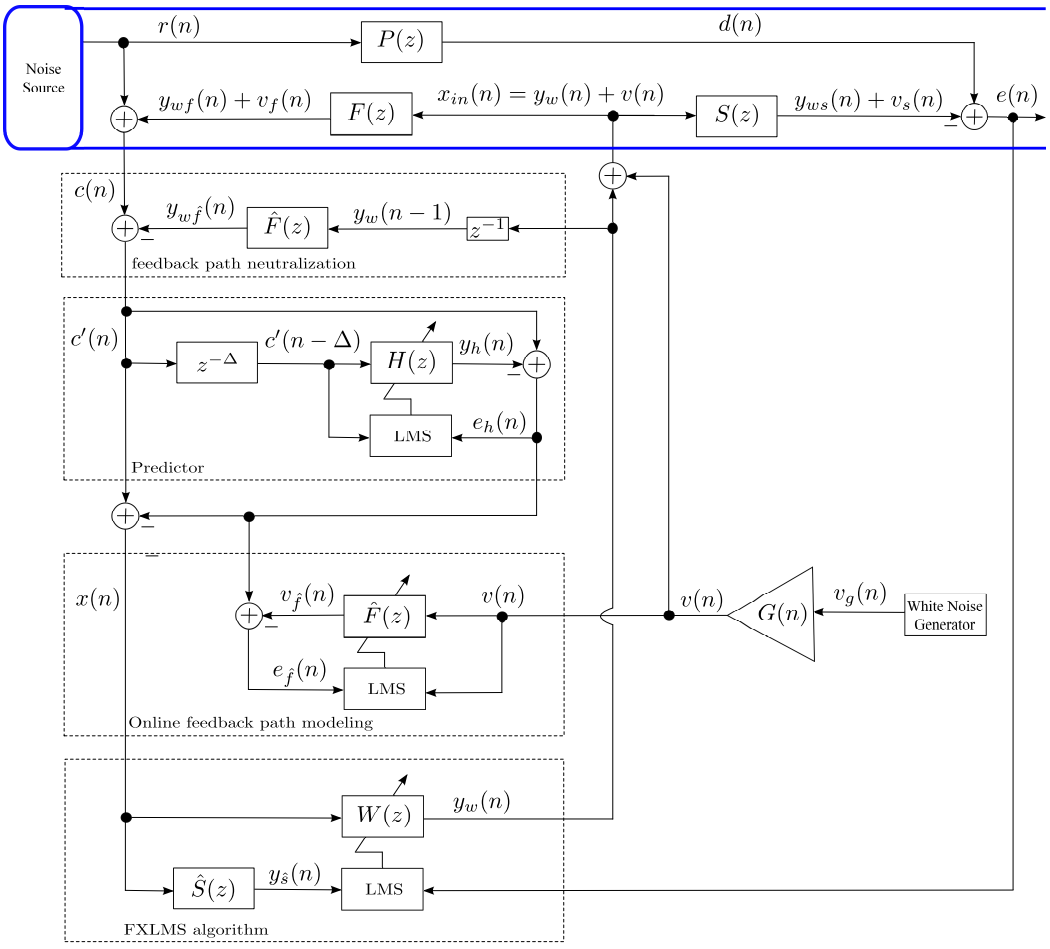

Figure 4.1: Block diagram of Kuo's method for online feedback path modeling and neutralization [70].

are compared with the existing methods through the simulation results.

4.1 Online FBPMN Without Gain Scheduling

4.1.1 Kuo's Method

The block diagram of Kuo's method [70] for single channel feedforward ANC system with online FBPMN is shown in Fig. 4.1. Here no gain scheduling is used, there-

fore $G(n) = 1$ in all operating conditions. It consists of filtered-x-LMS (FxLMS) adaptive algorithm based ANC filter $W(z)$, the adaptive LMS algorithm based linear prediction filter $H(z)$, adaptive FBPM filter $\hat{F}(z)$, and static FBPN filter $\hat{F}(z)$. The weights of adaptive FBPM filter are copied to static FBPN filter. Online FBPM is achieved by additive auxiliary noise $v(n) = v_g(n)$ (as $G(n) = 1$) being modeled as white Gaussian noise (WGN). The same signal $v(n)$ can also been employed for OSPM; however, in this chapter we mainly concentrate on online FBPMN. Assuming that $W(z)$ is an FIR filter, its output $y_w(n)$ is computed as

$$y_w(n) = w(n) * x(n) = \boldsymbol{w}^T(n)\boldsymbol{x}_{w(n),x(n)}(n), \tag{4.1}$$

where $w(n)$ is the impulse response of $W(z)$, $\boldsymbol{w}(n) = [w_0(n), w_1(n), \cdots, w_{L_w-1}(n)]^T$ is the impulse response coefficient vector of $W(z)$ at time n, and $\boldsymbol{x}_{w(n),x(n)}(n) = [x(n), x(n-1), \cdots, x(n-L_w+1)]^T$ is the input signal vector of filter $W(z)$ with input $x(n)$ at time n. The weight update equation for ANC filter $W(z)$ is given as

$$\boldsymbol{w}(n+1) = \boldsymbol{w}(n) + \mu_w e(n)\boldsymbol{x}_{\mathrm{LMS},y_{\hat{s}}(n)}(n), \tag{4.2}$$

where μ_w is the step-size parameter, and $\boldsymbol{x}_{\mathrm{LMS},y_{\hat{s}}(n)}(n) = [y_{\hat{s}}(n), y_{\hat{s}}(n), \cdots, y_{\hat{s}}(n-L_w+1)]^T$ is the filtered reference signal vector at time n. The reference signal $x(n)$ filtered through $\hat{S}(z)$ is computed as

$$y_{\hat{s}}(n) = \hat{s}(n) * x(n) = \hat{\boldsymbol{s}}^T(n)\boldsymbol{x}_{\hat{s}(n),x(n)}(n), \tag{4.3}$$

where $\hat{s}(n)$ is the impulse response of $\hat{S}(z)$, $\hat{\boldsymbol{s}}(n) = [\hat{s}_0(n), \hat{s}_1(n), \cdots, \hat{s}_{L_s-1}(n)]^T$ is the impulse response coefficient vector of $\hat{S}(z)$ at time n, and $\boldsymbol{x}_{\hat{s}(n),x(n)}(n) = [x(n), x(n-1), \cdots, x(n-L_s+1)]^T$ is the input signal vector of filter $\hat{S}(z)$ with input $x(n)$ at time n. From Fig. 4.1, the residual error signal $e(n)$ picked-up by

the error microphone is given by

$$e(n) = d(n) - y_{ws}(n) - v_s(n), \tag{4.4}$$

where $d(n) = p(n) * r(n)$, $p(n)$ is the impulse response of $P(z)$, and $r(n)$ is the original unwanted noise at the reference microphone; $y_{ws}(n) = s(n) * y_w(n)$, $s(n)$ is the impulse response of $S(z)$; and $v_s(n) = s(n) * v(n)$ denotes the contribution of the additive auxiliary noise at the error microphone. The corrupted reference signal $c(n)$ picked-up by the reference microphone given as

$$c(n) = r(n) + y_{wf}(n) + v_f(n), \tag{4.5}$$

where $y_{wf}(n) = f(n) * y_w(n-1)$, $f(n)$ is the impulse response of $F(z)$, and $y_w(n-1)$ is one sample delayed (inherent delay associated with the feedback path) version of $y_w(n)$; and $v_f(n) = f(n) * v(n)$ denotes the contribution of the additive auxiliary noise at the reference microphone. In Fig. 4.1, the output of the FBPN filter $\hat{F}(z)$ is subtracted from $c(n)$ to compute the desired response, $c'(n)$, of linear prediction filter $H(z)$ as

$$c'(n) = c(n) - y_{w\hat{f}}(n), \tag{4.6}$$

where the signal $y_{w\hat{f}}(n)$ (estimate of $y_{wf}(n)$) is the output of FBPN filter, and is computed as

$$y_{w\hat{f}}(n) = \hat{f}(n) * y_w(n-1) = \hat{\boldsymbol{f}}^T(n) * \boldsymbol{x}_{\hat{f}(n), y_w(n-1)}(n), \tag{4.7}$$

where $\hat{f}(n)$ is the impulse response of $\hat{F}(z)$, $\hat{\boldsymbol{f}}(n) = [\hat{f}_0(n), \hat{f}_1(n), \cdots, \hat{f}_{L_f-1}(n)]^T$ is the impulse response coefficient vector of $\hat{F}(z)$ at time n, and $\boldsymbol{x}_{\hat{f}(n), y_w(n-1)}(n) = [y_w(n-1), y_w(n-2), \cdots, y_w(n-L_f)]^T$ is the input signal vector of filter $\hat{F}(z)$ with input $y_w(n-1)$ at time n. In Fig. 4.1, the signal $c'(n)$ acts both as the desired

response and as an input excitation signal of $H(z)$. The output of $H(z)$ can be computed as

$$y_h(n) = h(n) * c'(n-\Delta) = \boldsymbol{h}^T(n)\boldsymbol{x}_{h(n),c'(n-\Delta)}(n), \tag{4.8}$$

where $h(n)$ is the impulse response of $H(z)$, $\boldsymbol{h}(n) = [h_0(n), h_1(n), \cdots, h_{L_h-1}(n)]^T$ is the impulse response coefficient vector of $H(z)$ at time n, $\boldsymbol{x}_{h(n),c'(n-\Delta)}(n) = [c'(n-\Delta), c'(n-\Delta-1), \cdots, c'(n-\Delta-L_h+1)]^T$ is the input signal vector of filter $H(z)$ with input $c'(n)$ at time n, and Δ is the decorrelation delay. The output of $H(z)$ is subtracted form its desired response $c'(n)$ to compute its error signal $e_h(n)$ as

$$e_h(n) = c'(n) - y_h(n). \tag{4.9}$$

The filter $H(z)$ is adapted using LMS algorithm as

$$\boldsymbol{h}(n+1) = \boldsymbol{h}(n) + \mu_h e_h(n)\boldsymbol{x}_{h(n),c'(n-\Delta)}(n), \tag{4.10}$$

where μ_h is the step-size parameter for weight updation of $H(z)$. In Fig. 4.1, the signal $e_h(n)$ is subtracted from $c'(n)$ to generate the interference (due to presence of feedback path) free signal, $x(n)$, for ANC filter and is computed as

$$x(n) = c'(n) - e_h(n) = c'(n) + y_h(n) - c'(n) = y_h(n). \tag{4.11}$$

The signal $e_h(n)$ also acts as the desired response of FBPM filter. The output of FBPM filter $v_{\hat{f}}(n)$ can be computed as

$$v_{\hat{f}}(n) = \hat{f}(n) * v(n) = \hat{\boldsymbol{f}}^T(n)\boldsymbol{x}_{\hat{f}(n),v(n)}(n), \tag{4.12}$$

where $\boldsymbol{x}_{\hat{f}(n),v(n)}(n) = [v(n), v(n-1), \cdots, v(n-L_f+1)]^T$ is the input signal vector of FBPM filter $\hat{F}(z)$ at time n. The output of FBPM filter $v_{\hat{f}}(n)$ is subtracted from $e_h(n)$ to compute its error signal $e_{\hat{f}}(n)$ as

$$e_{\hat{f}}(n) = e_h(n) - v_{\hat{f}}(n). \tag{4.13}$$

The weight update equation for FBPM filter is given by

$$\hat{\boldsymbol{f}}(n+1) = \hat{\boldsymbol{f}}(n) + \mu_f e_{\hat{f}}(n)\boldsymbol{x}_{\hat{f}(n),v(n)}(n), \tag{4.14}$$

where $\mu_f(n)$ is the step-size parameter for FBPM filter.

4.1.2 Remarks Regarding Kuo's Method

The following are the problems with Kuo's method

- The basic purpose of FBPN filter is to neutralize the effect of feedback path to have $x(n) = r(n)$. In Kuo's structure if we assume $\hat{F}(z) = F(z)$, then the output $y_h(n)$ (see (4.8)) can also be written as

$$y_h(n) = [h(n) * r(n-\Delta)] + [h(n) * v_f(n-\Delta)]. \tag{4.15}$$

  From above equation we can conclude that even for ideal case, i.e., for $\hat{F}(z) = F(z)$ and for $(h(n)*r(n-\Delta)) = r(n)$, the second term $(h(n)*v_f(n-\Delta)) \neq 0$. The term $(h(n) * v_f(n-\Delta))$ in $e_h(n)$ (desired response of FBPM filter) and in $x(n)$ will act as an interference, respectively, for FBPM filter and ANC filter. For ANC systems without gain scheduling, the interference term $(h(n)*v_f(n-\Delta))$ severely degrades the convergence of both the FBPM filter and ANC filter, and thus degrades the overall noise-reduction-performance (NRP) of ANC system.

- Information about the tap-weight length of $F(z)$ is required to select the proper value of decorrelation delay Δ

- Separate filters are used for FBPM and FBPN, this increases the computational complexity of Kuo's method.

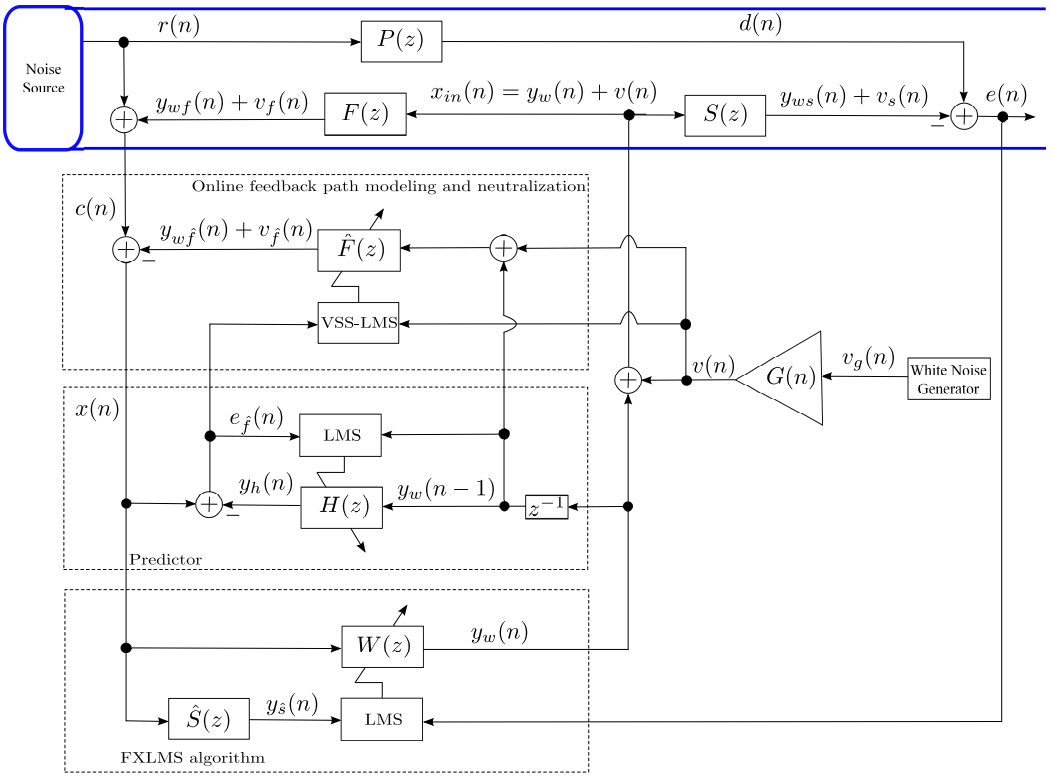

Figure 4.2: Block diagram of Akhtar's method for online feedback path modeling and neutralization [75].

- In Kuo's method linear prediction filter $H(z)$ is used which works only for narrow band predictable noise sources. Its performance will be degraded for broad-band input signals.
- As no gain scheduling is used, therefore the auxiliary noise, injected for online FBPMN, will degrade the NRP of ANC system at steady-state.

4.1.3 Akhtar's Method

The block diagram of Akhtar's method [75] is shown in Fig. 4.2. As no gain scheduling is used, therefore $G(n) = 1$ in all operating conditions. Here the action

of FBPN and FBPM filter is combined into a single FBPMN filter. It is claimed in [75] that the structure will work both for narrow-band and brad-band input signals. Also no decorrelation delay is required in Akhtar's structure. In addition to this, variable step-size (VSS) LMS adaptive algorithm is used for FBPMN filter. In Fig. 4.2, the output of the FBPMN filter $\hat{F}(z)$ is subtracted from $c(n)$ to compute $x(n)$ as

$$x(n) = c(n) - y_{w\hat{f}}(n) - v_{\hat{f}}(n) = [r(n) + y_{wf}(n) - y_{w\hat{f}}(n)] + [v_f(n) - v_{\hat{f}}(n)], \quad (4.16)$$

where the signals $c(n)$, and $y_{w\hat{f}}(n)$, respectively, are given by (4.5) and (4.7), and the signal $v_{\hat{f}}(n)$ is computed as

$$v_{\hat{f}}(n) = \hat{f}(n) * v(n) = \hat{\boldsymbol{f}}^T(n) * \boldsymbol{x}_{\hat{f}(n),v(n)}(n), \quad (4.17)$$

where $\boldsymbol{x}_{\hat{f}(n),v(n)}(n) = [v(n), v(n-1), \cdots, v(n-L_f+1)]^T$ is the input signal vector of filter $\hat{F}(z)$ with input $v(n)$ at time n. In Fig. 4.2, the signal $x(n)$ acts both as an input excitation signal of FxLMS adaptive algorithm based ANC filter and as the desired response of $H(z)$. The weight update equation of $W(z)$ is the same as given in (4.2). The one sample delayed version of the output of ANC filter acts as an input excitation signal of $H(z)$. The output of $H(z)$ can be computed as

$$y_h(n) = h(n) * y_w(n-1) = \boldsymbol{h}^T(n)\boldsymbol{x}_{h(n),y_w(n-1)}(n), \quad (4.18)$$

where $\boldsymbol{x}_{h(n),y_w(n-1)}(n) = [y_w(n-1), y_w(n-2), \cdots, y_w(n-L_w)]^T$ is the input signal vector of filter $H(z)$ with input $y_w(n-1)$ at time n. The output of $H(z)$ is subtracted form its desired response $x(n)$ (see Fig. 4.2) to compute its error signal $e_{\hat{f}}(n)$ (also used as an error signal of FBPMN filter) as

$$e_{\hat{f}}(n) = x(n) - y_h(n) = [r(n) + y_{wf}(n) - y_{w\hat{f}}(n) - y_h(n)] + [v_f(n) - v_{\hat{f}}(n)]. \quad (4.19)$$

The filter $H(z)$ is adapted using LMS algorithm as

$$\boldsymbol{h}(n+1) = \boldsymbol{h}(n) + \mu_h e_{\hat{f}}(n)\boldsymbol{x}_{h(n),y_w(n-1)}(n). \tag{4.20}$$

The signal $e_{\hat{f}}(n)$ is also used as an error signal of FBPMN filter. The weight update equation for FBPMN filter is given by

$$\hat{\boldsymbol{f}}(n+1) = \hat{\boldsymbol{f}}(n) + \mu_f(n) e_{\hat{f}}(n)\boldsymbol{x}_{\mathrm{VSS-LMS},v(n)}(n), \tag{4.21}$$

where $\boldsymbol{x}_{\mathrm{VSS-LMS},v(n)}(n) = [v(n), v(n-1), \cdots, v(n-L_f+1)]^T$ is the input signal vector of VSS-LMS adaptive algorithm at time n, and $\mu_f(n)$ is the VSS parameter computed as

$$\mu_f(n) = \mu_{f_{\min}}\rho(n) + \mu_{f_{\max}}(1-\rho(n)), \tag{4.22}$$

where $\mu_{f_{\min}}$ and $\mu_{f_{\max}}$ are experimentally determined upper and lower bounds for $\mu_f(n)$, and time-varying parameter $\rho(n)$ is computed as

$$\rho(n) = \frac{P_{e_{\hat{f}}}(n)}{P_x(n)}; \quad \rho(0) = 1, \lim_{n\to\infty}\rho(n) \to 0, \tag{4.23}$$

where $P_{e_{\hat{f}}}(n)$, and $P_x(n)$ can be estimated online using a low pass estimator as

$$P_q(n) = \lambda P_q(n-1) + (1-\lambda)q^2(n), \tag{4.24}$$

where $q(n)$ is the signal of interest, and $0.9 < \lambda < 1$ is a forgetting factor. In (4.19), the first term in square brackets acts as an interference, while the second term $(v_f(n) - \hat{v}_f(n))$ is the desired error signal for $\hat{F}(z)$. The interference term is decreasing in nature, therefore the step-size for FBPMN filter is small when interference is large, and subsequently increased to a higher value when interference becomes small (due to convergence of $H(z)$).

4.1.4 Remarks Regarding Akhtar's Method

- For LMS based adaptive filter with input $v(n)$, the excess mean-square-error (MSE) is given by [4]

$$\xi_{\text{excess}} \approx 0.5\mu_f L P_v \xi_{\min}, \tag{4.25}$$

  where μ_f is the step-size parameter, P_v is the input signal power of adaptive filter which can be estimated using (4.24), $\xi_{\min}$ is the minimum MSE corresponding to Weiner solution. It is very easy to conclude from (4.25) that, in steady state, the large value of step-size ($\mu_f = \mu_{f_{\max}}$) results in large excess MSE, and the small value of step-size will slow down the convergence of FBPMN filter. Therefore the proper selection of $\mu_{f_{\max}}$, in Akhtar's method, is very important.

- As no gain scheduling is used, therefore the auxiliary noise, injected for online FBPMN, will degrade the NRP of ANC system at steady-state.

The solution to the above problems is to use: 1) VSS that has decreasing trend, i.e., the step-size should converge to small value as the ANC system converges, 2) Gain scheduling strategy to reduce the contribution of auxiliary noise to the residual error and improve the NRP of ANC system.

4.1.5 Proposed Method-1

The block diagram of proposed structure [76] is shown in Fig. 4.3. In [76], this structure is used along with gain scheduling of auxiliary-noise-power. However, since in this section online FBPMN without gain scheduling is discussed. Therefore, for fair comparison of the existing structures with the proposed structure it

is assumed that $G(n) = 1 \; \forall \; n$, and the discussion about gain scheduling strategy will be deferred till the next section.

The proposed structure is similar to Kuo's structure except that in the proposed structure the action of FBPM and FBPN filter combined into a single FBPMN filter as did by Akhtar [75]. The weight update equation for $W(z)$ is the same as in (4.2). The weight update equation for $H(z)$ and $\hat{F}(z)$ are the same as in (4.20) and (4.21), respectively, but with the following exceptions: 1) the vector $\boldsymbol{x}_{h(n),y_w(n-1)}(n)$ in (4.20) is replaced by vector $\boldsymbol{x}_{h(n),x(n-\Delta)}(n) = [x(n-\Delta), x(n-\Delta-1), \cdots, x(n-\Delta-L_h+1)]^T$, 2) the VSS parameter $\mu_f(n)$ in (4.21) is replaced by a fixed step-size parameter μ_f, and 3) The vector $\boldsymbol{x}_{\text{VSS-LMS},v(n)}(n)$ is replaced by a vector $\boldsymbol{x}_{\text{LMS},v(n)}(n)$, where the vector $\boldsymbol{x}_{\text{LMS},v(n)}(n) = [v(n), v(n-1), \cdots, v(n-L_f+1)]^T$. The algorithm for the proposed method-1 is given in Table. 4.1

The advantage of the proposed structure over Kuo's structure is that for $\hat{F}(z) = F(z)$ the interference term $(h(n) * v_f(n-\Delta))$ (see (4.11) and (4.15)) in $x(n)$ will be equal to zero. This will improve the convergence of ANC system in proposed method-1 compared to Kuo's method. A similar structure is proposed in [74], but instead of using the delay of Δ samples, a one sample delay is used. However, it is shown in [35] that for delay $\Delta < L_f$, the filter $H(z)$ will incorrectly cancels the desired term $(v_f(n) - v_{\hat{f}}(n))$ from the error signal $e_{\hat{f}}(n)$ of FBPM filter. This means that for delay $\Delta < L_f$ the filter $\hat{F}(z)$ will not receive the desired error signal $(v_f(n) - v_{\hat{f}}(n))$ for its weight updation. We believe that same is the problem with Akhtar's structure [75], because in Akhtar structure also there is only one sample delay ($\Delta = 1$) between the desired response and the output of filter $H(z)$. It is because of this problem that the performance of Akhtar's structure is inferior to that of proposed structure (It will be clear from the simulation results presented

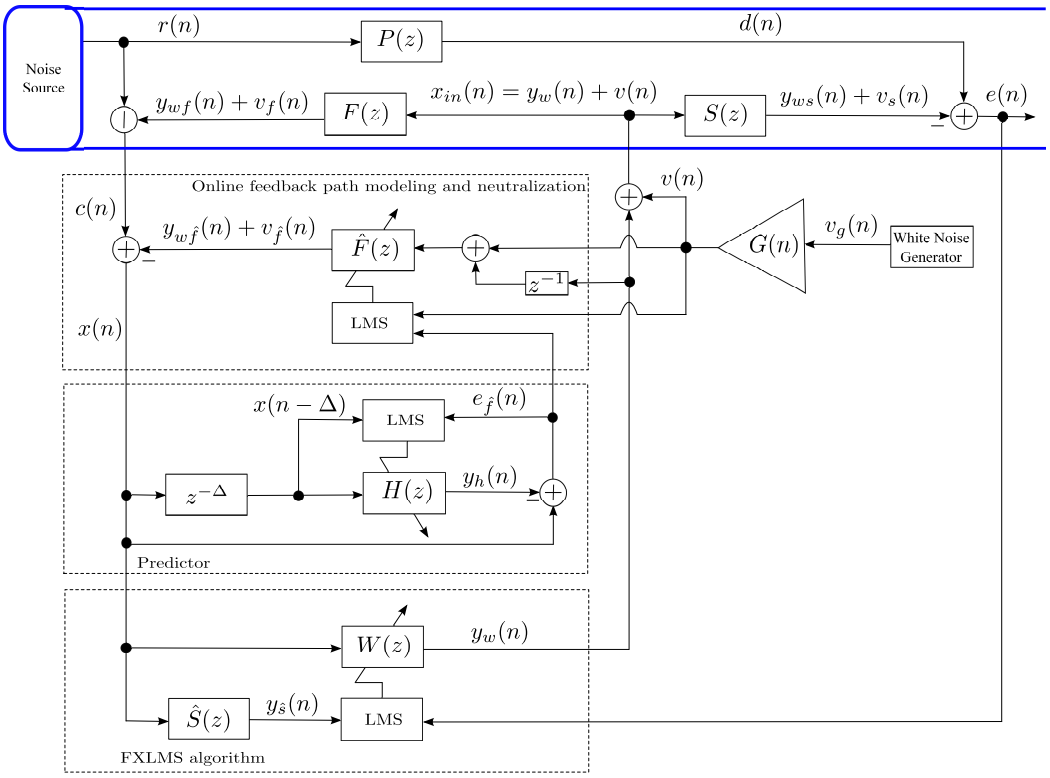

Figure 4.3: Block diagram of proposed method for online feedback path modeling and neutralization [76].

onward in Fig. 4.4 and Fig. 4.5).

4.1.6 Purpose of Decorrelation Delay

It is well known from the theory of signal processing that for random WGN signal $v(n)$, its autocorrelation function is defined as

$$E[v(n)v(n-l)] = \begin{cases} P_v & (l=0) \\ 0 & (\text{Otherwise}) \end{cases}, \tag{4.26}$$

where $E[\cdot]$ denotes the mathematical expectation, P_v is the power of signal $v(n)$ which can be estimated using (4.24), and l represents the delay between the two

Table 4.1: Algorithm for the proposed method-1

$$v(n) = G(n)v_g(n)\ (G(n) = 1\,\forall\, n)$$
$$y_{wf}(n) + v_f(n) = \boldsymbol{f}^T(n)\boldsymbol{x}_{f(n),(y_w(n-1)+v(n))}(n)$$
$$c(n) = r(n) + y_{wf}(n) + v_f(n)$$
$$y_{w\hat{f}}(n) + v_{\hat{f}}(n) = \hat{\boldsymbol{f}}^T(n)\boldsymbol{x}_{\hat{f}(n),(y_w(n-1)+v(n))}(n)$$
$$x(n) = c(n) - y_{w\hat{f}}(n) - v_{\hat{f}}(n)$$
$$y_h(n) = \boldsymbol{h}^T(n)\boldsymbol{x}_{h(n),x(n-\Delta)}(n);\ e_{\hat{f}}(n) = x(n) - y_h(n)$$
$$y_w(n) = \boldsymbol{w}^T(n)\boldsymbol{x}_{w(n),x(n)}(n)$$
$$y_{ws}(n) + v_s(n) = \boldsymbol{s}^T(n)\boldsymbol{x}_{s(n),(y_w(n)+v(n))}(n)$$
$$d(n) = \boldsymbol{p}^T(n)\boldsymbol{x}_{p(n),x(n)}(n);\ e(n) = d(n) - y_{ws}(n) - v_s(n)$$
$$y_{\hat{s}}(n) = \hat{\boldsymbol{s}}^T(n)\boldsymbol{x}_{\hat{s}(n),x(n)}(n)$$
$$\boldsymbol{h}(n+1) = \boldsymbol{h}(n) + \mu_h e_{\hat{f}}(n)\boldsymbol{x}_{h(n),x(n-\Delta)}(n)$$
$$\hat{\boldsymbol{f}}(n+1) = \hat{\boldsymbol{f}}(n) + \mu_f e_{\hat{f}}(n)\boldsymbol{x}_{\mathrm{LMS},v(n)}(n)$$
$$\boldsymbol{w}(n+1) = \boldsymbol{w}(n) + \mu_w e(n)\boldsymbol{x}_{\mathrm{LMS},y_{\hat{s}}(n)}(n)$$

samples. It is clear form (4.26) that for random WGN signals the consecutive samples are uncorrelated. It is shown in [35] that for a WGN signal filtered through filter $F(z)$ of tap-weight length L_f, i.e., $v_f(n) = f(n) * v(n)$, a delay of at least L_f samples are needed for the two samples to be uncorrelated, i.e.,

$$E[v_f(n)v_f(n-l)] = 0 \qquad \forall \qquad l \geq L_f. \tag{4.27}$$

It is known from the theory of adaptive signal processing that the output of adaptive filter will converge to that part of its desired response which is correlated

with its input signal. In Fig. 4.3, the signal $x(n-\Delta)$ acts as an input, and the signal $x(n)$ (given by (4.16)) acts as the desired response of $H(z)$. It is required that the output $y_h(n)$ should converge to $(r(n)+y_{wf}(n)-y_{w\hat{f}}(n))$, leaving the desired signal $(v_f(n)-v_{\hat{f}}(n))$ in the error signal $e_{\hat{f}}(n)$ of FBPMN filter. However from (4.27), it can be concluded that the signal $x(n)$ (desired response of $H(z)$ in [74]) and $x(n-1)$ (input of $H(z)$ in [74]) are correlated, and a delay of one sample, as used in [74], will not be able to decorrelate the term $(v_f(n)-v_{\hat{f}}(n))$ in $x(n)$ from the term $(v_f(n-1)-v_{\hat{f}}(n-1))$ in $x(n-1)$. Therefore the output $y_h(n)$ will not only cancel the interference term $(r(n)+y_{wf}(n)-y_{w\hat{f}}(n))$, but will also start canceling the desired term $(v_f(n)-v_{\hat{f}}(n))$ of FBPMN filter. From Fig. 4.2, it is clear that the same problem exists in Akhtar's structure as well, because in Akhtar's structure also there is one sample delay between the desired response $x(n)$ and input signal $(y_w(n-1)=w(n-1)*x(n-1))$ of $H(z)$. In proposed method-1, the delay $\Delta \geq L_f$ is sufficient to decorrelate the term $(v_f(n)-v_{\hat{f}}(n))$ in $x(n)$ (desired response of $H(z)$ in proposed method-1) from the term $(v_f(n-\Delta)-v_{\hat{f}}(n-\Delta))$ in $x(n-\Delta)$ (input of $H(z)$ in proposed method), and hence will not allow the output of $H(z)$ to falsely cancel the desired term $(v_f(n)-v_{\hat{f}}(n))$ from $e_{\hat{f}}(n)$. This will improve the convergence of the FBPMN filter in proposed method-1, and hence improves the convergence of ANC system.

4.1.7 Simulation Results

In this section, simulation results are presented to compare the performance of the proposed method-1 (see Fig. 4.3) with Kuo's [70] and Akhtar's method [75]. The performance comparison is carried out on the basis of following performance measures.

Table 4.2: Simulation parameters for online feedback path modeling and neutralization without gain scheduling.

	Parameters
No FBPN	$\mu_w = 3 \times 10^{-5}$, $\mu_h = 5 \times 10^{-4}$, $\mu_f = 5 \times 10^{-3}$.
Kuo's method [70]	$\mu_w = 3 \times 10^{-5}$, $\mu_h = 5 \times 10^{-4}$, $\mu_f = 5 \times 10^{-3}$, $\Delta = 32$.
Akhtar's method [75]	$\mu_w = 3 \times 10^{-5}$, $\mu_h = 5 \times 10^{-4}$, $\mu_{f_{\min}} = 3 \times 10^{-4}$, $\mu_{f_{\max}} = 5 \times 10^{-3}$.
Proposed method-1 [76]	$\mu_w = 3 \times 10^{-5}$, $\mu_h = 5 \times 10^{-4}$, $\mu_f = 5 \times 10^{-3}$, $\Delta = 32$.

- Relative modeling error of feedback path $\Delta D_f(n)$ being defined as

$$\Delta D_f(n) = 10\log_{10}\frac{||\boldsymbol{f}(n) - \hat{\boldsymbol{f}}(n)||^2}{||\boldsymbol{f}(n)||^2} \quad \text{dB}. \tag{4.28}$$

- Mean-noise-reduction (MNR) at the error microphone without auxiliary noise contribution being defined as

$$\text{MNR}_{d-y_{ws}}(n) = 10\log_{10}\frac{E[(d(n) - y_{ws}(n))^2]}{E[d^2(n)]} \quad \text{dB}. \tag{4.29}$$

- MSE in the reference signal $\Delta X(n)$ being defined as

$$\Delta X(n) = 10\log_{10} E[(x(n) - r(n))^2 \quad \text{dB}. \tag{4.30}$$

Using data from [4], the acoustic paths $P(z)$, $S(z)$, and $F(z)$ are modeled as FIR filters of tap-weight lengths 48, 16, and 32, respectively. The adaptive filters $W(z)$, $\hat{F}(z)$, and $H(z)$ are selected as FIR filters of tap-weight length 32, 32 and 16 respectively. In all methods, -5dB offline modeling is used for $\hat{F}(z)$. The ANC filter $W(z)$ and $H(z)$ are initialized by null vectors. The original unwanted noise

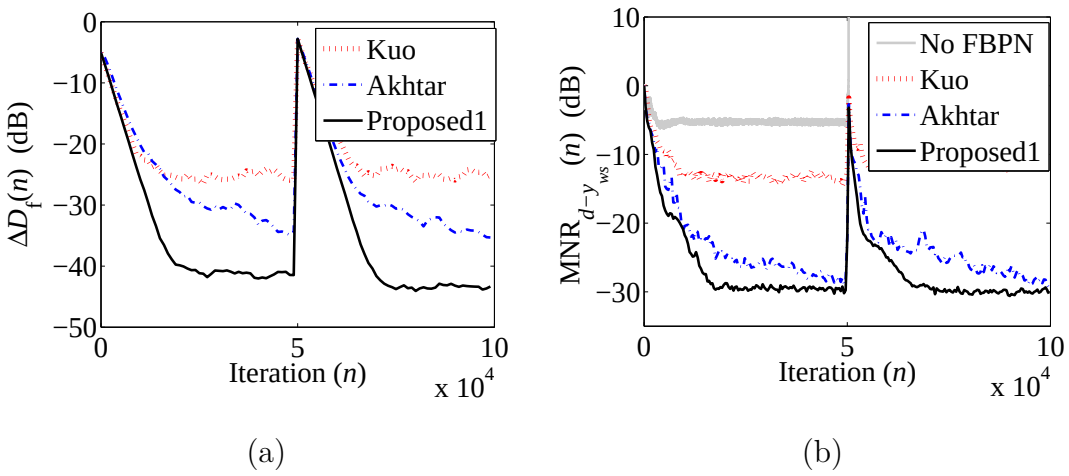

(a) (b)

Figure 4.4: (a) Relative modeling error, $\Delta D_f(n)$(dB), (b) Mean-noise-reduction without auxiliary noise, $\text{MNR}_{d-y_{ws}}(n)$ (dB).

signal $r(n)$, at the reference microphone, is a multi-tonal input with frequencies 100, 150, 300, 400, and 450 Hz, and its variance is adjusted to 2. A zero-mean WGN with variance 0.002 is added with $r(n)$ to account for any measurement noise. The modeling excitation signal, $v_g(n)$, is a zero-mean WGN with variance 0.05. The step-size parameters for adaptive filters are experimentally adjusted for fast and stable convergence and are given in Table. 4.2. The jumps in the middle of all the simulation results is due to the perturbation in the impulse responses of the acoustic paths $P(z)$, $S(z)$, and $F(z)$. The data for the perturbed acoustic paths is also obtained form [4]. The sampling frequency is 2kHz, and all the simulation results are averaged over 10 independent realizations.

- The curves for relative modeling error $\Delta D_f(n)$, as defined in (4.28), are shown in Fig. 4.4(a). In Kuo's method, the presence of the interference term $(h(n) * v_f(n-\Delta))$ in $x(n)$ (see (4.11) and (4.15)) will affect the convergence of both the FBPM filter and ANC filter. In Akhtar's method, the one sample

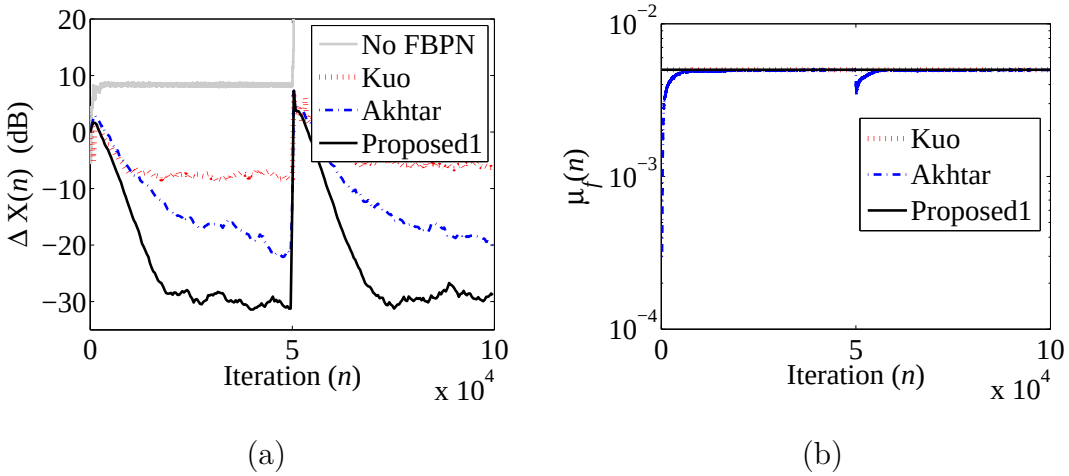

Figure 4.5: (a) Mean-square-error in the reference signal, $\Delta X(n)$ (dB), (b) Time-varying step-size parameter $\mu_f(n)$ for $\hat{F}(z)$.

delay between the desired response, $x(n)$, and the input signal, $y_w(n-1)$, of $H(z)$ can not stop $H(z)$ from canceling the desired term $(v_f(n) - v_{\hat{f}}(n))$ in $x(n)$, and thus will affect the convergence of FBPMN filter. The proposed structure solves the problems with Kuo's and Akhta's method and hence gives better performance than the previous methods.

- The curves for $\text{MNR}_{d-y_{ws}}(n)$, as defined in (4.29), are shown in Fig. 4.4(b). The improved modeling accuracy of FBPM filter will reduce the interference in the input signal of $W(z)$, and hence gives improved NRP. It is clear from Fig. 4.4(b) that the proposed method gives better performance than the previous methods.

- The curves for MSE in the reference signal $\Delta X(n)$, as defined in (4.30), are shown in Fig. 4.5(a). The better convergence of the FBPM filter will efficiently neutralize the feedback path coupling effect, thus results in reduced interference in the reference signal $r(n)$. It is clear from Fig. 4.5(a) that the

Table 4.3: Computational complexity comparison (Number of computations per iteration)

Name	$\times$	$+$	$\div$
No FBPN	$2L_w + L_s + 1$	$2L_w + L_s - 1$	–
Kuo [70]	$2L_w + 2L_h + 3L_f + L_s + 3$	$2L_w + 2L_h + 3L_f + L_s$	–
Akhtar [75]	$2L_w + 2L_h + 2L_f + L_s + 11$	$2L_w + 2L_h + 2L_f + L_s + 4$	1
Proposed1 [76]	$2L_w + 2L_h + 2L_f + L_s + 3$	$2L_w + 2L_h + 2L_f + L_s$	–

proposed method gives lower MSE compared to previous methods.

- Figure 4.5(b) shows the step-size, $\mu_f(n)$, variation of FBPM filter. In Kuo's and proposed method-1 fixed step-size is used, while in Akhtar's method VSS is used. As stated earlier, in Akhtar's method, initially a small value of step-size is used due to large value of interference term in the error signal of FBPM filter. In the later stage, the step-size increases accordingly as the interference decreases.

4.1.8 Computational Complexity Comparison

The computational complexity requirements of all the methods discussed in this section are given in Table. 4.3. The method without FBPN has the lowest computational complexity, but this method may cause the ANC system to become unstable. Among the methods with FBPN, the proposed method-1 (without gain scheduling) has the lower computational cost.

4.2 Online FBPMN With Gain Scheduling

In the previous section no gain scheduling of auxiliary noise is used, and auxiliary noise with fixed variance is injected in all operating conditions, i.e., $G(n) = 1 \forall n$. As the auxiliary noise contributes to the residual error, therefore its fixed variance $\forall n$ degrades the NRP of ANC system at the steady-state. The solution to the problem is to use auxiliary-noise-power (ANP) scheduling. For this purpose, the gain scheduling strategies are used to make $G(n)$ and hence the ANP time-varying. The ANP is varied in accordance with the convergence status of FBPMN filter. When FBPMN filter is far from actual feedback path, the gain scheduling strategy is desired to allow injection of auxiliary noise with large variance. This will result in fast convergence of FBPMN filter. At early stages of adaptation of ANC system, the large variance of auxiliary noise is masked by the large variance of the residual unwanted noise, and hence the contribution corresponding to auxiliary noise remains unnoticeable by the subject (observer). However, with the convergence of ANC system the original unwanted noise is reduced due to cancellation by the anti-noise, and is not able to mask the large value of auxiliary noise. It is desirable that as the FBPMN filter and the ANC system converges the gain scheduling strategy should allow the ANP to decrease. This will reduce the contribution of auxiliary noise to the residual error, and thus improves the NRP of ANC system. In this section a new gain scheduling strategies are proposed for online FBPMN.

4.2.1 Proposed Method-2 and Method-3

In this subsection a new gain scheduling strategy is proposed for online FBPMN. The proposed gain scheduling strategy is used with structure of Fig. 4.2, hereafter

referred as proposed method-2 [77] and with structure of Fig. 4.3, hereafter referred as proposed method-3 [76]. The auxiliary noise $v(n)$ injected into the ANC system for online FBPMN (can be used for OSPM as well) is given by

$$v(n) = G(n)v_g(n), \tag{4.31}$$

where $G(n)$ is a time-varying gain, and $v_g(n)$ is a stationary zero mean WGN signal with unit variance unless otherwise stated. In both Fig. 4.2 and Fig. 4.3, the error signal of the FBPMN filter, $e_{\hat{f}}(n)$, is time-varying (has decreasing trend) in nature, therefore the gain $G(n)$ in the proposed methods is computed by making $\{P_{(y_{w\hat{f}}+v_{\hat{f}})}(n) - P_{y_{w\hat{f}}}(n)\}$ to be equal to the power of $e_{\hat{f}}(n-1)$, and is given mathematically as

$$P_{(y_{w\hat{f}}+v_{\hat{f}})}(n) - P_{y_{w\hat{f}}}(n) = P_{e_{\hat{f}}}(n-1). \tag{4.32}$$

From Fig. 4.2 (or Fig. 4.3), the term $P_{(y_{w\hat{f}}+v_{\hat{f}})}(n)$ in (4.32) can be written as

$$P_{(y_{w\hat{f}}+v_{\hat{f}})}(n) = ||\hat{\boldsymbol{f}}(n)||^2 \left[E[(y_w(n-1))^2] + G^2(n)E[(v_g(n))^2]\right], \tag{4.33}$$

where $||\cdot||$ denotes the euclidean norm, $E[(y_w(n-1))^2] \approx P_{y_w}(n-1)$, and $v_g(n)$ is a zero-mean, unit variance WGN. Similarly the term $P_{y_{w\hat{f}}}(n)$ in (4.32) can be written as

$$P_{y_{w\hat{f}}}(n)) = ||\hat{\boldsymbol{f}}(n)||^2 P_{y_w}(n-1). \tag{4.34}$$

Substituting the value of $P_{(y_{w\hat{f}}+v_{\hat{f}})}(n)$ and $P_{y_{w\hat{f}}}(n)$, respectively, from (4.33) and (4.34) in (4.32), and solving for the time-varying gain $G(n)$ we get

$$G(n) = \sqrt{\frac{P_{e_{\hat{f}}}(n-1)}{||\hat{\boldsymbol{f}}(n)||^2}}, \tag{4.35}$$

where the power of the error signal $P_{e_{\hat{f}}}(n)$ can be estimated online using a low pass estimator as

$$P_{e_{\hat{f}}}(n-1) = \lambda P_{e_{\hat{f}}}(n-2) + (1-\lambda){e_{\hat{f}}}^2(n-1), \tag{4.36}$$

where $0.9 < \lambda < 1$ is a forgetting factor. In the proposed methods fixed step-size is used for the FBPMN filter, and the convergence is controlled by varying its input signal power, i.e, $P_v(n)$. The gain computed by (4.35) very quickly drops to a low value, thus resulting in a very small input signal power of the FBPMN filter. This will result in freezing of the adaptation of the FBPMN filter even if $\hat{F}(z)$ is far from $F(z)$. In order to avoid this problem the gain is filtered and is given by

$$G(n) = \alpha G(n-1) + \gamma \sqrt{\frac{P_{e_{\hat{f}}}(n-1)}{||\hat{\boldsymbol{f}}(n)||^2}}, \tag{4.37}$$

where α and γ controls the decay rate and the steady-state value of the time-varying gain $G(n)$. The parameter α is like a forgetting factor and varies between $0.99 < \alpha < 1$ while $\gamma > 0$ is typically selected as a very small value. The algorithms for proposed method-2 [77], and proposed method-3 [76] are given, respectively, in Table. 4.4, and 4.5.

4.2.2 Simulation Results for Online FBPMN With Gain Scheduling

In this section simulation results are presented to compare the performance of following methods

1. Methods without gain scheduling
    - ANC system with no FBPMN filter
    - Kuo's method [70]
    - Akhtar's method [75]
    - Proposed method-1 [76]
2. Methods with gain scheduling

Table 4.4: Algorithm for the proposed method-2 [77]

$$v(n) = G(n)v_g(n) \text{ } (G(n) = 1 \text{ for first iteration})$$
$$y_{wf}(n) + v_f(n) = \boldsymbol{f}^T(n)\boldsymbol{x}_{f(n),(y_w(n-1)+v(n))}(n)$$
$$c(n) = r(n) + y_{wf}(n) + v_f(n)$$
$$y_{w\hat{f}}(n) + v_{\hat{f}}(n) = \hat{\boldsymbol{f}}^T(n)\boldsymbol{x}_{\hat{f}(n),(y_w(n-1)+v(n))}(n)$$
$$x(n) = c(n) - y_{w\hat{f}}(n) - v_{\hat{f}}(n)$$
$$y_h(n) = \boldsymbol{h}^T(n)\boldsymbol{x}_{h(n),y_w(n-1)}(n);\ e_{\hat{f}}(n) = x(n) - y_h(n)$$
$$y_w(n) = \boldsymbol{w}^T(n)\boldsymbol{x}_{w(n),x(n)}(n)$$
$$y_{ws}(n) + v_s(n) = \boldsymbol{s}^T(n)\boldsymbol{x}_{s(n),(y_w(n)+v(n))}(n)$$
$$d(n) = \boldsymbol{p}^T(n)\boldsymbol{x}_{p(n),x(n)}(n);\ e(n) = d(n) - y_{ws}(n) - v_s(n)$$
$$y_{\hat{s}}(n) = \hat{\boldsymbol{s}}^T(n)\boldsymbol{x}_{\hat{s}(n),x(n)}(n);\text{Compute } G(n) \text{ using (4.37)}$$
$$\boldsymbol{h}(n+1) = \boldsymbol{h}(n) + \mu_h e_{\hat{f}}(n)\boldsymbol{x}_{h(n),y_w(n-1)}(n)$$
$$\hat{\boldsymbol{f}}(n+1) = \hat{\boldsymbol{f}}(n) + \mu_f e_{\hat{f}}(n)\boldsymbol{x}_{\text{LMS},v(n)}(n)$$
$$\boldsymbol{w}(n+1) = \boldsymbol{w}(n) + \mu_w e(n)\boldsymbol{x}_{\text{LMS},y_{\hat{s}}(n)}(n)$$

- Proposed method-2 [77]: Using structure of Fig. 4.2 (Akhtar's structure) along with gain scheduling as given in (4.37). In proposed method-2 fixed step-size, instead of VSS, is used for FBPMN filter.
- Proposed method-3 [76]: Using structure of Fig. 4.3 (Proposed method-1) along with gain scheduling as given in (4.37).

The modeling excitation signal, $v_g(n)$, is a zero-mean WGN with variance 0.05 for methods without gain scheduling, and with variance 1 for methods using gain

Table 4.5: Algorithm for the proposed method-3 [76]

$v(n) = G(n)v_g(n)$ ($G(n) = 1$ for first iteration)

$y_{wf}(n) + v_f(n) = \boldsymbol{f}^T(n)\boldsymbol{x}_{f(n),(y_w(n-1)+v(n))}(n)$

$c(n) = r(n) + y_{wf}(n) + v_f(n)$

$y_{w\hat{f}}(n) + v_{\hat{f}}(n) = \hat{\boldsymbol{f}}^T(n)\boldsymbol{x}_{\hat{f}(n),(y_w(n-1)+v(n))}(n)$

$x(n) = c(n) - y_{w\hat{f}}(n) - v_{\hat{f}}(n)$

$y_h(n) = \boldsymbol{h}^T(n)\boldsymbol{x}_{h(n),x(n-\Delta)}(n)$; $e_{\hat{f}}(n) = x(n) - y_h(n)$

$y_w(n) = \boldsymbol{w}^T(n)\boldsymbol{x}_{w(n),x(n)}(n)$

$y_{ws}(n) + v_s(n) = \boldsymbol{s}^T(n)\boldsymbol{x}_{s(n),(y_w(n)+v(n))}(n)$

$d(n) = \boldsymbol{p}^T(n)\boldsymbol{x}_{p(n),x(n)}(n)$; $e(n) = d(n) - y_{ws}(n) - v_s(n)$

$y_{\hat{s}}(n) = \hat{\boldsymbol{s}}^T(n)\boldsymbol{x}_{\hat{s}(n),x(n)}(n)$;Compute $G(n)$ using (4.37)

$\boldsymbol{h}(n+1) = \boldsymbol{h}(n) + \mu_h e_{\hat{f}}(n)\boldsymbol{x}_{h(n),x(n-\Delta)}(n)$

$\hat{\boldsymbol{f}}(n+1) = \hat{\boldsymbol{f}}(n) + \mu_f e_{\hat{f}}(n)\boldsymbol{x}_{\mathrm{LMS},v(n)}(n)$

$\boldsymbol{w}(n+1) = \boldsymbol{w}(n) + \mu_w e(n)\boldsymbol{x}_{\mathrm{LMS},y_{\hat{s}}(n)}(n)$

scheduling strategy given in (4.37). It is important to note that for the methods with no gain scheduling additive auxiliary noise with small variance is used, otherwise it will degrade the NRP of ANC system. It is shown in [22] that for LMS adaptive algorithm, the convergence of the mean-square-error (MSE) is guaranteed if the step-size is selected within the bounds given by

$$0 < \mu_f < \frac{2}{3P_v(n)}, \tag{4.38}$$

where $P_v(n)$ is the power of input excitation signal $v(n)$ of FBPMN filter and can be estimated using a low pass estimator as

$$P_q(n) = \lambda P_q(n-1) + (1-\lambda)q^2(n), \tag{4.39}$$

where $q(n)$ is the signal of interest, and $0.9 < \lambda < 1$ is a forgetting factor. It is clear from (4.38), that the allowable range of step-size μ_f for which the LMS algorithm remains stable is inversely proportional to the power of input excitation signal. In those methods which are using gain scheduling, auxiliary noise with large variance is injected. Therefore, in those methods, the allowable stable range for step-size μ_f will be small. As a result, for stable operation, the step-size (for $\hat{F}(z)$) with small value is selected compared to the methods with no gain scheduling. The step-size parameters and other simulation parameters for various methods are given in Table. 4.6. All other simulation conditions are exactly the same as used for the simulation results of Fig. 4.4, and Fig. 4.5. For comparison of different methods, the following performance measures are used

- Time-varying gain $G(n)$
- Relative modeling error of feedback path $\Delta D_f(n)$ as defined in (4.28)
- Norm of interference terms: This performance measure can be explained as follows.

  Using (4.3) and (4.16), the weight update equation for ANC filter $W(z)$ given by (4.2) can also be written like this

$$\begin{aligned} \boldsymbol{w}(n+1) &= \boldsymbol{w}(n) + \mu_w e(n) \boldsymbol{x}_{\mathrm{LMS},y_{\hat{s}}(n)}(n) \\ &= \boldsymbol{w}(n) + \mu_w e(n) \left[\boldsymbol{x}_{\mathrm{LMS},r_{\hat{s}}(n)}(n) + \boldsymbol{x}_{\mathrm{LMS},y_{wf\hat{s}}(n)}(n) - \right. \\ &\quad \left. \boldsymbol{x}_{\mathrm{LMS},y_{w\hat{f}\hat{s}}(n)}(n) + \boldsymbol{x}_{\mathrm{LMS},v_{f\hat{s}}(n)}(n) - \boldsymbol{x}_{\mathrm{LMS},v_{\hat{f}\hat{s}}(n)}(n) \right] \end{aligned} \tag{4.40}$$

where $y_{\hat{s}}(n)$ is given by

$$y_{\hat{s}}(n) = r_{\hat{s}}(n) + y_{wf\hat{s}}(n) - y_{w\hat{f}\hat{s}}(n) + v_{f\hat{s}}(n) - v_{\hat{f}\hat{s}}(n), \tag{4.41}$$

and $\boldsymbol{x}_{\mathrm{LMS},r_{\hat{s}}(n)}(n) = [r_{\hat{s}}(n), r_{\hat{s}}(n-1), \cdots, r_{\hat{s}}(n-L_w+1)]^T$, $\boldsymbol{x}_{\mathrm{LMS},y_{wf\hat{s}}(n)}(n) = [y_{wf\hat{s}}(n), y_{wf\hat{s}}(n-1), \cdots, y_{wf\hat{s}}(n-L_w+1)]^T$, $\boldsymbol{x}_{\mathrm{LMS},y_{w\hat{f}\hat{s}}(n)}(n) = [y_{w\hat{f}\hat{s}}(n), y_{w\hat{f}\hat{s}}(n-1), \cdots, y_{w\hat{f}\hat{s}}(n-L_w+1)]^T$, $\boldsymbol{x}_{\mathrm{LMS},v_{f\hat{s}}(n)}(n) = [v_{f\hat{s}}(n), v_{f\hat{s}}(n-1), \cdots, v_{f\hat{s}}(n-L_w+1)]^T$, and $\boldsymbol{x}_{\mathrm{LMS},v_{\hat{f}\hat{s}}(n)}(n) = [v_{\hat{f}\hat{s}}(n), v_{\hat{f}\hat{s}}(n-1), \cdots, v_{\hat{f}\hat{s}}(n-L_w+1)]^T$ are the input signal vectors corresponding to inputs $r_{\hat{s}}(n)$, $y_{wf\hat{s}}(n)$, $y_{w\hat{f}\hat{s}}(n)$, $v_{f\hat{s}}(n)$, and $v_{\hat{f}\hat{s}}(n)$ respectively. where the signals $r_{\hat{s}}(n)$, $y_{wf\hat{s}}(n)$, $y_{w\hat{f}\hat{s}}(n)$, $v_{f\hat{s}}(n)$, and $v_{\hat{f}\hat{s}}(n)$, respectively are given by

$$\begin{aligned}
r_{\hat{s}}(n) &= \hat{s}(n) * r(n) = \hat{\boldsymbol{s}}^T(n)\boldsymbol{x}_{\hat{s}(n),r(n)}(n) \\
y_{wf\hat{s}}(n) &= \hat{s}(n) * y_{wf}(n) = \hat{\boldsymbol{s}}^T(n)\boldsymbol{x}_{\hat{s}(n),y_{wf}(n)}(n) \\
y_{w\hat{f}\hat{s}}(n) &= \hat{s}(n) * y_{w\hat{f}}(n) = \hat{\boldsymbol{s}}^T(n)\boldsymbol{x}_{\hat{s}(n),y_{w\hat{f}}(n)}(n) \\
v_{f\hat{s}}(n) &= \hat{s}(n) * v_f(n) = \hat{\boldsymbol{s}}^T(n)\boldsymbol{x}_{\hat{s}(n)*v_f(n)}(n) \\
v_{\hat{f}\hat{s}}(n) &= \hat{s}(n) * v_{\hat{f}}(n) = \hat{\boldsymbol{s}}^T(n)\boldsymbol{x}_{\hat{s}(n),v_{\hat{f}}n}(n),
\end{aligned} \tag{4.42}$$

where $\boldsymbol{x}_{\hat{s}(n),r(n)}(n) = [r(n), r(n-1), \cdots, r(n-L_s+1)]^T$, $\boldsymbol{x}_{\hat{s}(n),y_{wf}(n)}(n) = [y_{wf}(n), y_{wf}(n-1), \cdots, y_{wf}(n-L_s+1)]^T$, $\boldsymbol{x}_{\hat{s}(n),y_{w\hat{f}}(n)}(n) = [y_{w\hat{f}}(n), y_{w\hat{f}}(n-1), \cdots, y_{w\hat{f}}(n-L_s+1)]^T$, $\boldsymbol{x}_{\hat{s}(n)*v_f(n)}(n) = [v_f(n), v_f(n-1), \cdots, v_f(n-L_s+1)]^T$, and $\boldsymbol{x}_{\hat{s}(n),v_{\hat{f}}(n}(n) = [v_{\hat{f}}(n), v_{\hat{f}}(n-1), \cdots, v_{\hat{f}}(n-L_s+1)]^T$. Using $e(n) = d(n) - y_{ws}(n) - v_s(n)$, the weight update equation in (4.40) can be written

as

$$\begin{aligned}\boldsymbol{w}(n+1) &= \boldsymbol{w}(n) + \mu_w(d(n) - y_{ws}(n))\boldsymbol{x}_{\mathrm{LMS},r_{\hat{s}}(n)}(n) + \\ &\quad \mu_w(d(n) - y_{ws}(n)) \left[\boldsymbol{x}_{\mathrm{LMS},y_{wf\hat{s}}(n)}(n) - \boldsymbol{x}_{\mathrm{LMS},y_{w\hat{f}\hat{s}}(n)}(n)\right] + \\ &\quad \mu_w(d(n) - y_{ws}(n)) \left[\boldsymbol{x}_{\mathrm{LMS},v_{f\hat{s}}(n)}(n) - \boldsymbol{x}_{\mathrm{LMS},v_{\hat{f}\hat{s}}(n)}(n)\right] - \\ &\quad \mu_w v_s(n) \left[\boldsymbol{x}_{\mathrm{LMS},r_{\hat{s}}(n)}(n) + \boldsymbol{x}_{\mathrm{LMS},y_{wf\hat{s}}(n)}(n) - \boldsymbol{x}_{\mathrm{LMS},y_{w\hat{f}\hat{s}}(n)}(n)\right] - \\ &\quad \mu_w v_s(n) \left[\boldsymbol{x}_{\mathrm{LMS},v_{f\hat{s}}(n)}(n) - \boldsymbol{x}_{\mathrm{LMS},v_{\hat{f}\hat{s}}(n)}(n)\right]. \qquad (4.43)\end{aligned}$$

In (4.43), the vector $\mu_w(d(n) - y_{ws}(n))\boldsymbol{x}_{\mathrm{LMS},r_{\hat{s}}(n)}(n)$ is the desired correction term for weight update of $W(z)$, while the vectors corresponding to last four terms in (4.43) acts as an interference for $W(z)$. These interference terms are required to be as small as possible in order to allow the filter $W(z)$ to converge to the optimal solution.

- Mean-noise-reduction (MNR) at the error microphone without auxiliary noise contribution as defined in (4.29)

- MNR at the error microphone with auxiliary noise contribution being defined as

$$\mathrm{MNR}(n) = 10\log_{10}\frac{E[e^2(n)]}{E[d^2(n)]} \quad \mathrm{dB}. \qquad (4.44)$$

- Figure 4.6(a) shows the plot of time-varying gain $G(n)$. In Kuo's, Akhtar's and proposed method-1, no gain scheduling is used and hence $G(n) = 1 =$ 0dB in all operating conditions. The comparison of the proposed method-1 with Kuo's and Akhtar's method is shown previously in Fig. 4.4, and Fig. 4.5. The results of Kuo's, Akhtar's, and proposed method-1 are repeated here for comparison with proposed method-2 and proposed method-3. In proposed method-2, and proposed method-3, the gain is time-varying and is

Table 4.6: Simulation parameters for online feedback path modeling and neutralization without and with gain scheduling.

	Parameters
	Methods without gain scheduling
No FBPN	$\mu_w = 3 \times 10^{-5}$, $\mu_h = 5 \times 10^{-4}$, $\mu_f = 5 \times 10^{-3}$.
Kuo's method [70]	$\mu_w = 3 \times 10^{-5}$, $\mu_h = 5 \times 10^{-4}$, $\mu_f = 5 \times 10^{-3}$, $\Delta = 32$.
Akhtar's method [75]	$\mu_w = 3 \times 10^{-5}$, $\mu_h = 5 \times 10^{-4}$, $\mu_{f_{\min}} = 3 \times 10^{-4}$, $\mu_{f_{\max}} = 5 \times 10^{-3}$.
Proposed method-1 [76]	$\mu_w = 3 \times 10^{-5}$, $\mu_h = 5 \times 10^{-4}$, $\mu_f = 5 \times 10^{-3}$, $\Delta = 32$.
	Methods with gain scheduling, i.e, using (4.37)
Proposed method-2 [77]	$\mu_w = 3 \times 10^{-5}$, $\mu_h = 5 \times 10^{-4}$, $\mu_f = 1 \times 10^{-3}$ $\alpha = 0.9992$, $\gamma = 3 \times 10^{-3}$.
Proposed method-3 [76]	$\mu_w = 3 \times 10^{-5}$, $\mu_h = 5 \times 10^{-4}$, $\mu_f = 1 \times 10^{-3}$, $\Delta = 32$, $\alpha = 0.9992$, $\gamma = 3 \times 10^{-3}$.

computed using (4.37). It is clear from Fig. 4.6(a) that gain in proposed method-2 and proposed method-3 is large at early stages of adaptation of ANC system or when the acoustic paths are perturbed in the middle of simulation, and is reduced to a small value as the FBPMN filter converges. The gain in proposed method-3 converges faster than proposed method-2. The different gain variation in proposed method-2 and proposed method-3 is due to different structure of ANC system used in these methods.

- The curves for relative modeling error as defined in (4.28) are shown in Fig.

4.6(b). As stated earlier, in Kuo's structure the presence of the interference term $(h(n) * v_f(n-\Delta))$ (see (4.15)) in $e_h(n)$ and in $x(n)$ will affect, respectively, the convergence of the FBPM filter and ANC filter. Therefore, the performance of Kuo's method is inferior to all other methods in terms of modeling accuracy of FBPM filter. In Akhtar's method VSS is used for FBPMN filter. The performance of Akhtar's method is better than the Kuo's method but worst than the proposed method-1. The proposed method-2 uses the same structure of Akhtar's method. However in proposed method-2 a gain scheduling strategy of (4.37) is used, and fixed step-size is used for FBPMN filter. Similarly the proposed method-3 uses the same structure as used in proposed method-1. However in proposed method-3 gain scheduling strategy of (4.37) is used to vary the gain $G(n)$. It is clear from Fig. 4.6(b) that the performance of the proposed method-3 is better than all the other methods.

- In Fig. 4.6(c) the norm of the interference terms, as described in (4.43), are plotted. It is clear from figure that the proposed method-3 gives better performance in terms of reducing the norm of interference.

- The curves for MNR performance without auxiliary noise contribution are shown in Fig. 4.7(a). In the case of ANC systems with no FBPN filter, no additive auxiliary noise is injected, therefore $E[e^2(n)] = E[(d(n) - y_{ws}(n))^2]$. The absence of FBPN filter results in large interference in the input signal of $W(z)$, therefore $W(z)$ is not able to generate the desired anti-noise signal $y_{ws}(n)$ at the error microphone. The absence of FBPN results in a large interference in the input signal of $W(z)$, and hence the ANC system may become unstable. This can be observed from Fig. 4.7(a), where the ANC system without FBPN filter becomes unstable after the acoustic paths per-

turbation in the middle of the simulation. All the proposed method results in improved performance compared to Kuo's and Akhtar's methods. The improved performance of the proposed methods is due to quick neutralization of the feedback path.

- Fig. 4.7(b) shows the curves for MNR(n) with auxiliary noise contribution. The improved NRP of the proposed methods is due to small contribution of $E[(d(n)-y_{ws}(n))^2]$ (see Fig. 4.7(a)) and $E[v_s^2(n)]$ (due to small value of gain (see Fig. 4.6(a))) in $E[e^2(n)]$.

- Fig. 4.7(c) shows the step-size variation for the FBPMN filter $\hat{F}(z)$. In Kuo's and in the proposed methods fixed step-size is used, while in Akhtar's method VSS is used. In the proposed method-2 and proposed method-3, the value of step-size for the FBPMN filter is smaller than that in Kuo's method and in proposed method-1. However, the proposed method-2 and proposed method-3 gives fast convergence of the FBPMN filter (see Fig. 4.6(b)). This is due to the large variance of additive auxiliary noise in the proposed method-2 and proposed method-3 compared to both the Kuo's method and proposed method-1. As no gain scheduling is used in Kuo's, Akhtar's and proposed method-1, therefore auxiliary noise with small variance is used otherwise the large variance of auxiliary noise will degrade the NRP of ANC systems. As stated earlier, in Akhtar's method initially a small value of step-size is used due to large value of interference term in the error signal of the FBPMN filter. In the later stage, the step-size increases accordingly as the interference decreases. When the acoustic paths are perturbed in the middle of simulation, then the interference in the error signal of $\hat{F}(z)$ increases, and correspondingly the step-size in Akhtar's method decreases again. As the

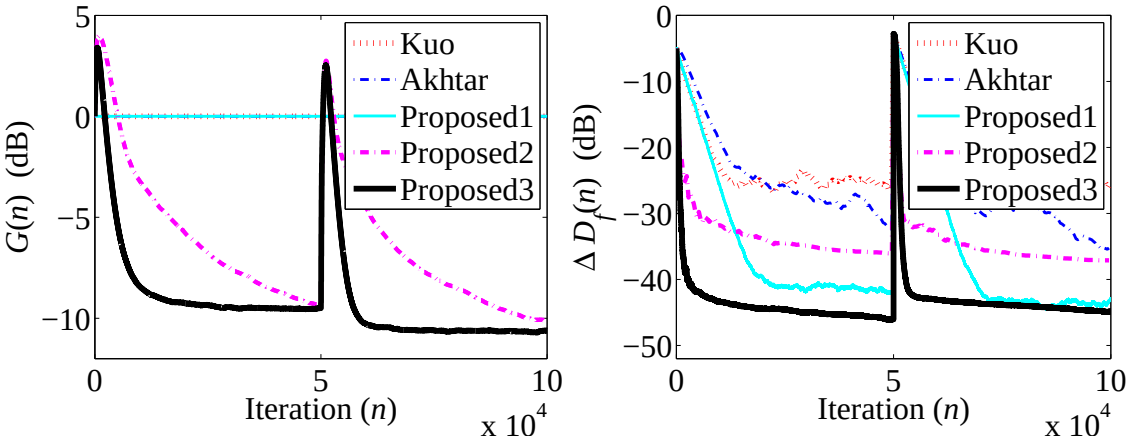

(a) (b)

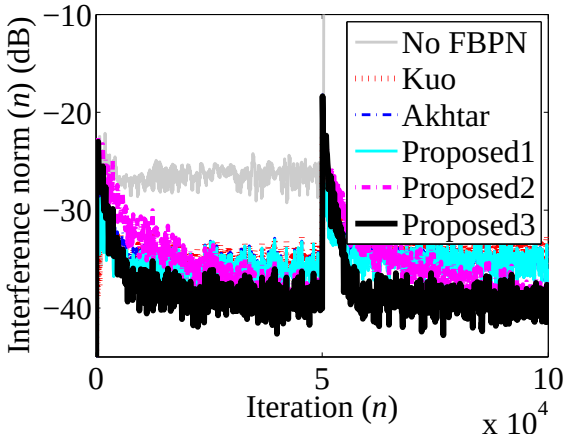

(c)

Figure 4.6: (a) The time-varying gain $G(n)$(dB), (b) Relative modeling error, $\Delta D_f(n)$(dB), (c) Norm of total interference for ANC filter in dB.

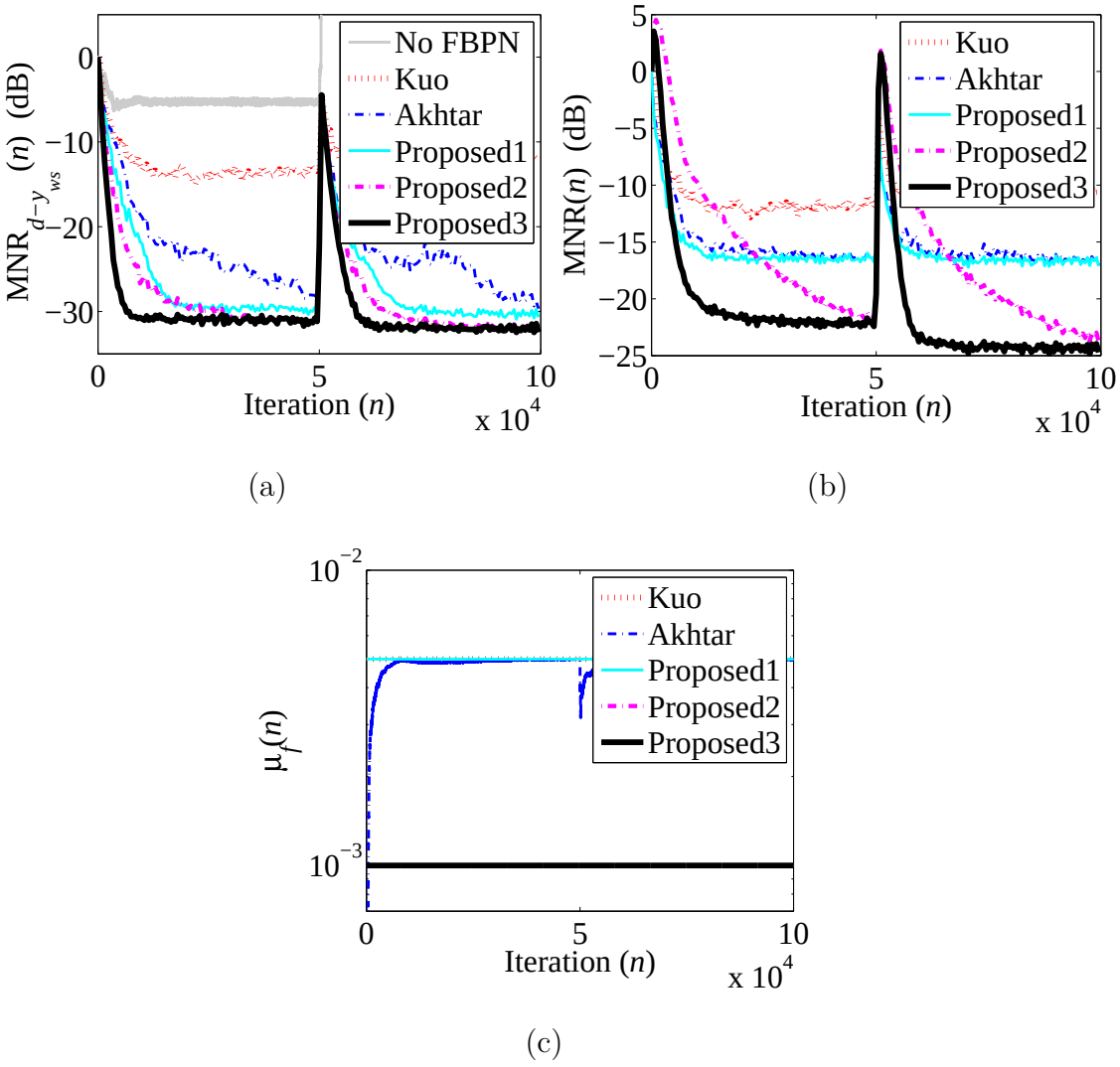

Figure 4.7: (a) Mean-noise-reduction without auxiliary noise, $\text{MNR}_{d-y_{ws}}(n)$ (dB), (b) Mean-noise-reduction with auxiliary noise, $\text{MNR}(n)$ (dB), (c) Time-varying step-size parameter $\mu_f(n)$ for $\hat{F}(z)$.

ANC system converges, after acoustic paths perturbation, then the step-size in Akhtar's method again converging towards the maximum value.

4.2.3 Remarks Regarding Proposed Method-2 and Method-3

- In proposed method-2 and proposed method-3 the gain is time-varying, and is computed using (4.37). The small value of the gain at steady-state reduces the contribution of auxiliary noise to the residual error, and thus improves the NRP of ANC system.

- The time-varying gain $G(n)$ computed using (4.35) drops very quickly. Although this is desirable as far as NRP of ANC system is concerned. However, the quick drop of the gain will reduce the power of input excitation signal of adaptive FBPMN filter and its adaptation process freezes. In order to avoid this situation, it is required to control the decay rate of the gain $G(n)$ in (4.35). For this reason the gain is required to be filtered through a low pass filter involving two tuning parameters α and γ (see (4.37)). These parameters controls the decay rate of the gain $G(n)$ in (4.35). However,these parameters needs to be tuned again and again with changing characteristics of the original unwanted noise, otherwise the NRP of ANC system will be degraded.

4.2.4 Effect of Relative Modeling Error of Feedback Path $\Delta D_f(n)$ on MNR(n)

In this section the effect of $-\Delta D_f(n)$ on $-$MNR(n) of ANC system is studied. For this case study the concept of offline modeling is used and the weights of fixed FBPN filter in Fig. 1.12 are initialized for $-\Delta D_f(n)$ of 1 to 60 dB with a step of 1 when moving from 1 to 60 dB. For each step of $-\Delta D_f(n)$ the corresponding value of $-$MNR(n) is obtained by averaging the last 50000 samples of $-$MNR(n) out of 100000 samples. The required simulation parameters are the same as used for Fig. 4.4. For this case study the $-$MNR(n) is plotted versus $-\Delta D_f(n)$ in Fig. 4.8. It is clear from Fig. 4.8 that for $-\Delta D_f(n) \geq 18$ dB the $-$MNR(n) is independent of $-\Delta D_f(n)$.

In this case the concept of offline modeling is used, and no auxiliary noise is injected. Therefore, the last three terms in (4.43) are zero, and the only interference term for $\boldsymbol{w}(n)$ in (4.43) is $\mu_w(d(n)-y_{ws}(n))[\boldsymbol{x}_{\text{LMS},y_{wf\hat{s}}(n)}(n)-\boldsymbol{x}_{\text{LMS},y_{w\hat{f}\hat{s}}(n)}(n)]$. For FBPN filter with modeling accuracy of -18 dB and higher the condition $||[\boldsymbol{x}_{\text{LMS},y_{wf\hat{s}}(n)}(n)-\boldsymbol{x}_{\text{LMS},y_{w\hat{f}\hat{s}}(n)}(n)]|| << ||\boldsymbol{x}_{\text{LMS},r_{\hat{s}}(n)}(n)||$ is true, which implies that the interference term $\mu_w(d(n)-y_{ws}(n))[\boldsymbol{x}_{\text{LMS},y_{wf\hat{s}}(n)}(n)-\boldsymbol{x}_{\text{LMS},y_{w\hat{f}\hat{s}}(n)}(n)]$ has negligible effect on the convergence of tap-weights of $\boldsymbol{w}(n)$ towards optimal value, therefore the $-$MNR(n) is independent of $-\Delta D_f(n)$ for $-\Delta D_f(n) \geq 18$ dB.

From this case study it can be concluded that higher modeling accuracy does not mean less MNR, however higher modeling accuracy results in large stability margins of ANC system. The above discussion lead us to the development of self-tuned ANP scheduling strategy with matching step-size for online FBPMN in ANC systems, referred as proposed method-4 [78], and will be discussed in the

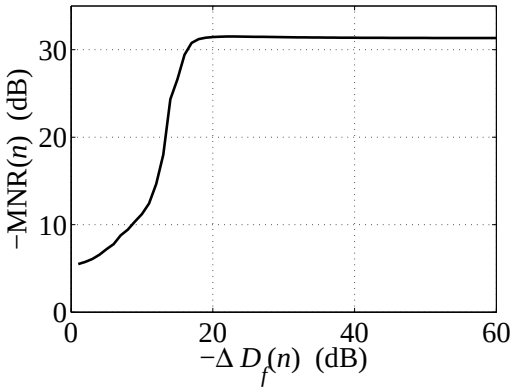

Figure 4.8: Effect of relative modeling error, $\Delta D_f(n)$ (dB) as defined in (4.28) on MNR(n) (dB) as defined in (4.44).

following subsection.

4.2.5 Proposed Method-4

In ANC systems, online FBPMN is needed: 1) to solve the potential instability problem associated with fix/time-varying feedback path, and 2) to improve the NRP of ANC system. Auxiliary noise injected for online FBPM degrades the NRP of ANC system. The solution to the problem is to use ANP scheduling. The previous proposed methods for online FBPMN with gain scheduling needs two tuning parameters α, and γ (see (4.37)). These tuning parameters are required to be tuned with changing characteristics of the original unwanted noise. In this subsection a new method is proposed [78], in which a self-tuned ANP scheduling strategy with matching step-size for adaptive FBPMN filter is used. The advantage of the proposed method-4 is that no tuning parameters are required for ANP scheduling, and improved steady-state NRP is achieved.

The block diagram of proposed method-4 is the same as for proposed method-3 (see Fig. 4.3). However, in proposed method-4, instead of fixed step-size, a

matching step-size (kind of VSS) is used for FBPMN filter. In proposed method-4 the gain is computed using (4.35). In proposed method-4, instead of filtering the gain using (4.37) the idea of matching step-size is used to compensate for the bad effect on modeling accuracy of FBPMN filter due to quick drop of the gain. The idea of matching step-size will eliminate the use of tuning parameters while still allowing $\Delta D_f(n) \leq -18$dB (see Fig. 4.8 for the effect of $\Delta D_f(n)$ on MNR(n)). The word matching step-size is used to emphasis on the fact that the step-size for each tap-weight of $\hat{F}(z)$ will adjust its value automatically to compensate for the decrease in the gain of the input signal value due to gain scheduling.

4.2.6 Matching Step-Size Calculation for FBPMN Filter in Proposed Method-4

To explain the matching step-size, consider Fig. 4.3 where the VSS-LMS based weight update equation for FBPMN filter can be written as

$$\hat{\boldsymbol{f}}(n+1) = \hat{\boldsymbol{f}}(n) + \boldsymbol{\mu}_f(n) e_{\hat{f}}(n) \boldsymbol{x}_{\text{VSS-LMS},v(n)}(n), \tag{4.45}$$

where $\hat{\boldsymbol{f}}(n) = [\hat{f}_0(n), \hat{f}_1(n), \cdots, \hat{f}_{L_f-1}(n)]^T$ is the impulse response coefficient vector of $\hat{F}(z)$ at time n, $\boldsymbol{x}_{\text{VSS-LMS},v(n)}(n) = [v(n), v(n-1), ...v(n-L_f+1)]^T$ is the input signal vector at time n, and $\boldsymbol{\mu}_f(n)$ is a diagonal matrix having matching step-size entries on its diagonal for the tap-weights of $\hat{F}(z)$. In (4.45), both the signal $e_{\hat{f}}(n)$, and the vector $\boldsymbol{x}_{\text{VSS-LMS},v(n)}(n)$ are functions of the diagonal gain matrix $\boldsymbol{G}(n)$ being defined as

$$\boldsymbol{G}(n) = \text{diag}[G(n), G(n-1), \cdots, G(n-L_f+1)], \tag{4.46}$$

where $\boldsymbol{G}(n)$ has dimensions $L_f \times L_f$. The error signal $e_{\hat{f}}(n)$ and the input signal vector $\boldsymbol{x}_{\text{LMS},v(n)}(n)$ of FBPMN filter in terms of gain matrix $\boldsymbol{G}(n)$ are given,

respectively, by

$$\begin{aligned} e_{\hat{f}}(n) &= \Big[r(n) + y_{wf}(n) - y_{w\hat{f}}(n)\Big] + \\ &\quad \Big[\boldsymbol{f}^T(n) - \hat{\boldsymbol{f}}^T(n)\Big]\boldsymbol{G}(n)\boldsymbol{x}_{\mathrm{LMS},v_g(n)}(n), \end{aligned} \tag{4.47}$$

and

$$\boldsymbol{x}_{\mathrm{VSS-LMS},v(n)}(n) = \boldsymbol{G}(n)\boldsymbol{x}_{\mathrm{LMS},v_g(n)}(n) \tag{4.48}$$

where $\boldsymbol{f}(n) = [f_0(n), f_1(n), \cdots, f_{L_f-1}(n)]^T$ is the impulse response coefficient vector of unknown path $F(z)$ at time n, and $\boldsymbol{x}_{\mathrm{LMS},v_g(n)}(n) = [v_g(n), v_g(n-1), ...v_g(n-L_f+1)]^T$. In case of ANC system without gain scheduling the gain matrix will be identity matrix of size $L_f \times L_f$ and is given by $\boldsymbol{G}(n) = \boldsymbol{I}$.

The gain scheduling will reduce the contribution of auxiliary noise at the error microphone, but it is clear from (4.47) and (4.48) that it will decrease the power of the error signal, and the input excitation signal of the FBPMN filter. This will reduce the magnitude of the tap-weight correction term of the FBPMN filter and thus degrades the modeling accuracy of the FBPMN filter. As the feedback path $\boldsymbol{f}(n)$ is unknown, therefore the effect of gain on the error signal $e_{\hat{f}}(n)$ can not be compensated. However the effect of the gain on the input signal vector of FBPMN filter can be compensated by using the matching step size. Therefore, instead of fixed step-size μ_f used in proposed method-3, here we compute the matching step-size $\mu_{f_i}(n)$ $(i = 0, 1, 2, \cdots L_f - 1)$ for each tap-weight of $\hat{\boldsymbol{f}}(n)$ as

$$\begin{aligned} \boldsymbol{\mu}_f(n) &= \mathrm{diag}[\mu_{f_0}(n), \mu_{f_1}(n), \cdots, \mu_{f_{L_f-1}}(n)] \\ &= \mathrm{diag}[\mu_{f_0}(n), \mu_{f_0}(n-1), \cdots, \mu_{f_0}(n-L_f+1)] \\ &= \mu_f \boldsymbol{G}^{-1}(n) \end{aligned} \tag{4.49}$$

where $\boldsymbol{\mu}_f(n)$ is a diagonal matrix having matching step-size entries $\mu_f/G(n-i)$ for $(i = 0, 1, 2, \cdots L_f - 1)$ on its main diagonal. $\mu_{f_0}(n) = \mu_f/G(n)$ is matching step-

size for the first tap-weight $\hat{f}_0(n)$ of FBPMN filter at time n and can alternatively be computed by satisfying the condition that the product of step-size and gain at two consecutive iterations are made equal, and is given mathematically as

$$\mu_{f_0}(n)G(n) = \mu_{f_0}(n-1)G(n-1) \quad \forall \quad n \geq 1, \tag{4.50}$$

From (4.50) the step-size $\mu_{f_0}(n)$ is computed as

$$\mu_{f_0}(n) = \frac{\mu_{f_0}(n-1)G(n-1)}{G(n)} \quad \forall \quad n \geq 1, \tag{4.51}$$

where $G(0) = 1$, and $\mu_{f_0}(0) = \mu_f$. $\boldsymbol{G}^{-1}(n)$ is inverse of gain matrix $\boldsymbol{G}(n)$. As $\boldsymbol{G}(n)$ is a diagonal matrix, therefore its inverse can be computed by taking the reciprocal of each entry such that $\boldsymbol{G}(n)\boldsymbol{G}^{-1}(n) = \boldsymbol{I}$.

Using (4.45), (4.48), and (4.49) the weight update equation of FBPMN filter in terms of matching step-size matrix $\boldsymbol{\mu}_f(n)$ and the gain matrix $\boldsymbol{G}(n)$ (leaving $e_{\hat{f}}(n)$ in the update equation as it is, because the effect of gain $G(n)$ on the error signal $e_{\hat{f}}(n)$ can not be compensated) can be written as

$$\hat{\boldsymbol{f}}(n+1) = \hat{\boldsymbol{f}}(n) + \mu_f \boldsymbol{G}^{-1}(n) e_{\hat{f}}(n) \boldsymbol{G}(n) \boldsymbol{x}_{\text{LMS},v_g(n)}(n), \tag{4.52}$$

Replacing $\mu_f \boldsymbol{G}^{-1}(n)$ with $\boldsymbol{\mu}_f(n)$ and $\boldsymbol{G}(n)\boldsymbol{x}_{\text{LMS},v_g(n)}(n)$ with $\boldsymbol{x}_{\text{VSS-LMS},v(n)}(n)$ in (4.52) we will get (4.45). Equation (4.52) can be further simplified and written as

$$\hat{\boldsymbol{f}}(n+1) = \hat{\boldsymbol{f}}(n) + \mu_f e_{\hat{f}}(n) \boldsymbol{x}_{\text{LMS},v_g(n)}(n), \tag{4.53}$$

where μ_f is a fixed step-size parameter. The original proposed method-4 (see (4.52)), and its simplified version (see (4.53)) needs L_f more memories to store, respectively, the diagonal values of gain matrix $\boldsymbol{G}(n)$, and the vector $\boldsymbol{x}_{\text{LMS},v_g(n)}(n)$ compared to proposed method-3. However, the computational complexity of the simplified version of proposed method-4 is lower than the proposed method-3 [76]

because in the simplified version of proposed method-4 the gain $G(n)$ computed using (4.35) need not to be filtered through a low pass filter. Also the computation complexity of simplified version of proposed method-4 given by (4.53) is lower than the actual proposed method-4 (given by (4.45)). This is because in simplified version fixed step-size μ_f, instead of matching step-size $\mu_f(n)$, is used.

From (4.53) we can conclude that the use of matching step-size $\boldsymbol{\mu}_f(n) = \mu_f \boldsymbol{G}^{-1}(n)$ in the weight update equation (4.52) of the FBPMN filter will partially compensate the gain scheduling effect on the modeling accuracy of the FBPMN filter. This is because the matching step-size removes the effect of the gain from the input signal vector $\boldsymbol{G}(n)\boldsymbol{x}_{\text{LMS},v_g(n)}(n)$ (note that vector $\boldsymbol{x}_{\text{LMS},v_g(n)}(n)$ is used in (4.53) instead of $\boldsymbol{x}_{\text{VSS-LMS},v(n)}(n)$) for weight updation of FBPMN filter. However this compensation is partial because the effect of gain on $e_{\hat{f}}(n)$ can not be removed as the feedback path $\boldsymbol{f}(n)$ is unknown. The algorithm for the proposed method-4 is shown in Table. 4.7.

4.2.7 Simulation Results for Online FBPMN With Gain Scheduling

In this section simulation results are presented to compare the performance of Kuo's [70], Akhtar's [75], and proposed method-3 [76] with proposed method-4 [78]. Previously it is shown through simulation results that proposed method-3 is better than both proposed method-1 and proposed method-2. Therefore, for simplicity of representation of simulation results the proposed method-1 and proposed method-2 are not considered here. The performance measures and the required simulation parameters are exactly the same as used for the simulation results of Fig. 4.6 and Fig. 4.7.

Table 4.7: Algorithm for the proposed method-4 [78]

$v(n) = G(n)v_g(n)$ ($G(n) = 1$ for first iteration)

$y_{wf}(n) + v_f(n) = \boldsymbol{f}^T(n)\boldsymbol{x}_{f(n),(y_w(n-1)+v(n))}(n)$

$c(n) = r(n) + y_{wf}(n) + v_f(n)$

$y_{w\hat{f}}(n) + v_{\hat{f}}(n) = \hat{\boldsymbol{f}}^T(n)\boldsymbol{x}_{\hat{f}(n),(y_w(n-1)+v(n))}(n)$

$x(n) = c(n) - y_{w\hat{f}}(n) - v_{\hat{f}}(n)$

$y_h(n) = \boldsymbol{h}^T(n)\boldsymbol{x}_{h(n),x(n-\Delta)}(n)$; $e_{\hat{f}}(n) = x(n) - y_h(n)$

$y_w(n) = \boldsymbol{w}^T(n)\boldsymbol{x}_{w(n),x(n)}(n)$

$y_{ws}(n) + v_s(n) = \boldsymbol{s}^T(n)\boldsymbol{x}_{s(n),(y_w(n)+v(n))}(n)$;$d(n) = \boldsymbol{p}^T(n)\boldsymbol{x}_{p(n),x(n)}(n)$

$e(n) = d(n) - y_{ws}(n) - v_s(n)$;$y_{\hat{s}}(n) = \hat{\boldsymbol{s}}^T(n)\boldsymbol{x}_{\hat{s}(n),x(n)}(n)$

Compute $G(n)$ using (4.35); Compute $\boldsymbol{\mu}_f(n)$ using (4.49)

$\boldsymbol{h}(n+1) = \boldsymbol{h}(n) + \mu_h e_{\hat{f}}(n)\boldsymbol{x}_{h(n),x(n-\Delta)}(n)$

$\hat{\boldsymbol{f}}(n+1) = \hat{\boldsymbol{f}}(n) + \boldsymbol{\mu}_f(n)e_{\hat{f}}(n)\boldsymbol{x}_{\mathrm{LMS},v(n)}(n)$

$\boldsymbol{w}(n+1) = \boldsymbol{w}(n) + \mu_w e(n)\boldsymbol{x}_{\mathrm{LMS},y_{\hat{s}}(n)}(n)$

- Figure 4.9(a) shows the plot of gain, $G(n)$, in dB. In Kuo's and Akhtar's method no gain scheduling is used, therefore the $G(n) = 0$ dB in all operating conditions. In proposed method-3 the gain computed using (4.35) is then filtered through a low pass filter, having parameters α and γ. Theses two parameters control the decay rate and steady-state value of $G(n)$, and avoid freezing of the convergence of FBPMN filter when the input excitation signal of FBPMN filter goes low due to gain scheduling. In the proposed method-4, the use of matching step-size eliminates the need of low pass filtering.

In the proposed method-4 the gain is computed using (4.35) and settles to lower steady-state value compared to other methods. After the acoustic path perturbation at $n = 2 \times 10^5$, a similar trend is observed for gain variation as it was before the perturbation.

- Figure 4.9(b) shows the curves for relative modeling error as defined in (4.28). It is clear form Fig. 4.9(b) that all the methods can achieve the desirable modeling accuracy limit of -18 dB. The proposed method-3 outperforms in terms of modeling accuracy of $\hat{F}(z)$. The reason is that the two tuning parameters control the decay rate of $G(n)$, thus resulting in large input power and fast convergence of $\hat{F}(z)$. In the proposed method-4 the gain drops very quickly (see Fig. 4.9(a) for gain variation). The effect of this decrease is partially compensated by adjusting the step-size of FBPMN filter, which will allow the proposed method-4 to achieve sufficient modeling accuracy for $\hat{F}(z)$ even if the input signal power $P_v(n)$ of the signal $v(n)$ for FBPMN filter drops to a very low value due to gain scheduling.

- In Fig. 4.9(c) the norm of interference terms, as described in (4.43), are plotted. At steady-state the conditions $||\boldsymbol{x}_{\text{LMS},y_{wf\hat{s}}(n)}(n) - \boldsymbol{x}_{\text{LMS},y_{w\hat{f}\hat{s}}(n)}(n)|| << ||\boldsymbol{x}_{\text{LMS},r_{\hat{s}}(n)}(n)||$ and $||\boldsymbol{x}_{\text{LMS},v_{f\hat{s}}(n)}(n) - \boldsymbol{x}_{\text{LMS},v_{\hat{f}\hat{s}}(n)}(n)|| << ||\boldsymbol{x}_{\text{LMS},r_{\hat{s}}(n)}(n)||$ are true and out of the last four interference terms the contribution of interference term $\mu_w v_s(n)[\boldsymbol{x}_{\text{LMS},r_{\hat{s}}(n)}(n) + \boldsymbol{x}_{\text{LMS},y_{wf\hat{s}}(n)}(n) - \boldsymbol{x}_{\text{LMS},y_{w\hat{f}\hat{s}}(n)}(n)]$ is significant. The signal $v_s(n)$ is a function of gain, therefore the small value of the gain in the proposed method-4 reduces the contribution of $v_s(n)$ and hence reduces the effect of the remaining significant interference term $\mu_w v_s(n)[\boldsymbol{x}_{\text{LMS},r_{\hat{s}}(n)}(n) + \boldsymbol{x}_{\text{LMS},y_{wf\hat{s}}(n)}(n) - \boldsymbol{x}_{\text{LMS},y_{w\hat{f}\hat{s}}(n)}(n)]$, thus resulting in small total interference in the weight update equation of $\boldsymbol{w}(n)$ as shown in

Fig. 4.9(c).

- Figure 4.10(a) shows the plot of $\text{MNR}_{d-y_{ws}}(n)$. In case of ANC systems without FBPN, no auxiliary noise is injected therefore $E[e^2(n)] = E[(d(n) - y_{ws}(n))^2]$, and the absence of FBPN filter results in large interference in the input signal of $W(z)$, therefore $W(z)$ is not able to generate the desired anti-noise signal $y_{ws}(n)$ at the error microphone. The structure proposed by Kuo also result in large interference in the input signal of $W(z)$, thus degrades the NRP. It is clear from Fig. 4.10(a) that the Akhtar's, the proposed method-3 and the proposed method-4 outperforms in terms of $\text{MNR}_{d-y_{ws}}(n)$ compared to Kuo's method. The reason behind this improved performance is not only the different strategy of weight adaptation of FBPMN filter but also the the different structure of the overall ANC system.

- Figure 4.10(b) shows the MNR performance of various methods. It is clear that the proposed method-4 results in lower MNR value compared to other methods. The improved NRP is due to small contribution of $E[v_s^2(n)]$ (due to small value of gain $G(n)$) in $E[e^2(n)]$ at steady-state.

- Figure 4.10(c) shows the step-size variation for the first tap of $\hat{F}(z)$. In Kuo's, Akhtar's and proposed method-3 same step-size is used for all the tap-weights of $\hat{F}(z)$, while in proposed method-4 different step-size is used for each tap-weight of $\hat{F}(z)$. For the sake of convenience, in all the methods, only the step-size variation for the first tap-weight of $\hat{F}(z)$, i.e., $\mu_{f_0}(n)$ is plotted. In Kuo's and proposed method-3 the value of step-size is constant for all operating conditions, while in Akhtar's and the proposed method-4 VSS is used. In Akhtar's method the step-size is minimum at the start and then increase to a

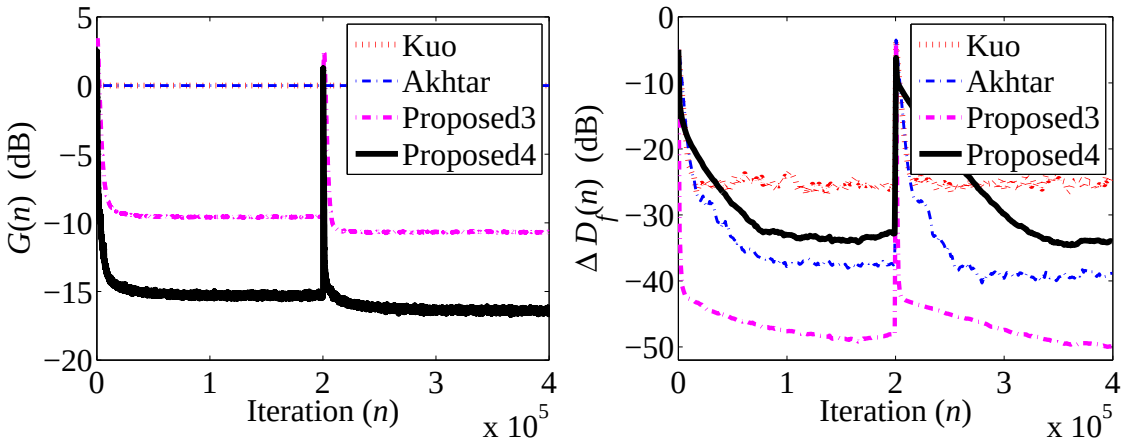

(a)

(b)

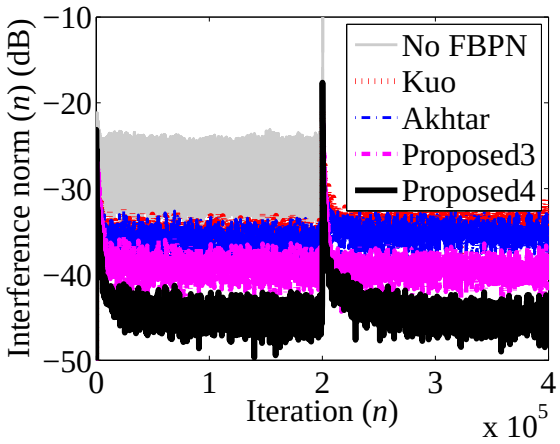

(c)

Figure 4.9: (a) The time-varying gain $G(n)$(dB), (b) Relative modeling error, $\Delta D_f(n)$(dB), (c) Norm of total interference for ANC filter in dB.

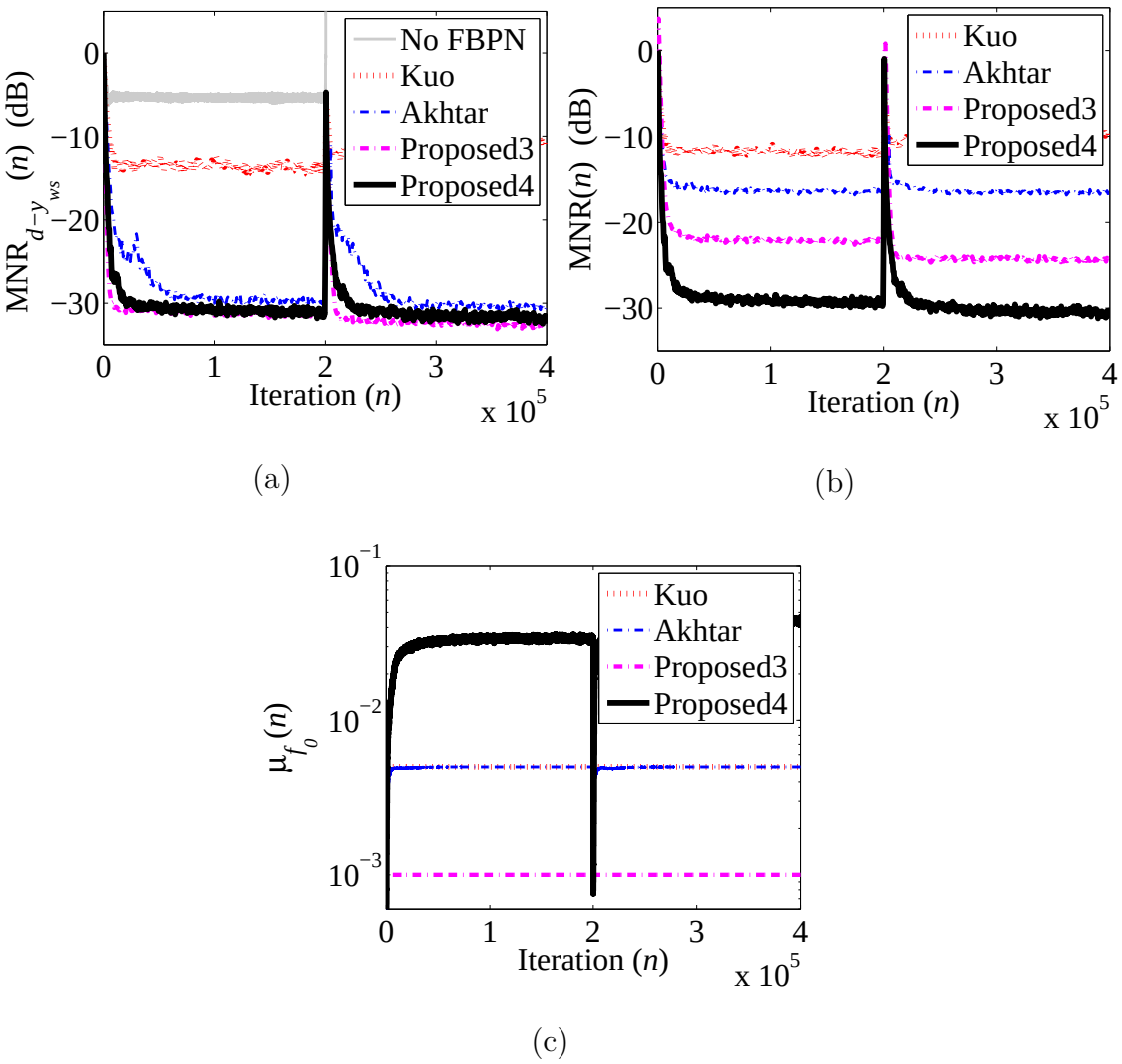

Figure 4.10: (a) Mean-noise-reduction without auxiliary noise, $\text{MNR}_{d-y_{ws}}(n)$ (dB), (b) Mean-noise-reduction with auxiliary noise, $\text{MNR}(n)$ (dB), (c) Time-varying step-size parameter $\mu_{f_0}(n)$ for first tap-weight of $\hat{F}(z)$.

Table 4.8: Computational complexity comparison (Number of computations per iteration)

Name	×	+	÷	√
Methods without gain scheduling				
No FBPN	$2L_w + L_s + 1$	$2L_w + L_s - 1$	–	–
Kuo [70]	$2L_w + 2L_h + 3L_f + L_s + 3$	$2L_w + 2L_h + 3L_f + L_s$	–	–
Akhtar [75]	$2L_w + 2L_h + 2L_f + L_s + 11$	$2L_w + 2L_h + 2L_f + L_s + 4$	1	–
Proposed1 [76]	$2L_w + 2L_h + 2L_f + L_s + 3$	$2L_w + 2L_h + 2L_f + L_s$	–	–
Methods with gain scheduling				
Proposed2 [77]	$2L_w + 2L_h + 3L_f + L_s + 9$	$2L_w + 2L_h + 3L_f + L_s + 2$	1	1
Proposed3 [76]	$2L_w + 2L_h + 3L_f + L_s + 9$	$2L_w + 2L_h + 3L_f + L_s + 2$	1	1
Proposed 4[78]	$2L_w + 2L_h + 3L_f + L_s + 7$	$2L_w + 2L_h + 3L_f + L_s + 1$	1	1

maximum value as the filter $\boldsymbol{h}(n)$ converges (see (4.22) for step-size variation in Akhtar's method). For the proposed method-4 the step-size variation for the first tap $\hat{f}_0(n)$ is computed using (4.51). In the proposed method-4 the values of the step-size is matched for each tap-weight in order to compensate the effect of time-varying gain, $G(n)$, on input vector in the update equation of $\hat{F}(z)$ (see (4.52)). With the decrease in the $P_{e_{\hat{f}}}(n)$ the gain and hence the input signal power of $\hat{F}(z)$ decreases and correspondingly the step-size increases to avoid freezing of the convergence of $\hat{F}(z)$. The perturbation in acoustic paths at $n = 2 \times 10^5$ results in increase in $G(n)$, therefore the step-size decreases (see (4.49)). After paths perturbation as $\hat{F}(z)$ and ANC system converges, the gain decrease and the step-size increases again.

4.2.8 Computational Complexity Comparison

The computational complexity requirements of different methods are shown in Table. 4.8. The method with no FBPN filter has the lowest computational complexity, but this method may cause the ANC system to become unstable. Among the methods with FBPN, the proposed method-1 (without gain scheduling) has the lowest computational cost. The computation of the gain increases the computational requirement of the algorithms, that is why the methods using gain scheduling have higher computational requirements compared to the methods without gain scheduling. It is clear from Table. 4.8 that all the methods using gain scheduling have almost same computational requirements.

4.3 Summary

In the first section of this chapter, existing methods for online FBPMN without gain scheduling are discussed, and their shortcomings are highlighted. A new structure is proposed to rectify the problems with the existing methods. The performance of the proposed structure is compare with the existing methods through the simulation results, and it is found that the proposed structure performs better than the existing methods.

Auxiliary noise injected for online FBPMN contributes to the residual error, and thus degrades the NRP of ANC system. In the second section of this chapter, different gain scheduling strategies are proposed to reduce the contribution of auxiliary noise to the residual and hence to improve the NRP of ANC systems.

Chapter 5

Conclusion and Future Recommendations

5.1 Conclusion

In ANC literature, many configurations of ANC systems are available. The focus of this thesis is on the filtered-x-LMS (FxLMS) adaptive algorithm based single channel feedforward configuration of ANC system. In this configuration, an anti-noise signal (to cancel the original unwanted noise) is generated with the help of reference and error microphones, ANC filter, and secondary source (loudspeaker). The two of the most important issues in feedforward configuration are 1) online secondary path modeling (OSPM), and 2) online feedback path modeling and neutralization (FBPMN). Generally, for OSPM and online FBPMN a system identi-

fication approach, in which an additional auxiliary noise is injected, is used. In this thesis different ideas of gain scheduling (to vary auxiliary-noise-power (ANP)) to improve the noise-reduction-performance (NRP) of active noise control (ANC) systems have been discussed.

OSPM: For stable operation of FxLMS adaptive algorithm based ANC system, an estimate of the secondary path is required such that the phase difference between the actual secondary path and its estimate is within $\pm 90^{\circ}$ bound [15]. The secondary path is an electro-acoustic path, that contains the transfer function of electronic components and the acoustic path, and hence this secondary path may be time-varying. In order to track the variation in the secondary path, to keep the phase difference within $\pm 90^{\circ}$ bound, a system identification techniques is used in which an auxiliary noise (usually a WGN) is injected into the ANC system.

Online FBPMN: The anti-noise signal generated by the loudspeaker will not only travel down stream to cancel the unwanted noise at the summing junction, but also travel upstream through the feedback path and corrupt the reference signal picked up by the reference microphone. This is called as *feedback path coupling* in ANC literature. This feedback coupling causes an interference in the reference signal of ANC filter, and hence may cause the ANC system to become unstable at some frequency. In order to avoid this undesirable scenario, it is required to neutralize the effect of the feedback coupling. For the neutralization of the feedback path effect, an estimate of the model of the feedback path is required. Similar to secondary path, the feedback path is also an electro-acoustic path, and hence may be time-varying. In order to know the correct estimate of the feedback path a system identification techniques is used in which an auxiliary noise (usually a WGN) is injected into the ANC system.

The basic objective of an ANC system is to reduce the unwanted noise at the summing junction. For stable operation of ANC system online SPM and FBPMN is required. For online SPM and FBPMN, an additional auxiliary noise is injected into the ANC system. If this additional noise is injected with fixed variance in all operating conditions, then at steady-state it will degrade the NRP of ANC system. In order to achieve the online SPM and FBPMN on one hand, and to improve the NRP on the other hand, an auxiliary noise with time-varying variance is needed. During early stages of adaptation of ANC system when the estimate of secondary path and feedback path are far from the actual values, an auxiliary noise with large variance is injected. However, when ANC system converges, and the estimates of the secondary and feedback path are close enough to the true values, the variance of auxiliary noise is reduce to a small value. This will improve the NRP of an ANC system. The main focus of this thesis is to investigate the new gain scheduling strategies to have the time-varying variance of the auxiliary noise.

Chapter 2: In this chapter, the existing methods for OSPM without gain scheduling (auxiliary noise with fixed variance is used in all operating conditions) are discussed. A simplified structure for OSPM with the modified FxLMS (MFxLMS) adaptive algorithm has been proposed. The advantage of the simplified structure is that it reduces the computational complexity of the MFxLMS algorithm based OSPM without having any compromise on the performance of ANC system.

Chapter 3: In this chapter, the existing methods for OSPM with gain scheduling are discussed. The drawbacks with the existing gain scheduling strategies are highlighted and some new gain scheduling strategies have been proposed to improve the modeling accuracy of SPM filter and the NRP of an ANC system.

Chapter 4: This chapter has dealed with the second most important issue associated with the feedforward configuration of ANC system, i.e., the issue of online FBPMN. In the first part of this chapter, the existing methods for online FBPMN without gain scheduling have been discussed. A new structure has been proposed for online FBPMN without gain scheduling. The performance of the existing methods has been compared with the proposed method through the simulation results.

In the second part of this chapter, a gain scheduling strategy has been proposed to improve the NRP of ANC system. In addition to this, a self-tuned ANP scheduling strategy with matching step-size for FBPMN filter has been proposed that requires no tuning parameters and further improves the NRP of ANC systems.

5.2 Future Recommendations

In this thesis, single channel feedforward ANC system is discussed. The single channel ANC system is effective to reduce the unwanted noise in a narrow duct. When it is required to cancel the noise in an enclosure or in a large dimension duct, then using a single channel ANC system to reduce the unwanted noise is not effective. This is because in an enclosure or in a large dimension duct the noise field is complicated. In this scenario the use of multi-channel ANC system is recommended. In multi-channel ANC system, several reference and error microphones, and secondary sources (loudspeakers) are used to cancel the unwanted noise [73], [79]-[82]. One of the future task could be to extend the ideas of proposed gain scheduling strategies (used for OSPM, and online FBPMN) to multi-channel ANC systems.

In this thesis, only linear ANC systems are considered. In linear case both

the primary and secondary paths are assumed to be linear, and filtered-x-LMS (FxLMS) adaptive algorithm is the common choice due to robustness and ease of implementation. However, in actual practice the primary path may be non-linear, the noise and the secondary path may have a non-linear distortion. In such scenarios, for better performance, the linear ANC systems must be replaced by a non-linear ANC systems employing non-linear controller. In addition to this, the devices such as ADC, DAC, power amplifier with linear characteristics are costly. However, if we have a non-linear ANC system employing non-linear controller then we can select less expensive devices having non-linear characteristics, and thus the cost of the overall ANC system may be reduced.

Several non-linear ANC systems have been presented in the literature. In [83] a Volterra FxLMS (VFxLMS) adaptive algorithm is proposed, which performs better than the FxLMS algorithm when 1) the reference noise is non-linear noise process and at the same time the secondary path estimate is of non-minimum phase, and 2) the primary path exhibits non-linearity. In [84] the filtered-s-LMS (FsLMS) algorithm is proposed that performs better than VFxLMS algorithm. In FsLMS algorithm the non-linear expansion of the original unwanted noise is used. This non-linear expansion involves the trigonometric functions and the delayed samples of the original unwanted noise. In [18] computationally efficient adaptive non-linear filters are proposed for non-linear ANC system. In [18] the concept of virtual secondary path is introduced to deal with linear and non-linear secondary paths within a single framework. In [85, 86] Fourier non-linear (FN) and even mirror FN (EMFN) filters, derived from the truncation of multidimensional generalized Fourier series, are presented. These filters have both (1) the property of universal approximator and (2) the property of orthogonality, and hence performs

better than VFxLMS and FsLMS non-linear filters. Because of the wide area of application of non-linear ANC system, one future task could be to extend the idea of gain scheduling for non-linear ANC systems to improve its NRP.

The basic building block of an ANC system is adaptive filter. In this thesis, we considered only the time domain adaptive filtering. In some applications long length adaptive FIR filters are needed to achieve the desired performance. One solution to the complexity problem is to use adaptive IIR filters that need few coefficients. With adaptive IIR filters we have the problems of algorithm instability, slow convergence and trapping in a local minimum. Another strategy to reduce the computation is to use the frequency domain adaptive filtering (FDAF) where block updating strategy is used. In FDAF, the fast Fourier transform (FFT) algorithm efficiently perform filter convolution and the gradient correlation needed for weight updation [87]-[90]. In block updating strategy the block of data is accumulated first and then the filter output computation and adaptive weight updation is performed once for each block. In addition to computational savings, the FDAF algorithm tends to decorrelate the correlated input signal due to inherent property of FFT, and hence can improve the convergence of ANC system. The future task could be to develop the gain scheduling strategy for frequency domain ANC system.

Bibliography

[1] C. M. Harris, *Handbook of acoustical measurements and noise control*, 3rd ed., New York: McGraw-Hill, 1991.

[2] L. L. Beranek, and I. L. Ver, *Noise and vibration control engineering: Principles and applications*, New York: Wiley, 1992.

[3] P. A. Nelson, and S. J. Elliot, *Active Control of Sound*, San Diego, CA: Academic, 1992.

[4] S. M. Kuo, and D. R. Morgan, *Active noise control systems-algorithms and DSP implementation*, New York: Wiley, 1996.

[5] S. J. Elliot, *Signal Processing for Active Control*, London, U.K.: Academic Press, 2001.

[6] B. Widrow, and S. D. Stearns, *Adaptive signal processing*, Englewood Cliffs, NJ: Prentic-Hall, 1985.

[7] L. Ljung, *System identification: Theory for the user*, Englewood Cliffs, NJ: Prentic-Hall, 1987.

[8] M. Bellanger, *Adaptive digital signal processing*, Marcel Dekker Inc., 1987.

[9] P. Lueg, "Process of silencing sound oscillations," U.S. Patent, no. 2,043,416, Jun. 09, 1936.

[10] J. C. Burgess, "Active adaptive sound control in a duct: A computer simulation," *J. Acoust. Soc. Am.*, vol. 70, pp. 715-720, Sep. 1981.

[11] G. E. Warnaka, J. Tichy, and L. A. Poole, "Improvements in adaptive active attenuators," *Proc. Inter-noise*, pp. 307-310, Jun. 1981.

[12] G. E. Warnaka, L. A. Poole, and J. Tichy, "Active acoustic attenuators," *U.S. Patent*, no. 4,473,906, Sep. 25, 1984.

[13] J. Makhoul, "Linear prediction: A tutorial review," *Proc. IEEE*, vol. 63, pp. 561-580. Apr. 1975.

[14] M. M. Sondhi, and D. A. Berkley, "Silencing echoes on the telephone network," *Proc. IEEE*, vol. 68, pp. 948-963. Aug. 1980.

[15] D. R. Morgan, "An analysis of multiple correlation cancellation loops with a filter in the auxiliary path," *IEEE Trans. Acoust., Speech,Signal Processing*, ASSP vol. 28, pp. 454-467, Aug. 1980.

[16] B. Widrow, D. Shur, and S. Shaffer, "On adaptive inverse control," in *Proc. 15th Asilomar Conf.*, pp. 185-189, 1981.

[17] Y. H. Lim, Y. S. Cho, I. W. Cha, and D. H. Youn, "Adaptive nonlinear prefilter for compensation of distortion in nonlinear systems," *IEEE Trans. Signal. Process.*, vol. 46, no. 06, pp. 1726-1730, Jun. 1998.

[18] D. Zhou, and V. DeBrunner, "Efficient adaptive nonlinear filters for nonlinear active noise control," *IEEE Trans. Circuits Syst.*, vol. 54, no. 03, pp. 669-681, Mar. 2007.

[19] S. D. Snyder, and C. H. Hansen, "The effect of transfer function estimation errors on the filtered-X LMS algorithm," *IEEE Trans. Signal Process.*, vol. 42, no. 04, pp. 950-953, Apr. 1994.

[20] S. J. Elliot, and P. A. Nelson, "Active noise control," *IEEE Signal Process. Mag.*, vol. 10, no. 04, pp. 12-35, Oct. 1993.

[21] L. J. Eriksson, and M. C. Allie, "Use of random noise for online transducer modeling in an adaptive active attenuation system," *J. Acoust. Soc. Am.*, vol. 85, no. 02, pp. 797-802, Feb. 1989.

[22] A. Feuer, and E. Weinstein, "Convergence analysis of LMS filters with uncorrelated Gaussian data," *IEEE Trans. Acoust., Speech,Signal Processing*, ASSP, vol. 33, no. 01, pp. 222-230, Feb. 1985.

[23] V. P. Ipatov, "Ternary Sequences with Ideal Periodic Autocorrelation Properties," *Radio Engineering and Electronic Physics*, vol. 24, pp. 75-79, 1979.

[24] H. D. Luke, "Sequences and arrays with perfect periodic correlation," *IEEE Trans. AES*, vol. 24, pp. 287-294, 1988.

[25] M. Antweiler, L. Bomer, and H. D. Luke, "Perfect ternary arrays," *IEEE Trans. IT* , vol. 36, pp. 696-705, 1990.

[26] C. Antweiler, and M. Dorbecker, "Perfect sequence excitation of the NLMS algorithm and its application to acoustic echo control," *Annales des Telecommunications*, vol. 49, no. 07-08, pp. 386-397, 1994.

[27] C. Antweiler, and M. Antweiler, "System identification with perfect sequences based on the NLMS algorithm," *International Journal of Electronics and Communications (AEU)*, vol. 49, no. 03, pp. 129-134, 1995.

[28] C. Antweiler, "Multi-channel system identification with perfect sequences," *Advances in Digital Speech Transmission*, U. H. R. Martin, and C. Antweiler, Eds., SPIE. John Wiley and Sons, pp. 171-198, 2008.

[29] P. V. C. Antweiler, and A. Telle, "NLMS-type system identification of MISO systems with shifted perfect sequences," In *Proc. IWAENC 2008*, Seattle, Washington, USA, 2008.

[30] S. Muller, and P. Massarani, "Transfer-function measurement with Sweeps," *Journal of the Audio Engineering Society*, vol. 49, no. 6, pp. 443-471, June 2001.

[31] A. Telle, C. Antweiler, and P. Vary, "Der perfekte Sweep-ein neues Anregungssignal zur adaptiven Systemidentifikation zeitvarianter akustischer Systeme," in *Proc. of German Annual Conference on Acoustics (DAGA)*, Berlin, Germany, pp. 341-342, Mar. 2010.

[32] Y. Suzuki, F. Asano, H.Y. Kim, and T. Sone, "An optimum computer-generated pulse signal suitable for the measurement of very long impulse responses," *Journal of the Acoustical Society of America*, vol. 97, no. 2, pp. 1119-1123, Feb. 1995.

[33] C. Antweiler, A. Telle, P. Vary, and G. Enzner, "Perfect-sweep NLMS for time-variant acoustic system identification," *in Int. Conf. on Acoustics, Speech and Signal Processing (ICASSP)*, Kyoto, Japan, pp. 517-520, Mar. 2012.

[34] C. Bao, P. Sas, and H. V. Brussel, "Comparison of two online identification algorithms for active noise control," in *Proc. Recent Advances in Active Control of Sound Vibration*, pp.38-51, 1993.

[35] S. M. Kuo, and D. Vijayan, "A secondary path modeling technique for active noise control systems," *IEEE Trans. Speech Audio Processing*, vol. 05, no. 04, pp.374-377, Jul. 1997.

[36] C. Bao, P. Sas, and H. Van Brussel, "Adaptive active control of noise in 3-D reverberant enclosures," *J. Sound Vibr.*, vol. 161, no. 03, pp.501-514, 1993.

[37] M. Zhang, H. Lan, and W. Ser, "Cross-updated active noise control system with online secondary path modeling," *IEEE Trans. Speech Audio Processing.*, vol. 09, no. 05, pp.598-602, Jul. 2001.

[38] M. T. Akhtar, M. Abe, and M. Kawamata, "A new variable step size LMS algorithm-based method for improved online secondary path modeling in active noise control systems," *IEEE Trans. Audio, Speech Lang. Process.*, vol. 12, no. 02, pp. 720-726, Mar. 2006.

[39] S. Ahmed, M. T. Akhtar, and M. Tufail, "A variable step size based method for Online secondary path modeling in active noise control System," in *Proc. of the Second APSIPA Annual Summit and Conference,*, Biopolis, Singapore, pp. 549-554, Dec. 2010.

[40] M. T. Akhtar, M. Abe, and M. Kawamata, "Adaptive filtering with averaging-based algorithm for feedforward active noise control systems," *IEEE Signal Process. Lett.*, vol. 11, no. 06, pp. 557-560, Jun. 2004.

[41] M. T. Akhtar, M. Abe, and M. Kawamata, "A New structure for feedforward active noise control systems with improved online secondary path modeling," *IEEE Trans. Speech Audio Process.*, vol. 13, no. 5, pp. 1082-1088, Sep. 2005.

[42] R. H. Kwong, and E. W. Johnston, "A Variable Step Size LMS Algorithm," *IEEE Trans. on Signal Process.*, vol. 40, no. 07, pp. 1633-1642, Jul. 1992.

[43] S. Ahmed, M.T. Akhtar, and W. Mitsuhashi, "Modified-FxLMS algorithm-based active noise control systems with reduced complexity and improved noise-reduction-performance," in *Proc. of 2012 International Workshop on Nonlinear Circuits, Communications and Signal Processing, NCSP'12*, Honolulu, Hawaii, USA, pp. 691-694, Mar. 2012.

[44] M. T. Akhtar, M. Abe, and M. Kawamata, "Noise power scheduling in active noise control systems with online secondary path modeling," *IEICE Electron. Express.*, vol. 4, no. 02, pp. 66-71, 2007.

[45] A. Carini, and S. Malatini, "Auxiliary noise power scheduling for feedforward active noise control," in *Proc. ICASSP 2008, Int. Conf. Acoust., Speech, Signal Process.*, Las Vegas, Nevada, USA, pp. 341-344, Mar 30-Apr 04. 2008.

[46] A. Carini, and S. Malatini, "Optimal variable step-size NLMS algorithms with auxiliary noise power scheduling for feedforward active noise control," *IEEE Trans. Audio, Speech Lang. Process.*, vol. 16, no. 08, pp. 1383-1395, Nov. 2008.

[47] S. Ahmed, A. Oishi, M. T. Akhtar, and W. Mitsuhashi, "Auxiliary noise power scheduling for online secondary path modeling in single channel feedforward active noise control systems," in *Proc. ICASSP 2012, Int. Conf. Acoust., Speech, Signal Process.*, Kyoto, Japan, pp. 317-320, Mar. 2012.

[48] S. Ahmed, M. T. Akhtar, and W. Mitsuhashi, "Varying auxiliary-noise-power for improved noise reduction in active noise control systems with online secondary path modeling," in *Proc. of Acoustics 2012 Hong Kong Conference and Exhibition*, Hong Kong, May. 2012.

[49] S. Ahmed, M. T. Akhtar, and X. Zhang, "Robust auxiliary-noise-power scheduling in active noise control systems with online secondary path modeling," *IEEE Trans. Audio, Speech Lang. Process.*, vol. 21, no. 04, pp. 749-761, Apr. 2013.

[50] S. Yamamoto, and S. Kitayama, "An adaptive echo canceller with variable step gain method," *Trans. IEICE Japan,* vol. E65 (1) pp. 1-8, Jan. 1982.

[51] D. T. M. Slock, "On the convergence behavior of the LMS and the normalized LMS algorithms," *IEEE Trans. Signal. Process.*, vol. 41, no. 09, pp. 2811-2825, Sep. 1993.

[52] J. Nagumo, and A. Noda, "A learning method for system identification," *IEEE Trans. Automat. Contr.*, vol. AC-12, no. 3, pp. 282-287, Jun. 1967.

[53] N. J. Bershad, "Analysis of the normalized LMS algorithm with Gaussian inputs," *IEEE Trans. Acoust., Speech, Signal Processing*, vol. ASSP-34, no. 04, pp. 793-806, Aug. 1986.

[54] N. J. Bershad, "Behavior of the ϵ-normalized LMS algorithm with Gaussian inputs," *IEEE Trans. Acoust., Speech, Signal Processing*, vol. ASSP-35, no. 05, pp. 636-644, May. 1987.

[55] T. Aboulnasr, and K. Mayyas, "A robust variable step-size LMS-type algorithm: Analysis and simulations," *IEEE Trans. Signal Process.,* vol. 45, no. 03, pp. 631-639, Mar. 1997.

[56] J. E. Greenberg, "Modified LMS algorithm for speech processing with an adaptive noise canceller," *IEEE Trans. Speech Audio Process.*, vol .06, no. 04, pp. 338-351 , 1998.

[57] S. J. Elliott, I. M. Stotbers, and P. A. Nelson, "A multiple error LMS algorithm and its application to the active control of sound and vibration," *IEEE Trans. Acoust., Speech, Signal Process.*, vol. ASSP-35, no. 10, pp. 1423-1434, 1987.

[58] C. C. Boucher, S. J. Elliott, and P. A. Nelson, "Effect of errors in the plant model on the performance of algorithms for adaptive feedforward control," in *Proc. Inst. Elect. Eng.,* vol. 138, pp. 313-319, 1991.

[59] M. Wu, X. Qiu, and G. Chen, "The statistical behavior of phase error for deficient-order secondary path modeling," *IEEE Signal Process. Lett.*, vol. 15, pp. 313-316, 2008.

[60] M. Zhang, H. Lan, and W. Ser, "A robust online secondary path modeling method with auxiliary-noise-power scheduling strategy and norm constraint manipulation," *IEEE Trans. Speech Audio Process.*, vol. 11, no. 01, pp. 45-53, Jan. 2003.

[61] M. A. Swinbanks, "The active control of sound propagation in long ducts," *J. Sound Vib.*, vol. 27, no. 03, pp. 411-436, Apr. 1973.

[62] K. Eghtesadi , and H. G. Leventhall, "Active attenuation of noise: The Chelsea diploe," *J. Sound Vib.*, vol. 75, no. 01, pp. 127-134, Mar. 1981.

[63] G. B. Chaplin, and R. A. Smith, "Waveform synthesis-the Essex solution to repetitive noise and vibratio," in *Proc. Inter-noise*, Edinburgh, UK, pp. 399-402, 1983.

[64] Jr. E. Ziegler, "Selective active cancellation system for repetitive phenomena," *U.S. Patent*, no. 4,878,188, Oct. 1989.

[65] L. J. Eriksson, "Recursive algorithm for active noise control," in *Proc. Int. Symp. Active Control of Sound Vib.*, pp. 137-146, 1991.

[66] L. J. Eriksson, and M. C. Allie, "Correlated active attenuation system with error and correction signal input," *U.S. Patent*, no. 5,206,911, Apr. 1993.

[67] L. J. Eriksson, M. C. Allie, and R. A. Greiner, "The selection and application of an IIR adaptive filter for use in active sound attenuation," *IEEE Trans. Acoust., Speech, and Signal Process.*, vol. 35, no. 04, pp. 433-437, 1987.

[68] L. J. Eriksson, "Active sound attenuation system with on-line feedback path cancellation," *U.S. Patent*, no. 4,677,677, Jun. 1987.

[69] S. M. Kuo, and J. Luan, J, "On-line modeling and feedback compensation for multiple-channel active noise control systems," *Appl. Signal Process.*, vol. 01, no. 02, pp. 64-75, 1994.

[70] S. M. Kuo,"Active noise control system and method for on-line feedback path modeling," *U.S. Patent*, no. 6,418,227, Jul. 9, 2002.

[71] M. T. Akhtar, M. Abe, and M. Kawamata, "On active noise control systems with online acoustic feedback path modeling," *IEEE Trans. Audio, Speech Lang. Process.*, vol. 15, no. 02, pp. 593-600, Feb. 2007.

[72] M. T. Akhtar, M. Tufail, M. Abe, and M. Kawamata, "Acoustic feedback neutralization in active noise control systems," *IEICE Electron. Exp.*, vol. 04, no. 07, pp. 221-226, Apr. 2007.

[73] M. T. Akhtar, M. Abe, M. Kawamata, and W. Mitsuhashi, "A simplified method for online acoustic feedback path modeling and neutralization in multichannel active noise control systems," *Signal Process.*, vol. 89, no. 06, pp. 1090-1099, Jun. 2009.

[74] Z. Mehmood, M. Tufail, and S. Ahmed, "A new variable step size method for online feedback path modeling in active noise control systems' ," in *Proc. 13th Int. Multi-Topic Conf. (INMIC)*, Islamabad, Pakistan, Dec. 2009.

[75] M. T. Akhtar, and W. Mitsuhashi, "Variable step-size based method for acoustic feedback modeling and neutralization in active noise control systems," *Applied Acoust.*, vol. 72, no. 05, pp. 297-304, Apr. 2011.

[76] S. Ahmed, M. T. Akhtar and X. Zhang, "Controlling auxiliary-noise-power for efficient neutralization of acoustic feedback in active noise control systems," in *Proc. of TENCON 2012*, Cebu, Philippines, Nov. 2012.

[77] S. Ahmed, M. T. Akhtar, and X. Zhang, "Online acoustic feedback mitigation with improved noise-reduction performance in active noise control systems," *IET Signal Process.*, vol. 07, no. 06, pp. 505-514, Jun. 2013.

[78] S. Ahmed, M. T. Akhtar and X. Zhang, "Self-tuned auxiliary-noise-power scheduling with matching step-size for online acoustic feedback path mitigation in active noise control," in *Proc. IEICE Tech. Rep. EA2014-18*, Sendai, Japan, vol. 114, no. 178, pp. 37-42, Aug. 2014.

[79] M. T. Akhtar, M. Abe, M. Kawamata, and A. Nishihara, "Online secondary path modeling in multichannel active noise control systems using variable step size," *Signal Process.*, vol. 88, no. 08, pp. 2019-2029, Aug. 2008.

[80] S. Ahmed, and M. Tufail, "A new variable step size method for online secondary path modeling in multichannel $(1 \times 2 \times 2)$ active noise control systems," in *Proc. of International conference on information and emerging technologies (ICIET), 2010*, Karachi, Pakistan, Jun. 2010.

[81] M. T. Akhtar, and W. Mitsuhashi, "Variable step-size based onlineacoustic feedback neutralization in multiple-channel ANC systems," in *Proc. 53rd IEEE Int. Midwest Symp. Circuits Syst.*, Seattle, WA, USA, pp. 1073-1076, Aug. 2010.

[82] S. Ahmed, M. T. Akhtar, M. Tufail, and W. Mitsuhashi, "On online acoustic feedback path modeling in multichannel active noise control systems," in *Proc. of 6th Triangle Symposium on Advanced ICT*, KAIST, Daejeon, Korea, pp. 204-208, Aug. 2011.

[83] L. Tan, and J. Jiang, "Adaptive volterra filter for active control of nonlinear noise processes," *IEEE Trans. on Signal Process.*, vol. 49, no. 08 pp. 1667-1676, Aug. 2001.

[84] D. P. Das, and G. Panda, "Active mitigation of non-linear noise processes using novel filterd-s-LMS algorithm," *IEEE Trans. on Speech and Audio Process.*, vol. 12, no. 03 pp. 313-322, May 2004.

[85] A. Carini, and G.L. Sicuranza, "Even mirror Fourier nonlinear filters," in *Proc. of the of ICASSP 2013, International Conference on Acoustic, Speech, Signal Process.*, Vancouver, Canada, pp. 5608 - 5612, May. 2013

[86] A. Carini, and G. L. Sicuranza, "Fourier nonlinear filters," *Signal Process.*, vol. 94, pp. 183-194, Jan. 2014.

[87] M. Dentino, J. McCool, and B. Widrow, "Adaptive filtering in the frequency domain," in *Proc. IEEE*, vol. 66, 1658-1659, Dec.1978.

[88] E. R. Ferrara, "Fast implementation of LMS adaptive filters," *IEEE Trans. Acoust., Speech, Signal Processing*, vol. ASSP-28, pp. 474-475, 1980.

[89] P. C. W. Sommen, and J. A. K. S. Jayasinghe, "On frequency-domain adaptive filtersusing the overlap-add method," in *Proc. IEEE Intl. Symp.Circuits Systems*, pp. 27-30, Espoo, Finland, June 1988.

[90] J. J. Shynk, "Frequency-domain and multirate adaptive filtering," *IEEE Signal Processing Mag.*, vol. 9, pp. 1437, Jan. 1992.

ACKNOWLEDGEMENTS

First of all I would like to thank almighty Allah who gave me the health, energy and chance to carry out this research.

I wish to thank my Supervisor Prof. Xi Zhang who has always been there to listen and to overcome the crises. I would like to thank him for providing me all the facilities, support, and guidance during my research, and for allowing me to carry out the research in my own way. I am thankful to my Co-Supervisor Prof. Kota Takahashi for reading/commenting the thesis, and helping me to improve the quality of the thesis.

I would like to express my sincere gratitude to Dr. Muhammad Tahir Akhtar for his guidance, commitment and dedication. I would like to thank him for his hard work in revising the thesis to improve its quality.

I am also indebted to Prof. Yoshikazu Washizawa for his generous support and guidance.

I consider it an honour to work with Professor Wataru Mitsuhashi. I would use this opportunity to say thanks to him for his encouragement, support, and advice to keep up the good work.

I would like to say thanks to the supervisory committee members Professor Wataru Mitsuhashi, Associate Professor Kota Takahashi, Associate Professor Hideyuki Nomura, and Associate Professor Feng Chao Xiao for their scientific advice to improve the quality of the thesis.

I would like to say special thanks to my parents, brother and sister for their invaluable support throughout my career.

I would like to acknowledge The Ministry of Education, Culture, Sports, Science and Technology (MEXT), Japan for the financial support to cover all my expenses.

At last, but not the least I owe my deepest gratitude to my Lab mates especially to Dai-Wei Wang, and all other friends for their love, treasuring memories, and support during the entire period of my stay in Japan.

About the Author ...

Shakeel Ahmed received the BE degree in electrical engineering from NWFP University of Engineering and Technology Peshawar, Pakistan in 2005, MS degree in Systems engineering from Pakistan Institute of Engineering and Applied Sciences (PIEAS), Islamabad, Pakistan, under a fellowship programme in 2007. In 2007 he joined PIEAS as a faculty member in the Department of Electrical Engineering. He received Japanese government scholarship (MEXT), from April 2011 to March 2015, for PhD degree. His research interests include adaptive signal processing for linear and non-linear active noise control systems.

List of Publications

Journal Papers:

[1]. **S. Ahmed**, M. T. Akhtar, and X. Zhang, "Online acoustic feedback mitigation with improved noise-reduction performance in active noise control systems," *IET Signal Process.*, vol. 07, no. 06, pp. 505-514, Jun. 2013. (**Chapter 4 contents**)

[2]. **S. Ahmed**, M. T. Akhtar, and X. Zhang, "Robust auxiliary-noise-power scheduling in active noise control systems with online secondary path modeling," *IEEE Trans. Audio, Speech Lang. Process.*, vol. 21, no. 04, pp. 749-761, Apr. 2013. (**Chapter 3 contents**)

International Conference Papers:

[1]. **S. Ahmed**, M. T. Akhtar and X. Zhang, "Controlling auxiliary-noise-power for efficient neutralization of acoustic feedback in active noise control systems," in *Proc. of TENCON 2012*, Cebu, Philippines, Nov. 2012.

[2]. **S. Ahmed**, M. T. Akhtar, and W. Mitsuhashi, "Varying auxiliary-noise-power for improved noise reduction in active noise control systems with online secondary path modeling," in *Proc. of Acoustics 2012 Hong Kong Conference and Exhibition*, Hong Kong, May. 2012.

[3]. **S. Ahmed**, A. Oishi, M. T. Akhtar, and W. Mitsuhashi, "Auxiliary noise power scheduling for online secondary path modeling in single channel feedforward active noise control systems," in *Proc. ICASSP 2012, Int. Conf. Acoust., Speech, Signal Process.*, Kyoto, Japan, pp. 317-320, Mar. 2012.

[4]. **S. Ahmed**, M. T. Akhtar, and W. Mitsuhashi, "Modified-FxLMS algorithm-based active noise control systems with reduced complexity and improved noise-reduction-performance," in *Proc. of 2012 International Workshop on Nonlinear Circuits, Communications and Signal Processing, NCSP'12*, Honolulu, Hawaii, USA, pp. 691-694, Mar. 2012.

[5]. **S. Ahmed**, M. T. Akhtar, M. Tufail, and W. Mitsuhashi, "On online acoustic feedback path modeling in multichannel active noise control systems," in *Proc. of 6th Triangle Symposium on Advanced ICT*, KAIST, Daejeon, Korea, pp. 204-208, Aug. 2011.

Domestic Workshop Papers:

[1]. **S. Ahmed**, M. T. Akhtar and X. Zhang, "Self-tuned auxiliary-noise-power scheduling with matching step-size for online acoustic feedback path mitigation in active noise control," in *Proc. IEICE Tech. Rep. EA2014-18*, Sendai, Japan, vol. 114, no. 178, pp. 37-42, Aug. 2014.